Molecular Characterization of Methanotrophic and Chemoautotrophic Communities at Cold Seeps

Dissertation
zur Erlangung des Grades eines
Doktors der Naturwissenschaften
- Dr. rer. nat. -

dem Fachbereich Biologie/Chemie der
Universität Bremen
vorgelegt von

Tina Lösekann

Bremen
März 2006

Die Untersuchungen zur vorliegenden Doktorarbeit wurden in der Zeit von September 2002 bis März 2006 am Max-Planck-Institut für Marine Mikrobiologie in Bremen durchgeführt.

1. Gutachterin: Prof. Dr. A. Boetius
2. Gutachter: Prof. Dr. R. Amann

Weitere Prüfer:
Prof. Dr. U. Fischer
Dr. K. Knittel

Tag des Promotionskolloquiums: 30. März 2006

Table of Contents

Summary

Cold seeps are complex ecosystems based on chemosynthesis. Sulfide and methane are available in high concentrations and support a variety of highly adapted microorganisms and symbiont-bearing invertebrates. The anaerobic oxidation of methane (AOM) is a key biogeochemical process at cold seeps and is assumed to be mediated by a consortium of anaerobic methanotrophic archaea (ANME) and sulfate-reducing bacteria.

In this thesis I used 16S rRNA-based molecular methods to identify and quantify methanotrophic and chemoautotrophic, sulfur-oxidizing communities at two cold seeps and collaborated with scientists from other disciplines to correlate the molecular results with biogeochemical, geological, and physical data sets. Two types of cold seeps were studied, the Arctic Haakon Mosby Mud Volcano (HMMV; 1250 m water depth) and the Hydrate Ridge at the Cascadia Margin (700 m water depth) off the coast of Oregon.

The actively methane-seeping HMMV hosts novel clades of aerobic and anaerobic methanotrophs. The distribution of the methanotrophic guilds is controlled by fluid flow and bioirrigation activities of marine invertebrates. The center of the volcano is characterized by high upward fluid flow. High numbers of novel aerobic methanotrophs were detected in the upper millimeters of the sediment. These dominated the microbial community in surface sediments of HMMV. At sites with decreased upward fluid flow, a new group of ANME archaea (ANME-3) was identified, dominating the zone of AOM in 1-4 cm sediment depth. In this zone, the microbial biomass was almost entirely comprised by ANME-3 archaea which form consortia with sulfate-reducing bacteria of the *Desulfobulbus* branch. In bioirrigated sediments populated by siboglinid tubeworms, sulfate is transported deeper into the sediment and here the AOM consortia were found at the base of the tubeworm roots.

The symbioses between bacteria and the tubeworms at HMMV were characterized. Two species of tubeworms coexist at the same site and represent the dominant megafauna at HMMV. The symbionts of *Sclerolinum contortum* were identified as chemoautotrophic sulfur oxidizers and are closely related to symbionts of vestimentiferan tubeworms. The symbionts of *Oligobrachia haakonmosbiensis* represent a novel symbiont lineage. The molecular results in combination with stable carbon isotope analysis suggest that this species may harbor both chemoautotrophic sulfur-oxidizing and methane-oxidizing symbionts.

Another focus of the thesis was to compare microbial communities in gas hydrate bearing shallow subsurface sediments with surface communities at Hydrate Ridge. The microbial diversity in these habitats was similar. Cells of the ANME-1 clade dominated the archaeal community in shallow subsurface sediments with highest numbers in depths directly above two gas hydrate layers. A novel type of microbial consortium was detected consisting of ANME-1 archaea and sulfate-reducing bacteria of the *Desulfosarcina/Desulfococcus* branch. The microbial community in gas hydrate melts was dominated by either ANME-1 or ANME-2 archaea. These cells had very low rRNA contents, indicating that they may have been inactive for extended periods. In contrast, ANME cells in sediments surrounding gas hydrates had high rRNA contents even at 1 m below the seafloor suggesting that sulfate and methane are available for the microbial community in distinct subsurface horizons.

Zusammenfassung

Die sogenannten ‚cold seeps' sind komplexe Ökosysteme, die auf Chemosynthese basieren. Sowohl Sulfid als auch Methan kommen in großen Konzentrationen vor und gewährleisten das Vorkommen von besonders angepassten Mikroorganismen und Invertebraten, die mikrobielle Symbionten beherbergen. Die anaerobe Methanoxidation (engl. Anaerobic Oxidation of Methane, AOM) ist ein biogeochemischer Schlüsselprozess an ‚cold seeps'. AOM wird von einem Konsortium aus anaeroben, methanotrophen Archaeen (ANME) und sulfatreduzierenden Bakterien (SRB) katalysiert.

In dieser Arbeit habe ich Methoden basierend auf 16S rRNA-Analysen angewandt, um die methanotrophen und chemoautotrophen Schwefel-oxidierenden mikrobiellen Gemeinschaften an zwei unterschiedlichen ‚cold seeps' zu identifizieren und zu quantifizieren. Darüber hinaus habe ich mit Wissenschaftlern verschiedenster Disziplinen zusammengearbeitet, um die Ergebnisse meiner molekularbiologischen Untersuchungen mit biogeochemischen, geologischen und physikalischen Datensätzen zu kombinieren. Zwei unterschiedliche ‚cold seep' Typen wurden untersucht: Der Arktische Schlammvulkan Haakon Mosby (engl. Haakon Musby Mud Volcano, HMMV; 1250 m Wassertiefe) und der Hydratrücken vor der Küste Oregons (Cascadia Margin, 700 m Wassertiefe).

Der HMMV stößt aktiv Methan aus und beherbergt neue Gruppen aerober und anaerober methanotropher Mikroorganismen. Die Verteilung dieser Gruppen ist von Stärke und Verlauf des Fluid-Flusses und vom Ausmaß der Bioirrigation durch Invertebraten abhängig. Im Zentrum des HMMV herrschen starke, aufwärtsgerichtete Fluid-Flüsse. Dort wurden in den oberen Millimetern des Sediments hohe Abundanzen neuer aerober Methanotropher entdeckt. Diese stellten den größten Teil der mikrobiellen Lebensgemeinschaft in den Oberflächensedimenten. Eine neue Gruppe von ANME-Archaeen (ANME-3) konnte an Standorten mit verringerten aufwärtsgerichteten Fluid-Flüssen identifiziert werden. Diese Gruppe dominierte die AOM-Zone in 1-4 cm Sedimenttiefe und stellte dort fast die gesamte mikrobielle Biomasse. Diese Archaeen bilden zusammen mit Sulfat-reduzierenden Bakterien des Zweiges *Desulfobulbus* mikrobielle Konsortien. In Sedimenten, in denen durch die Bioirrigationaktivitäten siboglinider Röhrenwürmer das Sulfat tiefer eingebracht wird, wurden mikrobielle Konsortien unterhalb Wurzeln der Würmer entdeckt.

Die Symbiose der Bakterien und der Röhrenwürmer am HMMV wurde ebenfalls charakterisiert. Zwei Arten von Röhrenwürmern koexistieren am selben Standort und repräsentieren die dominierende Megafauna. Die Symbionten von *Sclerolinum contortum* wurden als chemoautotrophe Schwefeloxidierer identifiziert und sind nahe Verwandte der Symbionten der *Vestimentifera*. Die Symbionten von *Oligobrachia haakonmosbiensis* gehören zu einer neuen Symbionten-Linie, die nicht mit bekannten Schwefel- oder Methanoxidierern verwandt ist. Die molekularbiologischen Ergebnisse lassen in Kombination mit den Ergebnissen der Analyse stabiler Kohlenstoffisotope vermuten, dass diese Wurmspezies wahrscheinlich sowohl chemoautotrophe Schwefel-oxidierende wie auch Methan-oxidierende Symbionten besitzt.

Ein weiterer Schwerpunkt dieser Arbeit war der Vergleich der mikrobiellen Gemeinschaften von oberflächennahen, Gashydrat-enthaltenden Tiefensedimenten und Oberflächensedimenten am Hydratrücken. Die mikrobielle Diversität dieser Habitate war ähnlich. Zellen der ANME-1 Archaeen dominierten die mikrobielle Lebensgemeinschaft in oberflächennahen Tiefensedimenten. Sie zeigten höchste Abundanzen direkt über zwei Schichten von Gashydrat. Dort wurde eine neue Variante eines Konsortiums bestehend aus ANME-1 Archaeen und Sulfat-reduzierenden Bakterien aus der *Desulfosarcina/Desulfococcus*-Gruppe entdeckt. Die mikrobielle Gemeinschaft in geschmolzenen Gashydraten wurde entweder von ANME-1 oder von ANME-2 Archaeen dominiert. Diese Zellen zeichneten sich durch einen geringen rRNA-Gehalt aus, was darauf hinweisen könnte, dass sie für einen längeren Zeitraum inaktiv gewesen sind. Im Gegensatz dazu besitzen Zellen in den Gashydrat-umgebenden Sedimenten einen hohen rRNA-Gehalt sogar 1 m unterhalb der Sedimentoberfläche. Diese Tatsache lässt vermuten, dass Sulfat wie auch Methan der mikrobiellen Lebensgemeinschaft in bestimmten Horizonten des Tiefensediments zur Verfügung stehen.

Part I

Combined Presentation of Results

A Introduction

At first glance, the deep-sea floor appears to be a desert – a barren, cold, and dark environment which is inhabited by very few specialized species. This anthropocentric view has been revised during the last decades. Today there is little doubt that the biodiversity in the deep-sea is very high and may be comparable to that of tropical forests. Reducing habitats such as hydrothermal vents and cold seeps are productivity hot spots in the deep-sea and represent oases of microbial and metazoan life. These unique habitats fascinated me ever since my early studies of microbiology. In the absence of sunlight diverse chemosynthetic communities build up spectacular high amounts of biomass using only inorganic compounds (including methane) as energy and carbon source. Remarkably little is known about the biodiversity in these ecosystems. During my thesis I focused on the characterization of methanotrophic and chemoautotrophic microbial communities at cold seeps, which represent key players in these ecosystems.

1 Reducing Habitats in the Ocean

The so-called 'reducing habitats' in the ocean are characterized by the absence of oxygen and high concentrations of reduced substances such as sulfide. Oxygen may be depleted in these zones because of high oxygen consumption in connection with high deposition rates of organic matter and/or the venting of reduced fluids from subsurface sources. On the ocean floor reducing habitats can be found in upwelling areas, at the intersection of the seafloor with oxygen minima in the water column, around large food falls, hydrothermal vents, and cold seeps. Reducing habitats are fascinating, because they are often populated by enormous biomasses of organisms which derive their energy from the oxidation of abundant energy-rich reduced substrates such as sulfide or methane. As chemical energy drives the synthesis of organic carbon, this microbial process is called chemosynthesis – in analogy to the process of photosynthesis with light as energy source. Chemosynthesis was first observed more than 100 years ago by the Russian microbiologist Sergei Winogradsky, but this process was considered to play no significant role in the carbon cycle of the photosynthetically dominated Earth's surface. The biogeochemical significance of chemosynthesis emerged only upon the discovery of deep-sea hydrothermal vent systems, where photosynthetic production of plant organic biomass at the base of the food web is hypothesized to be virtually replaced by chemosynthetic production of microbial organic carbon (Van Dover 2000). The complex

chemosynthetic communities at vents are comprised of a variety of highly adapted microorganisms and symbiont-bearing invertebrates which play an important role for the ocean's biodiversity and the transfer of carbon to the deep sea.

1.1 Oxygen Minimum Zones

Oxygen minimum zones (OMZ) are defined as zones of the water column where oxygen concentrations are below 0.5 ml oxygen l^{-1}. Generally, OMZs are formed in areas of the ocean which receive a high load of organic matter due to high surface productivity, e.g. in upwelling regions. In OMZs oxygen is already depleted in the water column due to aerobic degradation processes of sinking organic matter. Where OMZs intercept the continental margins, extensive stretches of the seafloor are exposed to severe oxygen depletion ranging from the shelf to upper bathyal depths (10-1,300 m). The anaerobic degradation of organic matter via fermentation, sulfate reduction, and methanogenesis produces large amounts of reduced substances like sulfide and methane which are utilized by chemosynthetic microorganisms. The largest OMZs are located in the eastern Pacific Ocean, in the Arabian Sea, in the Bay of Bengal, off southwest Africa, and off California. Regions such as the Baltic Sea, the Black Sea or some Norwegian fjords exhibit hypoxia (<0.2 ml oxygen l^{-1}) irrespective of water depth. Deep-water hypoxia can be found in shallow-sill basins such as the California continental borderlands (Levin 2003).

1.2 Large Organic Falls

Large organic falls (whales, woods, kelp) provide concentrated packages of organic carbon to the nutrient limited seafloor of the deep-sea. Although these food falls are more or less unpredictable in time and space, they are rapidly located and devoured by specialized, opportunistic fauna (Smith 1985). Degradation occurs by microorganisms and animal communities adapted to the use of high carbon concentrations. Although little is known about the abundance of organic falls, the fast detection and exploitation of these pulsed deliveries of organic material by deep-sea benthic invertebrates suggest that food falls are common (Van Dover 2000). Decomposing whale carcasses have been intensively studied during the last decades and are considered to be persistent, organic and sulfide-rich habitats at the deep-sea floor. The anaerobic breakdown of bone lipids via sulfate reduction provides sulfide which attracts a large, species-rich, and trophically complex assemblage that lives on the skeleton. Interestingly, a high diversity of endemic species has been found associated with sunken whales such as the bone-degrading worm *Osedax* (Rouse *et al*. 2004). It has been

suggested that - at least for metazoans - whale falls might provide dispersal stepping stones for vent and seep species dependent on sulfide availability at the deep-sea floor (Smith *et al.* 1989, Feldman *et al.* 1998, Smith & Baco 2003). Moreover, large organic falls facilitated the repeated invasion of chemosynthetic species from shallow low-sulfide environments to deep-sea high sulfide-environments such as hydrothermal vents and cold seeps (Distel *et al.* 2000).

1.3 Hydrothermal Vents

Deep-sea hydrothermal vents and their associated fauna were first discovered along the Galapagos Rift in the eastern Pacific (Corliss *et al.* 1979). Vents are now known to occur along all active mid ocean ridges and back-arc spreading centers from fast to ultra-slow spreading ridges. Fluid composition of magmatically driven vent systems results from the reaction of seawater with cooling basalt at high temperatures. The fluids are especially enriched in hydrogen sulfide, hydrogen, methane, manganese, and other transition metals (iron, zinc, copper, lead, cobalt, aluminium). The energy derived from the oxidation of reduced hydrothermal fluid compounds supports exceptionally productive biological communities (reviewed in Van Dover 2000). During explorations of deep-sea hydrothermal vents symbiotic associations between sulfur-oxidizing, chemoautotrophic bacteria and marine invertebrates were first discovered (Cavanaugh *et al.* 1981, Felbeck 1981). It is now known that associations with thiotrophic and methanotrophic bacteria occur in a wide taxonomic range of invertebrates which live in reducing environments (Childress *et al.* 1986, Fisher 1990, Feldman *et al.* 1998).

1.4 Cold Seeps

About one decade after the discovery of the hydrothermal vent communities, another type of chemosynthesis-based ecosystem, the so-called 'cold seeps' were discovered at the deep-sea floor (Paull *et al.* 1984, Kennicutt *et al.* 1985, Suess *et al.* 1985). Cold seeps are located at both active and passive continental margins and are characterized by focused fluid flow which is not induced by hydrothermal activity. Both sulfide and methane are available in high concentrations and support chemosynthetic communities similar to those found at hydrothermal vents. Methane is released from subsurface reservoirs and ascends as free gas or dissolved in fluids to the sediment surface. Large amounts of sulfide are formed due to the process of anaerobic oxidation of methane (AOM). Cold seeps are often associated with gas hydrate deposits. Gas hydrates are solid ice-like structures consisting of gas (predominantly methane) which is encaged inside ice crystals. They form under conditions of low

temperature, high hydrostatic pressure, and gas in excess of solubility (Kvenvolden 1988, Buffet 2000). Environmental changes such as increasing water temperature or decreasing sea level alter the hydrate stability field and may cause decomposition of gas hydrates. Hence, gas hydrates represent one of the most dynamic organic carbon reservoirs on Earth. The knowledge about the global distribution of gas hydrates is incomplete making estimates about the total amount of methane stored in gas hydrates highly speculative. However, conservative estimates suggest that more organic carbon is stored in gas hydrates deep in the ocean than in any other fossil fuel or gas reservoir on Earth (Kvenvolden 1988).

A major type of cold seep system is represented by gas-emitting submarine mud volcanoes. Mud volcanoes are present at tectonically active and inactive areas of continental margins. These geological features result from the emission of semi-liquid material (mud breccia) extruded by a deep pressure source forming mounds and craters on the seafloor (Dimitrov 2002). The rising muds are often enriched in methane and represent a window between the deep geosphere and the biosphere. According to Kopf (2003), the contribution of mud volcanoes to the global methane emission ranges between 0.4% and 22.7% and may be underestimated in global carbon budgets.

Other types of cold seeps include hydrocarbon seeps and asphalt volcanoes which are abundant in the Gulf of Mexico (Joye *et al.* 2004, MacDonald *et al.* 2004). Active sites are characterized by elevated concentrations of simple (C_1-C_5) and complex (oil) hydrocarbons and in the case of asphalt volcanoes associated with asphalt flows. Only a small fraction of sulfate reduction activity is coupled to AOM in these systems (Aharon & Fu 2000, Orcutt *et al.* 2005). The high concentrations of sulfide in the sediments are mainly produced by microbial degradation of hydrocarbons other than methane coupled to the reduction of sulfate.

Despite the large amounts of methane which are stored in the ocean, only little methane escapes from marine sediments due to AOM. This process shields our atmosphere effectively from the aggressive greenhouse gas methane today. However, in former periods of Earth's history large-scale decomposition of gas hydrates and the according increase of methane concentrations in the atmosphere have influenced the global climate and probably caused global warming events (Katz *et al.* 1999, Norris & Rohl 1999, Hesselbo *et al.* 2000, Kennett *et al.* 2000, Hinrichs *et al.* 2003). Thus, the study of AOM is an important contribution to our understanding and the quantification of the global carbon cycle as well as future and past climate changes.

2 Key Biogeochemical Processes in Reducing Habitats

The spectacular ecosystems found associated with reducing habitats are based on the availability of chemical energy from reduced compounds, such as sulfide and hydrogen at hydrothermal vents or less readily metabolizable compounds such as methane and other hydrocarbons at cold seeps. In the following, the major biogeochemical processes, which provide energy to the ecosystem's food web, are presented.

2.1 Methanogenesis

Most methane in the ocean is biogenic, i.e. it is produced by thermogenic transformation of organic matter or by microbial methanogenesis. Microbial methanogenesis is a process mediated by a specialized group of microorganisms, the methanogenic archaea *(Methanobacteriales, Methanococcales, Methanomicrobiales, Methanosarcinales, Methanopyrales)*. They are strict anaerobes and occur only in anoxic habitats. In the oxic zone of marine sediments organic material can be fully degraded to CO_2. Once oxygen is depleted, the mineralization of organic matter is carried out by a sequence of interacting bacterial groups. Methanogenic archaea represent the last stage of this sequence. They can only use a narrow spectrum of substrates, primarily H_2/CO_2 (reaction 1) and acetate (reaction 2). Within the sulfate-penetrated seafloor sulfate-reducing bacteria compete successfully for these few substrates and thus methanogenesis is of little significance in the sulfate zone (Wellsbury & Parkes 2000). Only a few 'non-competitive' substrates such as methylamines are used by methanogens and not by sulfate reducers (Oremland *et al.* 1982). Below the sulfate-penetrated zone of the seafloor, there are no other electron acceptors than CO_2 available and methane accumulates as the main terminal product of organic matter degradation.

$$4 H_2 + CO_2 \rightarrow CH_4 + 2 H_2O \qquad\qquad\qquad (1)$$
$$CH_3COO^- + H+ \rightarrow CH_4 + CO_2 \qquad\qquad\qquad (2)$$

The process of microbial methanogenesis is mediated in several enzymatic steps. Only the last step is common for all methanogenic substrates and is catalyzed by the methyl-coenzyme M reductase (MCR). Methyl-conenzyme M can be formed from coenzyme M and acetate and is subsequently reduced with coenzyme B to methane with the concomitant formation of the heterodisulfide of coenzyme M and coenzyme B (reaction 3). Since the generation of the heterodisulfide in the oxidative part of the energy metabolism is not coupled with net ATP formation, the energy required for growth of methanogens must be

generated in the reductive part, i.e. the exergonic reduction of the heterodisulfide (Thauer 1998).

$$CH_3 - S - CoM \, + \, H - S - CoB \rightarrow CH_4 \, + \, HS - CoM - S - S - CoB \qquad\qquad (3)$$

Before the finding of vast gas hydrate deposits on deeper areas of continental margins (>500 m) it was believed that most of the methane in the ocean is produced in shelf and near-shore sediments. Today it is known that subsurface zones of continental margins may also provide high fluxes of gas (Kvenvolden 1988). In the abyssal open ocean primary productivity is much lower and most of the organic matter is already degraded in the water column. Organic matter that reaches the seafloor in these zones is mainly decomposed by aerobic processes (Wenzhofer & Glud 2002).

2.2 Anaerobic Oxidation of Methane

The anaerobic oxidation of methane (AOM) is the major sink of methane in reducing habitats, where methane and sulfate are concurrently available. The process of AOM coupled to the reduction of sulfate has been postulated three decades ago to explain conspicuous pore water profiles of methane and sulfate measured in organic-rich, anoxic sediments which showed the simultaneous consumption of both substances (Martens & Berner 1974, Barnes & Goldberg 1976). Today it is established that methane in marine sediments is oxidized under anoxic conditions. AOM activity has been demonstrated in several marine habitats and can be the dominant sulfate-consuming process, e.g. in sediments above gas hydrates or at methane seeps (Michaelis *et al.* 2002, Treude *et al.* 2003). AOM activity is often restricted to a narrow zone of the sediments forming steep gradients of pore water constituents (Fig. 1). Highest AOM activities are found at sites with highest methane flux, thus cold seeps are hot spots of AOM in the ocean.

AOM is an effective biological barrier to methane and shields the atmosphere from the aggressive greenhouse gas (Hinrichs & Boetius 2002 and references therein). More than 80% of the methane produced annually in the ocean is consumed before it reaches the atmosphere (Reeburgh 1996). The previously estimated 75 Tg/yr of methane consumed by AOM (not including the high AOM rates at cold seeps) indicate that AOM consumes nearly twice the annual increase in the atmospheric inventory of methane (40 Tg/yr) (Hinrichs & Boetius 2002). Hence, this process is crucial in maintaining a sensitive balance of our atmosphere's greenhouse gas content. Moreover, Earth's atmosphere was rich in methane and poor in

oxygen for the longest time and the extension of our knowledge of how life can be based on methane as energy source is important for our understanding of the evolution of biochemical cycles.
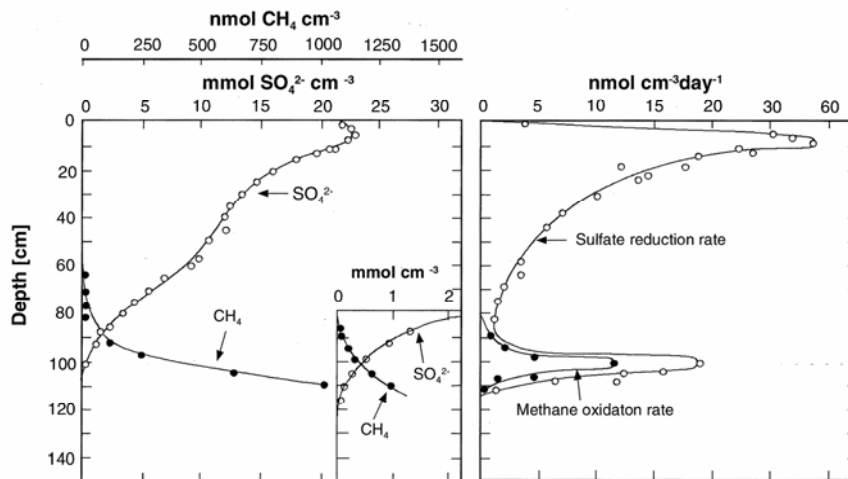
Figure 1 AOM-associated depth profiles from Skagerrak sediments (Denmark). (Left) Sulfate and methane concentrations, the enlarged insert shows the sulfate-methane-transition zone. (Right) Radiotracer rate measurements of AOM and sulfate reduction showing the coupling of both processes in anoxic sediments. (Modified from Iversen & Jørgensen 1985)

The metabolic process of AOM is proposed to be a reversed methanogenesis coupled to the reduction of sulfate, involving methanotrophic archaea (ANME) and sulfate-reducing bacteria (SRB). ANME and SRB are assumed to interact syntrophically (Hoehler *et al.* 1994) and form microbial consortia which oxidize methane with equimolar amounts of sulfate, yielding bicarbonate and sulfide (reaction 4) (Nauhaus *et al.* 2002). In the following, the term 'microbial consortium' refers to the close association of microbial cells in which two or more different microorganisms maintain a permanent cell-to-cell contact and form an organized structure.

The free energy yield of AOM is very small and has to be shared by both partner organisms of the consortium. AOM mediating microorganisms are slow-growing but build up high amounts of biomass at cold seeps. Often authigenic carbonates form due to localized increases in alkalinity caused by AOM activity and the availability of cations from the overlying seawater (Bohrmann *et al.* 1998, Luff & Wallmann 2003). Furthermore, sulfide as the by-product of AOM nourishes sulfur-based chemosynthetic communities such as mats of colorless, sulfur-oxidizing bacteria, symbiont-bearing mussels, clams, and tubeworms (MacDonald *et al.* 1989, Sahling *et al.* 2002, Sibuet & Olu-Le Roy 2002).

The net reaction of AOM can be formulated as:

$$CH_4 + SO_4^{2-} \rightarrow HCO_3^- + HS^- + H_2O \qquad \Delta G^0 = \text{-16.6 kJ/reaction} \qquad (4)$$

All attempts to isolate microorganisms capable of net AOM failed so far. Thus, little is known about the physiology of anaerobic methane oxidizers, the metabolic pathways, and involved enzymes. Recent progress has been made in enriching these microorganisms (Nauhaus *et al.* 2002, Girguis *et al.* 2003). Nauhaus *et al.* (2002) demonstrated AOM under laboratory conditions and showed that AOM and SR are coupled in a 1:1 ratio as predicted by the stochiometry of the two processes. The rates increased with increasing methane partial pressure showing that AOM strongly depends on the availability of dissolved methane.

In many syntrophic associations hydrogen is transferred as intermediate between both partners (Schink 1997) and 'interspecies hydrogen transfer' has also been proposed for AOM mediating consortia. Sulfate-reducing bacteria are able to scavenge hydrogen at very low concentrations and thereby maintain hydrogen partial pressure low enough for favorable energy yields by AOM. However, hydrogen production has not yet been observed in methanogens even at very low-hydrogen conditions (Valentine *et al.* 2000). Moreover, thermodynamically considerations contradict the idea that hydrogen serves as an intermediate, because too much energy is lost during the diffusion of intermediates at low concentrations (Sörensen *et al.* 2001). This also applies for acetate and methanol (Sörensen *et al.* 2001). Formiate appears to be a suitable intermediate but laboratory experiments using formiate did not show an effect on AOM (Nauhaus *et al.* 2002). Electrons may also serve as intermediates that are transferred by electron-shuttling compounds.

Recently, the analysis of genes and biochemical components in samples from habitats, where methane-oxidizing microbial communities are abundant, supported the hypothesis that AOM is in terms of biochemistry a reversal of methanogenesis (Hallam *et al.* 2003, Krüger *et al.* 2003, Hallam *et al.* 2004, Meyerdierks *et al.* 2005). Genes were retrieved which are very similar to those encoding the three subunits of methyl-coenzyme M reductase (MCR), the terminal enzyme in methanogenesis. The deduced proteins were phylogenetically related to MCR subunits of the *Methanosarcinales* and could be assigned to ANME-1 and ANME-2 archaea. Moreover, proteins could be purified from ANME-1 dominated methanotrophic mats fueled by AOM (Krüger *et al.* 2003). The dominant protein consisted of three subunits with N-terminal amino acid sequences matching those of the retrieved genes. This protein harbored a nickel factor which was apparently a heavier (951 Da) variant of factor F_{430} (905 Da), the unique nickel porphinoid in MCR (Thauer 1998). These studies show that ANME archaea

may catalyze the initial reaction of AOM by an enzyme which shares an evolutionary origin with MCRs in methanogenic archaea, but has been optimized for 'reverse methanogenesis'.

2.3 Sulfate Reduction

In marine sediments the most important anaerobic degradation process of organic matter is the dissimilatory sulfate reduction mediated by sulfate-reducing bacteria (Jørgensen 1982a). This is mainly due to high concentrations of sulfate which are transported into the seafloor by penetrating seawater (28 mM sulfate). Concentrations of sulfate at the sediment-water interface are more than 50 times higher as all other electron acceptors with higher standard free energies such as oxygen, nitrate, iron, and manganese (D'Hondt et $al.$ 2002).

Dissimilatory sulfate reduction can be described by the following net equation (Kasten & Jörgensen 2000):

$$2\ CH_2O + SO_4^{2-} \rightarrow 2\ HCO_3^- + H_2S \qquad\qquad (5)$$

The reduction of sulfate to sulfide is an eight-electron reduction and proceeds through a number of intermediate stages. Sulfate has first to be activated by means of ATP. The enzyme ATP sulfurylase catalyzes the attachment of the sulfate ion to a phosphate of ATP leading to the formation of adenosine phosphosulfate (APS). The sulfate in APS is subsequently reduced to sulfite by the enzyme APS reductase with the release of AMP. Once sulfite is formed, sulfide is produced by the enzyme sulfite reductase. During this process electron transport reactions occur leading to proton motive force formation which drives ATP synthesis by an ATP synthase (Madigan & Martinko 2006).

Estimates of the overall significance of dissimilatory sulfate reduction for the degradation of organic matter suggest that the combined processes of aerobic respiration and sulfate reduction account for most of the organic carbon oxidation. In reducing habitats sulfate reduction can be the dominant pathway of organic carbon oxidation (Kasten & Jörgensen 2000). As discussed above, sulfate reduction is also the dominant process in the anaerobic oxidation of methane (Boetius et $al.$ 2000, Nauhaus et $al.$ 2002) and other hydrocarbons (Zengler et $al.$ 1999, Joye et $al.$ 2004). The sulfide produced by sulfate reduction can be utilized by sulfur-oxidizing, chemoautotrophic communities.

2.4 Oxidation of Sulfide

The oxidation of sulfide (SOx) is a process that requires the coexistence of sulfide and oxygen or nitrate (Jørgensen 1982b, Fossing et $al.$ 1995b). Such interface environments are the

chemocline of stratified water bodies (e.g. Black Sea, meromictic lakes), marine or limnic sediments where the accumulation of organic matter has led to intensive sulfide production, and hydrothermal vents where sulfide-rich, reduced fluids are emitted. The spectacular high biomass of sulfur-based chemosynthetic communities at cold seeps has been an enigma for a long time, as known sources of sulfide which would provide a sufficient high flux of sulfide (e.g. hydrothermal venting) were absent. Today it is known that sulfide is generated as an end-product of sulfate-dependent AOM in the anoxic layers of the sediment (see above). The microbially mediated SOx has been shown to be three orders of magnitude faster than the spontaneous chemical oxidation at neutral pH (Nelson *et al.* 1986). Microorganisms use also other common reduced sulfur compounds such as elemental sulfur or thiosulfate as electron donors (reactions 6-9). The final product of sulfur oxidation is in most cases sulfate. The oxidation of sulfide, which is the most reduced sulfur compound, takes place in stages (Fig. 2). The first oxidation step leads to the formation of elemental sulfur which is stored internally by many sulfur-oxidizing bacteria. The oxidation of elemental sulfur can bridge periods when sulfide is not available (Madigan & Martinko 2006).

$$H_2S + 2\ O_2 \rightarrow SO_4^{2-} + 2\ H^+ \qquad \Delta G^0 = \text{-798.2 kJ/ reaction} \qquad (6)$$

$$HS^- + \tfrac{1}{2}\ O_2 + H^+ \rightarrow S^0 + H_2O \qquad \Delta G^0 = \text{-209.4 kJ/ reaction} \qquad (7)$$

$$S^0 + H_2O + 1\ \tfrac{1}{2}\ O_2 \rightarrow SO_4^{2-} + 2\ H^+ \qquad \Delta G^0 = \text{-587.1 kJ/ reaction} \qquad (8)$$

$$S_2O_3^{2-} + H_2O + 2\ O_2 \rightarrow 2\ SO_4^{2-} + 2\ H^+ \qquad \Delta G^0 = \text{-818.3 kJ/ reaction} \qquad (9)$$

The central intermediate during the oxidation of sulfide, elemental sulfur, and thiosulfate is sulfite. Sulfite can be subsequently oxidized to sulfate in two ways. The most widespread pathway employs the enzyme sulfite oxidase which transfers directly electrons from sulfite to cytochrome c. Thereby, a proton motive force is generated from electron flow in the membrane and ATP is synthesized by membrane bound ATP synthases. The other pathway involves the reverse activity of adenosine phosphosulfate (APS) reductase, an enzyme which is essential for sulfate-reducing bacteria. During the oxidation of sulfite to sulfate, AMD is converted to ADP. Carbon is fixed autotrophically via the Calvin cycle. The electrons required for this process come from reverse electron flow. Some microorganisms can use nitrate as an alternative electron acceptor under anoxic conditions (Madigan & Martinko 2006). Famous examples are the large vacuolated sulfide oxidizers *Beggiatoa*, *Thioploca* and *Thiomargarita* (Fossing *et al.* 1995b, McHatton *et al.* 1996, Schulz *et al.* 1999).
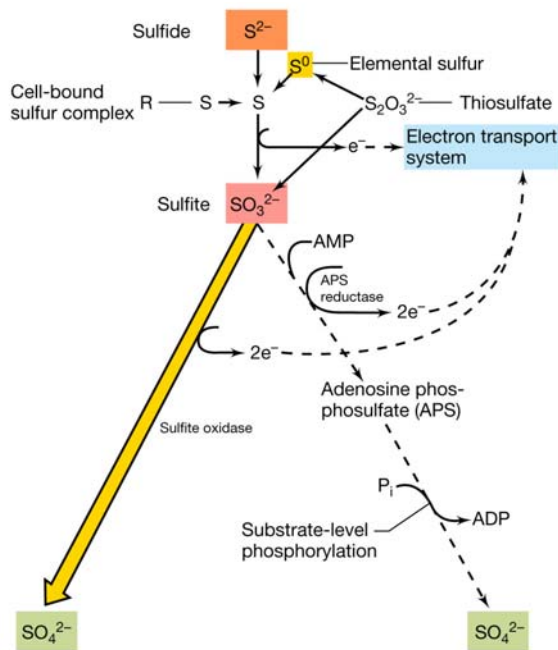
Figure 2 Oxidation of reduced sulfur compounds by sulfur-oxidzing bacteria (from Madigan & Martinko 2006).

2.5 Aerobic Oxidation of Methane

The microbially mediated aerobic oxidation of methane (MOx) takes place in habitats where methane and oxygen are concurrently available. In limnic systems most of the methane, which is produced in the anoxic zone of the sediments by organic matter degradation, reaches the oxic zones and is oxidized aerobically. In contrast, in marine systems most of the methane is already oxidized anaerobically in the sulfate-penetrated sediments before it reaches oxic zones. Moreover, the penetration depth of oxygen is very limited in methane-rich marine sediments (Wenzhofer & Glud 2002), because oxygen is often already depleted in the top millimeters due to the microbial degradation of organic matter (Fig. 3). Hence, microniches supporting the MOx are very restricted in marine sediments and the aerobic oxidation of methane is only a minor sink for methane in the ocean.
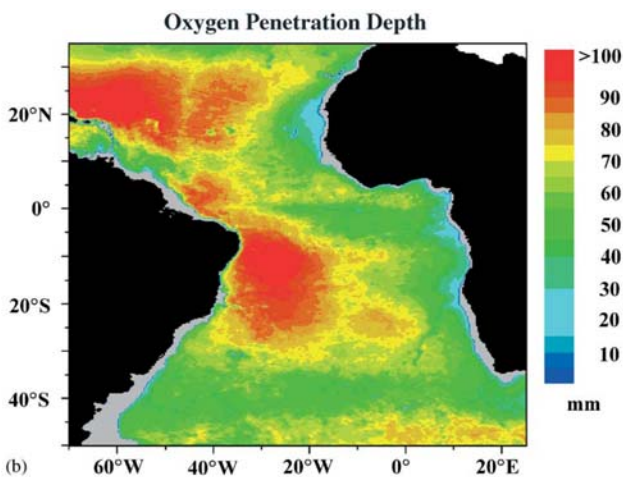
Figure 3 Estimated oxygen penetration depth in the Atlantic (from Wenzhofer & Glud 2002).

The first methane-oxidizing (methanotrophic) bacterium was isolated in 1906 by Söhngen (Söhngen 1906), and until today many methanotrophic strains were isolated. Since pure cultures are available, the biochemical pathway of the MOx has been resolved completely (Fig. 4). The initial oxidation of methane is catalyzed by a class of enzymes called methane monooxygenases. Methane monooxygenases utilize two reduction equivalents, which come from cytochrome c, to split the O-O bonds of dioxygen. One of the oxygen atoms is reduced to H_2O, and the other is incorporated into methane to form methanol. Due to the activity of dehydrogenases, methanol is subsequently oxidized to formaldehyde, formate, and CO_2 as end products (Hanson & Hanson 1996). Typical redox cofactors such as quinones or NADH are reduced in these oxidation steps and enter the electron transport chain. A proton motive force is established from electron flow in the membrane and fuels ATP generation by membrane bound ATP synthases (Madigan & Martinko 2006). In the presence of copper all methanotrophic bacteria express the particulate form of methane monooxygenase (pMMO), and thus the presence of this enzyme or its gene can be used as a functional marker for methanotrophy. Under copper-limited conditions some methanotrophs are able to synthesize a soluble form of the methane monooxygenase (sMMO).

The oxidation of methane with oxygen is highly exergonic (reaction 10) and aerobic methanotrophs are characterized by fast growth.

$$CH_4 + 2\ O_2 \rightarrow CO_2 + 2\ H_2O \qquad \Delta G^0 = \text{-773 kJ/reaction} \qquad (10)$$
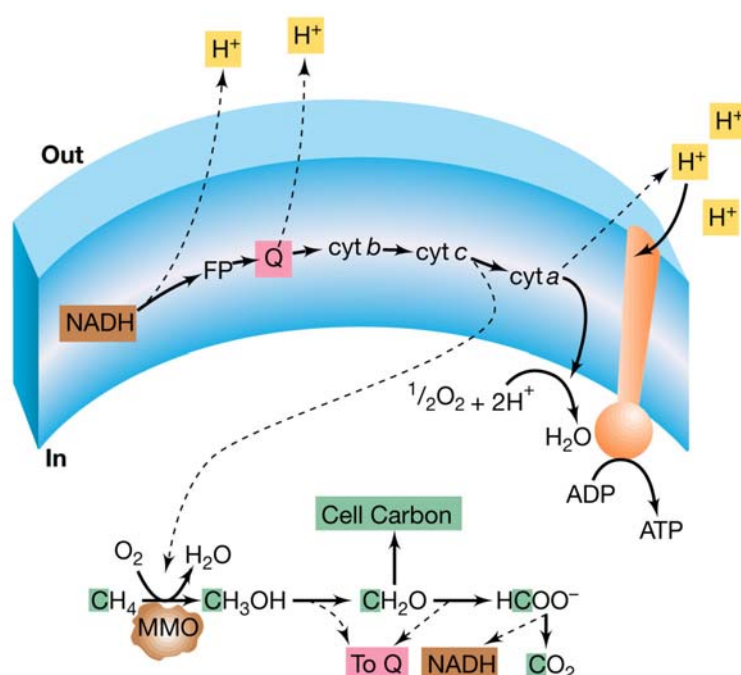
Figure 4 Oxidation of methane by aerobic methanotrophic bacteria. MMO, methane monooxygenase; FP, flavoprotein; cyt, cytochrome; Q, quinine. Although not depicted as such, MMO is a membrane-associated enzyme (from Madigan & Martinko 2006).

Carbon is assimilated into biomass by two distinct mechanisms, the ribulose monophosphate (RuMP) pathway or the serine pathway (Hanson & Hanson 1996). The RuMP pathway is more efficient as formaldehyde delivers all carbon atoms for cell material. Moreover, formaldehyde is already at the same oxidation level and thus no reducing power is needed. In contrast, the serine pathway is fueled by acetyl-CoA which is synthesized by one molecule formaldehyde and one molecule CO_2. This pathway needs more energy in form of ATP and additionally reducing power.

2.6 Oxidation of other reduced elements

In some reducing environments, especially hydrothermal vent systems, vast amounts of reduced substances such as hydrogen, iron, manganese, and ammonium are emitted. The microbial oxidation of these compounds plays an important role in these ecosystems (Reysenbach & Shock 2002 and literature therein). These biogeochemically complex processes are not further discussed here as they were not a focus of this thesis.

3   Key Players at Reducing Habitats

In the following, I introduce those microorganisms and symbiotic associations which represent the key players at cold seep systems and other reducing habitats, with the focus on those that I studied in my thesis. Other important key players in reducing habitats include denitrifiers, a variety of metal oxidizers and reducers, and methanogens, but these groups were not subject of this study.

3.1 Anaerobic Methane-Oxidizing Archaea

Methanotrophic archaea (ANME) associated with sulfate-reducing bacteria in AOM mediating consortia have been identified with culture-independent methods. Highly ^{13}C-depleted archaeal biomarkers (crocetane, archaeol, hydroxyarchaeol, pentamethylicosane [PMI]) were detected in active cold seep sediments (e.g. Elvert *et al.* 1999, Hinrichs *et al.* 1999, Pancost *et al.* 2000, Thiel *et al.* 2001). Lipid biomarkers of methanotrophic archaea often display δ^{13}C values of -100‰ and lower showing that these archaea eventually derived their carbon from methane. Additionally, isotopic light bacterial lipids that are commonly found in sulfate-reducing bacteria were detected with δ^{13}C between -50‰ and -100‰ (Hinrichs *et al.* 2000, Hinrichs & Boetius 2002). The depletion in ^{13}C relative to the source methane shows that these bacteria incorporated methane-derived carbon too. 16S rRNA gene

sequences belonging to ANME have been obtained from many methane-rich, marine habitats but not from any other aquatic environment (Fig. 5). Two archaeal clades were most frequently found, ANME-1 and ANME-2. FISH surveys confirmed that these sequences originated from cells in microbial consortia that are associated with sulfate-reducing bacteria (Fig. 6) (Boetius *et al.* 2000). Recently, Orphan (Orphan *et al.* 2001b) established a method that combines FISH and secondary ion mass spectroscopy, and showed that the biomass of ANME-1, ANME-2 and their sulfate-reducing partners is highly depleted in ^{13}C.
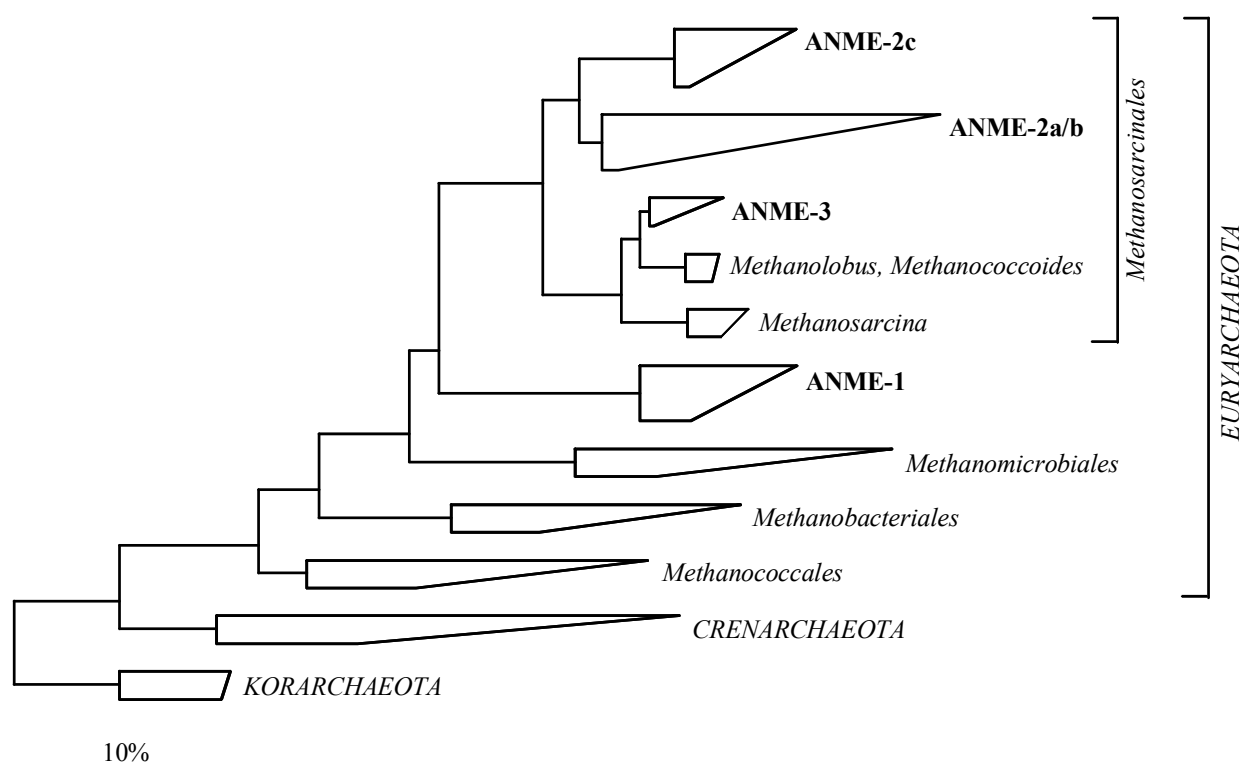
Figure 5 Phylogenetic tree based on 16S rRNA phylogeny showing the affiliations of ANME archaea with other major groups of the domain *Archaea*.

ANME-1 archaea are distantly related to *Methanosarcinales* and *Methanomicrobiales* and have been found to be associated with SRB of the *Desulfosarcina-Desulfococcus* branch (DSS) in microbial mats (Michaelis *et al.* 2002, Knittel *et al.* 2005). These methanotrophic mats form microbial reefs fueled by AOM that were found in the Black Sea above methane seeps. ANME-1 archaea were one major component of the mats and make up 10-45% of the total microbial biomass. Moreover, ANME-1 were frequently detected in deeper layers of cold seep sediments, where they occur as single cells (Orphan *et al.* 2001b, Knittel *et al.* 2005, Orcutt *et al.* 2005) and aggregated cells (Orphan *et al.* 2002, Orcutt *et al.* 2005). It is

intriguing that single ANME-1 cells without close contact to SRB were detected. So far, it is not known whether single ANME-1 cells interact with free-living SRB to perform AOM or ANME-1 cells are capable to oxidize methane without a bacterial partner. The sulfate-reducing archaeon *Archaeoglobus fulgidus* possesses almost all genes necessary for methanogenesis (Klenk *et al.* 1997), thus it might be possible that one organism combines the metabolic capabilities of methane oxidation and sulfate reduction.

ANME-2 archaea are more closely related to *Methanosarcinales* than ANME-1 and form structured microbial consortia with sulfate-reducing DSS (ANME-2/DSS). ANME-2/DSS consortia were the first AOM mediating microbial consortia which were microscopically visualized (Boetius *et al.* 2000). The consortia were discovered in surface sediments of Hydrate Ridge overlying gas hydrates. Up to 90% of the microbial biomass (1.4×10^{10} cells/ml) in the surface sediments was comprised by ANME-2/DSS consortia. An average consortium from Hydrate Ridge consists of a core of 100 archaeal cells surrounded by a shell of 200 bacterial cells.
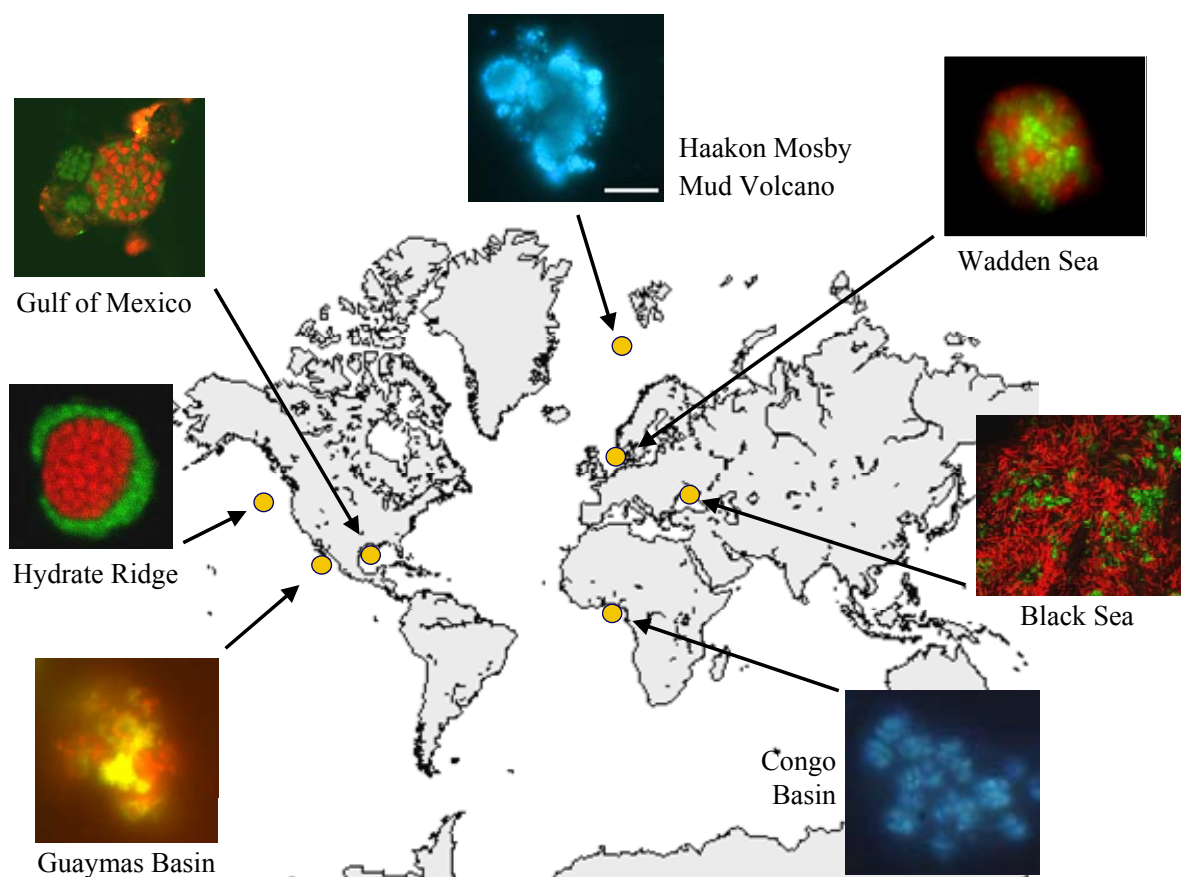
Figure 6 Epifluorescence micrographs of AOM mediating consortia from cold seep habitats. Archaeal cells are stained with probes specific for ANME archaea (shown in red). Bacterial cells are stained with probes specific for *Deltaproteobacteria* (shown in green). Cells of consortia from the Congo Basin and the Haakon Mosby Mud Volcano are stained with DAPI (shown in blue). Pictures provided by K. Knittel and K. Ishii.

Recent work at an Arctic mud volcano has shown that there are environments that are dominated by a third type of ANME group which has not been recognized before (Lösekann 2002). This novel group was designated ANME-3 and is closely related to *Methanococcoides* species. ANME-3 archaea form structured shell-type consortia and are specifically associated with SRB of the *Desulfobulbus* branch (ANME-3/DBB).

At cold seeps AOM consortia build up huge amounts of biomass that is supported by methane-based chemosynthesis in the absence of molecular oxygen. Thus, AOM microorganisms may be the microbial key players around 2.7 Gyr ago, when methane was stable in marine habitats and the increased oxygenation of Earth resulted in favorable sulfate concentrations (Hinrichs & Boetius 2002).

3.2 Sulfate-Reducing Bacteria

Sulfate-reducing bacteria (SRB) play a key role in anaerobic degradation of organic matter and are abundant in anoxic, marine sediments. Sulfate reducers are a polyphyletic group of microorganisms. Most SRB are affiliated with the *Deltaproteobacteria* and found in twelve genera. Moreover, some SRB belong to deep-branching, thermophilic lineages of *Nitrospirae (Thermodesulfobacterium, Thermodesulfovibrio)*, to the *Firmicutes (Desulfotomaculum, Desulfosporosinus)*, and to the *Archaea (Archaeoglobus, Caldivirga)*. All SRB have as a common feature the ability to use sulfate as terminal electron acceptor (Rabus *et al.* 2002). The range of electron donors utilized by SRB is fairly broad including a great variety of low molecular mass compounds from the fermentative breakdown of organic matter. Some specialized SRB can utilize hydrocarbons, even crude oil (Harms *et al.* 1999, Joye *et al.* 2004, Orcutt *et al.* 2005).

At cold seeps several seep-endemic clades of sulfate-reducing *Deltaproteobacteria* have been identified designated as SEEP-SRB1 (*Desulfococcus/Desulfosarcina* rel.), SEEP-SRB2 (unaffiliated), SEEP-SRB3 (*Desulfobulbus* rel.), and SEEP-SRB4 (*Desulforhopalus* rel.) all of which are only distantly related to cultivated species (Knittel *et al.* 2003).

Single cells of the *Desulfococcus/Desulfosarcina* branch are widespread in marine, anoxic environments and cold seep sediments and reach high numbers *in situ* (e.g. Llobet-Brossa *et al.* 1998, Sahm *et al.* 1999b, Ravenschlag *et al.* 2000, Knittel *et al.* 2003, Mussmann *et al.* 2005). The high abundance in various habitats underlines the importance of this versatile group. SEEP-SRB1 of the *Desulfococcus/Desulfosarcina* represents the group which is associated with ANME-2 in AOM mediating consortia (Knittel *et al.* 2003) and also occurs as partner of ANME-1 (Michaelis *et al.* 2002). Very ^{13}C-depleted specific fatty acids which are

likely derived from SEEP-SRB2, SEEP-SRB3, and SEEP-SRB4 suggest that these seep-specific groups are also involved in the process of AOM.

3.3 Sulfide-Oxidizing Bacteria

Little is known about the diversity and abundance of sulfide-oxidizing bacteria (SOB) in the ocean. Mainly, the large, colorless SOB including the gliding and non-gliding filamentous forms of *Beggiatoa*, *Thiothrix,* and *Thioploca,* as well as *Thiomargarita* have been studied. They attracted much attention in the past due to their size and the high amounts of biomass they build up at oxic-anoxic interfaces (Fig. 7). Other important sulfide oxidizers found at vents and seeps belong to the genus *Arcobacter*. These vibrio-shaped *Epsilonproteobacteria* produce large amounts of sulfur precipitates which look like cotton balls (Wirsen *et al.* 2002). Dense mats of colorless, filamentous SOB or *Arcobacter*-types may form conspicuous white patches on the seafloor that are known from many reducing habitats including hydrothermal vents, cold seeps, upwelling areas, and productive shallow water areas (Fossing *et al.* 1995b, Gallardo *et al.* 1995, Jannasch *et al.* 1989, Jörgensen 1977b, Larkin & Henk 1996, Sahling *et al.* 2002). Since organic carbon input is low at hydrothermal vent and cold seeps, mats of SOB are an important food source for the local fauna.

All large SOB (diameter >4 µm) can bridge periods of reduced sulfide supply by oxidizing internal sulfur inclusions as long as oxygen is available. An additional adaptation to changing environmental conditions is the presence of intracellular vacuoles for storage of nitrate which is used during anoxic periods as alternative electron acceptor. The large vacuole accounts for up to 98% of the cell volume and gives the cells a hollow appearance.
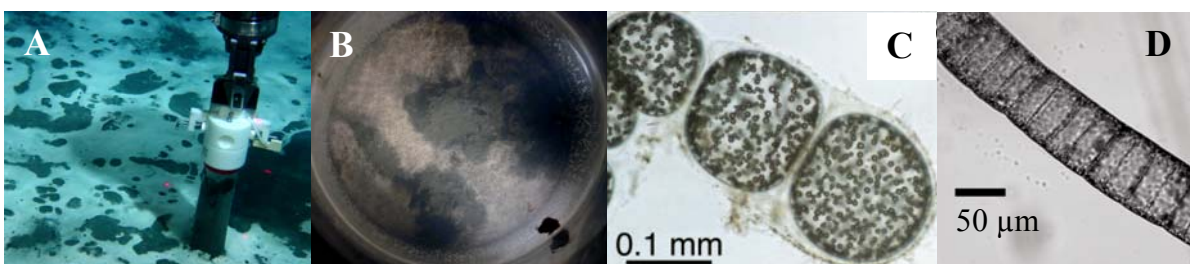
Figure 7 Colorless sulfur-oxidizing bacteria. (A) Sampling of white bacterial mats at the Haakon Mosby Mud Volcano (MPI Bremen, Ifremer). (B) Sediment core from Hydrate Ridge with *Beggiatoa* mat on the sediment surface. (C) Light micrograph of typical *Thiomargarita* chain (from Schulz *et al.* 1999). (D) Light micrograph of filamentous *Beggiatoa* species (from Kalanetra *et al.* 2004).

In the past, the genera of large, filamentous SOB were recognized on the basis of phenotypic characters, e.g. *Beggiatoa* species were differentiated by the width of their filaments (Larkin 1983). Although molecular tools are now available to examine the phylogeny of microorganisms based on the comparative analysis of their 16S rRNA genes, only a limited number of sequences has been deposited in the public databases. It seems likely that the diversity of SOB is currently underestimated and that many new strains remain to be discovered. Available 16S rRNA sequences show, that *Beggiatoa* and *Thioploca* are members of the same clade of *Gammaproteobacteria*, while *Thiotrix* form a separated lineage (Teske *et al.* 1999) (Fig. 8).
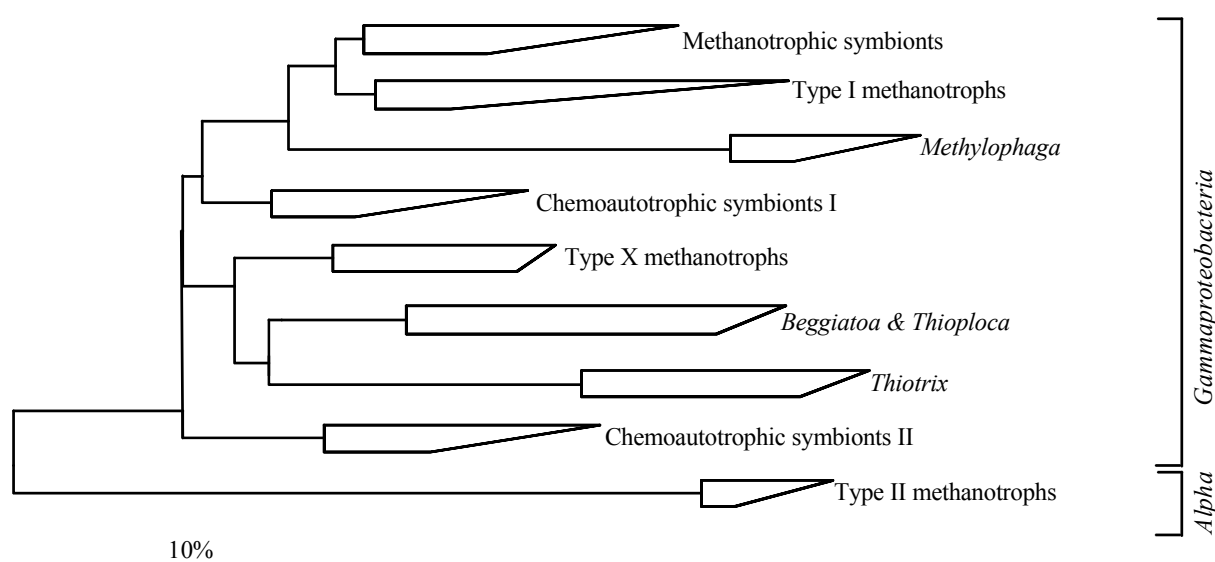
Figure 8 Phylogenetic tree based on 16S rRNA phylogeny showing the placement of free-living and symbiotic clades of methanotrophic and sulfur-oxidizing bacteria within the *Gammaproteobacteria*. Type II methanotrophs are used as outgroup and belong to the *Alphaproteobacteria*.

SOB can be traced in the environment through their unique lipid biomarker signatures. Several studies suggest that fatty acids such as 16:1ω7 and 18:1ω7 are diagnostic for sulfur-oxidizing bacteria in reducing marine sediments (Jacq *et al.* 1989, McCaffrey *et al.* 1989, Guezennec & Fiala-Medioni 1996, Zhang *et al.* 2005).

3.4 Aerobic Methane-Oxidizing Bacteria

The ability to oxidize single carbon (C_1-) substrates is unique to a group of microorganisms called methylotrophic bacteria. A subgroup of methylotrophs, the methane-oxidizing (methanotrophic) microorganisms, is able to use methane as electron donor and sole carbon source. Methanotrophic bacteria are obligate aerobes and rely on the presence of molecular

oxygen for the initial oxygenation of the chemically stable methane molecule (Madigan & Martinko 2006). They are widespread in aquatic and terrestrial environments, where methane and oxygen are concurrently available, and inhabit oxic-anoxic transition zones (Hanson & Hanson 1996). They thrive as free-living cells in the oxic water column, at the oxic sediment-water interface, or in symbiotic associations with marine invertebrates. All aerobic methanotrophs show the ability to form resting stages such as cysts or endospores which enable them to survive even long periods of anoxia or without methane.

Methanotrophic bacteria form two major groups based on their internal cell structure, phylogeny, and carbon assimilation pathway. Type I methanotrophs possess bundles of disc-shaped vesicle throughout the cell and use the ribulose monophosphate (RuMP) pathway for carbon assimilation (Madigan & Martinko 2006). Based on 16S rRNA phylogeny, type I methanotrophs are represented by the family *Methanococcaceae* of *Gammaproteobacteria* including the genera *Methylobacter, Methylomonas, Methylomicrobium,* and *Methylosphaera* (Garrity *et al.* 2001). A subgroup of type I methantrophs designated type X belongs also to the *Gammaproteobacteria* and includes the genera *Methylococcus* and *Methylocaldum.* They use both the RuMP and the serine pathway for carbon assimilation, grow at higher temperatures, and possess DNA with a higher G+C content than most of the type I methanotrophs (Hanson & Hanson 1996). In contrast, the membrane system of type II methanotrophs consists of paired membranes that run along the periphery of the cell. They use the serine pathway for carbon assimilation (Madigan & Martinko 2006). All type II methanotrophs belong to the *Alphaproteobacteria* and are represented by the family *Methylocystaceae* including the genera *Methylocystis, Methylopila, and Methylosinus* (Garrity *et al.* 2001).

When methane escapes from the anoxic zones of seep sediments, aerobic methanotrophs can reach locally high abundances (Durisch-Kaiser *et al.* 2005) and show high rates of activity (Valentine *et al.* 2001). In addition to FISH probes that are specific for aerobic methanotrophs (Eller *et al.* 2000, Gulledge *et al.* 2001), lipid biomarkers are useful environmental markers for the presence and identification of aerobic methanotrophs. In type I and type X methanotrophs fatty acids with 16 carbon atoms such as 16:1ω8c are most abundant, whereas in type II methanotrophs mainly fatty acids with 18 carbon atoms such as 18:1ω8c are found (Hanson & Hanson 1996).

3.5 Symbiont-Bearing Invertebrates

Symbiotic associations with chemoautotrophic, sulfur-oxidizing and methanotrophic bacteria occur in a wide taxonomic range of invertebrates which live in reducing environments at

redox boundaries where reduced compounds and oxygen are present in close proximity (Felbeck *et al.* 1981, Childress *et al.* 1986, Fisher 1990, Feldman *et al.* 1998). In these symbioses bacteria have a better access to reduced compounds such as methane or sulfide and to oxidants enabling them to fix CO_2, while the eukaryotic hosts acquire carbon from the symbionts either through translocation of nutrients or direct digestion of bacteria.

The morphology of the symbioses varies widely as might be expected from the diverse phylogenetic origins of the hosts. However, a common characteristic is that in all host species the digestive system is absent or reduced in function. Thus, the bacterial population is the primary means of carbon acquisition given the inability of the host to feed on particulate organic matter. Until today pure cultures of symbionts are not available and much of what is known about the symbionts is based on the study of intact symbioses by transmission electron microscopy, radiotracer experiments, stable carbon isotope signatures, and enzyme activity assays.

Sulfur-based symbioses are by far the most common chemosynthetic symbioses known to date (Nelson & Fisher 1995). Chemoautotrophic sulfur-oxidizing symbionts oxidize reduced sulfur compounds and use the energy gained for autotrophic carbon fixation. Methane-based symbioses are only found in very few metazoan species, although the oxidation of methane and sulfide yields similar free energies. Constraints on methane-based symbioses are most likely linked to the concentration of methane in the environment or its biological availability. Many host species have evolved abilities to bind sulfide and concentrate it above ambient levels, whereas such capabilities are not known for methane.

Cold seeps are mainly populated by symbiont-bearing bivalve clams *(Thyasiridae, Vesicomyidae, Lucinidae, Solemyidae)*, bathymodiolid mussels *(Mytilidae)*, and tube-dwelling annelids *(Siboglinidae)* (Sibuet & Olu 1998). Members of the familiy *Siboglinidae* include vestimentiferan tubeworms found at hydrothermal vents (e.g. *Riftia pachyptila*) and cold seeps (e.g. *Lamellibrachia* spp.), as well as frenulate and moniliferan tubeworms (e.g. *Siboglinum* spp., *Sclerolinum* spp.) which mainly inhabit sedimentary non-seep environments (Fig. 9). Most siboglinids harbor chemoautotrophic, sulfur-oxidizing symbionts. The only exception is the species *Siboglinum poseidoni* which harbors methanotrophic symbionts (Schmaljohann & Flügel 1987). Symbiotic cells are embedded in a specialized interior tissue called the trophosome which is the main tissue in the trunk of these animals. Sulfide from the environment is transported to the symbionts with the blood. Sulfide is extremely poisonous to aerobic eukaryotic organisms because of the inhibition of cytochrome c oxidase and the conversion of hemoglobin to sulfhemoglobin which is unable to

carry oxygen. To circumvent the toxic effects of sulfide, siboglinids have evolved unique hemoglobin which is able to bind sulfide tightly. This binding is reversible, allowing transport from the outside medium to the symbionts and preventing release into the host tissue. In addition, the blood is able to concentrate sulfide above ambient levels (Felbeck & Distel 2002).

Most clams and mussels (e.g. *Calyptogena* spp., *Acharax* spp.; Fig. 9) harbor chemoautotrophic, sulfur-oxidizing symbionts inside of specialized gill cells where they are in close contact with the surrounding seawater. These animals typically concentrate sulfide through their foot which is in contact with reduced fluids. Toxic effects of sulfide are prevented by the presence of sulfide-binding transport proteins other than hemoglobin or by the activity of sulfide oxidases which transform sulfide to the less toxic form of thiosulfate (Felbeck & Distel 2002). Symbiotic associations with methanotrophic bacteria have been also described for species of deep-sea mussels of the genus *Bathymodiolus* (reviewed in DeChaine & Cavanaugh 2005). Moreover, dual symbioses have been reported in some species of bathymodiolid mussels which harbor chemoauotrophic, sulfur-oxidizing symbionts and methanotrophic symbionts.
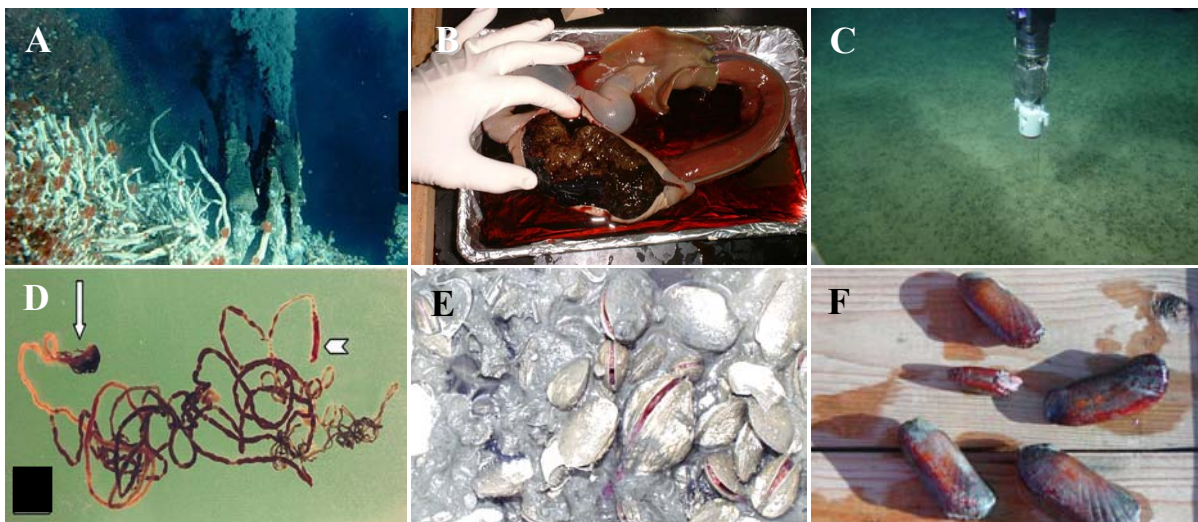
Figure 9 Symbiont-bearing invertebrates. (A) Hydrothermal vents with colonies of vestimentiferan tubeworms (from www.cascadia.ctc.edu). (B) Dissection of the giant vestimentiferan tubeworm *Riftia pachyptila* exposing the symbiont-bearing trophosome tissue (from www.ocean.udel.edu). (c) Sediments populated with frenulate and moniliferan tubeworms at the Haakon Mosby Mud Volcano (MPI Bremen, Ifremer). (D) Frenulate tubeworm *Oligobrachia mashikoi* removed from its tube (from Sassayama *et al.* 2003). (E+F) *Calyptogena* and *Acharax* specimens sampled at Hydrate Ridge (MPI Bremen, GEOMAR).

Based on 16S rRNA phylogeny, most symbionts belong to the *Gammaproteobacteria* (Fig. 8). Methanotrophic symbionts form a distinct clade which is closely related to type I

methanotrophs. Chemoautotrophic, sulfur-oxidizing symbionts are phylogenetically more diverse, and three major clades became evident so far. Group I contains symbionts from vent and seep vestimentiferan tubeworms as well as symbionts from lucinid, thyasirid, and solemyid clams. Group II contains mainly symbionts from vesicomyid mussels. Symbionts from frenulate tubeworms group into separate lineages and no symbiont sequence from moniliferan tubeworms is available to date.

4 Cultivation-Independent Methods for the Identification of Microorganisms

The overwhelming majority of microbial species (>99%) has not been cultivated in the laboratory yet (Amann *et al.* 1995a). Thus, pure cultures of environmentally abundant species are often not available and the present knowledge of microbial key players is derived from cultivation-independent techniques. In the following, the most important cultivation-independent methods will be briefly introduced.

4.1 The Full Cycle rRNA Approach

The rRNA of the ribosomal small subunit is currently the molecule of choice for microbial molecular systematic studies. To assess the microbial diversity of complex environmental samples, DNA is extracted and 16S rRNA genes are amplified by specific primers followed by cloning and sequencing. Comparative sequence analysis with existing 16S rRNA gene databases facilitates the identification of known and unknown species in the environment. 16S rRNA gene libraries can address the question "who's out there?", but offer very limited information about the *in situ* abundance and ecological niches of individual microorganisms.

The fluorescence *in situ* hybridization (FISH) with rRNA targeted oligonucleotide probes is the complementary method to 16S rRNA cloning and closes the cycle of the rRNA approach (Amann *et al.* 1995a). FISH permits the identification and quantification of single microbial cells in their natural environment. Moreover, interspecies associations such as microbial consortia can be visualized. The availability of comprehensive 16S rRNA databases which contain currently 300,000 sequences of 16S rRNA genes (GenBank, February 2006), permits the design of nucleic acid probes that are specific for groups of microorganisms ranging from phyla to individual species. FISH probes are complementary to sequences on the 16S rRNA in the target cells and carry a fluorescent dye. Upon *in situ* hybridization, the probes bind specifically to the rRNA in the target cells by complementary base pairing. Positive, hybridized cells can then be visualized by epifluorescence microscopy.

4.2 Lipid biomarkers

An additional tool for the cultivation-independent identification of microorganisms is the analysis of lipid biomarkers. Archaeal and bacterial cells differ with respect to the structure of their cell membrane lipids. Typical archaeal biomarkers are characterized by isoprenoid chains and ether linkages, whereas bacterial biomarkers are fatty acids with ester linkages. The specific composition of lipid biomarkers in a given environment can be used to identify and quantify certain microbial groups. Moreover, the stable carbon isotopic signature of biomarkers bears information about the carbon source they were synthesized from. In biologically mediated processes, the heavy isotope ^{13}C is discriminated against ^{12}C leading to a significant ^{13}C-depletion of the lipid biomass compared to the source. The ratio of $^{13}C/^{12}C$ is given as $\delta^{13}C$-value compared to the 'Pee Dee Belemnite' standard is highly negative for methane of microbial origin (-110‰ to -50‰), whereas the value for thermogenic methane is less negative (-50‰ to -20‰) (Whiticar 1999). The effect of kinetic isotope fractionation is especially useful to track carbon derived from isotopically light sources such as methane. When methane is incorporated into microbial biomass, the stable carbon isotope composition of biomarkers extracted from these microorganisms is very light with values diagnostic for methanotrophy. The typical fractionation factor for AOM is -50 to -60‰ (Hinrichs & Boetius 2002 and literature therein).

4.3 Metagenomics

Environmental genomic studies provide insights into the metabolic potential of uncultured microorganisms. This approach involves the extraction of high molecular weight DNA from an environmental sample. The recovered 'metagenome' is subsequently cloned into small- or large-insert vectors without prior PCR amplification. Sequence analyses of metagenomic libraries allow the reconstruction of metabolic pathways and might also aid enrichment and cultivation efforts of yet uncultivated microorganisms (Tyson & Banfield). So far, metagenomic studies have focused on pelagic habitats, because sediments still pose a lot of practical and technological problems to the methods involved. The first metagenomic study including a whale fall as reducing habitat shows distinct genetic characteristics for this environment compared to other marine samples and soils (Tringe *et al.* 2005).

5 Thesis Outline

Cold seeps are fascinating deep-sea ecosystems which support complex chemosynthetic communities. During the last years new insights were gained into the identity of the microbial players responsible for key biogeochemical processes at cold seeps such as free-living and symbiotic chemoautotrophic sulfur oxidizers as well as anaerobic methanotrophs. However, quantitative data of their *in situ* distribution is often lacking. For a comprehensive understanding of the ecosystem functioning at cold seeps, an integrated approach including identification and quantification of microbial communities combined with activity measurements and the geochemical characterization of the habitat is essential.

In this thesis I used 16S rRNA-based molecular methods to identify and quantify microbial communities at two cold seeps and collaborated with scientists from other disciplines to correlate my molecular results with biogeochemical, geological, and physical data sets.

For each study site, the following questions were of particular interest:

· Which key microbial players are present?

· How abundant are they?

· What environmental factors may control their distribution?

· Do surface and subsurface communities differ from each other?

· What environmental factors may select the dominating phylotypes?

· Are there interspecies associations?

One study site was the Haakon Mosby Mud Volcano (HMMV), a cold seep located in the Arctic Ocean. Already during my master thesis in 2002 I found the first evidence that the HMMV hosts multiple methanotrophic guilds in distinct habitats which differed in various geochemical parameters. Thus, the HMMV is an interesting habitat to study the diversity and community composition of microbial communities and to determine those parameters which control their distribution. In the framework of a German/French collaboration program new samples were obtained from the HMMV in 2003. I completed the data sets which were obtained during my master thesis and confirmed the preliminary results. Moreover, I investigated the microbial communities in habitats which have not been described before such as bacterial mats and subsurface sediments. Furthermore, I characterized the symbioses between bacteria and siboglinid tubeworms which are the dominant megafauna at HMMV.

The second study site was Hydrate Ridge, a cold seep located at the Cascadia Margin coast off Oregon. I participated in a research cruise to Hydrate Ridge in 2002 and sampled shallow subsurface sediments and gas hydrates which are characterized by sulfate limited concentrations. At this time it was unknown whether the same groups of anaerobic methanotrophs (ANME-1, ANME-2) occur in surface sediments, subsurface sediments, and gas hydrates.

B   Results and Discussion

In the following, I summarize the results from each study site investigated in this thesis including those presented in manuscripts as well as those which will be published in collaboration with others. At the end of this section, the data are discussed in a broader context and an outlook for future research on cold seep communities is given.

1 Haakon Mosby Mud Volcano (Barents Sea)

One of the major objectives of this thesis was to identify and quantify the microbial communities in sediments of the Haakon Mosby Mud Volcano (HMMV) by comparative 16S rRNA gene sequence analysis and fluorescence *in situ* hybridizations.

The HMMV is a methane-venting cold seep which is situated at the Norwegian-Barents-Spitzbergen continental margin (72° 00.25'N, 14° 43.50'E) in a water depth of 1,250 m. It is an interesting study site, because the specific geostructure of the HMMV supports multiple types of chemosynthetic communities on a scale of several hundred meters. The mud volcano has a circular zonation (Fig. 10): a) In the center, methane-rich muds and fluids are expelled from the deep geosphere to the seafloor, b) the sediments surrounding the central area are densely covered with bacterial mats of filamentous sulfur-oxidizing bacteria, and c) the outer rim is colonized by siboglinid tubeworms (Pimenov *et al.* 2000).
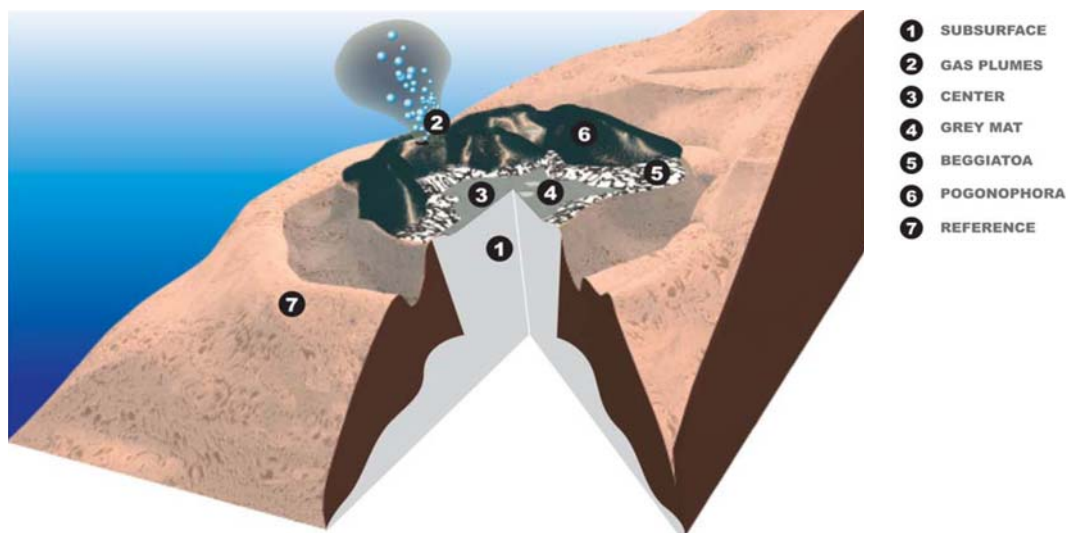
Figure 10. A schematic diagram of the HMMV. The vertical height is exaggerated ca. 50-fold, numbers refer to distinct habitats. 'Beggiatoa' refers to sediments covered with white bacterial mats which primarily consist of *Beggiatoa* species and 'Pogonophora' refers to sediments populated by siboglinid tubeworms. Modified from (Niemann & Lösekann *et al.* subm).

1.1 Methanotrophic Microbial Communities in Surface Sediments

The microbial diversity and community structure of surface sediments were studied in detail at the HMMV. Several sites were examined (Fig. 10): Freshly expelled mud from the volcano center (3) and sediments populated with chemosynthetic communities such as grey bacterial mats (4), white bacterial mats (5), and siboglinid tubeworms (6). Most results summarized in the following sections are presented in detail in publications #1 and #2 of this thesis.

Aerobic Methane-Oxidizing Bacteria

Dense populations of novel aerobic methanotrophic bacteria which are closely affiliated with *Methylobacter* and *Methylophaga* species were found in freshly expelled surface sediments of the volcano center (55 ± 9% of total cells), and to a lesser extent in sediments covered with white bacterial mats (9 ± 2% of total cells). Both habitats are characterized by high methane concentrations over the entire vertical profile (Niemann & Lösekann *et al.* subm) and a limited oxygen penetration depth of a few millimeters (de Beer *et al.* 2006). The HMMV is the first cold seep for which high *in situ* abundance of aerobic methanotrophs could be demonstrated. Anaerobic methanotrophs were not detected at this site. Analyses of biomarkers and rate measurements of methane oxidation are consistent with the 16S rRNA based results. High concentrations of $\delta^{13}C$ depleted (-89‰) bacterial fatty acids (e.g. $C_{16:1\omega8c}$) assigned to *Methylobacter* species were found, whereas archaeal AOM biomarker were below the detection limit. Aerobic methane oxidation rates were high (0.3 µmol cm^{-3} d^{-1}) and AOM activity could not be detected.

These high population densities of aerobic methanotrophs were only found in a thin horizon close to the sediment surface. Aerobic methanotrophs rely on the availability of oxygen as electron acceptor in order to oxidize methane. They are excluded from deeper sediment layers, because these zones are anoxic due to the high flux of oxygen-depleted fluids from below.

The groups of aerobic methanotrophs found in the sediments were also detected in bottom waters above HMMV by FISH but in very low numbers. This finding is consistent with previous studies showing that the aerobic oxidation of methane in the water column above HMMV is of minor significance (Damm & Budéus 2003, Sauter *et al.* 2006). Water currents may facilitate the dispersal of aerobic methanotrophs and may enable them to colonize suitable sedimentary habitats such as the center sediments of HMMV.

Discovery of a New Type of AOM Consortium

A new type of AOM consortium was discovered during the initial characterization of surface sediments at the HMMV (Lösekann 2002). 16S rRNA gene libraries from sediments covered with white bacterial mats (*Beggiatoa* sp.) were dominated by a novel archaeal clade named ANME-3, which belongs to the *Euryarchaeota* and is most closely related to *Methanococcoides burtonii* (93-96%) within the order *Methanosarcinales*. Although the ANME-3 group does not include any cultivated species, it is more closely related to the cultivated genera *Methanosarcina*, *Methanococcoides*, *Methanohalophilus*, and *Methanolobus* than the other two groups so far linked to AOM, ANME-1 and ANME-2. ANME-3 sequences are most similar (93-96%) to *Methanococcoides burtonii*. Single sequences of this archaeal clade were retrieved previously from different seep habitats (Orphan *et al.* 2001a, Knittel *et al.* 2005, S. K. Heijs *et al.*, database release) but were not assigned to a specific AOM consortium. ANME-3 consortia were microscopically visualized for the first time at the HMMV. *In situ* analyses showed that ANME-3 archaea mainly occur in consortium with sulfate-reducing bacteria of the *Desulfobulbus* branch (hereafter ANME-3/DBB, Fig. 11-a/b), but also occurred without physically associated bacteria or were associated with yet unidentified bacteria forming "mixed-type" aggregates (Fig. 11-c). Interestingly, a substantial number of single ANME-3 cells were detected in sediments covered with grey or white bacterial mats at HMMV (Fig. 11-d).
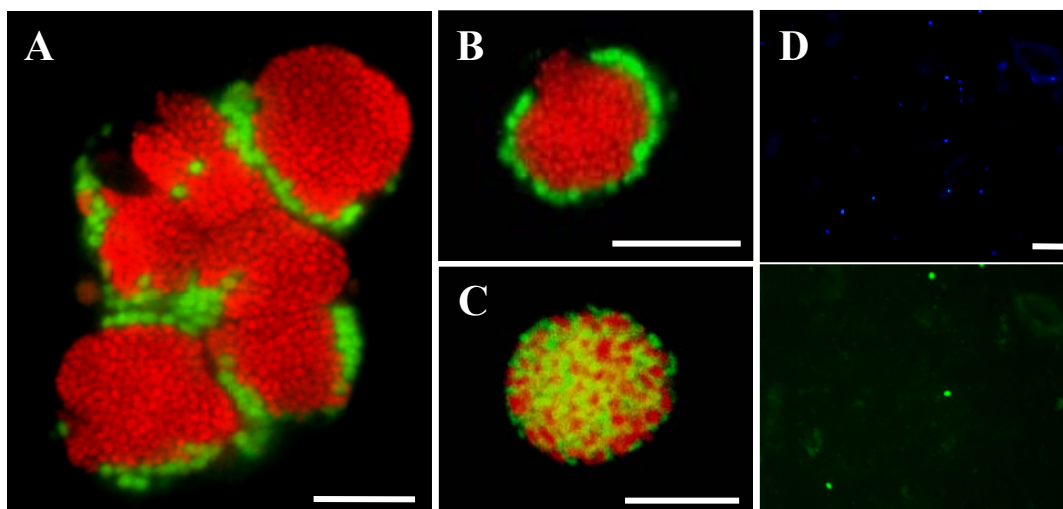
Figure 11. Epifluorescence micrographs of microbial consortia in HMMV surface sediments after *in situ* hybridization with 16S rRNA targeted oligonucleotide probes. (A+B) ANME-3 archaea (red) stained with probe ANME3-1249 and *Desulfobulbus* spp. (green) stained with probe DBB660. (C) ANME-3 archaea (red) stained with probe ANME3-1249 and *Bacteria* (green) stained with probe EUB338 I-III. (D) DAPI staining (blue, upper picture) and single ANME-3 cells stained with probe ANME3-1249 (green, lower picture). Scale bars 10 μm.

The HMMV is the only cold seep known to host a dominant biomass of ANME-3. ANME-1 and ANME-2 were also detected but at most sites in much lower abundance. High AOM rates were measured in the surface sediments directly underlying white bacterial mats and coincided with high numbers of ANME-3/DBB consortia (up to 2×10^7 aggregates/ml). The AOM zone below the white bacterial mats was restricted to 1-4 cm sediments depth due to the limited penetration depth of sulfate from bottom waters into the sediments (de Beer *et al.* 2006). In this zone ANME-3/DBB aggregates accounted for 60-95% of total cells. Furthermore, high concentrations of highly ^{13}C-depleted (-109‰) archaeal lipids could be assigned specifically to ANME-3 and were detected in the same layer (Niemann *et al.* in prep a). AOM rates and biomarker profiles matched perfectly the depth profile of aggregate counts with highest abundance in 1-2 cm sediment depth. These results support the conclusion that ANME-3 archaea are responsible for AOM at HMMV and represent a new type of an AOM mediating consortium.

Close to gas ebullition sites and at the transition from the inner center to the periphery of the mud flows (Fig. 10), circular patches of reduced, gassy sediments of 10-100 cm diameter were found, covered by grey bacterial mats. Total numbers of ANME-2 and ANME-3 aggregates were similar to those in sediments covered with white mats (up to 2×10^7 aggregates/ml). Highest numbers were detected in 2-4 cm sediment depth coinciding with high AOM rates and high concentrations of strongly ^{13}C-depleted ANME specific biomarkers (Niemann *et al.* in prep a). ANME-2 and ANME-3 aggregates coexist at this site (ratio 70:30) indicating that these groups may share similar habitat preferences. *In situ* microsensor profiles showed a sulfide production zone below 2 cm sediment depth and an overlap of oxygen and sulfide in the surface sediments. The sulfide produced in the sediments by AOM supports a diverse thiotrophic community in the grey mats (compare section 1.3). It remains unknown, which geological processes cause the formation of these fragmented habitats for AOM communities in the center of the HMMV. A relatively stable supply of methane and sulfate needs to be available within these sediment patches to build up the observed biomass of the slow-growing AOM populations.

High biomass of anaerobic methanotrophs was only found in zones of few centimeters thickness at both sites covered with bacterial mats. The upper boundary of the AOM zone is determined by the penetration depth of oxygen. ANME archaea are sensitive to oxygen and thus excluded from the upper oxygenated surface layers. The lower boundary of the AOM zone is defined by the thermodynamics of AOM. The available energy for the AOM

mediating microorganisms is lower in deeper layers due to decreasing sulfate concentrations and increasing sulfide concentrations and limits the ANME population density.

ANME cells were also detected in sediments populated by siboglinid tubeworms but in much lower abundance compared to sediments covered with white or grey bacterial mats. Very few ANME-1 cells (max. 1% of total cells) and low numbers of ANME-3/DBB consortia were detected in the surface sediments down to 15 cm depth. The sediments at this site are bioirrigated by the worms which pump seawater deep into the sediments (de Beer *et al.* 2006). Fluid flow rates were considerably lower than in the center or bacterial mat area. Thus, the sulfate/methane transition zone is shifted to deeper sediment horizons and growth of ANME cells is rather limited in the upper sediment layers. Accordingly, AOM and sulfate reduction rates peaked in deeper sediments (below 60 cm depth) coinciding with a subsurface peak of ANME consortia and their specific biomarker lipids. This zone is characterized by the presence of hydrates at around 70 cm, which could have positive effects on the availability of methane and sulfate fluxes. The sulfate supply at this depth could come from the bioirrigation activity of the tubeworms (Cordes *et al.* 2005).

1.2 Microbial Communities in Subsurface Sediments
(data not presented in a manuscript)

The microbial diversity of HMMV subsurface sediments was studied at three sites (Fig. 10): Freshly expelled muds from the volcano center (sample from 465 cm depth), sediments covered with white bacterial mats (sample from 458 cm depth) and sediments populated with siboglinid tubeworms (sample from 410 cm depth). Gas hydrates occurred in fine layers to bulk ice of several cm thicknesses at the HMMV in the outer zone of the center at depths up to 25 cm. The depth of the gas hydrate layer increased to about 2-5 m towards the outer rim of the HMMV populated by tubeworms (Klages *et al.* 2004).

Subsurface sediments of the center and the zone covered with bacterial mats showed very little evidence for microbial activity. At the tubeworm field the AOM zone was shifted to deeper sediment layers and in 70 cm depth elevated AOM rates were measured.

Archaeal diversity was very low in HMMV subsurface sediments and only three lineages became evident at each site (see appendix). All archaeal clone libraries were dominated by sequences of *Crenarchaeota*, namely the marine benthic group C (MBGC; center 67/110 clones, bacterial mat 56/59 clones, tubeworm field 69/105 clones). Sequences of the MBGC were also obtained from hydrate-bearing deep subsurface sediments of the Cascadia Margin (Inagaki *et al.* 2006). However, this group is not exclusively associated with methane

rich habitats as it is also widespread in non-seep sediments (e.g Chandler *et al.* 1998, Vetriani *et al.* 1999, Li *et al.* 1999c, Teske *et al.* 2002; Schäfer *et al.*, database release). From subsurface center sediments, sequences affiliated with *Methanofollis aquaemaris* were also frequently obtained (50/118 clones). Sequences of ANME were only recovered from subsurface sediments of the tubeworm field. These sequences were affiliated with ANME-2a (26/105 clones) and ANME-2c (9/105 clones).

The overall bacterial diversity in the subsurface sediments was higher compared to the archaeal diversity. A detailed overview of obtained clone sequences is given in the appendix. Intriguingly, the bacterial diversity was highest in subsurface sediments of the center. In contrast, the clone libraries of center surface sediments revealed the lowest diversity compared to the sediments covered with bacterial mats and the tubeworm field. As muds are expelled in the center from a deep source (2-3 km below seafloor), it is tempting to speculate that the microbial lineages obtained from these subsurface sediments may originated from microbial communities thriving even deeper in the subsurface biosphere. However, lineages which are widespread in subsurface sediments, such as the JS1 clade were not retrieved (Parkes *et al.* 2005, Inagaki *et al.* 2006). The presence of aerobic methanotrophs in deep oxygen-depleted sediments of the center and the white bacterial mats site may be explained by horizontal and vertical mixing processes of surface and subsurface sediments during the transport of muds from the center to the rim of the volcano.

The sediment layers from which the clone libraries were constructed were not suitable for FISH analysis mainly due to very low cell numbers ($<<10^8$ cells/ml). Thus, the *in situ* abundance of groups dominating the clone libraries remains unknown.

1.3 Microbial communities in Mats of Sulfur-Oxidizing Bacteria
(data not presented in a manuscript)

To gain insights into the sulfide-oxidizing community at HMMV several mat samples including the uppermost millimeters of the sediment were investigated by comparative 16S rRNA gene analysis. The presence of filamentous sulfur-oxdizing bacteria was verified with DAPI staining before clone libraries were constructed. These experiments revealed a diverse community of filamentous sulfur-oxidizing bacteria in samples from the grey mats. Filaments which resemble *Beggiatoa* were found with widths of 1.5 μm, 3 μm und 5 μm, respectively. Big coccoid cells (10-20 μm in diameter) occurring as single cells or in chains were also very abundant. In contrast to mats which were microscopically investigated immediately after sampling (Klages *et al.* 2004), cells resembling *Thiomargarita* (>100 μm

in diameter) were not detected. In white mats mainly 9 μm wide filaments were detected indicating that most likely a single strain of *Beggiatoa* dominates the community. Here neither *Thiomargarita* nor the big coccoid cells detected in grey mats were present. This finding is consistent with previous investigations of living material from white mats (Klages *et al.* 2004).

The bacterial 16S rRNA gene libraries constructed from grey mat material were dominated by members of the methanotrophic groups HMMV-MetI and HMMV-MetII which are also found in sediments of the center and beneath white mats (see appendix). Moreover, clades assumed to be involved in sulfide-oxidation such as *Leucothrix mucor* and a group distantly related to *Arcobacter* species were represented in high numbers. *Arcobacter* species were found at hydrothermal vents and have been shown to produce large amounts of filamentous sulfur in laboratory culture (Taylor & Wirsen 1997, Taylor *et al.* 1999, Wirsen *et al.* 2002). The presence of *Arcobacter* agrees well with the observed macrostructure of the grey mats which share some similarities with filamentous sulfur mats at hydrothermal vents. The diversity of *Deltaproteobacteria* was rather low and only three groups were present with one being seep-specific (SEEP-SRB4).

In white mats, the bacterial diversity was extremely high (see appendix). Members of the *Deltaproteobacteria* were most frequently recovered. In addition, the bacterial clone libraries comprised an extraordinary high number of sequences affiliated with uncultured clades (e.g. OD1, OP5, OP8, OP9, OP11, TM6, WS3, WS6), which were mostly represented by a single sequence or just a few ones. The diversity in the uppermost millimeters of the sediment including the mats appears to be negatively correlated with the morphological diversity of putative sulfide-oxidizers observed in the mats.

Sequences of the large sulfur oxidizers such as *Beggiatoa, Thiomargarita,* and *Thioploca* known from cold seeps and reducing environments were not recovered from either mat material although 292 clones have been analyzed and microscopical investigation of the mat suggested their presence. This lack of these sequences in clone libraries constructed from bacterial mats has been reported previously (Heijs *et al.* 2005). Only living filaments are appear to be suitable for PCR amplification as a high content of endogenous DNAses degrades chromosomal DNA rapidly upon cell lysis (S. Hinck, pers. communication).

Preliminary FISH analyses showed high autofluorescence of the microorganisms in the mat samples. Moreover, unspecific binding of both monolabeled and HRP-labeled probes hampered the community analysis by FISH. However, DAPI staining revealed that total cell numbers were very high (up to 9×10^9 cells/ml) suggesting that the microbial community in

the mats is active and proliferating. Cells showing the conspicuous morphology of methanotrophs of the HMMV-MetI clade were very abundant in the grey mat material. Published probes for sulfide-oxidizing bacteria including several probes specific for *Beggiatoa* and *Arcobacter* (Snaidr *et al.* 1997, Mussmann *et al.* 2003) gave no specific hybridization signals at recommended formamide concentrations. Thus, further effort should be made to design new probes and to verify their specificity carefully.

1.4 Symbioses between Bacteria and Siboglinid Tubeworms

About 300-400 m from the center of the HMMV dense colonies of symbiont-bearing siboglinid tubeworms populate the sediments stretching over an area of about 400 m^2 around the HMMV (Fig. 10). The results summarized in the following section are presented in detail in publication #3 of this thesis.

All members of the family *Siboglinidae* live in obligate symbiosis with bacterial endosymbionts and rely on the chemosynthetic capabilities of their symbionts for nutrition (Felbeck 1981, Southward *et al.* 1986). The symbionts are housed in an interior vascularized tissue called the trophosome (Southward 1982). The tubeworms provide their symbionts with both oxygen from the water column and energy-rich compounds from the anoxic sediments. The tubeworm species at HMMV have been described previously (Smirnov 2000) and two new species were identified, *Sclerolinum contortum (Monilifera, Siboglinidae)* and *Oligobrachia haakonmosbiensis (Frenulata, Siboglinidae)*, which coexist at the same site. These species represent the dominant megafauna at HMMV and reach very high biomasses of 1-2 kg wet weight m^{-2} as determined by box coring. The symbionts in only two frenulate species (Kimura *et al.* 2003, Naganuma *et al.* 2005) and no moniliferan species have been examined to date. Hence, the abundant tubeworm species at HMMV offered the opportunity to extend the current knowledge about these rarely sampled clades of siboglinid tubeworms and their associated symbionts. The symbioses were investigated by comparative sequence analysis of 16S rRNA, 18S rRNA, and protein-coding genes, fluorescence *in situ* hybridization, and lipid biomarker analyses.

The posterior parts of the worm tubes are buried in the reduced sediments (approximately 15 cm and 60 cm depth for *S. contortum* and *O. haakonmosbiensis,* respectively) while the anterior ends extend a few centimeters into the oxygenated water column (-1°C *in situ* temperature). The *in situ* profiles of sulfide and oxygen overlapped in the top centimeters indicating that the tubeworms actively pump seawater into the sulfidic sediments (de Beer *et al.* 2006). Just below the base of the *O. haakonmosbiensis* worms and above the

first fine layers of gas hydrates, elevated rates of anaerobic methane oxidation were found to coincide with a subsurface peak of microbial aggregates mediating this process (Niemann & Lösekann *et al.* subm).

Molecular analysis of the symbionts revealed that the *S. contortum* symbiont is closely related to gammaproteobacterial chemoautotrophic sulfur-oxidizing symbionts of vestimentiferan hosts. In *O. haakonmosbiensis* two closely related symbionts were found which belong to the *Gammaproteobacteria* and group with the symbiont of another frenulate siboglinid, *O. mashikoi* from Japan. These symbiont sequences form a separate clade unaffiliated with known methane- or sulfur-oxidizing bacteria. Fluorescence *in situ* hybridizations with symbiont-specific oligonucleotide probes confirmed that the dominant bacterial phylotypes originated from endosymbionts residing inside the host trophosome. In both host species genes coding for ribulose-1,5-bisphosphate carboxylase/oxygenase (RubisCO) and adenosine-5'-phosphosulfate reductase (APS) were present, whereas genes diagnostic for methanotrophy such as genes coding for the particulate and soluble methane monooxygenase or methanol dehydrogenase were not detected. The $\delta^{13}C$ values of bacterial fatty acids and cholesterol in both host species were depleted with median values of -43‰ for *S. contortum* and -70‰ for *O. haakonmosbiensis*.

The molecular data suggest that *S. contortum* harbors chemoautotrophic sulfur-oxidizing symbionts. The stable carbon isotopic values of biomarkers are extremely negative, but can be accomplished by chemoautotrophic CO_2 fixation at HMMV. In contrast, the metabolic mode of the *O. haakonmosbiensis* symbionts could not be unambiguously determined. The molecular data suggest that *O. haakonmosbiensis* harbors chemoautotrophic sulfur-oxidizing symbionts, but the stable carbon isotopic values of biomarkers were too negative to be accomplished by chemoautotrophic CO_2 fixation alone. However, the presence of a methane-oxidizing symbiont was not confirmed as molecular data and biomarkers specific for type I methanotrophs are lacking.

1.5 Diversity of *mcrA* Genes (data not presented in a manuscript)

The process of AOM is thought to be a reversed methanogenesis. Methyl-coenzyme M reductase (MCR) catalyzes the last enzymatic step of methanogenesis. Recent studies suggest that *mcrA* genes could substitute for 16S rRNA genes in determining phylogenetic relationships among methanogens (Luton *et al.* 2002). Two *mcrA* groups (a and b) correspond to ANME-1, and three *mcrA* groups (c, d and e) correspond to ANME-2 (Hallam *et al.* 2003, Inagaki *et al.* 2004).
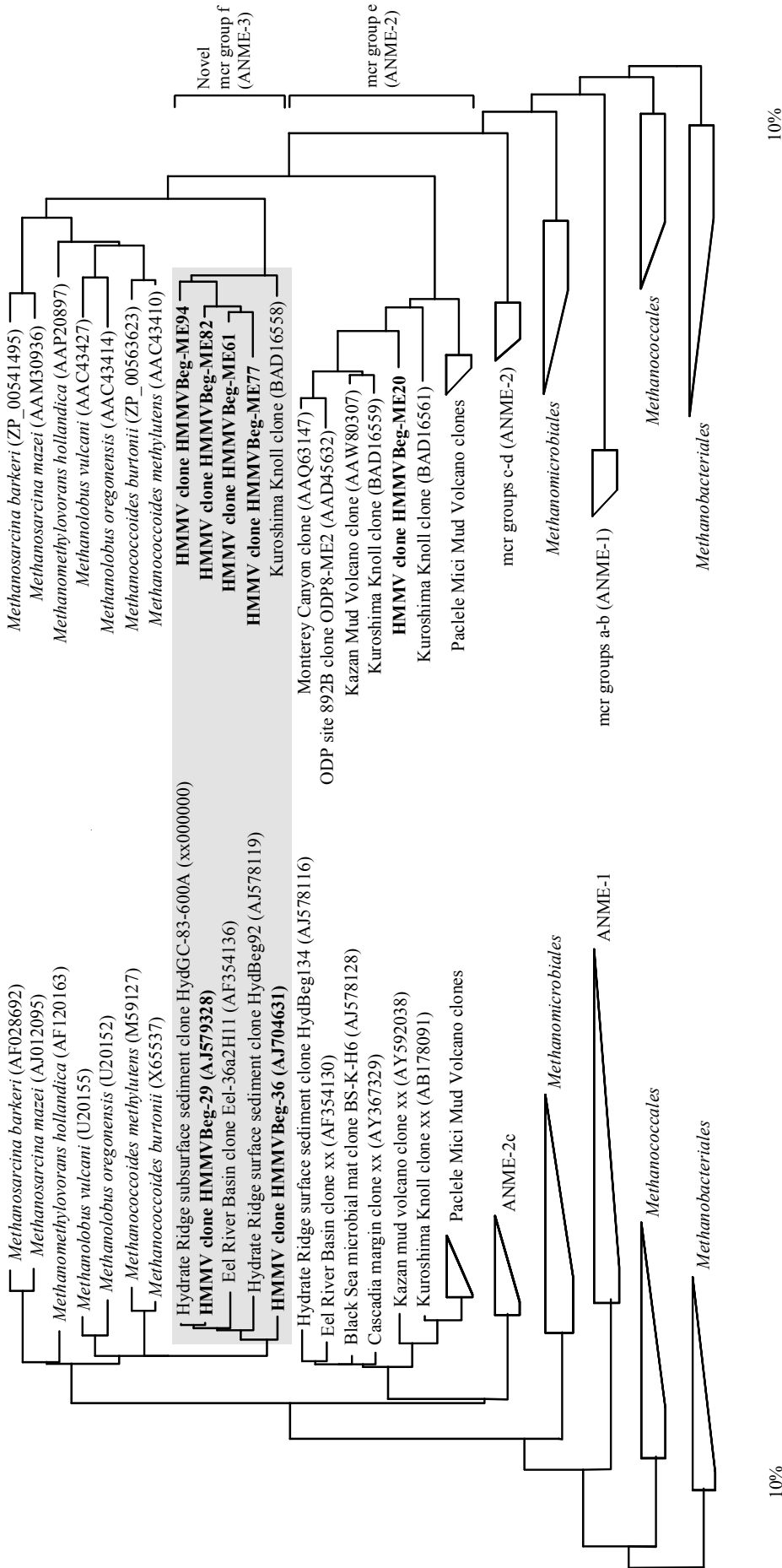
Figure 12. Comparison of 16S rRNA gene and *mcrA*-based phylogenetic trees. The 16S rRNA gene tree was calculated with nearly full-length sequences by maximum-likelihood analysis in combination with filters, which consider only 50% conserved regions of the 16S rRNA of *Archaea*. The *mcrA* tree is built from deduced amino acid sequences by neighbor-joining analysis in combination with filters, which consider only 30% conserved regions of the *mcrA* gene fragment. Branching orders not supported by all calculation methods are shown as multifurcations.

To identify ANME-3 associated *mcrA* genes a *mcrA* clone library from HMMV surface sediments covered with white bacterial mats was constructed. FISH surveys have shown that the 1-2 cm sediment horizon is dominated by ANME-3 which accounted for 95 ± 2% of total cells. Of >100 screened clones only five *mcrA* phylotypes became evident. One phylotype represented by clone HMMVBeg-ME20 fell into the previously defined ANME-2 associated *mcrA* group e (Hallam *et al.* 2003). Representatives of the other phylotypes grouped with one sequence from cold seep sediments (Kuroshima Knoll, Inagaki *et al.* 2004) forming a novel clade in the following referred to as group f. This group was more closely related to cultivated methanogens than *mcrA* groups a-e are. According to congruent 16S rRNA gene phylogeny, these sequences probably originated from ANME-3 (Fig. 12).

In order to estimate the potential for catalytic activity of the novel group f of *mcrA* gene sequences, the deduced amino acid sequences were aligned with representative sequences of ANME-1, ANME-2, and methanogens as references as described previously (Hallam *et al.* 2003, Alain *et al.* 2005). Since active sites encoded by the *mcrA* fragment were conserved, the *mcrA* of groups c-f may have the potential to catalyze the terminal step in methanogenesis. In contrast, ANME-1 associated *mcrA* groups a and b harbor amino acid substitutions at universally conserved positions (e.g. motif $VX_2CCX_4CX_5C$) which could alter active-site geometry and therefore protein function (Krüger *et al.* 2003). These modifications, however, were neither found in ANME-2 nor in ANME-3 associated groups and thus are not diagnostic for the catalytic potential of AOM.

2 Cascadia Margin (Hydrate Ridge, Coast off Oregon)

The second major objective of this thesis was to characterize microbial communities in sulfate-limited habitats at Hydrate Ridge (HR) which have not been investigated before, i.e. shallow gas hydrate bearing subsurface sediments and pure gas hydrates. The results of these studies are presented in detail in publication #4 of this thesis. Moreover, surface sediments of HR were investigated to extend the current knowledge about the distribution of different types of AOM consortia, namely ANME-2 subgroups a/c and ANME-3 (publications #4 and #5 of this thesis). To understand the diversity and activity of anaerobic methanotrophs in hydrate-bearing sediments is important, because they may affect methane concentrations and hence processes of decomposition and formation of gas hydrates.

Hydrate Ridge (HR) is an accretionary structure formed as the result of the subduction of the Juan de Fuca plate underneath the North American plate (Suess *et al.* 1999). Fluids rich in

methane rise from deep sediments and form massive gas hydrates (methane vol% >95, Suess *et al.* 1999) in the overlying sediments, some of which outcrop at the seafloor. *In situ* methane concentrations reach up to 70 mM (Torres *et al.* 2002) which is the equilibrium solubility at *in situ* conditions (600-800 m water depth, 4-6°C). Gas ebullition occurs at high fluid flow sites. Sulfur-based chemosynthetic communities such as bacterial mats of filamentous sulfur-oxidizing bacteria (*Beggiatoa* sp.) and symbiont-bearing clams of the genus *Calyptogena* are indicators for AOM activity in the underlying sediments and the presence of surficial gas hydrates (Sahling *et al.* 2002, Torres *et al.* 2002, Tryon *et al.* 2002).

2.1 Detection and Quantification of ANME-2 subgroups in Surface Sediments

AOM rates reported for surface sediments of HR were extremely high (several μmol cm^{-3} d^{-1}) and correlated with the presence of high numbers of AOM consortia (>10^{10} cells/ml sediment) (Boetius *et al.* 2000, Knittel *et al.* 2003, Treude *et al.* 2003). These consortia consist of ANME-2 archaea and sulfate-reducing bacteria of the *Desulfosarcina/Desulfococcus* group (DSS).

The clade of ANME-2 archaea is divided in two major subgroups, ANME-2a/b and ANME-2c. To investigate the distribution of these subgroups in surface sediments, I used 16S rRNA targeted oligonucleotide probes specific for each subgroup. The FISH surveys revealed that the ANME-2 subgroups can be distinguished from each other by the morphology of the consortia they form as described in publication #5 of this thesis (Knittel *et al.* 2005). ANME-2c archaea were associated with DSS and mainly formed spherical 'shell-type' consortia consisting of an inner core of archaea which is partially or fully surrounded by an outer shell of SRB (Fig. 13-b). Shell-type ANME-2c/DSS consortia were predominantly found at medium-flow sites such as those inhabited by *Calyptogena* clams (75-80% of total consortia in 1-2 cm depth). In contrast, ANME-2a archaea and DSS formed mainly 'mixed-type' consortia in which archaeal and bacterial cells were completely mixed and grew in direct contact (Fig. 13-c). Mixed-type ANME-2a/DSS consortia were predominant at sites with high methane and sulfide concentrations as marked by the coverage of the sediments with bacterial mats (45-80% of total consortia in 1-2 cm depth). Hence, the dominance of ANME-2 subgroups is linked to a specific type of chemosynthetic community populating the surface.

2.2 Detection of ANME-3 in Surface Sediments

Since ANME-3 sequences were retrieved from surface (Knittel *et al.* 2005) and shallow subsurface sediments of HR (see publication #4 of this thesis), the presence of this novel type of AOM consortium was tested with FISH. Indeed, presence of ANME-3 could be confirmed and aggregates were detected, but only in low numbers (estimated 1×10^4 aggregates cm^{-3}) in 3-4 cm sediment depth in sediments covered with bacterial mats. Here, ANME-3 formed spherical or irregular shaped consortia which were partially surrounded by DSS cells (Fig. 13-a). At HMMV, ANME-3 archaea were associated with *Desulfobulbus* species (DBB) showing that this group of anaerobic methanotrophs can interact with different groups of sulfate-reducing bacteria.

2.3 Methanotrophic Communities in Shallow Subsurface Sediments and Gas Hydrates

The microbial diversity in Cascadia margin sediments, especially of Hydrate Ridge, has been intensively studied including surface, subsurface and gas hydrate samples (Cragg *et al.* 1996, Bidle *et al.* 1999, Marchesi *et al.* 2001, Boetius & Suess 2004, Lanoil *et al.* 2005, Inagaki *et al.* 2006), but an analysis of the shallow subsurface (>20 cm to a few meters below seafloor) and pure gas hydrates has been lacking. During my thesis I examined a 1.5 m gravity core bearing two distinct gas hydrate layers, massive gas hydrates, and sediments directly attached to the outside of gas hydrates.

Sequences of ANME-1 and ANME-2 dominated the archaeal clone libraries constructed from deep sediments (1 m below seafloor) and pure gas hydrate melts. Fluorescence *in situ* hybridizations confirmed the presence of ANME throughout the 1.5 m sediment core. Abundance of ANME-1 and ANME-2 in shallow subsurface sediments was highest (10^9 cells cm^{-3}) in 23 and 73 cm depth directly above two gas hydrate layers. When integrated over depth, cells of ANME-1 dominated the archaeal community. A novel type of microbial consortium was detected in 23 cm sediment depth: ANME-1 and sulfate-reducing DSS, occurred as shell-type ANME-1/DSS aggregates in relatively high abundance (Fig. 13-d).

The microbial community in gas hydrate melts was dominated by either ANME-1 or ANME-2 archaea (Fig. 13-e). The cells had very low rRNA contents, indicating that they may have been inactive for extended periods. In contrast, ANME cells in sediments surrounding gas hydrates had high rRNA contents even at 1 m depth below the seafloor suggesting that sulfate and methane are available for the microbial community in distinct subsurface horizons.
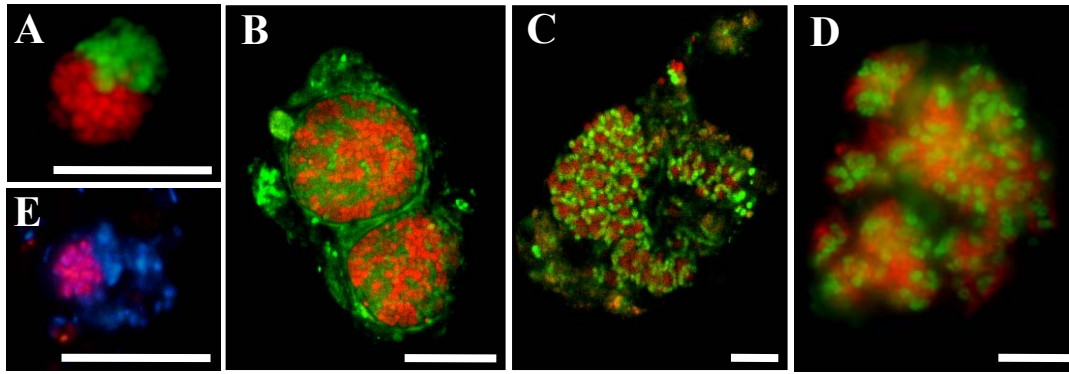
Figure 13. Epifluorescence micrographs of microbial consortia in HR sediments after *in situ* hybridization with 16S rRNA targeted oligonucleotide probes. (A) Surface: ANME-3 archaea (red) stained with probe ANME3-1249 and DSS (green) stained with probe DSS658. (B) Surface: ANME-2c archaea (red) stained with probe ANME2c-622 and DSS (green) stained with probe DSS658. (C) Surface: ANME-2a archaea (red) stained with probe ANME2a-647 and DSS (green) stained with probe DSS658. (D) Shallow subsurface: ANME-1 archaea (red) stained with probe ANME1-350 and DSS (green) stained with probe DSS658. (E) Gas hydrate: DAPI staining and ANME-2 archaea (magenta) stained with probe EelMS-932. Scale bars, 10 μm.

3 Final Discussion

In this thesis, a variety of different habitats at cold seeps was investigated. Major aims were to identify and quantify key microbial players in order to determine environmental factors which control their distribution and activity in the ecosystem. In the following, I will discuss the results obtained during my thesis according to the main questions posed in chapter IA-5 (thesis outline).

3.1 Key Microbial Players and Their Distribution

Anaerobic Methanotrophs

Anaerobic methanotrophs (ANME) are key microbial players in cold seep systems. They mediate the anaerobic oxidation of methane (AOM) in a consortium with sulfate-reducing bacteria (SRB). The process of AOM reduces the emission of the greenhouse gas methane from the ocean to the atmosphere significantly.

Lipid biomarker data and DNA signatures indicate the ubiquitous presence of ANME archaea in anoxic, methane rich sediments. So far, ANME signatures have been detected at all cold seeps investigated and were also found in sulfate-methane transition zones of coastal environments (e.g. Orphan *et al.* 2001a, Michaelis *et al.* 2002, Reed *et al.* 2002, Hallam *et al.* 2003, Knittel *et al.* 2003, Mills *et al.* 2003, Inagaki *et al.* 2004, Ishii *et al.* 2004, Heijs *et al.* 2005, Knittel *et al.* 2005). The current data sets indicate that the presence of

ANME groups is limited to the upper meters of the sediments, because their 16S rRNA genes have not yet been recovered from deeper layers.

Highest activity and biomass of anaerobic methanotrophs were only detected in near-surface sediments (Boetius *et al.* 2000, Knittel *et al.* 2003, Treude *et al.* 2003, Knittel *et al.* 2005, Orcutt *et al.* 2005). Results obtained from the HMMV confirm the conclusion that the magnitude of key biogeochemical processes at cold seeps is correlated with the biomasses of the corresponding microbial players. The vertical distribution of cells matched the vertical distribution of activities at all sites investigated. This applies for both aerobic and anaerobic methane oxidizers at HMMV and is in good agreement to previous studies from other active cold seeps such as Hydrate Ridge (Boetius *et al.* 2000, Knittel *et al.* 2003) or hydrocarbon seeps at the Gulf of Mexico (Orcutt *et al.* 2005). Moreover, it was demonstrated that concentrations of lipid biomarkers correlated well with single cell counts (Niemann *et al.* in prep a).

In shallow subsurface sediments, low concentrations of sulfate and high concentrations of sulfide make AOM thermodynamically more unfavorable compared to surface sediments. However, in depths down to 1 m anaerobic methanotrophs reach relatively high numbers as demonstrated for Hydrate Ridge shallow subsurface sediments. Future studies are needed to test whether this type of AOM community is able to exploit methane at very low sulfate concentrations and represent a common low-activity compartment in cold seep ecosystems.

I also aimed to further characterize the novel group of anaerobic methanotrophs ANME-3. A few years ago, only two ANME-3 sequences from the Eel River Basin and from Hydrate Ridge, respectively, were published. Research conducted in this thesis extended the number of ANME-3 sequences and elucidated the role of ANME-3 in AOM. Today, there is little doubt that ANME-3 archaea consume methane under anaerobic conditions. Studies at HMMV revealed that high numbers of ANME-3 consortia coincide with high AOM rates and specific ^{13}C-depleted lipid biomarker signatures. At this time (March 2006), ANME-3 sequences have been retrieved from other cold seeps, too, and the clade contains 129 sequences from five different habitats (Fig 14). The sequence similarity of ANME-3 is 95-100% indicating that several genera are represented. Sequences from an AOM bioreactor, the Monterey Canyon, the Kuroshima Knoll, and a Lost City hydrothermal vent chimney fell adjacent to the ANME-3 clade. These sequences are not targeted by the currently used ANME-3 probes.

Sequence analysis of *mcrA* genes obtained from HMMV identified a clade of *mcrA* sequences which correspond to ANME-3 based on congruent 16S rRNA phylogeny.

Metagenomic libraries can now be screened for the presence ANME-3 *mcrA* genes and positive clones can be assigned to ANME-3. Sequencing of adjacent sequence stretches would provide new insights into the genome organization and metabolic potential of ANME-3. Additionally, further physiological studies are needed to test their preferred and realized niches in the environment.
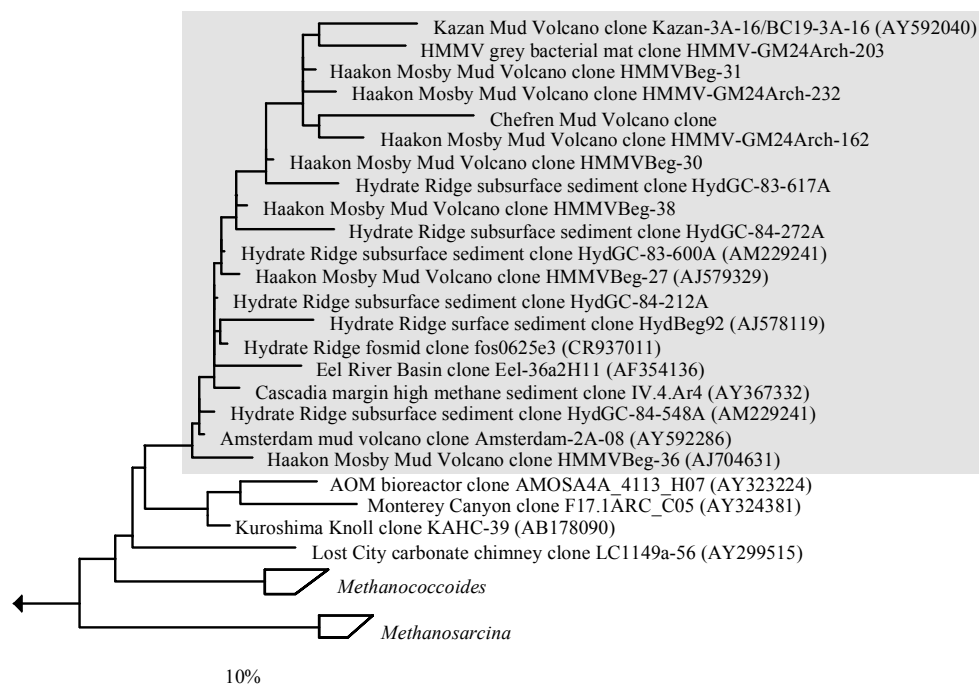
Figure 14. Phylogenetic tree based on 16S rRNA gene phylogeny showing the affiliations within the ANME-3 clade (shaded box). At least one representative sequence is shown from all ANME-3 hosting habitats known so far.

Chemoautotrophic Sulfide Oxidizers

AOM is the main sulfide-generating process at cold seeps and supports enormous biomasses of bacterial mats and symbiont-bearing invertebrates. These sulfide-oxidizing chemoautotrophic communities oxidize all the sulfide produced in the anoxic zones of the sediments. The distribution of chemoautotrophic communities at cold seeps depends mainly on the magnitude of the sulfide-generating processes in the sediments. Mats of sulfur-oxidizing bacteria mark sites with high fluid flow and high concentrations of sulfide in the underlying sediments (de Beer *et al.* 2006, Joye *et al.* 2004, Sahling *et al.* 2002, Tryon *et al.* 2002,). All large, sulfur-oxidizing bacteria can also use nitrate as an electron acceptor for the oxidation of sulfide and therefore do not depend on oxic conditions. In contrast, symbiont-bearing invertebrates need access to oxygen and reduced compounds from the sulfidic, anoxic

zones. The animals have different strategies to supply their symbionts with both electron donors and electron acceptors. Some hosts are motile or bridge oxic-anoxic interfaces due to their size. Bivalves, clams, and tubeworms are ecosystem engineers and alter their environment by dwelling, burrowing, and bioirrigation activities. In general, benthic animals can be found at medium and low flux sites with lower sulfide concentrations compared to areas inhabited by bacterial mats (de Beer *et al.* 2006, Sahling *et al.* 2002). This is mainly due to the high levels of sulfide which is extremely toxic for most aerobic respiring organisms. Moreover, the tubes of tubeworms would channel high upward fluid flow and the bioirrigation of the sediments is limited.

3.2 Difference between Surface and Subsurface Communities

One objective of my thesis was to compare surface and subsurface microbial communities in order to examine whether the same clades of key microbial players are present in surface sediments and deeper sediment layers.

The composition of surface and shallow subsurface communities of Hydrate Ridge was similar based on 16S rRNA gene analysis. Sequences affiliated with ANME groups clearly dominated the archaeal 16S rRNA clone libraries from either sample and lineages of the *Crenarchaeota* were not detected. Bacterial 16S rRNA clone libraries were phylogenetically highly diverse and most lineages were obtained from both surface and shallow subsurface samples. The microbial diversity in gas hydrates was highly reduced and mainly lineages involved in AOM (ANME-1, ANME-2, DSS) were obtained. Sequences unique to gas hydrates were not retrieved from the investigated samples.

In contrast, the microbial communities in deep subsurface sediments (few to hundreds of meters below seafloor) are distinctly different from those in surface and shallow subsurface sediments. Groups of *Crenarchaeota* dominate archaeal 16S rRNA clone libraries and genes of ANME have not been retrieved yet from these depths. Instead, sequences belonging to the 'marine benthic group B' (MBGB), the 'miscellaneous crenarchaeotic group' (MCG) and the 'marine crenarchaeotic group I' (MGI) of *Crenarchaeota* are widely distributed in deep subsurface sediments (Biddle *et al.* 2006, Inagaki *et al.* 2006, Parkes *et al.* 2005).

The results obtained in this thesis confirmed the predominance of crenarchaeotal groups in subsurface sediments. Clone libraries constructed from HMMV subsurface sediments (4-5 m depth) were dominated by sequences affiliated with the 'marine group C' (MBGC). The metabolic traits of these yet uncultivated crenarchaeotal groups are unknown. Recently, Biddle *et al.* (2006) investigated archaeal communities in deep subsurface sediments off Peru,

which are dominated by members of MBGB and MGC. Based on carbon flow reconstructions the authors showed that archaeal cells in the deep subsurface oxidize methane to gain energy, but do not assimilate methane-derived carbon. Therefore, these groups may consume methane and catalyze the process of AOM.

3.3 Interspecies Associations at Cold Seeps

Interspecies Correlation of ANME groups and their Bacterial Partners

During this thesis novel types of microbial consortia were identified showing that interspecies associations in cold seep habitats are very versatile. Previous work showed that ANME archaea form diverse associations with SRB. ANME-1 cells form mat-type consortia with DSS and ANME-2 form shell-type and mixed-type consortia with DSS (Boetius *et al.* 2000, Knittel *et al.* 2003, Michaelis *et al.* 2002). In this thesis, consortia of ANME-3 archaea and *Desulfobulbus* species were visualized for the first time in HMMV surface sediments. ANME-3 archaea also form associations with DSS as shown in Hydrate Ridge surface sediments. Moreover, I identified consortia of ANME-1 and DSS at Hydrate Ridge. It is likely that other forms of syntrophic associations between ANME archaea and SRB remain to be discovered in yet unexplored cold seep systems.

One important question for the understanding of the process of AOM is whether it obligatorily requires the syntrophic interaction between ANME archaea and SRB in the form of symbiotic associations. Highest biomasses were found where ANME archaea form physically close associations with SRB indicating that this life style may be energetically favorable. However, all ANME groups occur as both microbial consortia with SRB and single cells: Single ANME-1 cells are frequently detected in deeper surface layers of cold seeps (Knittel *et al.* 2005, Orphan *et al.* 2002, Orcutt *et al.* 2005), ANME-2 have been shown to occur as single cells without contact to SRB in methanotrophic mats of the Black Sea (K. Knittel, pers. communication), and single ANME-3 cells were detected in surface sediments covered with white or grey bacterial mats at HMMV. The occurrence of single cells supports the conclusion that ANME may interact with free-living SRB or may catalyze AOM without a bacterial partner.

Interspecies Correlation of ANME Archaea and Marine Invertebrates

Tubeworms may even have a mutualistic association with AOM mediating consortia (Boetius 2005, Cordes *et al.* 2005). It has been shown that *Lamellibrachia* spp. from the Gulf of Mexico take up sulfide from the sulfidic subsurface sediment zones with their deeply

buried roots (Cordes *et al.* 2003, Freytag *et al.* 2001). The animals transport sulfate into the sediments by bioirrigation and may also release sulfate through their roots as a by-product of sulfide oxidation mediated by their symbionts. Thus, the tubeworms locally increase the sulfate concentrations in the sediments and remove sulfide. The tubeworms' roots likely represent a favorable niche for AOM mediating consortia, because AOM is thermodynamically favored in the vicinity of the roots. Cordes *et al.* (2005) presented a model showing that AOM fueled by the release of sulfate from the tubeworms roots could provide 60% of the sulfide needed to support the tubeworms for several decades.

3.4 Environmental Selection of ANME Groups

Fluid Flow and Bioirrigation as Selection Factors

Previous studies of ANME enrichments have shown that increasing methane partial pressures clearly stimulates the rate of AOM. The temperature optimum ranged between 4°C and 16°C indicating that at least one partner in the AOM mediating consortium is psychrophilic. Variations of pH, salinity, and sulfate concentration did not influence the AOM activity laboratory studies (Nauhaus *et al.* 2002, Nauhaus *et al.* 2005). Thus, populations of ANME are adapted to cold temperatures and high methane fluxes, which are commonly found at cold seeps. The results of this thesis in combination with those from scientists of other disciplines suggest that fluid flow controls the distribution of methanotrophic guilds at cold seeps.

For example, at HMMV aerobic methanotrophs reached high numbers only in sediments of the center where upward fluid rates were high. Balancing upward flow with downward diffusion and local consumption, it was calculated that the rising subsurface fluids (3-6 m yr^{-1}) restrict availability of oxygen and sulfate to a few millimeters below seafloor in the active centre of HMMV (de Beer *et al.* 2006). These environmental conditions exclude anaerobic methanotrophs from this site and allow high activities of aerobic methanotrophs. The zone of aerobic methane oxidation was very thin, and could not prevent most methane from escaping to the water column. However, in most marine sediments oxygen and methane do not overlap, and thus the aerobic oxidation of methane is of minor significance in the oceans.

In contrast, sites covered with mats of sulfur-oxidizing bacteria at HMMV were associated with high AOM rates. This is due to decreased fluid flow rates (0.3-0.6 m yr^{-1}) transporting methane rich fluids to the surface and a deeper sulfate penetration depth compared to the center (few centimeters) (de Beer *et al.* 2006). In the sulfate-penetrated zone of the methane-rich sediments, growth of anaerobic methanotrophs is favored. High numbers of

AOM consortia were indeed detected in this thin horizon below the zone of oxygen penetration and above the zone of sulfate depletion.

Another important factor controlling the distribution of methanotrophic communities at cold seeps are activities of benthic animals. At cold seeps, symbiont-bearing invertebrates are often the dominant megafauna (Sahling *et al.* 2002, Sibuet & Olu-Le Roy 2002). These animals need access to oxygen and reduced substances to fulfill their symbionts' needs. Bioturbation of bivalves and clams or bioirrigation by tubeworms are factors which change the biogeochemical zonation of sediments. At HMMV symbiont-bearing siboglinid tubeworms are highly abundant and these worms engineer their environment by pumping seawater deep into the sediments. The worms reach down to 60 cm into the sediments and their bioirrigation activity considerably increases the oxygen penetration depth (10 cm depth). Thereby anaerobic methanotrophs are excluded from surface sediments. However, sulfate is transported deep into the sediments and directly fuels AOM at the base of the tubeworms (70 cm depth).

It has been assumed that increasing upward flow rates provide more dissolved methane to cold seep surface communities, which adapt their population size to the available energy. However, the current research at HMMV has shown that very high fluid flow rates of subsurface fluids limit the diffusion of electron acceptors into the sediments and thus restrict the activity and biomass of microbial communities. Already at flow rates of $>1 \text{m yr}^{-1}$, which are commonly found at cold seeps (Freund *et al.* 1997, Henry *et al.* 1992, Henry *et al.* 1996, Levin *et al.* 2003b), anaerobic methane consumption is inhibited and the efficiency of this microbial filter against methane emission into the water column is considerably decreased.

Dominance of ANME Groups

ANME-1 and ANME-2 co-occur in Hydrate Ridge and Black Sea microbial mats as well as in many other methane-rich habitats. Now it is also known that there are habitats where ANME-3 is abundant and may coexist with ANME-1 and/or ANME-2 as in Hydrate Ridge surface sediments of HMMV surface sediments covered with grey mats.

The *in situ* quantification showed that the ANME groups are present at very different levels suggesting that different mechanisms select for the dominant phylotype in a given habitat. ANME-1 dominated in Black Sea microbial mats (40-50% of total cells) and ANME-2 were restricted to small microniches (1% of total cells). In Hydrate Ridge sediments ANME-2 and ANME-3 aggregates co-occurred in the surface. Here, ANME-2 clearly dominated the microbial community and numbers of ANME-3 aggregates were several orders

of magnitude lower. In deeper sediment layers of Hydrate Ridge, ANME-1 cells were frequently detected down to 1 m below seafloor. At HMMV, ANME-3 dominated the microbial community (95% of total cells) in surface sediments covered with bacterial mats and neither ANME-1 nor ANME-2 could be detected.

In order to identify environmental parameters which may select the dominating ANME group in a habitat, I compared literature data from cold seeps for which 16S rRNA sequence information is available and the dominating phylotype was identified by FISH (Table 1). At all sites excess methane was available as the main carbon and energy source. Based on *in vitro* incubations, it was shown that temperature influenced the intensity of AOM, with ANME-2 and ANME-3 being more adapted to cold temperatures than ANME-1 (Nauhaus *et al.* 2005, Niemann *et al.* in prep b). The variation of other environmental parameters, such as sulfate concentration, pH and salinity, did not influence the activity of ANME-1 or ANME-2 communities *in vitro* (Nauhaus *et al.* 2005).

Another factor influencing the dominance of ANME groups appears to be their oxygen tolerance. ANME-1 seem to be more sensitive to oxygen than ANME-2 and ANME-3. This conclusion is supported by low ANME-1 cell numbers in oxygenated sediments of Hydrate Ridge which are periodically flushed with oxic bottom water. In contrast, microbial mats in the Black Sea were comprised by large quantities of ANME-1 cells. The ANME-2 subgroups seem to differ in their oxygen tolerance, too (Knittel *et al.* 2005). ANME-2a aggregates were predominant in surface sediments of Hydrate Ridge which are covered with bacterial mats and which are characterized by an oxygen penetration depth of a few millimeters. In contrast, ANME-2c dominated in sediments which were populated with *Calyptogena* clams. At this site oxygen penetrated deeper into the sediments due to bioturbation activities of the clams.

Factors which may select for ANME-3 cannot be determined at the moment. Environmental parameters measured in the ANME-3 dominated habitat at HMMV are similar to those measured in ANME-2 dominated habitats. In surface sediments covered with grey mats at HMMV, both ANME-2 and ANME-3 co-occur in high abundances suggesting that these groups share similar habitat preferences.

Table 1 Geochemical Characterization of Cold Seep Sites and Occurrence of Methanotrophic Groups

Habitat	Water depth [m]	Temp. [°C]	Oxygen penetration [mm]	Sulfate penetration† [cm]	Sulfide conc. [mM]	Methane oxidation rate [µmol cm⁻³ d⁻¹]	MOx Bacteria	16S rRNA Gene Sequences			References
								ANME-1	ANME-2	ANME-3	
HMMV	1250	-1									(De Beer et al. 2006, Niemann et al. in prep)
Center surface			1-3	1-3	<0.01	Up to 0.3	+*	-	-	-	
Center subsurface				-		DL	-	-	-	-	
Grey mat surface			2	>4		Up to 0.8	+	-	+*	+	
White mat surface (*Beggiatoa* spp.)			1	4	4	Up to 0.7	+	-	-	+*	
White mat subsurface (*Beggiatoa* spp.)						DL	-	-	-	-	
Tubeworms surface (*Siboglinidae*)			3-10	~80	0.15	Up to 0.01	-	+	-	+	
Tubeworms subsurface (*Siboglinidae*)						Up to 0.4	-	-	+	-	
Cascadia Margin	780	4									(Sahling et al. 2002, Treude et al. 2003, Knittel et al. 2005)
White mat surface (*Beggiatoa* spp.)			1	4	10-26	Up to 0.2	-	+	+*	+	
Clam bed surface (*Calyptogena* spp.)			10	8	0-10	Up to 2.7	-	+	+*	-	
Subsurface sediment				‡	2-11	DL	-	+*	+	+	
Gas hydrates				-		DL	-	+*	+*	-	
Black Sea Mats	250	9	-	-	1	Up to 18	-	+*	+	-	(Michaelis et al. 2002, Knittel et al. 2003, Knittel et al. 2005)

†Calculated based on balancing upward flow with downward diffusion and local consumption (De Beer et al. 2006). ‡Sulfate detectable down to 150 cm (<5 mM) in investigated core. DL = near or below the detection limit of the method, ND = no data available. *dominating phylotype *in situ*.

3.5 Outlook

In this thesis I used 16S rRNA-based molecular methods to identify and quantify microbial communities at two cold seeps. A few important environmental factors controlling the distribution of key microbial players were determined, yet further *in situ* and physiological research is needed for a comprehensive understanding of cold seep ecosystems.

The characterization of *in situ* parameters which structure microbial niches in the environment is essential for interpreting microbial diversity and distribution patterns. Therefore it is important to obtain as many *in situ* data as possible. An important task for the future would be to develop analytical tools to measure microbial activities directly on the seafloor, because the commonly used *ex situ* measurements always introduce artefacts.

Moreover, enrichment experiments should be continued to obtain ANME in pure culture for physiological and biochemical characterization. The development of flow-through microcosms which enable manipulation experiments would be important to study the ecophysiology of AOM communities.

Another aim should be to obtain full genome sequences from ANMEs. Enrichment cultures are available which are enriched in single ANME cells. I isolated single ANME-1 cells by fluorescence activated cell sorting (FACS) with high purity. Further effort should be made to sort a sufficient number of cells for DNA extraction and subsequent whole genome sequencing. The genome sequence of ANME would provide valuable insights into the metabolic potential of ANME and this knowledge may aid enrichment and isolation efforts.

It is still not known whether ANME archaea are capable of oxidizing methane without bacterial partner. Further development of methods for the detection of mRNA in single cells would be useful to prove whether ANME archaea express genes diagnostic for sulfate reduction and methane oxidation. During my thesis, I worked on the adaptation of a mRNA-FISH protocol to cells of ANME-1. The preliminary experiments show that the application of digested probes (<100 base pairs) is most promising. The continuation of these experiments would be an important task for the future.

This thesis and previous studies have shown that the ANME phylotypes are globally distributed and occur in anoxic, methane rich sediments worldwide (Knittel *et al.* 2005). However, it may be that the resolution of the 16S rRNA gene, which is currently the gene of choice for microbial molecular systematic studies, is too limited to elucidate biogeographical

patterns of anaerobic methanotrophs. Sequencing of other marker genes or the ITS region of 16S rRNA genes would provide additional information to examine microdiversity among closely related ANME phylotypes.

During this work, a novel group of anaerobic methanotrophs and novel associations between AOM mediating archaea and bacteria were discovered. It is likely that not yet investigated habitats provide unexpected ecological niches for microbial life and that a much greater diversity of anaerobic methanotrophs and microbial associations remains to be discovered. For example, it is not known which groups of microorganisms mediate AOM in hydrothermal subsurface sediments and it would be interesting to study this type of high-temperature habitat.

Another interesting aspect for future research would be to study the abundance and function of *Crenarchaeota* at cold seeps. Different groups of *Crenarchaeota* are frequently found in clone libraries of cold seep sediments, but quantitative data about their distribution is lacking. For this project, new specific probes have to be developed and applied.

To elucidate the identity of the filamentous sulfur oxidizers forming mats at HMMV, I recommend using pure mat material without sediment contamination for further analysis. Moreover, the amplification of 16S rRNA genes from living, single filaments is the most promising approach and was successful at other sites (Mussmann *et al.* 2003).

C References

Aharon P, Fu B (2000) Microbial sulfate reduction rates and sulfur and oxygen isotope fractionations at oil and gas seeps in deepwater Gulf of Mexico. Geochimica et Cosmochimica Acta 64:233-246

Alain K, Holler T, Musat F, Elvert M, Treude T, Kruger M (2005) Microbiological investigation of methane- and hydrocarbon-discharging mud volcanoes in the Carpathian Mountains, Romania. Environmental Microbiology doi:10.1111/j.1462-2920.2005.00922.x

Amann RI, Ludwig W, Schleifer K-H (1995a) Phylogenetic identification and in situ detection of individual microbial cells without cultivation. Microbiological Reviews 59:143-169

Barnes RO, Goldberg ED (1976) Methane production and consumption in anoxic marine sediments. Geology 4:297-300

Biddle JF, Lipp JS, Lever MA, Lloyd KG, Sorensen KB, Anderson R, Fredricks HF, Elvert M, Kelly TJ, Schrag DP, Sogin ML, Brenchley JE, Teske A, House CH, Hinrichs K-U (2006) Heterotrophic Archaea dominate sedimentary subsurface ecosystems off Peru. Proceedings of the National Academy of Sciences USA 103:3846-3851

Bidle KA, Kastner M, Bartlett DH (1999) A phylogenetic analysis of microbial communities associated with methane hydrate containing marine fluids and sediments in the Cascadia margin (ODP8 site 892B). FEMS Microbiology Letters 177:101-108

Boetius A (2005) Microfauna-Macrofauna Interaction in the Seafloor: Lessons from the Tubeworm. PLoS Biology 3:e102

Boetius A, Suess E (2004) Hydrate Ridge: a natural laboratory for the study of microbial life fueled by methane from near-surface gas hydrates. Chemical Geology 205:291-310

Boetius A, Ravenschlag K, Schubert C, Rickert D, Widdel F, Gieseke A, Amann R, Jørgensen BB, Witte U, Pfannkuche O (2000) A marine microbial consortium apparently mediating anaerobic oxidation of methane. Nature 407:623-626

Bohrmann G, Greinert J, Suess E, Torres M (1998) Authigenic carbonates from the Cascadia subduction zone and their relation to gas hydrate stability. Geology 26:647-650

Buffet BA (2000) Chlathrate hydrates. Annual Reviews of Earth and Planetary Science 28:477-507

Cavanaugh CM, Gardiner SL, Jones ML, Jannasch HW, Waterbury JB (1981) Prokaryotic cells in the hydrothermal vent tube worm Riftia pachyptila Jones: possible chemoautotrophic symbionts. Science 213:340-342

Chandler DP, Brockman FJ, Bailey TJ, Fredrickson JK (1998) Phylogenetic diversity of archaea and bacteria in a deep subsurface paleosol. Microbial Ecology 36:37-50

Childress JJ, Fisher CR, Brooks JM, Kennicutt II MC, Bidigare R, Anderson AE (1986) A methanotrophic marine molluscan *(Bivalvia, Mytilidae)* symbiosis: mussels fueled by methane. Science 233:1306-1308

Cordes EE, Arthur MA, Shea K, Arvidson RS, Fisher CR (2005) Modeling the mutualistic interactions between tubeworms and microbial consortia. PLOS Biology 3:1-10

Cordes EE, Bergquist DC, Shea K, Fisher CR (2003) Hydrogen sulphide demand of long-lived vestimentiferan tube worm aggregations modifies the chemical environment at deep-sea hydrocarbon seeps. Ecology Letters 6:212-219

Corliss JB, Dymond J, Gordon LI, Edmond JM, von Herzen RP (1979) Submarine thermal springs on the Galapagos Rift. Science 203:1073-1083

References

Cragg BA, Parkes RJ, Fry JC, Weightman AJ, Rochelle PA, Maxwell JR (1996) Bacterial populations in sediments containing gas hydrates (ODP Leg 146: Cascadia Margin). Earth and Planetary Science Letters 139:497-507

Damm E, Budéus G (2003) Fate of vent-derived methane in seawater above the Haakon Mosby mud volcano (Norwegian Sea). Marine Chemistry 1969:1-11

de Beer D, Sauter E, Niemann H, Witte U, Schlüter M, Boetius A (2006) In situ fluxes and zonation of microbial activity in surface sediments of the Haakon Mosby Mud Volcano (in press). Limnology and Oceanography limn-51-03-10.3d

DeChaine EG, Cavanaugh CM (2005) Symbioses of methanotrophs and deep-sea mussels (Mytilidae: Bathymodiolinae). In: Overmann J (ed) Molecular basis of symbioses. Springer-Verlag, Berlin

D'Hondt S, Rutherford S, Spivack AJ (2002) Metabolic activity of subsurface life in deep-sea sediments. Science 295:2067-2070

Dimitrov LI (2002) Mud volcanoes - the most important pathway for degassing deeply buried sediments. Earth-Science Reviews 59:49-76

Distel DL, Baco AR, Chuang E, Morrill W, Cavanaugh C, Smith CR (2000) Marine ecology: Do mussels take wooden steps to deep-sea vents? Nature 403:725-726

Durisch-Kaiser E, Klauser L, Wehrli B, Schubert C (2005) Evidence of Intense Archaeal and Bacterial Methanotrophic Activity in the Black Sea Water Column. Applied and Environmental Microbiology 71:8099-8106

Eller G, Stubner S, Frenzel P (2000) Group-specific 16S rRNA targeted probes for the detection of type I and type II methanotrophs by fluorescence in situ hybridisation. FEMS Micobiology Letters 198:91-97

Elvert M, Suess E, Whiticar MJ (1999) Anaerobic methane oxidation associated with marine gas hydrates: superlight C-isotopes from saturated and unsaturated C20 and C25 irregular isoprenoids. Naturwissenschaften 86:295-300

Felbeck H (1981) Chemoautotrophic potential of the hydrothermal vent tube worm, *Riftia pachyptila* Jones *(Vestimentifera)*. Science 213:336-338

Felbeck H, Childress JJ, Somero GN (1981) Calvin-Benson cycle and sulfide oxidation enzymes in animals from sulfide-rich habitats. Nature 293:291

Felbeck H, Distel DL (2002) Prokaryotic symbionts of marine invertebrates. In: Dworkin M (ed) The Prokaryotes (Electronic version). Springer Verlag, New York

Feldman RA, Shank TM, Black MB, Baco AR, Smith CR, Vrijenhoek RC (1998) Vestimentiferan on a whale fall. The Biological Bulletin 194:116-119

Fisher CR (1990) Chemoautotrophic and methanotrophic symbioses in marine invertebrates. Reviews of Aquatic Sciences 2:399-436

Fossing H, Gallardo VA, Jørgensen BB, Hüttel M, Nielsen LP, Schulz H, Canfield DE, Forster S, Glud RN, Gundersen JK, Küver J, Ramsing NB, Teske A, Thamdrup B, Ulloa O (1995b) Concentration and transport of nitrate by the mat-forming sulphur bacterium *Thioploca*. Nature 374:713-715

Freund C, Gehring P, Holak TA, Pluckthun A, Wallmann K, Linke P, Suess E, Bohrmann G, Sahling H, Schluter M, Dahlmann A, Lammers S, Greinert J, von Mirbach N (1997) Quantifying fluid flow, solute mixing, and biogeochemical turnover at cold vents of the eastern Aleutian subduction zone. Geochimica et Cosmochimica Acta 61: 5209-5219

Freytag JK, Girguis PR, Bergquist DC, Andras JP, Childress JJ, Fisher CR (2001) A paradox resolved: Sulfide acquisition by roots of seep tubeworms sustains net chemoautotrophy. Proceedings of the National Academy of Sciences USA 98:13408-13413

Gallardo VA, Carrasco FD, Roa R, Canete JI (1995) Ecological patterns in the benthic macrobiota across the continental shelf off central Chile. Ophelia 40:167-188

Garrity GM, Winters M, Searles DB (2001) Taxonomic outline of the prokaryotic genera. In: Bergey's manual of systematic bacteriology, Vol 2nd edition. Springer Verlag, New York

Girguis PR, Orphan VJ, Hallam SJ, DeLong EF (2003) Growth and methane oxidation rates of anaerobic methanotrophic archaea in a continuous-flow bioreactor. Applied and Environmental Microbiology 69:5472-5482

Guezennec J, Fiala-Medioni A (1996) Bacterial abundance and diversity in the Barbados Trench determined by phospholipid analysis. FEMS Microbiology Ecology 19:83-93

Gulledge J, Ahmad A, Steudler PA, Pomerantz WJ, Cavanaugh CM (2001) Family- and genus-level 16S rRNA-targeted oligonucleotide probes for ecological studies of methanotrophic bacteria. Applied and Environmental Microbiology 67:4726-4733

Hallam SJ, Girguis PR, Preston CM, Richardson PM, DeLong EF (2003) Identification of methyl coenzyme M reductase A (mcrA) genes associated with methane-oxidizing archaea. Applied and Environmental Microbiology 69:5483-5491

Hallam SJ, Putnam N, Preston CM, Detter JC, Rokhsar D, Richardson PM, DeLong EF (2004) Reverse Methanogenesis: Testing the Hypothesis with Environmental Genomics. Science 305:1457-1462

Hanson RS, Hanson TE (1996) Methanotrophic Bacteria. Microbiological Reviews 60:439-471

Harms G, Zengler K, Rabus R, Aeckersberg F, Minz D, Rosello-Mora R, Widdel F (1999) Anaerobic oxidation of o-xylene, m-xylene, and homologous alkylbenzenes by new types of sulfate-reducing bacteria. Applied and Environmental Microbiology 65:999-1004

Heijs SK, Sinninghe Damste JS, Forney LJ (2005) Characterization of a deep-sea microbial mat from an active cold seep at the Milano mud volcano in the Eastern Mediterranean Sea. FEMS Microbiology Ecology 54:47-56

Henry P, Foucher JP, Le Pichon X, Sibuet M, Kobayashi K, Tarits P, Chamot-Rooke N, Furuta T, Schultheiss P (1992) Interpretation of Temperature-Measurements from the Kaiko-Nankai Cruise: Modeling of Fluid-Flow in Clam Colonies. Earth and Planetary Science Letters 109:355-371

Henry P, Le Pichon X, Lallemant S, Lance S, Martin JB, Foucher, JP, Fiala-Medioni A, Rostek F, Guilhaumou N, Pranal V, Castrec M (1996) Fluid flow in and around a mud volcano field seaward of the Barbados accretionary wedge: Results from Manon cruise. Journal of Geophysical Research-Solid Earth 101:20297-20323

Hesselbo SP, Gröcke DR, Jenkyns HC, Bjerrum CJ, Farrimond P, Morgans Bell HS, Green OR (2000) Massive dissociation of gas hydrate during a Jurassic oceanic anoxic event. Nature 406:392-395

Hinrichs K-U, Boetius A (2002) The anaerobic oxidation of methane: New insights in microbial ecology and biogeochemistry. In: Wefer G, Billett D, Hebbeln D, Jörgensen BB, Schlüter M, Van Weering TC (eds) Ocean Margin Systems. Springer, Berlin

Hinrichs KU, Hayes JM, Sylva SP, Brewer PG, DeLong EF (1999) Methane-consuming archaebacteria in marine sediments. Nature 398:802-805

Hinrichs K-U, Hmelo LR, Sylva SP (2003) Molecular fossil record of elevated methane levels in late pleistocene coastal waters. Science 299:1214-1217

Hinrichs K-U, Summons RE, Orphan V, Sylva SP, Hayes JM (2000) Molecular and isotopic analysis of anaerobic methane-oxidizing communities in marine sediments. Organic Chemistry 31:1685-1701

References

Hoehler TM, Alperin MJ, Albert DB, Martens CS (1994) Field and laboratory studies of methane oxidation in an anoxic marine sediment: Evidence for a methanogen-sulfate reducer consortium. Global Biogeochemical Cycles 8:451-463

Inagaki F, Nunoura T, Nakagawa S, Teske A, Lever M, Lauer A, Suzuki M, Takai K, Delwiche M, Colwell FS, Nealson KH, Horikoshi K, D'Hondt S, Jorgensen BB (2006) Biogeographical distribution and diversity of microbes in methane hydrate-bearing deep marine sediments on the Pacific Ocean Margin. Proceedings of the National Academy of Sciences USA 103:2815-2820

Inagaki F, Tsunogai U, Suzuki M, Kosaka A, Machiyama H, Takai K, Nunoura T, Nealson KH, Horikoshi K (2004) Characterization of C1-Metabolizing Prokaryotic Communities in Methane Seep Habitats at the Kuroshima Knoll, Southern Ryukyu Arc, by Analyzing pmoA, mmoX, mxaF, mcrA, and 16S rRNA Genes. Applied and Environmental Microbiology 70:7445-7455

Ishii K, Mu[ss]mann M, MacGregor BJ, Amann R (2004) An improved fluorescence in situ hybridization protocol for the identification of bacteria and archaea in marine sediments. FEMS Microbiology Ecology 50:203-212

Iversen N, Jørgensen BB (1985) Anaerobic methane oxidation rates at the sulfate-methane transition in marine sediments from Kattegat and Skagerrak (Denmark). Limnology and Oceanography 30:944-955

Jacq E, Prieur D, Nichols DC, White T, Porter T, Geesey GG (1989) Microscopic examination and fatty acid characterization of filamentous bacteria colonizing substrate around subtidal hydrothermal vents. Archives of Microbiology 152:64-71

Jannasch HW, Taylor CD, Wirsen CO (1989) Massive natural occurrence of unusual large bacteria *(Beggiatoa sp.)* at a hydrothermal deep-sea vent site. Nature 342:834-836

Jörgensen BB (1977) Distribution of colorless sulfur bacteria *(Beggiatoa spp.)* in a coastal marine sediment. Marine Biology 41:19-28

Jørgensen BB (1982a) Mineralization of organic matter in the sea bed - the role of sulphate reduction. Nature 296:643-645

Jørgensen BB (1982b) Ecology of the sulphur cycle with special reference to anoxic-anoxic interface environments. Phil. Trans R. Soc. Lond. B 298:543-561

Joye SB, Boetius A, Orcutt BN, Montoya JP, Schulz HN, Erickson MJ, Lugo SK (2004) The anaerobic oxidation of methane and sulfate reduction in sediments from Gulf of Mexico cold seeps. Chemical Geology 205:219-238

Kalanetra KM, Huston SL, Nelson DC (2004) Novel, Attached, Sulfur-Oxidizing Bacteria at Shallow Hydrothermal Vents Possess Vacuoles Not Involved in Respiratory Nitrate Accumulation. Applied and Environmental Microbiology 70:7487-7496

Kasten S, Jörgensen BB (2000) Sulfate Reduction in Marine Sediments. In: Schulz HD, Zabel M (eds) Marine Geochemistry. Springer Verlag, Berlin, p 263 - 281

Katz ME, Pak DK, Dickens GR, Miller KG (1999) The Source and Fate of Massive Carbon Input During the Latest Paleocene Thermal Maximum. Science 286:1531-1533

Kennett JP, Cannariato KG, Hendy IL, Behl RJ (2000) Carbon isotopic evidence for methane hydrate instability during quaternary interstadials. Science 288:128-133

Kennicutt MC, Brooks JM, Bidigare RR, Fay RR, Wade TL, MacDonald TJ (1985) Vent-type taxa in a hydrocarbon seep region on the Lousiana slope. Nature 317:351-353

Kimura H, Sato M, Sasayama Y, Naganuma T (2003) Molecular characterization and in situ localization of endosymbiotic 16S ribosomal RNA and RuBisCO genes in the pogonophoran tissue. Marine Biotechnology 5:261-269

Klages M, Thiede J, Foucher JP (eds) (2004) The Expedition ARKTIS XIX/3 of the Research Vessel Polarstern in 2003, Vol 488. Buchhandlung Kamloth, Bremen

Klenk HP, Clayton RA, Tomb JF, White O, Nealson K, al e (1997) The complete genome sequence of the hyperthermophilic, sulphate-reducing archaeon *Archaeoglobus fulgidus*. Nature 390:364-370

Knittel K, Boetius A, Lemke A, Eilers H, Lochte K, Pfannkuche O, Linke P, Amann R (2003) Activity, distribution, and diversity of sulfate reducers and other bacteria in sediments above gas hydrate (Cascadia Margin, Oregon). Geomicrobiology Journal 20:269-294

Knittel K, Lösekann T, Boetius A, Kort R, Amann R (2005) Diversity and distribution of methanotrophic archaea at cold seeps. Applied and Environmental Microbiology 71:467-479

Kopf AJ (2003) Global methane emission through mud volcanoes and its past and present impact on the Earth´s climate. International Journal of Earth Sciences 92:806-816

Krüger M, Meyerdierks A, Glöckner FO, Amann R, Widdel F, Kube M, Reinhardt R, Kahnt J, Böcher R, Thauer RK, Shima S (2003) A conspicuous nickel protein in microbial mats that oxidize methane anaerobically. Nature 426:878-881

Kvenvolden K (1988) Methane hydrate - a major reservoir of carbon in the shallow geosphere? Chemical Geology 71:41 - 51

Lanoil BD, Duc MTL, Wright M, Kastner M, Nealson KH, Bartlett D (2005) Archaeal diversity in ODP legacy borehole 892b and associated seawater and sediments of the Cascadia Margin. FEMS Microbiology Ecology 54:167-177

Larkin JM, Henk MC (1996) Filamentous sulfide-oxdizing bacteria at hydrocarbon seeps at the Gulf of Mexico. Microscopy Research and Techniques 33:23-31

Larkin JM (1983) *Beggiatoa, Thiothrix,* and *Thioploca*. Annual Reviews of Microbiology 37:341-367

Levin LA (2003a) Oxygen minimum zone benthos: adaptation and community reponse to hypoxia. Oceanography and Marine Biology: an Annual Review 41:1-45

Levin LA, Ziebis W, Mendoza GF, Growney VA, Tryon MD, Brown KM, Mahn C, Gieskes JM, Rathburn AE (2003b) Spatial heterogeneity of macrofauna at northern California methane seeps: influence of sulfide concentration and fluid flow. Marine Ecology Progress Series 265:123-139

Li L, Kato C, Horikoshi K (1999c) Microbial diversity in sediments collected from the deepest cold-seep area, the Japan trench. Marine Biotechnology 1:391-400

Llobet-Brossa E, Rossello-Mora R, Amann R (1998) Microbial community composition of wadden sea sediments as revealed by fluorescence *in situ* hybridization. Applied and Environmental Microbiology 64:2691-2696

Lösekann T (2002) Molekularbiologische Untersuchungen der Diversität und Struktur mikrobieller Lebensgemeinschaften in methanreichen, marinen Sedimenten (Haakon Mosby Schlammvulkan), Diplomarbeit an der Universität Bremen

Luff R, Wallmann K (2003) Fluid flow, methane fluxes, carbonate precipitation and biogeochemical turnover in gas hydrate-bearing sediments at Hydrate Ridge, Cascadia Margin: Numerical modeling and mass balances. Geochimica et Cosmochimica Acta 67:3403-3421

Luton PE, Wayne JM, Sharp RJ, Riley PW (2002) The *mcrA* gene as an alternative to 16S rRNA in the phylogenetic analysis of methanogen population in landfill. Microbiology 148:3521-3530

MacDonald IR, Bohrmann G, Escobar E, Abegg F, Blanchon P, Blinova V, Bruckmann W, Drews M, Eisenhauer A, Han X, Heeschen K, Meier F, Mortera C, Naehr T, Orcutt B, Bernard B, Brooks J, de Farago M (2004) Asphalt Volcanism and Chemosynthetic Life in the Campeche Knolls, Gulf of Mexico. Science 304:999-1002

References

MacDonald IR, Boland GS, Baker JS, Brooks JM, Kennicutt II MC, Bidigare RR (1989) Gulf of Mexico chemosynthetic communities: II. Spatial distribution of seep organisms and hydrocarbons at Bush Hill. Marine Biology 101:235-247

Madigan MT, Martinko JM (2006) Brock - Biology of Microorganisms, Pearson Prentice-Hall, London

Marchesi JR, Weightman AJ, Cragg BA, Parkes RJ, Fry JC (2001) Methanogen and bacterial diversity and distribution in deep gas hydrate sediments from the Cascadia Margin as revealed by 16S rRNA molecular analysis. FEMS Microbiology Ecology 34:221-228

Martens CS, Berner RA (1974) Methane production in the interstitial waters of sulfate-depleted marine sediments. Science 185:1167-1169

McCaffrey MA, Farrington JW, Repeta DJ (1989) Geochemical implication of the lipid composition of Thioploca spp. from the Peru upwelling region - 16°S. Organic Geochemistry 14:61-68

McHatton SC, Barry JP, Jannasch HW, Nelson DC (1996) High nitrate concentrations in vacuolate, autotrophic marine *Beggiatoa* spp. Applied and Environmental Microbiology 62:954-958

Meyerdierks A, Kube M, Lombardot T, Knittel K, Bauer M, Glockner FO, Reinhardt R, Amann R (2005) Insights into the genomes of archaea mediating the anaerobic oxidation of methane. Environmental Microbiology 7:1937-1951

Michaelis W, Seifert R, Nauhaus K, Treude T, Thiel V, Blumenberg M, Knittel K, Gieseke A, Peterknecht K, Pape T, Boetius A, Amann R, Jörgensen BB, Widdel F, Peckmann J, Pimenov NV, Gulin MB (2002) Microbial reefs in the Black Sea fueled by anaerobic oxidation of methane. Science 297:1013-1015

Mills HJ, Hodges C, Wilson K, MacDonald IR, Sobecky PA (2003) Microbial diversity in sediments associated with surface-breaching gas hydrate mounds in the Gulf of Mexico. FEMS Microbiology Ecology 46:39-52

Mussmann M, Ishii K, Rabus R, Amann R (2005) Diversity and vertical distribution of cultured and uncultured Deltaproteobacteria in an intertidal mud flat of the Wadden Sea. Environmental Microbiology 7:405-418

Mussmann M, Schulz HN, Strotmann B, Kjaer T, Nielsen LP, Rosselló-Mora RA, Amann R, Jörgensen BB (2003) Phylogeny and distribution of nitrate-storing *Beggiatoa* spp. in coastal marine sediments. Environmental Microbiology 5:523-533

Naganuma T, Elsaied H, Hoshii D, Kimura H (2005) Bacterial Endosymbioses of Gutless Tube-Dwelling Worms in Nonhydrothermal Vent Habitats. Marine Biotechnology 7:416-428

Nauhaus K, Treude T, Boetius A, Kruger M (2005) Environmental regulation of the anaerobic oxidation of methane: a comparison of ANME-I and ANME-II communities. Environmental Microbiology 7:98-106

Nauhaus K, Boetius A, Krüger M, Widdel F (2002) In vitro demonstration of anaerobic oxidation of methane coupled to sulphate reduction in sediment from a marine gas hydrate area. Environmental Microbiology 4:296-305

Nelson DC, Fisher CR (1995) Chemoautotrophic and methanotrophic endosymbiotic bacteria at deep-sea vents and seeps. In: Karl DM (ed) Deep-sea hydrothermal vents. CRC Press, Boca Raton, p 125-167

Nelson DC, Jörgensen BB, Revsbach NP (1986) Growth pattern and yield of a chemoautotrophic Beggiatoa sp. in oxygen-sulfide microgradients. Applied and Environmental Microbiology 52:225-233

Niemann H, Lösekann T, de Beer D, Elvert M, Knittel K, Amann R, Sauter E, Schlüter M, Klages M, Foucher J, Boetius A (subm) Fluid flow controls distribution of methanotrophic microorganisms at submarine cold seeps. Nature.

Niemann H, Elvert M, Lösekann T, Jakob J, Nadalig T, Boetius A (in prep a) Distribution of methanotrophic guilds at Haakon Mosby Mud Volcano, Barents Sea.

Niemann H, Sauter E, Krüger M, Heinrich F, Lösekann T, Elvert M, Boetius A (in prep b) Aerobic and anaerobic methane oxidation in sediments of Haakon Mosby Mud Volcano, Barents Sea. in prep

Norris RD, Rohl U (1999) Carbon cycling and chronology of climate warming during the Palaeocene/Eocene transition. Nature 401:775-778

Orcutt B, Boetius A, Elvert M, Samarkin V, Joye SB (2005) Molecular biogeochemistry of sulfate reduction, methanogenesis and the anaerobic oxidation of methane at Gulf of Mexico cold seeps. Geochimica et Cosmochimica Acta 69:4267-4281

Oremland RS, Marsh LM, Polcin S (1982) Methane production and simultaneous sulphate reduction in anoxic, salt marsh sediments. Nature 296:143-145

Orphan VJ, Hinrichs K-U, Ussler III W, Paull CK, Taylor LT, Sylva SP, Hayes JM, DeLong EF (2001a) Comparative analysis of methane-oxidizing archaea and sulfate-reducing bacteria in anoxic marine sediments. Applied and Environmental Microbiology 67:1922-1934

Orphan VJ, House CH, Hinrichs K-U, McKeegan KD, DeLong EF (2001b) Methane-consuming archaea revealed by directly coupled isotopic and phylogenetic analysis. Science 293:484-487

Orphan VJ, House CH, Hinrichs K-U, McKeegan KD, DeLong EF (2002) Multiple archaeal groups mediate methane oxidation in anoxic cold seep sediments. Proceedings of the National Academy of Sciences USA 99:7663-7668

Pancost RD, Damsté JSS, de Lint S, van der Maarel MJEC, Gottschal JC, party tMss (2000) Biomarker evicence for widespred anaerobic methane oxidation in Mediterranean sediments by a consortium of methanogenic archaea and bacteria. Applied and Environmental Microbiology 66:1126-1132

Parkes RJ, Webster G, Cragg BA, Weightman AJ, Newberry CJ, Ferdelman TG, Kallmeyer J, Jorgensen BB, Aiello IW, Fry JC (2005) Deep sub-seafloor prokaryotes stimulated at interfaces over geological time. Nature 436:390-394

Paull CK, Hecker B, Commeau R, Freeman-Lynde RP, Neumann C, Corso WP, Golubic S, Hook JE, Sikes E, Curray J (1984) Biological communities at the Florida escarpment resemble hydrothermal vent taxa. Science 226:965-967

Pimenov NV, Savvichev AS, Rusanov II, Lein AY, Ivanov MV (2000) Microbiological processes of the carbon and sulfur cycles at cold methane seeps of the North Atlantic. Microbiology 69:709-720

Rabus R, Hansen T, Widdel F (2002) Dissimilatory Sulfate- and Sulfur-Reducing Prokaryotes. In: Dworkin M (ed) The Prokaryotes (Electronic version). Springer Verlag, New York

Ravenschlag K, Sahm K, Knoblauch C, Jørgensen BB, Amann R (2000) Community structure, cellular rRNA content and activity of sulfate-reducing bacteria in marine Arctic sediments. Appl. Environ. Microbiol. 66:3592-3602

Reeburgh WS (1996) "Soft spots" in the global methane budget. In: Lidstrom ME, Tabita FR (eds) Microbial Growth on C1 Compounds. Kluwer Academic Publishers, Dordrecht, p 334–342

Reed DW, Fujita Y, Delwiche ME, Blackwelder DB, Sheridan PP, Uchida T, Colwell FS (2002) Microbial communities from methane-bearing deep marine sediments in a forearc basin. Applied and Environmental Microbiology 68:3759-3770

Reysenbach A-L, Shock E (2002) Merging Genomes with Geochemistry in Hydrothermal Ecosystems 10.1126/science.1072483. Science 296:1077-1082

Rouse GW, Goffredi SK, Vrijenhoek RC (2004) *Osedax:* Bone-Eating Marine Worms with Dwarf Males. Science 305:668-671

Sahling H, Rickert D, Lee R, Linke P, Suess E (2002) Macrofaunal community structure and sulfide flux at gas hydrate deposits from the Cascadia convergent margin, NE Pacific. Marine Ecology Progress Series 231:121 - 138

Sahm K, Knoblauch C, Amann R (1999b) Phylogenetic affiliation and quantification of psychrophilic sulfate-reducing isolates in marine arctic sediments. Applied and Environmental Microbiology 65:3976-3981

Sassayama Y, Matada M, Fukumori Y, Umebayashi M, Matsuno A, Nakagawa T, Imajima M (2003) External morphology of the posterior end, the "opisthosoma", of the beard worm *Oligobrachia mashikoi (Pogonophora)*. Zoological Science 20:1411-1416

Sauter EJ, Muyakshin SI, Charlou JL, Schlüter M, Boetius A, Jerosch K, Damm E, Foucher JP, Klages M (2006) Methane discharge from a deep-sea submarine mud volcano into the upper water column by gas hydrate-coated methane bubbles (in press). Earth and Planetary Science Letters

Schink B (1997) Energetics of syntrophic cooperation in methanogenic degradation. Microbiology and Molecular Biology Reviews 61:262-280

Schmaljohann R, Flügel HJ (1987) Methane-oxidizing bacteria in *Pogonophora*. Sarsia 72:91-98

Schulz HN, Brinkhoff T, Ferdelman TG, Teske A, Jörgensen BB (1999) Dense Populations of a Giant Sulfur Bacterium in Namibian Shelf Sediments. Science 284:493-495

Sibuet M, Olu K (1998) Biogeography, biodiversity and fluid dependence of deep-sea cold-seep communities at active and passive margins. Deep-Sea Research II 45:517 - 567

Sibuet M, Olu-Le Roy K (2002) Cold seep communities on continental margins: structure and quantitative distribution relative to geological and fluid venting patterns. In: Wefer G, Billett D, Hebbeln D, Jörgensen BB, Schlüter M, Van Weering TC (eds) Ocean Margin Systems. Springer, Berlin, p 235-251

Smirnov RV (2000) Two new species of *Pogonophora* from the arctic mud volcano off northwestern Norway. Sarsia 85:141-150

Smith CR (1985) Food for the deep sea: Utilization, dispersal and flux of nekton falls at the Santa Catalina Basin floor. Deep-Sea Research 32:417-442

Smith CR, Baco AR (2003) Ecology of whale falls at the deep-sea floor. Oceanography and Marine Biology: an Annual Review 41:311-354

Smith CR, Kukert H, Wheatcroft RA, Jumars PA, Deming JW (1989) Vent fauna on whale remains. Nature 34:27-28

Söhngen NL (1906) Über Bakterien, welche Methan als Kohlenstoffnahrung und Energiequelle gebrauchen. Zentralblatt für Bakteriologie, Parasitenkunde und Infektionskrankheiten 15:513-517

Sörensen K, Finster K, Ramsing N (2001) Thermodynamic and Kinetic Requirements in Anaerobic Methane Oxidizing Consortia Exclude Hydrogen, Acetate, and Mehanol as Possible Electron Shuttles. Microbial Ecology 42:1f.

Snaidr J, Amann R, Huber I, Ludwig W, Schleifer KH (1997) Phylogenetic analysis and in situ identification of bacteria in activated sludge. Applied and Environmental Microbiology 63:2884-2896

Southward AJ, Southward EC, Dando PR, Barrett RL, Ling R (1986) Chemoautotrophic Function of Bacterial Symbionts in Small Pogonophora. Journal of the Marine Biological Association of the United Kingdom 66:415-437

Southward EC (1982) Bacterial symbionts in Pogonophora. Journal of the Marine Biological Association of the United Kingdom 46:579-616

Suess E, Torres ME, Bohrmann G, Collier RW, Greinert J, Linke P, Rehder g, Trehu A, Wallmann K, Winckler G, Zuleger E (1999) Gas hydrate destabilization: enhanced dewatering, benthic material turnover and large methane plumes at the Cascadia convergent margin. Earth and Planetary Sciences Letters 170:1-5

Suess E, Carson B, Ritger SD, Moore JC, Jones ML, Kulm GR, Cochrane GR (1985) Biological communities at vent sites along the subduction zone off Oregon. Bulletin of the Biological Society of Washington 6:475-484

Taylor CD, Wirsen CO (1997) Microbiology and Ecology of Filamentous Sulfur Formation. Science 277:1483-1485

Taylor CD, Wirsen CO, Gaill F (1999) Rapid Microbial Production of Filamentous Sulfur Mats at Hydrothermal Vents. Applied and Environmental Microbiology 65:2253-2255

Teske A, Hinrichs K-U, Edgcomb V, de Vera Gomez A, Kysela D, Sylva SP, Sogin ML, Jannasch HW (2002) Microbial diversity of hydrothermal sediments in the Guaymas Basin: evidence for anaerobic methanotrophic communities. Applied and Environmental Microbiology 68:1994-2007

Teske A, Sogin ML, Nielsen LP, Jannasch HW (1999) Phylogenetic relationships of a large marine Beggiatoa. Systematic and Applied Microbiology 22:39-44

Thauer RK (1998) Biochemistry of methanogenesis: a tribute to Marjory Stephenson. Microbiology 144:2377-2406

Thiel V, Peckmann J, Richnow HH, Luth U, Reitner J, Michaelis W (2001) Molecular signals for anaerobic methane oxidation in Black Sea seep carbonates and a microbial mat. Marine Chemistry 73:97-112

Torres ME, McManus J, Hammond DE, De Angelis MA, Heeschen KU, Colbert SL, Tryon MD, Brown KM, Suess E (2002) Fluid and chemical fluxes in and out of sediments hosting methane hydrate deposits in Hydrate Ridge, OR, I: Hydrological provinces. Earth and Planetary Sciences Letters 201:525-540

Treude T, Boetius A, Knittel K, Wallmann K, Jörgensen BB (2003) Anaerobic oxidation of methane above gas hydrates (Hydrate Ridge, OR). Marine Ecology Progress Series 264:1-14

Tringe SG, von Mering C, Kobayashi A, Salamov AA, Chen K, Chang HW, Podar M, Short JM, Mathur EJ, Detter JC, Bork P, Hugenholtz P, Rubin EM (2005) Comparative Metagenomics of Microbial Communities. Science 308:554-557

Tryon MD, Brown KM, Torres ME (2002) Fluid and chemical flux in and out of sediments hosting methane hydrate deposits on Hydrate Ridge, OR, II: Hydrological processes. Earth and Planetary Science Letters 201:541-557

Tyson GW, Banfield JF (2005) Cultivating the uncultivated: a community genomics perspective. Trends in Microbiology 13:411-415

Valentine DL, Blanton DC, Reeburgh WS (2000) Hydrogen production by methanogens under low-hydrogen conditions. Archives of Microbiology 174:415-421

Valentine DL, Douglas CB, Reeburgh WS, Kastner M (2001) Water column methane oxidation adjacent to an area of active hydrate dissociation, Eel River Basin. Geochim. Cosmochim. Acta 65:2633-2640

Van Dover CL (2000) The ecology of deep-sea hydrothermal vents, Princeton University Press, Princeton

Vetriani C, Jannasch HW, MacGregor BJ, Stahl DA, Reysenbach AL (1999) Population structure and phylogenetic characterization of marine benthic archaea in deep-sea sediments. Applied and Environmental Microbiology 65:4375-4384

Wellsbury P, Parkes RJ (2000) Deep Biosphere: source of methane for oceanic hydrate. In: Max MD (ed) Natural gas hydrate in oceanic and permafrost environments. Kluwer Academic Publishers, p 91-104

References

Wenzhofer F, Glud RN (2002) Benthic carbon mineralization in the Atlantic: a synthesis based on in situ data from the last decade. Deep Sea Research Part I: Oceanographic Research Papers 49:1255-1279

Whiticar MJ (1999) Carbon and hydrogen isotope systematics of bacterial formation and oxidation of methane. Chemical Geology 161:291-314

Wirsen CO, Sievert SM, Cavanaugh CM, Molyneaux SJ, Ahmad A, Taylor LT, DeLong EF, Taylor CD (2002) Characterization of an autotrophic sulfide-oxidizing marine Arcobacter sp. that produces filamentous sulfur. Applied and Environmental Microbiology 68:316-325

Zengler K, Richnow HH, Rosello-Mora R, Michaelis W, Widdel F (1999) Methane formation from long-chain alkanes by anaerobic microorganisms. Nature 401:266-269

Zhang CL, Huang Z, Cantu J, Pancost RD, Brigmon RL, Lyons TW, Sassen R (2005) Lipid Biomarkers and Carbon Isotope Signatures of a Microbial *(Beggiatoa)* Mat Associated with Gas Hydrates in the Gulf of Mexico. Applied and Environmental Microbiology 71:2106-2112

Part II

Publications

A List of Publications

This thesis includes five manuscripts. One manuscript is already published and another manuscript has been submitted. The other manuscripts will be submitted within the next months depending on the comments of the co-authors.

Manuscripts presented in this thesis

(1) Niemann, H., Lösekann, T., de Beer, D., Elvert, M., Nadalig, T., Knittel, K., Amann, R., Sauter, E., Schlüter, M., Klages, M., Foucher, J.P., Boetius, A. (submitted) Fluid flow controls distribution of methanotrophic microorganisms at submarine cold seeps. Nature.

Sampling onboard for lipid biomarker, DNA and FISH analyses, methane, sulfate, porosity, and AOM and sulfate reduction rates was done by Helge Niemann, Thierry Nadalig, and Antje Boetius. Cloning of 16S rRNA genes, phylogenetic analyses and FISH experiments were carried out by me. Lipid biomarker analysis, methane, sulfate, and rate measurements were mainly done by Helge Niemann and Antje Boetius. Parts of the sulfate data set were acquired by Eberhard Sauter and Michael Schlüter. Mapping of the habitats was done by Jean Paul Foucher, Michael Schlüter and Michael Klages. The manuscript was jointly written by Helge Niemann and Antje Boetius and benefited from comments of all co-authors. The manuscript has been submitted to 'Nature' in February 2006 and is currently in review.

(2) Lösekann, T., Knittel, K., Nadalig, T., Niemann, H., Boetius, A., and Amann, R. (in prep) Novel clusters of aerobic and anaerobic methane oxidizers at an Arctic cold seep (Haakon Mosby Mud Volcano, Barents Sea).

Sampling onboard was done by Thierry Nadalig and Antje Boetius. Cloning of 16S rRNA genes, phylogenetic analyses and FISH experiments were carried out by me under the supervision of Katrin Knittel. Aggregates were counted by Thierry Nadalig and me. The manuscript was written by me and benefited from the comments of all co-authors. The manuscript will be submitted to 'Applied and Environmental Microbiology' within the next months.

(3)   Lösekann, T., Niemann, H., Pradillon F., Knittel, K., Boetius, A., and Dubilier N. (in prep) Endosymbioses between bacteria and deep-sea siboglinid tubeworms from an Arctic cold seep (Haakon Mosby Mud Volcano, Barents Sea).

Sampling onboard was done by Helge Niemann and Antje Boetius. Cloning of 16S rRNA and 18S rRNA genes, phylogenetic analyses and FISH experiments were carried out by me or undergraduate students under my supervision. Cloning of protein-coding genes and the phylogenetic analyses were done by me. Lipid biomarker analyses were performed by Helge Niemann and Albert Robador during a lab rotation. Sequencing of 18S rRNA genes was done by Florence Pradillon. The manuscript was written by me and Nicole Dubilier and benefited from the comments of all co-authors. The manuscript will be submitted to 'Applied and Environmental Microbiology' within the next months.

(4)   Lösekann, T., Knittel, K., Treude, T., Nauhaus, K., Wallmann, K., Boetius, A., and Amann R. (in prep) Microbial diversity and community composition in gas hydrates and hydrate-bearing sediments of the Cascadia margin (Hydrate Ridge).

Sampling onboard was done by Tina Treude, Katja Nauhaus, and me. Cloning of 16S rRNA genes, phylogenetic analyses and FISH experiments were carried out by me. Ex situ rate measurements and methane measurements were performed by Tina Treude and Antje Boetius. Anoxic incubations were done by Katja Nauhaus. Data sets of porewater constituents were acquired from Klaus Wallmann. The manuscript was written by me and benefited from the comments of all co-authors. In the next months, the manuscript will be supplemented with additional biogeochemical data and submitted to 'Geobiology' or an adequate international, peer-reviewed journal.

(5)   Knittel, K., Lösekann, T., Boetius, A., Kort, R. and Amann, R. (2005) Diversity and distribution of methanotrophic archaea at cold seeps. Applied and Environmental Microbiology **71**: 467-479.

Sampling was carried out by Antje Boetius and Tina Treude. Phylogenetic analyses and FISH counts were carried out by Katrin Knittel. Evaluation of probes for ANME-2 subgroups was done by me. Epifluorescence micrographs were taken by Katrin Knittel and me. Scanning electron microscopy was performed by Katrin Knittel and Renate Kort. The manuscript was written by Katrin Knittel and benefited from the comments of

all co-authors. The manuscript was submitted to 'Applied and Environmental Microbiology' and has been published in January 2005.

Further manuscript

(1)   Niemann, H., Elvert, M., Lösekann, T., Jakob, J., Nadalig, T., and Boetius A. (in prep) Lipid signatures and distribution of methanotrophic microbial communities at Haakon Mosby Mud Volcano, Barents Sea. To be submitted to 'Geobiology'.

For this manuscript I provided a phylogenetic tree showing the affilations of ANME-3 archaea and epifluorescence micrographs.

B   Publications

<div align="center">

1

Fluid Flow Controls Distribution of

Methanotrophic Microorganisms

at Submarine Cold Seeps

</div>

Helge Niemann[1,2,+], Tina Lösekann[1,+], Dirk de Beer [1], Markus Elvert[1,*3], Thierry Nadalig[4,*5], Katrin Knittel[1], Rudolf Amann[1], Eberhard J. Sauter[2], Michael Schlüter[2], Michael Klages[2], Jean-Paul Foucher[4], Antje Boetius[1,2,6]

Fluid Flow Controls Distribution of Methanotrophic Microorganisms at Submarine Cold Seeps

Helge Niemann[1,2,+], Tina Lösekann[1,+], Dirk de Beer [1], Markus Elvert[1,*3], Thierry Nadalig[4,*5], Katrin Knittel[1], Rudolf Amann[1], Eberhard J. Sauter[2], Michael Schlüter[2], Michael Klages[2], Jean-Paul Foucher[4], Antje Boetius[1,2,6]

[1] Max Planck Institute for Marine Microbiology, 28359 Bremen, Germany

[2] Alfred Wegener Institute for Polar and Marine Research, 27515 Bremerhaven, Germany

[3] DFG Research Center on Ocean Margins, University of Bremen, 28334 Bremen, Germany

[4] Centre Ifremer de Brest, BP70, 29280 Plouzane, France

[5] UMR 7156 Université Louis-Pasteur/CNRS, Département Microorganismes, Génomes, Environnement, 67083 Strasbourg Cedex, France

[6] International University Bremen, 28759 Bremen, Germany

[+] These authors contributed equally to this work

[*] present address

Large quantities of methane are produced and stored in the seafloor of continental margins. However, the ocean is a minor global methane source[1], because most of this greenhouse gas is oxidized within the seafloor by anaerobic methanotrophic archaea (ANME) before it reaches the hydrosphere[2-4]. Even at cold seeps, which are characterized by high gas fluxes, most methane is scavenged by subsurface methanotrophs[5,6]. However, very little is known about environmental factors regulating the activity and distribution of the methanotrophic communities in nature. This was the focus of our field study of the methane emitting Haakon Mosby Mud Volcano (HMMV, 72°N, 14°44'E; 1250 m water depth, Barents Sea), combining *in situ* microsensor profiling of O_2, pH and H_2S with high-resolution quantification of microbial populations and their methane turnover. We identified three distinct key populations of aerobic and anaerobic methanotrophs; a novel clade of archaea named ANME-3, free-living populations of *Methylococcales*, and symbiotic pogonophoran tubeworms hosting methanotrophs. Their distribution was related to the horizontal gradient in fluid flow velocity, decreasing from the centre to the outer rim of HMMV. Our in situ data suggest that increasing upward fluid flow restricts the penetration depth of the main electron acceptors for methane oxidation, oxygen and sulphate, thereby limiting the vertical and horizontal dimensions of methanotrophic habitats. This mechanism reduces the capacity of the microbial methane filter, reinforcing greenhouse gas emission from the seafloor.

Anaerobic methanotrophic archaea (ANME), which form consortia with sulphate-reducing bacteria (SRB), were discovered a few years ago in cold seep environments[2-4]. Since then, the global occurrence of these consortia, their abundance in anoxic habitats and relevance as a filter against the emission of methane from the ocean have been confirmed by combinations of molecular, microbiological and biogeochemical methods[7]. Here, our main aim was to investigate environmental conditions, which enhance or repress methane turnover at a cold seep ecosystem, and determine the distribution and diversity of methanotrophs. Therefore, we studied fluid-flow and methane-turnover associated ecosystem patterns at a deep-water cold seep with *in situ* techniques to avoid artefacts by retrieval of supersaturated gaseous sediments. We selected the methane-rich HMMV as a model system. The HMMV is a circular structure of 1 km diameter and <10 m elevation above bottom. It is fuelled by gas migrating from depths of 2-3 km below seafloor, and characterized by a large gas flare above

the seafloor[8-10] (Fig. 1, Fig. 2-1, 2-2). The bare centre muds (Fig. 2-3) are encircled by thiotrophic bacterial mats (Fig. 2-4, 2-5), which are surrounded by fields of pogonophoran tubeworms (Fig. 2-6). Interestingly, there is almost no overlap between the habitats of the different types of methanotrophs, indicating a strong environmental control. Previous microbiological studies had detected aerobic and anaerobic methane turnover at this cold seep, but did not identify the responsible key organisms or factors determining their distribution and activity[8,11].
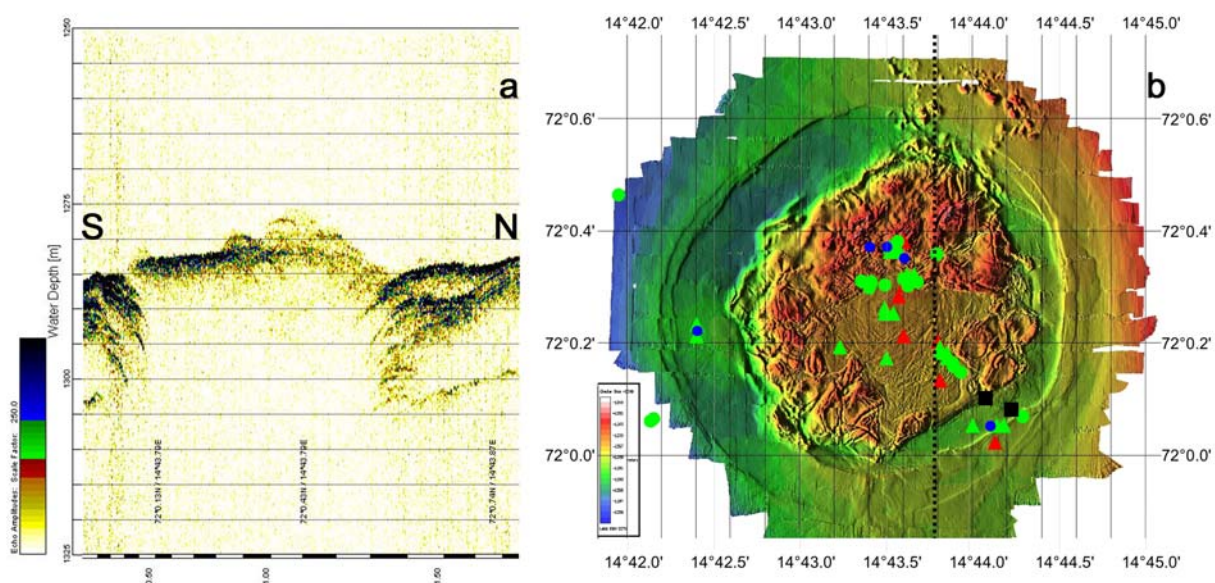
Figure 1. The Haakon Mosby Mud Volcano. a) Sediment echosounder image (PARASOUND) of a 1.8 km long profile crossing the mud volcano from south to north (see panel b for position). In the centre, the data do not show any mud layering, because the high gas content may considerably decrease penetration to high acoustic attenuation. At the northern and southern rims of the volcano, the signal penetration rises to around 30 m and a stack of sedimentary layers is displayed. Some of the layers could correspond to former mudflows. The black and white bars represent 100m horizontal distances. The y-axis (height) is 24-fold exaggerated. b) High-resolution bathymetric map of the HMMV showing sampling stations of POLARSTERN expedition ARK XIX/3b with ROV VICTOR 6000. Sediments were retrieved with ROV push cores (PC), TV guided multiple corer cores (TV-MUC), gravity corer cores (GC) and a TV guided grab sampler (TV-Grab). Water samples were obtained just above the sea floor with ROV PEP bottles (PEP) and from the water column with a CTD rosette (CTD) (data not shown here). The IFREMER software CARAIBES was used to process the microbathymetry data acquired by the multibeam echosounder (Reson SeaBat 8125 and EM2000, georeferenced by Posidonia USBL positioning) mounted on ROV VICTOR. The pink line indicates the position of the North-South PARASOUND transect (14° 43,8 E)[21].

The circular centre of the HMMV has a diameter of 500-600 m (~0.23 km^2), and consists of uniformly mixed, greyish, highly gassy clays. *In situ* profiling with microsensors in the centre showed that oxygen penetrated only a few mm into the seafloor (Fig. 2-3, Fig. 3a1). Exceptionally high cell numbers were detected in the top surface sediments, reaching $5.1 \pm 0.3 \times 10^9$ cells cm^{-3}, of which 50 ± 5 % belonged to type I aerobic methanotrophic bacteria of the order *Methylococcales* and *Methylophaga* (Fig. 2-3, Fig. 3a3). Accordingly, high concentrations of a ^{13}C-depleted, type I methanotroph specific fatty acid (FA; C16:1ω8c) were found in the same surface sediments (Fig. 3a4). Aerobic oxidation of methane (MOx) was restricted to the oxygenated surface of centre sediment, reaching ca. 0.9 mol m^{-2} yr^{-1} as estimated from integrated ^{14}CH$_4$ tracer turnover in the oxic zone of the sediments. The O$_2$ influx to this area was 1.3 mol m^{-2} yr^{-1} as determined by *in situ* microsensor profiling[12], indicating that oxygen is predominantly consumed by MOx, (molar MOx stoichiometry 1 CH$_4$:2 O$_2$). Most curiously, sulphate was depleted below 0.5 mM within the top few cm of seafloor, although sulphide was absent from the top 9 cm (Fig. 3a1). Anaerobic oxidation of methane (AOM) and sulphate reduction (SR) were below detection limit in the top 4 m of centre sediments based on push core and gravity core sampling. ANME cells were not detectable by FISH using all known ANME oligonucleotide probes. Furthermore, only minor amounts of AOM-related lipid biomarkers (<0.1 μg g-dw^{-1}) and low cell numbers (<<10^8 cells cm^{-3}) were found below 5 cm sediment depth (Fig. 3a3 and 3a4), reminiscent of the low biomass of deep biosphere microbial communities[13]. Obviously, the centre zone does not provide a habitat for AOM communities, despite the high methane concentrations in the sediments (recovered cores showed strong degassing). Concurrent to sulphate depletion, chloride concentrations dropped from 610 mM in bottom waters to <415 mM in the sediments (data not shown), indicating a significant upward flow of freshened subsurface fluids. High fluid flow velocities were also confirmed by *in situ* measurements and modelling of oxygen and temperature profiles[12]. Balancing upward flow with downward diffusion and local consumption, it was calculated that the rising subsurface fluids (3-6 m yr^{-1}) restrict availability of oxygen and sulphate, and hence the habitat for methanotrophs, to a few mm below seafloor in the active centre of HMMV[12].
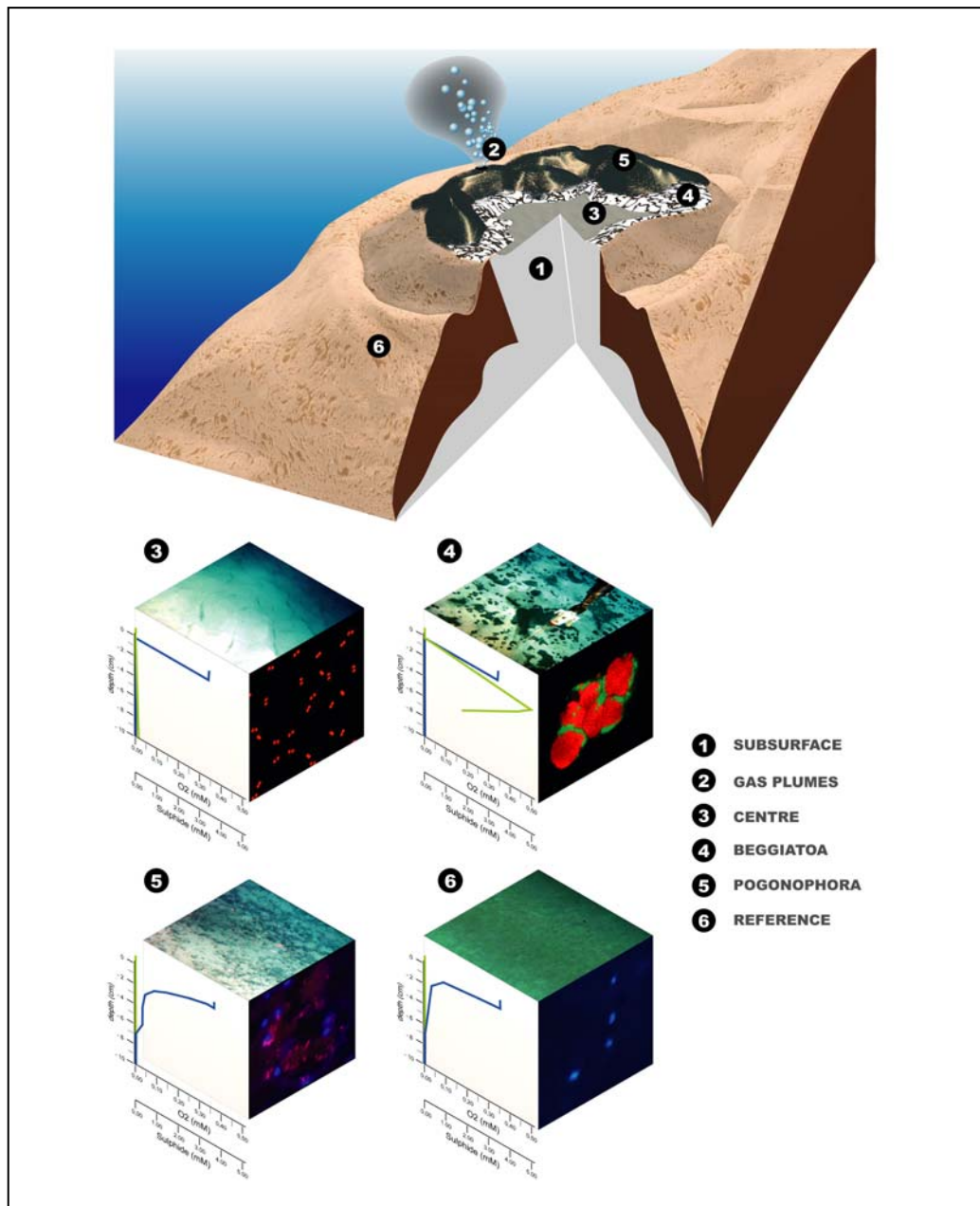
Figure 2. A schematic diagram of the different microbial habitats at HMMV. The vertical height is exaggerated ca. 50-fold. (2-1) Subsurface muds rising from a deep reservoir; (2-2) Gas and fluid channels in the northern centre of the volcano where free methane gas is released, immediately forming gas hydrate-coated methane bubbles and gas hydrate flakes in the water column[9]. The squares (2-3 to 2-6) show images of the seafloor on the top panel, idealized concentration gradients of oxygen and sulphide on the left panel and micrographs of the dominating microbial organisms on the right panel. (2-3) Central sediments colonized by aerobic methanotrophic bacteria (type I methanotrophs); (2-4) *Beggiatoa* mats covering sediments dominated by an ANME-3/DBB population; (2-5) Colonies of pogonophoran tubeworms harbouring symbiotic bacteria, which are probably aerobic methanotrophs according to the ^{13}C-depletion of the worm (micrograph: endosymbionts shown in pink, host nuclei shown in blue); (2-6) reference station at the flank of the volcano (1270 m water depth). Here, *in situ* oxygen penetration was >3 cm and no sulphate, chloride or temperature anomalies were found, suggesting that deviations associated with the mud volcano are related to fluid flow.

Encircling the mud volcano centre, a concentric area of 40-120 m width (~0.16 km^2) is covered by dense, patchy mats of sulphide-oxidizing bacteria (*Beggiatoa spp.*) (Fig. 2-4). *In situ* microsensor profiling into the *Beggiatoa* mats indicate a high sulphide production at 2-3 cm beneath the seafloor (Fig. 3b1), coinciding with a peak in AOM and SR (Fig. 3b2). In this layer, we found a novel consortium of archaea and sulphate-reducing bacteria (SRB) responsible for AOM. 16S rRNA gene analyses of DNA extracted from this layer revealed the presence of a cluster of archaeal sequences named ANME-3 (Supplement Fig. 1). Previously, single sequences of this cluster were only sporadically detected at seeps[14,15]. This investigation demonstrates their functioning as anaerobic methanotrophs. The AOM maximum (0.7 µmol cm^{-3} d^{-1}) at 2 cm below the *Beggiatoa* mats coincided with high numbers of microbial aggregates (20 × 10^6 aggregates cm^{-3}, i.e. 1.5 × 10^{10} cells cm^{-3} or 81% of total cell numbers) and elevated lipid biomarker concentrations (Fig. 3b3 and 3b4). Integrated *ex situ* AOM and SRR rates (Fig. 3b2) were equivalent to 4.5-5.5 mol m^{-2} yr^{-1}, i.e. ca. 5 times higher than average aerobic methane oxidation rates in the centre. Total sulphide production calculated from *in situ* microsensor profiles was 8.2 mol m^{-2} yr^{-1}. Stable C-isotope signatures of the archaeal lipids (*sn2*-hydroxyarchaeol, archaeol and penta-methyl-icosenes; all δ^{13}C-values <-98‰) indicated that methanotrophy is the main process for the build-up of archaeal biomass at this site. Interestingly, the ANME-3 form dense aggregates with a novel type of SRB (Fig. 2-4). Analyses of 16S rRNA genes and lipid biomarkers (substantial amounts of C17:1ω6c with a δ^{13}C of -70‰, see supplementary information) showed that the cells associated with ANME-3 are closely related to *Desulfobulbus* spp. (DBB). 95% of all ANME-3/DBB aggregates were found in the upper 4 cm below the *Beggiatoa* mats. Again, fluid flow velocities at this site provide the most likely explanation for their concentration in a very narrow depth horizon. In this area of HMMV, the upward porewater flow is ca. 0.3-0.6 m yr^{-1} [12]. *In situ* microsensor profiles show that oxygen penetrates only a few mm into the bacterial mats (Fig 3b1). Balancing upward fluid flow, consumption and downward diffusion of electron acceptors, it can be estimated that sulphate can penetrate only up to 4 cm beneath seafloor[12]. Accordingly, the active methanotrophic zone in the *Beggiatoa*-covered sediments is restricted to 1-4 cm beneath the seafloor, forming a thin horizon below the zone of oxygen penetration and above the zone of sulphate depletion.
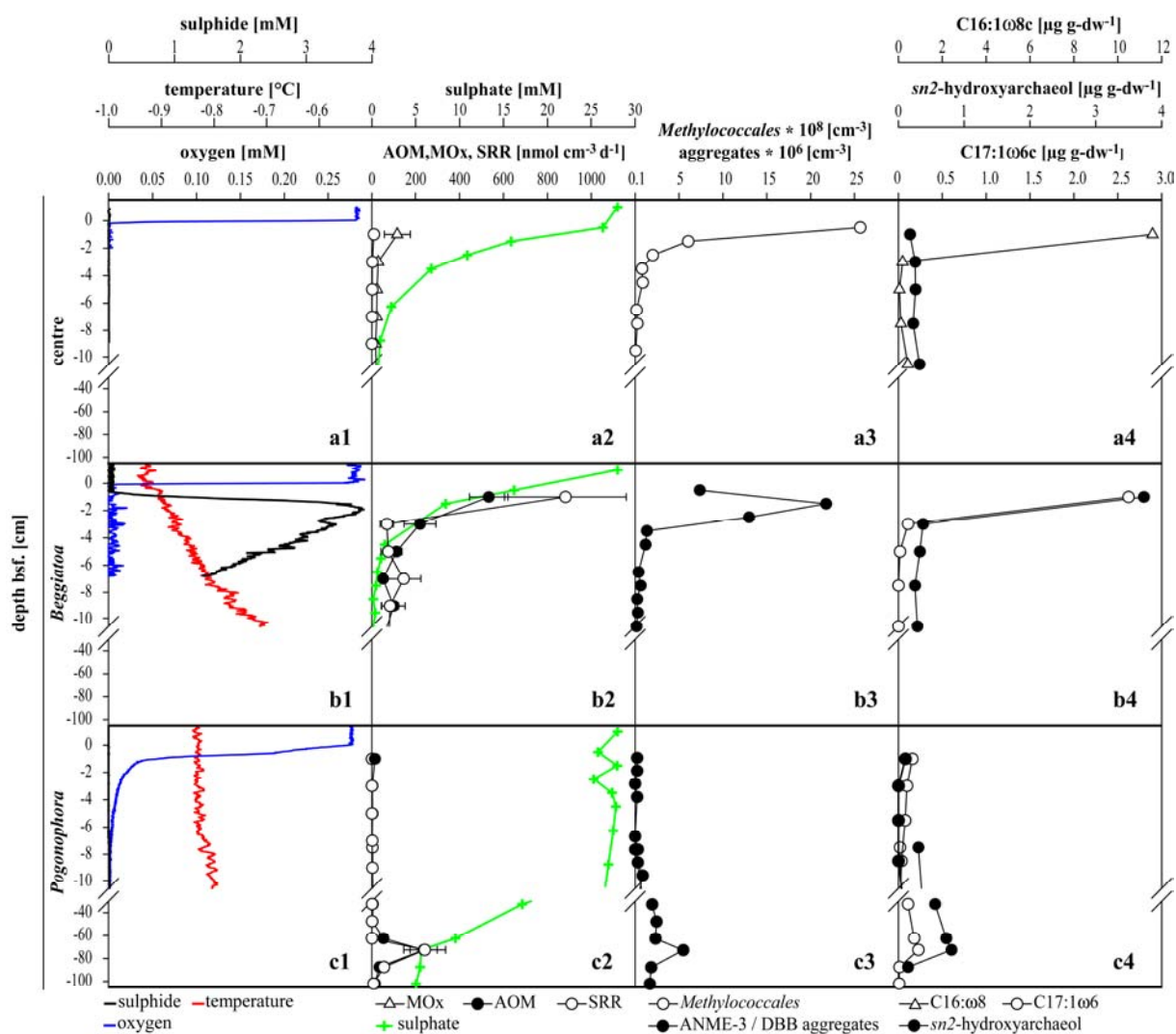
Figure 3. Vertical profiles of oxygen, sulphide and temperature (a1-c1); sulphate, *ex situ* methane and sulphate turnover (a2-c2), bacteria and aggregate counts (a3-c3) and selected lipid biomarker (a4-c4) from the centre (a), *Beggiatoa*-covered sediments (b) and the *Pogonophora* field (c). Oxygen, sulphide and temperature were measured *in situ* with microsensors mounted on a deep-sea profiling unit. AOM, SR, sulphate, cell and aggregate counts as well as lipid biomarker contents were determined using ROV pushcorer samples from the same sites.

The next major transition in HMMV habitats occurs about 300-400 m from its geographical centre, where the *Beggiatoa* mats are suddenly replaced by dense tubeworm colonies stretching over an area of about 0.4 km^2 around the HMMV (Fig. 2-5). Gravity cores from these tubeworm fields showed the presence of gas hydrates ca. 1 m below seafloor. Two pogonophoran species, *Oligobrachia haakonmosbiensis* and *Sclerolinum contortum*[16] populate this area of HMMV with biomasses of 1-2 kg wet weight m^{-2} (data not shown). *O. haakonmosbiensis* is a tubeworm of ca. 60 cm length and 0.5 mm diameter. The depleted

δ^{13}C-values (ca. -70 ‰) of lipids from the worm tissue indicate that the worms' carbon source is derived from methanotrophy (see supplementary information). In the pogonophoran fields, fluid flow rates were considerably lower than in the centre or bacterial mat area with <0.4 m yr^{-1} [12]. Balancing downward diffusion and upward fluid flow, sulphate penetration would theoretically be maximally 12 cm, without bioadvection by tubeworms. However, the measured deep oxygen and sulphate penetration in the tubeworm field (Fig. 2-5, 3c1) show that the tubeworms substantially increase the transport of electron acceptors into the sediments. Accordingly, the maximum in AOM was found at the base of the worm tubes (70 cm bsf), coinciding with a subsurface peak of ANME-3/DBB aggregates and their specific biomarker lipids (Fig. 3c2, 3c3, 3c4). Integrated methane turnover (without the potential methanotrophic activity of the tubeworm symbionts) was 7.1 mol m^{-2} yr^{-1}, indicating that total methane removal at this site is higher than in the other zones of HMMV, due to the bioadvection of oxygen and sulphate. In this regard, microbe-invertebrate symbioses have an advantage over free-living microbial populations because they can engineer their environment to increase access to both electron donor and electron acceptor by special migratory behaviour, mining, pumping and farming of benthic microbes[5,18,19].

In conclusion, we found that methane oxidation was the main energy source for biomass build-up in all different habitats of HMMV. Populations of aerobic or anaerobic methanotrophs comprised between 50-80% of the total microbial community (centre and *Beggiatoa* mat habitats). Whereas free-living methanotrophs reached 1-10 g C per m^2, the symbiotic, presumably methanotrophic, tubeworms even reached several kilograms of biomass per square meter. Total methane turnover in the Centre, *Beggiatoa* and *Pogonophora* habitats was 2, 8 and 28 × 10^5 mol yr^{-1}, respectively (sum 38 × 10^5 mol yr^{-1}). In comparison, methane emission to the hydrosphere from HMMV was estimated between 25 × 10^5 to 114 × 10^5 mol yr^{-1} [8,9], resulting in a total methane flux between 63-152 × 10^5 mol yr^{-1} (not including methane deposited as hydrate). Hence, the microbial filter at HMMV can control methane flux by 25% to 60%, which is a substantially lower than at other margin sites[1,7]. Our data suggest that porewater transport may be a main habitat-structuring factor at cold seep ecosystems, by regulating availability of electron acceptors. It is generally assumed that with increasing upward flow velocities, more dissolved methane is transported to the surface and

utilized by microbial communities, which adapt their population densities to the available energy. However, the fact that subsurface fluids of cold seep systems are generally depleted in electron acceptors introduces a negative switch in the fluid flow / microbial activity relationship: At increasing fluid flow rates, the downward diffusion of electron acceptors becomes increasingly limited. Here we have shown that the efficiency of the microbial filter against methane already decreases considerably at fluid flow rates >1m yr^{-1}, causing increased efflux of methane to the hydrosphere[9]. Velocities of decimetres to metres yr^{-1} are within the average range of fluid flow measured at cold seeps[17-20], hence the described inhibition of microbial methane consumption may be wide spread at seeps. Further quantitative *in situ* measurements of fluid flow and microbial methane consumption are necessary to constrain the relevance and control of methane emission from submarine mud volcanoes and other fluid-flow driven geo-bio-systems.

Methods

Sampling - Our studies took place during two cruises with R/V "L'Atalante" (2001) and R/V "Polarstern" (2003) both equipped with ROV "VICTOR 6000" as part of a French/German research initiative[21].Sediments were collected with gravity corers and ROV pushcores, and *in situ* microsensor profiles of temperature, oxygen, pH and sulphide were obtained along a radial transect from the centre to the east of the mud volcano (Fig. 1).

Sulphate reduction and methane oxidation rates - Microbial rates of aerobic (MOx) and anaerobic (AOM) methane oxidation and sulphate reduction (SR) in sediments were determined *ex situ* using $^{14}CH_4$ and $^{35}SO_4^{2-}$ tracers as described previously[5]. Directly after retrieval, sediment subsamples from the cores were transferred into 6 ml glass tubes or whole-injection cores, sealed with butyl rubber stoppers and $^{35}SO_4^{2-}$ and $^{14}CH_4$ was injected. Cores contained ca. 1 mM CH_4 during incubation. Glass tubes and cores were incubated for 24 h at *in situ* temperature before the SR and AOM reactions were stopped by mixing the sediment with 20% $ZnCl_2$ or 5% NaOH solution, respectively. MOx and AOM were distinguished according to the presence or absence of oxygen and SR during the tracer incubations. MOx, AOM and SR rate measurements on 3-5 replicate cores per area showed a standard error of 25 to 55% of the average value.

Lipid analysis - Lipid biomarker were extracted from frozen sediment samples and tubeworm tissue by successive sonication in solvent mixtures of decreasing polarity and further separated and derivatised as described previously[22,23] before injection into a HP 5890 Series II gas chromatograph equipped with a 50 m HP5 fused silica capillary column (0.32 mm i.d., 0.17 μm film thickness). Chromatographic conditions were as described previously[22] with slight modifications of the temperature gradient for the neutral lipid fraction. Column temperature was programmed from 60 to 150°C at a rate of 10°C min^{-1} and then at a rate of 4°C min^{-1} to 310°C (45 min isothermal). Compounds were identified on a Finnigan Trace MS. Stable carbon isotope composition of single compounds were determined using a HP 6890 Series gas chromatograph interfaced via a Combustion Interface III to a Finnigan Delta Plus isotope ratio mass spectrometer. Reported δ^{13}C-values (in per mill deviation from Pee Dee Belemnite, ‰) were corrected for the introduction of additional carbon atoms during derivatisation. δ^{13}C-values have an analytical error of ±1‰.

Fluorescence in situ hybridization - Cells of *Methylococcales* and ANME-3/DBB aggregates were quantified by FISH with monolabeled oligonucleotide probes according to previously described methods[14,24]. Novel probes used in this study were MetI-444 (CCTGCCTGTTTTCCTCCC) and MetII-844 (GCTCCACCACTAAGACCT) for HMMV type I methanotrophs, MPH-732 (GTAATGGCCCAGTGAGTC) for *Methylophaga* related species, and ANME3-1249 (TCGGAGTAGGGACCCATT) for ANME-3 archaea. For *Desulfobulbus* spp. we used probe 660[25].

Sulphate and chloride concentrations - Sulphate concentrations were determined from 5 ml sediment fixed in 50 ml corning vials with 25 ml zinc acetate solution (20%, w/v). An aliquot of the supernatant was injected into a Waters HPLC system (Waters 512 HPLC pump, I.C.-Pak anion-column, Waters WAT007355 4.6 x 50 mm, Waters 730 conductivity detector). Isophtalic acid (1mM) was used as a solvent at a constant flow rate of 1ml min^{-1}. Chloride concentrations were determined using a Metrohm[TM] 761 Compact IC with chemical suppression, equipped with a 250 x 4 mm ultra high capacity column (Metrosep[TM] A Supp 5) and a and conductivity detector. A carbonate buffer solvent (3.2 mM Na_2CO_3 / 1 mM $NaHCO_3$) was used at a flow of 0.7 ml min^{-1}. Total sulphate and chloride concentrations were corrected for porosity which was determined according to a previously described method[5].

Microsensor measurements - Microsensors, with tip diameters of ca. 20 μm, for oxygen, H_2S and pH were manufactured and used as described previously[26]. The sensors were calibrated after mounting on a deep sea profiling unit as described previously[27]. Total sulphide concentrations were calculated from H_2S and pH. The profiler was deployed on a free-falling lander or by a ROV. Profiles were recorded with a spatial resolution of 0.025 cm. A detailed description of in situ data and the geochemical models applied here is provided elsewhere[12].

References

1. Reeburgh, W. S. in *Microbial Growth on C_1 Compounds* (eds. Lidstrom, M. E. & Tabita, F. R.) 334-342 (Kluwer Academic Publishers, Dordrecht, 1996).

2. Hinrichs, K.-U., Hayes, J. M., Sylva, S. P., Brewer, P. G. & DeLong, E. F. Methane-consuming archaebacteria in marine sediments. *Nature* **398**, 802-805 (1999).

3. Boetius, A. et al. A marine microbial consortium apparently mediating anaerobic oxidation of methane. *Nature* **407**, 623-626 (2000).

4. Orphan, V. J., House, C. H., Hinrichs, K. U., McKeegan, K. D. & DeLong, E. F. Methane-consuming archaea revealed by directly coupled isotopic and phylogenetic analysis. *Science* **293**, 484-487 (2001).

5. Treude, T., Boetius, A., Knittel, K., Wallmann, K. & Jorgensen, B. B. Anaerobic oxidation of methane above gas hydrates at Hydrate Ridge, NE Pacific Ocean. *Marine Ecology Progress Series* **264**, 1-14 (2003).

6. Joye, S. B. et al. The anaerobic oxidation of methane and sulfate reduction in sediments from Gulf of Mexico cold seeps. *Chemical Geology* **205**, 219-238 (2004).

7. Hinrichs, K.-U. & Boetius, A. in *Ocean Margin Systems* (eds. Wefer, G., Billett, D. & Hebbeln, D.) 457-477 (Springer-Verlag, Berlin, Berlin, 2002).

8. Milkov, A. V. et al. Geological, geochemical, and microbial processes at the hydrate-bearing Haakon Mosby mud volcano: a review. *Chemical Geology* **205**, 347-366 (2004).

9. Sauter, E. et al. Methane discharge from a deep-sea submarine mud volcano into the upper water column by gas hydrate-coated methane bubbles. *Earth and Planetary Science Letters* (in press).

10. Damm, E. & Budéus, G. Fate of vent-derived methane in seawater above the Hakon Mosby mud volcano (Norwegian Sea). *Marine Chemistry* **82**, 1-11 (2003).

11. Pimenov, N. et al. Microbial processes of carbon cycle as the base of food chain of Håkon Mosby mud volcano benthic community. *Geo-Marine Letters* **19**, 89-96 (1999).

12. de Beer, D., Sauter, E., Niemann, H., Witte, U. & Boetius, A. In situ fluxes and zonation of microbial activity in surface sediments of the Håkon Mosby Mud Volcano. *Limnology and Oceanography* (accepted).

13. Parkes, R. J., Cragg, B. A. & Wellsbury, P. Recent studies on bacterial populations and processes in subseafloor sediments: A review. *Hydrogeology Journal* **8**, 11-28 (2000).

14. Knittel, K., Lösekann, T., Boetius, A., Kort, R. & Amann, R. Diversity and distribution of methanotrophic archaea at cold seeps. *Applied and Environmental Microbiology* **71**, 467-479 (2005).

15. Orphan, V. J. et al. Comparative analysis of methane-oxidizing archaea and sulfate-reducing bacteria in anoxic marine sediments. *Applied and Environmental Microbiology* **67**, 1922-1934 (2001).

16. Smirnov, R. V. Two new species of *Pogonophora* from the arctic mud volcano off northwestern Norway. *Sarsia* **85**, 141-150 (2000).

17. Wallmann, K. et al. Quantifying fluid flow, solute mixing, and biogeochemical turnover at cold vents of the eastern Aleutian subduction zone. *Geochimica et Cosmochimica Acta* **61**, 5209-5219 (1997).

18. Henry, P. et al. Interpretation of Temperature-Measurements from the Kaiko-Nankai Cruise - Modeling of Fluid-Flow in Clam Colonies. *Earth and Planetary Science Letters* **109**, 355-371 (1992).

19. Levin, L. A. et al. Spatial heterogeneity of macrofauna at northern California methane seeps: influence of sulfide concentration and fluid flow. *Marine Ecology Progress Series* **265**, 123-139 (2003).

20. Henry, P. et al. Fluid flow in and around a mud volcano field seaward of the Barbados accretionary wedge: Results from Manon cruise. *Journal of Geophysical Research-Solid Earth* **101**, 20297-20323 (1996).

21. Klages, M., Thiede, J. & Foucher, J. P. (eds.) The expedition ARKTIS XIX/3 of the research vessel Polarstern. (Alfred-Wegener-Institute for Polar and Marine Research, Bremerhaven, 2004).

22. Elvert, M., Boetius, A., Knittel, K. & Jorgensen, B. B. Characterization of specific membrane fatty acids as chemotaxonomic markers for sulfate-reducing bacteria involved in anaerobic oxidation of methane. *Geomicrobiology Journal* **20**, 403-419 (2003).

23. Niemann, H. et al. Methane emission and consumption at a North Sea gas seep (Tommeliten area). *Biogeosciences* **2**, 335-351 (2005).

24. Snaidr, J., Amann, R., Huber, I., Ludwig, W. & Schleifer, K. H. Phylogenetic analysis and in situ identification of bacteria in activated sludge. *Applied and Environmental Microbiology* **63**, 2884-2896 (1997).

25. Devereux, R., Kane, M. D., Winfrey, J. & Stahl, D. A. Genus-Specific and Group-Specific Hybridization Probes for Determinative and Environmental-Studies of Sulfate-Reducing Bacteria. *Systematic and Applied Microbiology* **15**, 601-609 (1992).

26. de Beer, D. et al. Transport and mineralization rates in North Sea sandy intertidal sediments, Sylt-Rømø Basin, Wadden Sea. *Limnology and Oceanography* **50**, 113-127 (2005).

27. Wenzhöfer, F. & Glud, R. N. Benthic carbon mineralization in the Atlantic: a synthesis based on in situ data from the last decade. *Deep-Sea Research Part I-Oceanographic Research Papers* **49**, 1255-1279 (2002).

Supplementary Information

16S rRNA gene analyses
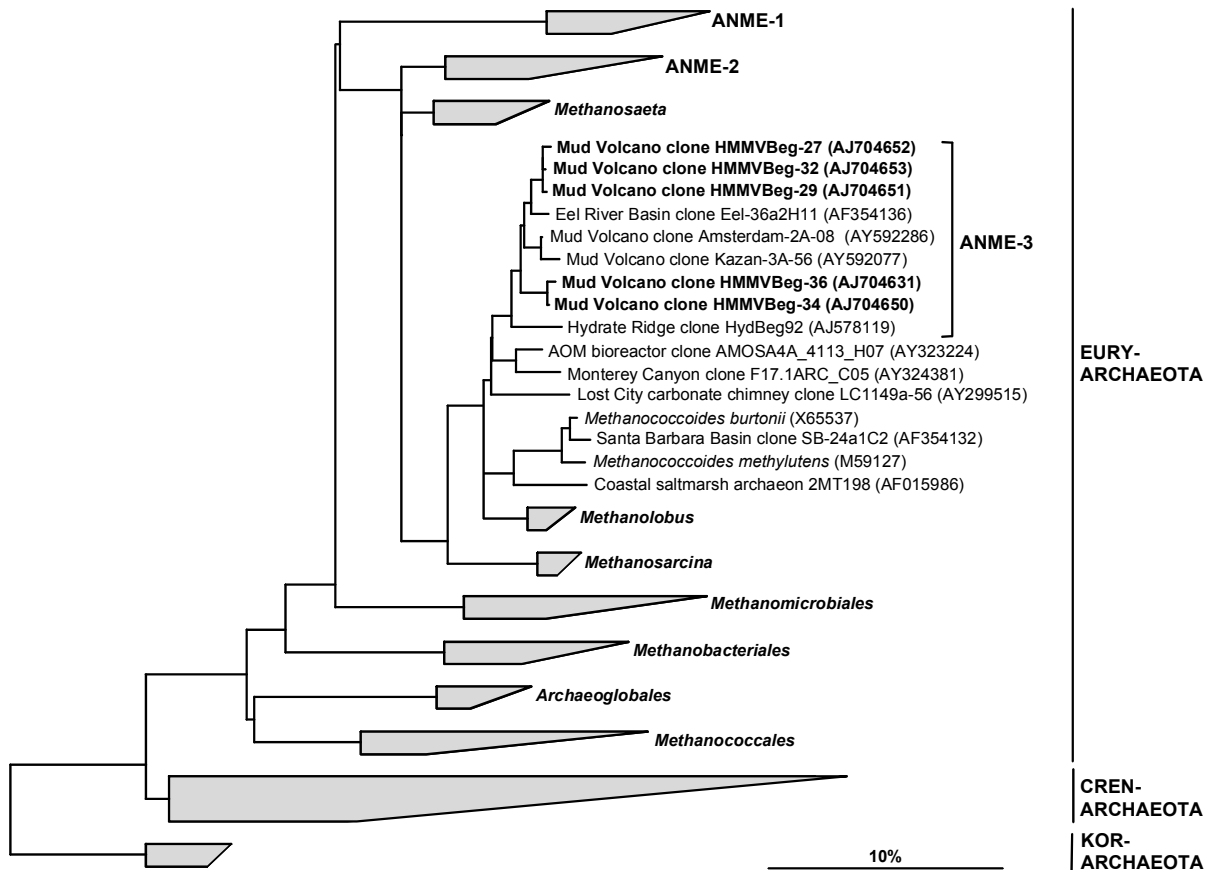
Figure S-1. Phylogenetic tree showing the affiliations of Haakon Mosby Mud Volcano 16S rRNA gene sequences to selected sequences of the domain *Archaea*. Using the ARB software package[1], the tree was calculated with nearly full-length sequences by maximum-likelihood analysis in combination with filters, which consider only 50% conserved regions of the 16S rRNA gene of *Archaea*. Branching orders that were not supported by all calculation methods are shown as multifurcations. Partial sequences were subsequently inserted into the reconstructed consensus tree by parsimony criteria, without allowing changes in the overall tree topology. Clone sequences from *Beggiatoa* covered HMMV sediments are in boldface type.

For comparative sequence analysis, a total of 67 clones carrying archaeal 16S rRNA gene sequences were obtained from HMMV near surface sediments covered with *Beggiatoa* mats. All sequences grouped and formed a new cluster within the order *Methanosarcinales*, termed ANME-3. This cluster has a distinct phylogenetic position and includes sequences from other methane seeps: the Eel River Basin[2], Hydrate Ridge[3], and Eastern Mediterranean Mud Volcanoes (Heijs et al., database release). All yet known ANME-3 16S rRNA gene sequences

are highly similar (95-100%) and targeted by probe ANME3-1249 as indicated by the brackets in Fig. S-1. Closest relatives were obtained from Monterey Canyon seep sediments[4] (95-98%), an AOM bioreactor with Monterey Canyon seep sediments[5] (94-97%), and a carbonate chimney of the Lost City hydrothermal vent field[6] (93-94%). Intriguingly, ANME-3 16S rRNA gene sequences were more closely related to cultivated methanogens (*Methanococcoides* spp., *and Methanolobus* spp., 95-96%) than any other ANME group.

Lipid biomarker signatures of the ANME-3 consortium

The sediments below Beggiatoa mats of HMMV are the first environment where ANME-3 populations have been found to dominate microbial biomass. Hence, we investigated the specific lipid biomarker fingerprint of ANME-3 in comparison to ANME-1 and -2. The archaeal lipids at this site were dominated by the glycerol diethers *sn2*-hydroxyarchaeol, archaeol and irregular isoprenoidal pentamethylicosenes (PMI) with four and five double bounds, all strongly depleted in ^{13}C ($\delta^{13}C$ <-98‰ vs. Pee Dee Belemnite). Neither PMIs with higher degrees of saturation, nor crocetane were detected, all of which are characteristic for ANME-1 and ANME-2 communities[7-11]. We conclude that dominant amounts of *sn2*-hydroxyarchaeol relative to archaeol, the presence of PMI's with five and four double bonds and the absence of other PMI's and crocetane are indicative for ANME-3.

Also for the first time, a new sulphate-reducing bacterium was identified as partner in an AOM consortium. 16S rRNA gene analysis in combination with FISH shows that a relative of *Desulfobulbus spp.* (DBB) is associated with ANME-3 at HMMV. Accordingly, high amounts of $C_{17:1\omega6c}$ were found, which was previously assigned as specific lipid biomarker to *Desulfobulbus spp.*[12,13]. This biomarker was also among the isotopically most depleted bacterial fatty acids retrieved from this site ($\delta^{13}C$: -70‰). In contrast, ANME-1 and ANME-2 are generally associated with sulphate-reducing bacteria of the *Desulfosarcina/Desulfococcus* (DSS) group[14,8,23]. DSS are characterised by dominant amounts of the FAs ai-$C_{15:0}$ and $C_{16:1\omega5c}$/cy$C_{17:1\omega5,6}$ when associated to ANME-1 or ANME-2, respectively[9,1511].

Lipid biomarker signatures of *Oligobrachia haakonmosbiensis*

Lipid analyses of whole tissue extracts of the pogonophoran worm *Oligobrachia haakonmosbiensis*[16] indicate that the worms carbon source is derived from methanotrophy. Lipids were extracted from the entire animal removed from its tube. Fatty acids of the worm

(e.g. cholesterol) and its symbiont (poly unsaturated fatty acids) were strongly depleted in ^{13}C with values of about -70‰ (methane $\delta^{13}C = -60$‰ at HMMV[17]). These values are typical for invertebrates harbouring methanotrophic symbionts[18].

1.   Ludwig, W. et al. ARB: a software environment for sequence data. *Nucleic Acids Research* **32**, 1363-1371 (2004).

2.   Orphan, V. J. et al. Comparative analysis of methane-oxidizing archaea and sulfate-reducing bacteria in anoxic marine sediments. *Applied and Environmental Microbiology* **67**, 1922-1934 (2001).

3.   Knittel, K., Lösekann, T., Boetius, A., Kort, R. & Amann, R. Diversity and distribution of methanotrophic archaea at cold seeps. *Applied and Environmental Microbiology* **71**, 467-479 (2005).

4.   Hallam, S. J., Girguis, P. R., Preston, C. M., Richardson, P. M. & DeLong, E. F. Identification of methyl coenzyme M reductase A (mcrA) genes associated with methane-oxidizing archaea. *Applied and Environmental Microbiology* **69**, 5483-5491 (2003).

5.   Girguis, P. R., Orphan, V. J., Hallam, S. J. & DeLong, E. F. Growth and methane oxidation rates of anaerobic methanotrophic archaea in a continuous-flow bioreactor. *Applied and Environmental Microbiology* **69**, 5472-5482 (2003).

6.   Schrenk, M. O., Kelley, D. S., Delaney, J. R. & Baross, J. A. Incidence and diversity of microorganisms within the walls of an active deep-sea sulfide chimney. *Applied and Environmental Microbiology* **69**, 3580-3592 (2003).

7.   Niemann, H. et al. Methane emission and consumption at a North Sea gas seep (Tommeliten area). *Biogeosciences* **2**, 335-351 (2005).

8.   Boetius, A. et al. A marine microbial consortium apparently mediating anaerobic oxidation of methane. *Nature* **407**, 623-626 (2000).

9.   Blumenberg, M., Seifert, R., Reitner, J., Pape, T. & Michaelis, W. Membrane lipid patterns typify distinct anaerobic methanotrophic consortia. *Proceedings of the National Academy of Sciences of the United States of America* **101** (2004).

10.   Elvert, M., Suess, E. & Whiticar, M. J. Anaerobic methane oxidation associated with marine gas hydrates: superlight C-isotopes from saturated and unsaturated C_{20} and C_{25} irregular isoprenoids. *Naturwissenschaften* **86**, 295-300 (1999).

11.   Elvert, M., Hopmans, E. C., Treude, T., Boetius, A. & Hinrichs, K.-U. Spatial variatons of archaeal-bacterial assambladges in gas hydrate bearing sediments at a cold seep: Implications from a high resolution molecular and isotopic approach. *Geobiology* **3**, 195-209 (2005).

12.   Taylor, J. & Parkes, R. J. The Cellular Fatty-Acids of the Sulfate-Reducing Bacteria, Desulfobacter Sp, Desulfobulbus Sp and Desulfovibrio-Desulfuricans. *Journal of General Microbiology* **129**, 3303-3309 (1983).

13.   Parkes, R. J. & Calder, A. G. The Cellular Fatty-Acids of 3 Strains of Desulfobulbus, a Propionate-Utilizing Sulfate-Reducing Bacterium. *Fems Microbiology Ecology* **31**, 361-363 (1985).

14. Knittel, K. et al. Activity, distribution, and diversity of sulfate reducers and other bacteria in sediments above gas hydrate (Cascadia margin, Oregon). *Geomicrobiology Journal* **20**, 269-294 (2003).

15. Elvert, M., Boetius, A., Knittel, K. & Jorgensen, B. B. Characterization of specific membrane fatty acids as chemotaxonomic markers for sulfate-reducing bacteria involved in anaerobic oxidation of methane. *Geomicrobiology Journal* **20**, 403-419 (2003).

16. Smirnov, R. V. Two new species of Pogonophora from the arctic mud volcano off northwestern Norway. *Sarsia* **85**, 141-150 (2000).

17. Damm, E. & Budéus, G. Fate of vent-derived methane in seawater above the Hakon Mosby mud volcano (Norwegian Sea). *Marine Chemistry* **82**, 1-11 (2003).

18. McKiness, Z. P., McMullin, E. R., Fisher, C. R. & Cavanaugh, C. M. A new bathymodioline mussel symbiosis at the Juan de Fuca hydrothermal vents. *Marine Biology* **148**, 109-116 (2005).

2

Novel Clusters of Aerobic and Anaerobic Methane Oxidizers at an Arctic Cold Seep (Haakon Mosby Mud Volcano, Barents Sea)

Tina Lösekann, Katrin Knittel, Thierry Nadalig, Helge Niemann,

Antje Boetius, and Rudolf Amann

Preliminary manuscript

Novel clusters of aerobic and anaerobic methane oxidizers at an Arctic mud volcano (Haakon Mosby Mud Volcano, Barents Sea)

Tina Lösekann[1], Katrin Knittel[1]*, Thierry Nadalig[2]†, Helge Niemann[1], Antje Boetius[1,3,4], and Rudolf Amann[1]

[1] Max Planck Institute for Marine Microbiology, Celsiusstrasse 1, 28359 Bremen, Germany

[2] Centre IFREMER de Brest, B.P. 70, 29280 Plouzane, France

[3] Alfred Wegener Institute for Polar and Marine Research, Am Handelshafen 12, 27515 Bremerhaven, Germany

[4] International University Bremen, Research II, Campusring 1, 28759 Bremen, Germany

†Present address: UMR 7156 Université Louis-Pasteur/CNRS, Département Microorganismes, Génomes, Environnement, 67083 Strasbourg Cedex, France

*Corresponding author. Mailing address: Max Planck Institute for Marine Microbiology, Celsiusstr. 1, D-28359 Bremen, Germany. Phone: 49 (0)4212028936. Fax: 49 (0)4212028580. E-Mail: kknittel@mpi-bremen.de.

Intended as an article in Applied and Environmental Microbiology
Section Microbial Ecology

Running title: Methane oxidizers at an Arctic mud volcano

ABSTRACT

Submarine mud volcanoes are formed by expulsions of mud, fluids and gases from deeply buried subsurface sources. They are often associated with intensive methane seepage and form highly reduced benthic habitats. In this study, the microbial diversity and community structure in methane rich sediments of the Haakon Mosby Mud Volcano (HMMV) was investigated by comparative sequence analysis of 16S rRNA genes and fluorescence *in situ* hybridization. In the active volcano center, which has a diameter of about 500 m, the main methane-consuming process was the bacterial aerobic oxidation. In this zone, aerobic methylotrophs belonging to three bacterial clusters that are closely affiliated with *Methylobacter* and *Methylophaga* species accounted for 55 ± 9% of total cells. In sediments covered with *Beggiatoa* mats encircling the center of the HMMV, a new group of archaea (ANME-3) was identified, dominating the zone of anaerobic methane oxidation. The ANME-3 cluster belongs to the *Euryarchaeota* and is most closely related to *Methanosarcinales*. ANME-3 form cell aggregates mostly associated with sulfate-reducing bacteria of the *Desulfobulbus* (DBB) branch. These ANME-3/DBB aggregates were highly abundant and accounted for 95 ± 2% of total cells. At the outer rim of the mud volcano the seafloor was colonized by tubeworms (*Siboglinidae*, formerly known as *Pogonophora*). Here, both aerobic and anaerobic methane oxidizers were found, however, in lower abundances compared to the inner part of the HMMV. Methane consumption in the tubeworm area might be dominated by the tubeworms' endosymbionts. Our results show that the HMMV represents an ecosystem depending on methanotrophy. The specific geostructure of this cold water deep-sea habitat offers distinct niches on scales of several hundred meters for all main phylogenetic types of microbial methanotrophs known to exist in the ocean.

INTRODUCTION

Large amounts of methane are stored in the ocean as crystalline gas hydrate or as free gas. Most of the methane released from these subsurface sources is consumed by microorganisms in anoxic subsurface sediments (54). This microbially mediated anaerobic oxidation of methane (AOM) reduces the emission of the greenhouse gas methane from the ocean to the atmosphere significantly [(21) and references therein].

The metabolic process of AOM is proposed to be a reversed methanogenesis coupled to the reduction of sulfate involving methanotrophic archaea (ANME) and sulfate-reducing bacteria (SRB). ANME archaea and SRB are assumed to interact syntrophically (23) and form microbial consortia that oxidize methane with equimolar amounts of sulfate, yielding

bicarbonate and sulfide (23, 43, 44). Sulfide produced as a by-product of AOM at cold seeps often supports chemosynthetic communities that derive energy from its oxidation. Two archaeal clades (ANME-1, ANME-2) oxidize methane under anoxic conditions (48, 49). ANME-2 archaea belonging to the order *Methanosarcinales* are associated with SRB of the *Desulfosarcina-Desulfococcus* branch forming structured consortia ["shell type" and "mixed type"; (3, 29)]. ANME-1 archaea, distantly related to *Methanosarcinales* and *Methanomicrobiales*, occur in sediments as single cells (29, 48) and aggregated cells (49) or are associated with SRB in microbial mats ["mat type" consortia; (29, 40)].

Neither ANME archaea nor their sulfate-reducing bacterial partners have been isolated in pure culture and the enzymes and biochemical pathways of AOM remain unknown. However, recent metagenomic studies have identified a modified methyl-coenzyme M-reductase ("methanase") that may catalyze the activation of methane under anoxic conditions (17, 18, 31).

While AOM reduces significantly the efflux of methane to the atmosphere, the microbially mediated aerobic oxidation of methane appears to be only a minor biological sink of methane in the ocean. Known aerobic methanotrophs belong to *Alpha-* and *Gammaproteobacteria* and depend on the availability of oxygen (19). Hence, in marine habitats aerobic methanotrophs are restricted to the oxic water column, the sediment-water interface or they exist as symbionts of mussels, clams and tubeworms.

This study provides for the first time a quantitative analysis of the composition and distribution of microbial communities at an active mud volcano. Offshore mud volcanoes are geological features formed as a result of the emission of semi-liquid material (mud breccia) extruded from deep sediment layers on the seafloor (11) and are often associated with methane seepage. This also applies to the Haakon Mosby Mud Volcano (HMMV), which has been discovered in 1990 (68) and is the only mud volcano in a polar region studied in greater detail [e.g. (7, 15, 16, 22, 33, 41, 51, 52, 58, 69, 70)]. According to Kopf (2003) (30), the contribution of mud volcanoes to the global methane emission ranges between 0.4% and 22.7% and may be underestimated in global carbon budgets.

MATERIAL AND METHODS

Site description and sample collection. The HMMV is an active cold seep, situated at the Norwegian-Barents-Spitzbergen continental margin (72° 00.25'N, 14° 43.50'E) in a water depth of 1250 m. Sediment samples were collected in August 2001 and June/July 2003 during joint cruises of the Alfred Wegener Institute and IFREMER with the research vessels

"L'Atalante" and "Polarstern", respectively, and the remotely operated vehicle (ROV) "VICTOR 6000" (IFREMER) in the framework of a German/French collaborative program (27). During dives with VICTOR 6000 signs of recent mud expulsion were observed in the northern part of the HMMV. The center is a flat circular area of about 500 m in diameter (230 m^2). It is encircled by sulfidic sediments covered by dense *Beggiatoa* mats in a stretch of about 40-120 m width (160 m^2). The outer rim of HMMV is composed of hill and trench sections, elevated by about 1-8 m compared to the center, and covered by dense accumulations of thread-like tubeworms *(Siboglinidae)* for a zone of 60-200 m (400 m^2). The two dominant species have been identified as *Sclerolinum contortum* and *Oligobrachia haakonmosbiensis* (59). The tubes of the worms have a diameter of a few mm and reach lengths of up to 60 cm. Only a small part of the tube extends up to 5 cm into the water column, whereas the main part is buried in the sediments. Siboglinid tubeworms are known to harbor endosymbionts, which can be either thiotrophic or methanotrophic (57, 61).

Sediment samples were recovered by video-guided multiple corer or ROV-operated push cores at different zones of HMMV: center sediments (two cores called "center": 72° 00.26'N, 14° 43.0'E; 72° 00.25'N, 14° 43.49'E), sediments underlying *Beggiatoa* mats (three cores called "*Beggiatoa* mat": 72° 00.26'N, 14° 43.00'E; 72° 00.16'N, 14° 43.88'E; 72° 00.18'N, 14° 43.85'E), and sediments colonized by siboglinid tubeworms (three cores called "tubeworm field": 72° 00.08'N, 14° 43.39'E; 72° 00.06'N, 14° 42.13'E; 72° 00.05'N, 14° 44.18'E). The sediment biogeochemistry of the sampled sites is described in detail in Niemann *et al.* (submitted) (46).

DNA extraction. Cores were sectioned in 1 cm thick layers and frozen at -20°C for DNA extraction at the home laboratory. Total community DNA was directly extracted from 2 g of wet sediments [center (72° 00.26'N, 14° 43.0'E) and mats (72° 00.26'N, 14° 43.00'E): 0-5 cm depth, tubeworms (72° 00.08'N, 14° 43.39'E): 6-17 cm depth] using the method of Zhou et al. (1996) (72). Crude DNA was purified with the Wizard DNA Clean-Up Kit (Promega, Madison, WI).

PCR amplification and clone library construction. Domain-specific primers were used to amplify almost full-length 16S rRNA genes from the extracted and purified chromosomal DNAs: for *Bacteria* primers GM3F [*E. coli* 16S rRNA position 0008 (42)] and EUB1492 (26), and for *Archaea* primers 20f (38) and Uni1392R (32) or 20f and Arch958R (9) were used. PCRs were performed with a Mastercycler Gradient (Eppendorf, Hamburg, Germany) as described previously (53). The annealing temperatures for amplification of archaeal 16S rRNA genes were 58°C, and for bacterial genes 42°C. PCR products of several reactions

were combined and purified with the QiaQuick PCR Purification Kit (Qiagen, Hilden, Germany). DNA was ligated in the pGEM T-Easy vector (Promega, Madison, WI) or the pCR4 TOPO vector (Invitrogen, Carlsbad, CA) and transformed into *E. coli* TOP10 cells (Invitrogen, Carlsbad, CA) according to the manufacturer's recommendations.

ARDRA. Clones known to contain the correctly sized insert of ca. 1.4 kb or 0.95 kb, respectively, were screened by amplified rRNA gene restriction analysis (ARDRA) in order to identify unique environmental clones. Two restriction enzymes (*Hae*III and *Rsa*I) were used for screening as described previously (53).

Sequencing and phylogenetic analysis. At least one representative of each ARDRA pattern was chosen for phylogenetic analysis. Sequencing was performed by *Taq* cycle sequencing with a model ABI377 sequencer (Applied Biosystems) with vector primers and universal rRNA gene specific primers. The presence of chimeric sequences in the clone libraries was determined with the CHIMERA_CHECK program of the Ribosomal Database Project II (http://rdp.cme.msu.edu/html/analyses.html). Potential chimeras were eliminated before phylogenetic trees were constructed. Sequence data were analyzed with the ARB software package (35). Phylogenetic trees were calculated by parsimony, neighbor-joining, and maximum-likelihood analysis with different sets of filters. For tree calculation, only almost full-length sequences (>1315 bp) were considered. Partial sequences were inserted into the reconstructed tree by parsimony criteria without allowing changes in the overall tree topology.

Fluorescence *in situ* hybridization (FISH). Subsamples of sediment cores were sliced into 1 cm intervals and fixed for 3-4 h with 3% formaldehyde (final concentration), washed twice with 1xPBS (10 mM sodium phosphate, 130 mM NaCl) and finally stored in 1xPBS/EtOH (1:1) at -20°C. Fixed samples were diluted 1:10 and treated by mild sonication for 20 s with a MS73 probe (Sonopuls HD70, Bandelin, Germany) at an amplitude of 42 μm and a power of <10 W. For FISH, an aliquot was filtered on 0.2 μm GTTP polycarbonate filters (Millipore, Eschborn, Germany). Hybridization with monolabeled probes and microscopy counts of hybridized and 4´,6´-diamidino-2-phenylindole (DAPI)-stained cells were performed as described previously (60). *In situ* hybridizations with horseradish peroxidase (HRP)-conjugated probes followed by tyramide signal amplification (CARD) were carried out to enhance the intensity of dim signals and performed as described by Pernthaler *et al.* (2002) (50), except for the cell wall permeabilization. For permeabilization of rigid archaeal cell walls, agarose embedded filters were incubated in 0.01 M HCl for 10 min at room temperature, subsequently incubated in 0.1 M HCl (1 min) or 1% Triton X-100 (10 min), and finally washed in MilliQ water and dehydrated in absolute ethanol. Hybridized samples were

examined with an epifluorescence microscope (Axiophot II microscope; Carl Zeiss, Jena, Germany). For each probe and sample 700-1000 DAPI-stained cells in 10-20 independent microscopic fields were counted. Micrographs of microbial aggregates were taken with a confocal laser scanning microscope (LSM510; Carl Zeiss, Jena, Germany). Monolabeled oligonucleotides were purchased from ThermoHybaid (Ulm, Germany), HRP-conjugated probes from Biomers (Ulm, Germany). Probe sequences and formamide concentrations required for specific hybridization are given in Table 1. The specificity of new probes was evaluated against reference strains having one or more mismatches.

Total cell counts and size measurements of ANME-3 aggregates. Total counts of individual cells were done by epifluorescence microscopy after staining with acridine orange according to the method of Meyer-Reil (1983) (39). Aggregate counts were done after *in situ* hybridization with probe Arch915 specific for the domain *Archaea*. Microbial aggregates stained with probe Arch915 were regarded as AOM consortia and later identified as ANME-3 consortia. Three individual cores recovered from sediments covered with *Beggiatoa* mats were examined for aggregate abundance. Total cell counts were defined as the sum of single cells plus an estimate on the number of the aggregated cells present in AOM consortia. Since the single cells per aggregate cannot be counted quantitatively, a semi-quantitative method was applied. In total, 172 individual aggregates of the sediment horizon with highest aggregate abundance at the *Beggiatoa* site of 2001 (1-2 cm) were measured after staining with DAPI. Average volumes were 150 μm^3 for spherical aggregates and 330 μm^3 for non-spherical aggregates. Cell numbers in the aggregates were calculated on the assumption that aggregates are either spheres or cylinders consisting of ANME-3 cells with a volume of 0.2 μm^3. Since most aggregates were associated with only very few SRB (compare Fig. 4), SRB cell numbers were neglected during calculation. The average volume of a spherical aggregate comprises approximately 750 ANME-3 cells, whereas cylindrical aggregates are built up on average from 1,650 ANME-3 cells. The observed ratio of spheres:cylinders (73:27) was taken into account, resulting in an average cell number of roughly 1,000 ANME-3 cells per HMMV aggregate. This estimate was corrected by the packing density η (74%, http://mathworld.wolfram.com/SpherePacking.html) for the closest packing of spheres resulting in an average cell number of 740 ANME-3 cells per HMMV aggregate.

Nucleotide sequence accession numbers. The sequence data reported here will appear in the EMBL, GenBank, and DDBJ nucleotide sequence databases under the accession no. AJ579313 to AJ579330 and no. AJ704631 to AJ704724.

TABLE 1 Oligonucleotide probes used in this study

Probe	Specificity	Probe sequence (5´-3´)	Target site[a] 16S rRNA positions	% FA[b]	Reference
NON338	Negative control	ACTCCTACGGGAGGCAGC	338-355	10	(70)
EUB338 I-III	most *Bacteria*	GCTGCCTCCCGTAGGAGT GCAGCCACCCGTAGGTGT GCTGCCACCCGTAGGTGT	338-355	35	(5)
Arch915	most *Archaea*	GTGCTCCCCGCCAATTCCT	915-935	35	(1)
DSS658	*Desulfosarcina* spp., *Desulfofaba* spp., *Desulfococcus* spp., *Desulfofrigus* spp.	TCCACTTCCCTCTCCCAT	658-685	60	(36)
DSV698	*Desulfovibrio* spp.	GTTCCTCCAGATATCTACGG	698-717	35	(36)
DSR651	*Desulforhopalus* spp.	CCCCCTCCAGTACTCAAG	651-668	35	(36)
DSB985	*Desulfobacter* spp., *Desulfobacula* spp.	CACAGGATGTCAAACCCAG	985-1003	20	(36)
DBB660	*Desulfobulbus* spp.	GAATTCCACTTTCCCCTCTG	660-679	60	(9)
DBB305	Subgroup of *Desulfobulbus* related sequences	AGTGCCAGTGTGACGGAT	305-322	25	This study
CF319a	*Cytophaga/Flavobacterium*	TGGTCCGTGTCTCAGTAC	319-336	35	(35)
MetI-444	HMMV-MetI (*Gammaproteobacteria*)	CCTGCCTGTTTTCCTCCC	444-461	60	(45)
MetII-844	HMMV-MetII (*Gammaproteobacteria*)	GCTCCACCACTAAGACCT	844-861	75	(45)
MPH-732	HMMV-MPH (*Gammaproteobacteria*)	GTAATGGCCCAGTGAGTC	732-749	40	(45)
ANME1-350	ANME-1 archaea	AGTTTTCGCGCCTGATGC	350-367	40	(3)
EelMS932	ANME-2 archaea	AGCTCCACCCGTTGTAGT	932-949	40	(3)
ANME3-397[c]	ANME-3 archaea	ATATGCTGGCACTCAGTG	397-414	40	(45)
ANME3-1249[d]	ANME-3 archaea	TCGGAGTAGGGACCCATT	1249-1266	20/40[d]	This study
Cren-444[c]	HMMV-Cren (*Crenarchaeota*)	CCCCCAGCTTTATACACT	444-461	55	This study

[a] *E. coli* numbering (4).
[b] Percent (Vol/Vol) formamide (FA) in hybridization buffer for FISH.
[c] Non-group hit with 0 weighted mismatches: *Methanohalobium evestigatum*.
[d] HRP-conjugated probe

RESULTS

Bacterial diversity in HMMV sediments. Three different sediment samples were selected for 16S rRNA gene library construction according to observed differences in sediment surface coverage: center sediment, sediment beneath *Beggiatoa* mats, and sediment from the tubeworm field. The composition of the bacterial 16S rRNA gene libraries varied significantly between the different sampling sites (Table 2).

Lowest bacterial diversity was observed in methane rich, oxic sediments of the volcano center. More than 90% of the clone sequences retrieved from this site (67/72) were related to methylotrophic *Gammaproteobacteria* (*Methylobacter*, *Methylophaga*; Fig. 1), whereas only few sequences (5/72) grouped within two other phylogenetic lineages, namely the *Cytophaga/Flavobacterium/Bacteroidetes* (CFB) and the WCHB1 cluster [sequences isolated from a hydrocarbon- and chlorinated-solvent-contaminated aquifer (14)].

The CFB phylum was the only group detected in all sites and clearly dominated the clone library constructed from methane rich, anoxic sediments covered with *Beggiatoa* mats

(59/132). Additionally, methylotrophic *Gammaproteobacteria* (37/132) and *Deltaproteobacteria* (22/132) related sequences were abundant at this site.

Bacterial diversity was highest in the clone library from the tubeworm site. There was a dominance of diverse deltaproteobacterial sequences (Table 2, Fig. 2) in these bioirrigated sediments. In contrast to the other sites, *Gammaproteobacteria* related sequences were not found. Other phylogenetic lineages that contain 1-9 clone sequences (i.e. 10% of total clones) included the *Actinobacteria, Acidobacterium/Holophaga*, *Planctomycetes*, *Verrucomicrobia*, *Betaproteobacteria*, the *Nitrospira* lineage, *Firmicutes*, and the uncultured WCHB1 and OP8 lineages. Many HMMV 16S rRNA gene clones showed high sequence similarity of more than 97% to sequences of uncultivated microorganisms from methane-rich habitats.

TABLE 2 Phylogenetic affiliations and frequencies of bacterial 16S rDNA clones

Phylogenetic affiliation	Next cultivated relative	% 16S rRNA gene similarity	No. of clones			
			Total	Center	*Beggiatoa*	Tubeworm
Gammaproteobacteria						
HMMV-MetI + HMMV-MetII	*Methylobacter marinus*	89-97	93	60	33	0
HMMV-MPH	*Methylophaga sulfidovorans*	89-93	15	7	4	0
	Legionella cincinnatiensis	85	1	0	1	0
Deltaproteobacteria						
	Desulfosarcina variabilis	90-96	14	0	1	13
	Desulfobacterium catecholicum	92-96	11	0	5	6
	Bacteriovorax stolpii	90-96	6	0	6	0
	Desulfonema magnum	92-93	4	0	4	0
	Desulfobacterium anilini	84-93	4	0	0	4
	Nitrospina gracilis	81	4	0	4	0
	Bdellovibrio bacteriovorus	76-83	3	0	0	3
	Desulfobulbus mediterraneus	93-94	2	0	0	2
	Desulfotignum balticum	86-91	2	0	0	2
	Desulfobacula phenolica	91-94	2	0	2	0
	Desulfofacinum infernum	85-88	2	0	0	2
	Desulfomonile tiedjei	88	1	0	0	1
	Desulfonatronum lacustre	79	1	0	0	1
Bacteriodetes						
Flexibacteraceae	*Cytophaga* sp.	89-100	67	4	57	6
Saprospiraceae	*Saprospira grandis*	89-100	2	0	2	0
WCHB1	no cultivated rel.	--	9	1	8	0
Actinobacteria	*Rubrobacter xylanophilus*	79-81	3	0	2	1
Acidobacterium/Holophaga						
	Acidobacterium capsulatum	78-82	3	0	0	3
	Geothrix fermentans	84	1	0	1	0
Planctomycetales	*Pirellula marina*	82-85	2	0	0	2
Verrucomicrobia	*Verrucomicrobium spinosum*	74-85	2	0	1	1
Betaproteobacteria	*Nitrosospira* sp.	97	1	0	0	1
Nitrospira	*Nitrospira marina*	81	1	0	0	1
Firmicutes	*Anaerovorax odorimutans*	89	1	0	1	0
Candidate division OP8	no cultivated rel.	--	1	0	0	1
Total no. of clones			258	72	132	50

Methylotrophic gammaproteobacterial groups HMMV-MetI, HMMV-MetII, and HMMV-MPH. All HMMV clone sequences related to aerobic methylotrophic *Gammaproteobacteria* were retrieved from surface sediments of the HMMV center (67/72) or from the adjacent *Beggiatoa* area (37/132). Sediments at both sites were methane-rich and showed an *in situ* oxygen penetration depth of only a few mm or less (8). Three sequence clusters could be defined: HMMV-MetI, HMMV-MetII, and HMMV-MPH (Fig. 1). HMMV-MetI and -MetII were most abundant in the libraries, closely related to each other and their members belong to the order *Methylococcales*. HMMV-MetI 16S rRNA gene sequences were closely related (94-97%) to sequences of methanotrophic mussel symbionts (12, 13). HMMV-MetII were most similar (96-99%) to clone sequence Hyd24-1 from gas hydrate bearing sediments of Hydrate Ridge (28). *Methylobacter marinus* was the closest cultivated relative of both clusters (89-97%). The third gammaproteobacterial cluster HMMV-MPH was related (87-94%) to the genus *Methylophaga*. The most similar sequences (92-100%) were obtained from marine bacterioplankton.
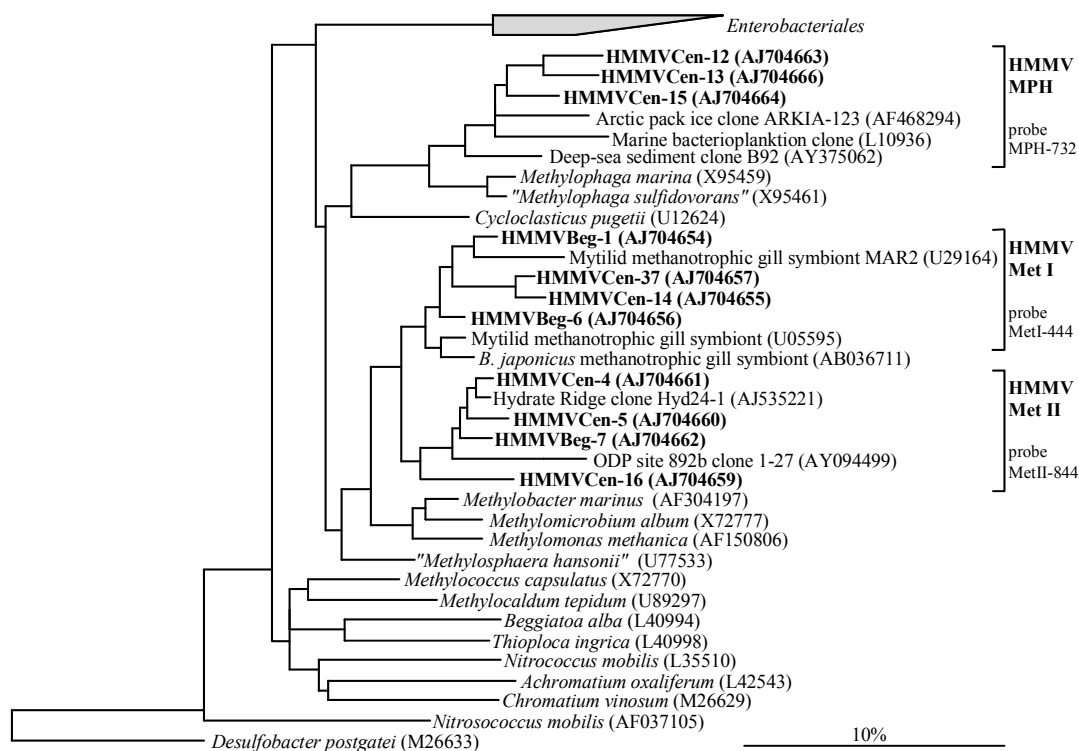
FIGURE 1 Phylogenetic tree showing the affiliations of Haakon Mosby Mud Volcano 16S rDNA clone sequences to selected sequences of the *Gammaproteobacteria*. The tree was calculated with nearly full-length sequences by maximum-likelihood analysis in combination with filters, which consider only 50% conserved regions of the 16S rRNA. Branching orders that were not supported by all calculation methods are shown as multifurcations. Partial sequences were subsequently inserted into the reconstructed consensus tree by parsimony criteria, without allowing changes in the overall tree topology. Clone sequences from HMMV sediments are in boldface type: clones HMMVCen-*, center sediments; clones HMMVBeg-*, *Beggiatoa* site. The bar represents 10% estimated phylogenetic divergence.

Deltaproteobacteria. Sequences within the *Deltaproteobacteria* were highly diverse (Fig. 2). Almost all known orders *(Desulfovibrionales, Desulfobacterales, Synthrophobacterales, Bdellovibrionales)* were represented. The majority of HMMV sequences was derived from the tubeworm site (34/50) and related to completely oxidizing *Desulfosarcina* and *Desulfobacterium* species (maximum similarity 96%). Sediments populated with siboglinid tubeworms were oxic in the upper 10 cm (8) and probably had the highest input of organic carbon other than methane, e.g. worm exudates and sedimented particles trapped by the worm tubes, supporting a variety of heterotrophic bacteria. Most clone sequences from sediments underlying *Beggiatoa* mats fell into the recently defined seep-specific clusters of sulfate-reducing bacteria, SEEP-SRB1, -SRB3, and -SRB4 [*Desulfobulbaceae, Desulfobacteraceae* (28)]. Additionally, non-SRB sequences of the *Deltaproteobacteria* were also present in HMMV clone libraries (Table 2). A minor fraction of clone sequences (3/50) was related to *Bacteriovorax stolpii* (90-91%). *Bacteriovorax* spp. and relatives are aerobic, obligatory predatory bacteria that forage on a wide variety of susceptible Gram-negative microorganisms (2) and thereby may control bacterial abundance. They have been found in a wide range of aquatic habitats, e.g. in freshwater and marine sediments, and biofilms (25).

Archaeal diversity in HMMV sediments. Three archaeal 16S rRNA gene libraries were constructed from center sediment, sediment beneath *Beggiatoa* mats, and sediment from the tubeworm field. ARDRA analysis revealed a rather low phylogenetic diversity. Five different archaeal groups became evident (Fig. 3). Three groups belonged to the *Euryarchaeota* and two groups to the *Crenarchaeota*. The differences between the sampling sites were pronounced. Libraries from the *Beggiatoa* site were dominated by a novel archaeal cluster named ANME-3 (29). In contrast, the marine benthic group C dominated the center sediments and ANME-3 sequences were not detected. Archaeal sequences recovered from the tubeworm site showed again the highest diversity of all three sites and included sequences affiliated with ANME-1 archaea *(Euryarchaeota)* as well as with marine benthic group B, C and marine group I archaea *(Crenarchaeota)*.

FIGURE 2 Phylogenetic tree showing the affiliations of Haakon Mosby Mud Volcano 16S rDNA clone sequences to selected sequences of the *Deltaproteobacteria*. The tree was calculated with nearly full-length sequences by maximum-likelihood analysis in combination with filters, which consider only 50% conserved regions of the 16S rRNA of *Deltaproteobacteria*. Branching orders that were not supported by all calculation methods are shown as multifurcations. Partial sequences were subsequently inserted into the reconstructed consensus tree by parsimony criteria, without allowing changes in the overall tree topology. Clone sequences from HMMV sediments are in boldface type: clones HMMVCen-*, center sediments; clones HMMVBeg-*, *Beggiatoa* site; clone HMMVPog-*, tubeworm site. The bar represents 10% estimated phylogenetic divergence.
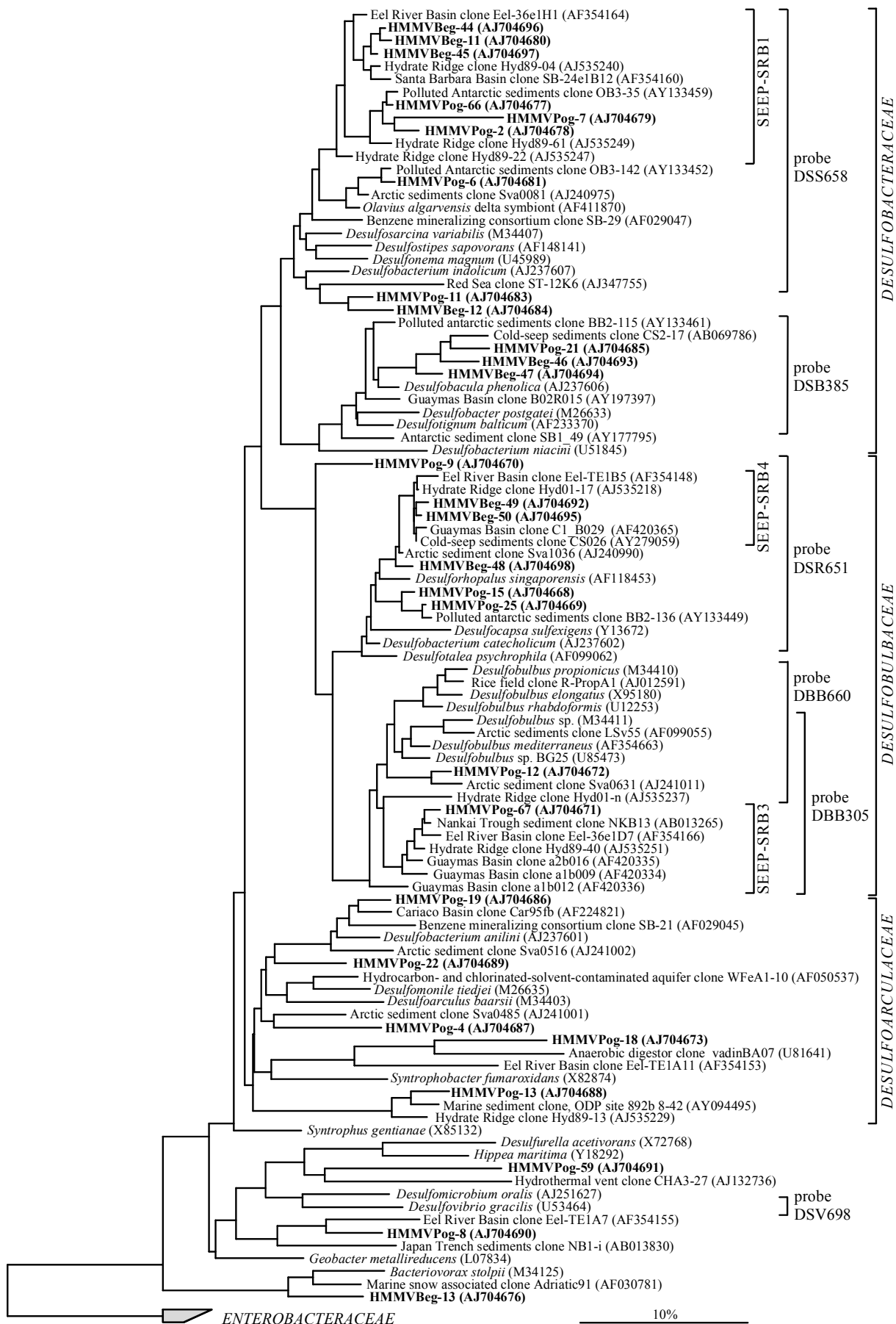
Euryarchaeota. All archaeal clone sequences retrieved from the *Beggiatoa* site (48/48) grouped forming a sequence cluster referred to as ANME-3. ANME-3 16S rRNA gene sequences are closely related (86-96%) to those of *Methanosarcinales* (Fig. 3). The ANME-3 cluster includes clone sequences from other methane seeps, the Eel River Basin (47), Hydrate Ridge (29) and the Amsterdam/Kazan mud volcanoes of the eastern Mediterranean (S. K. Heijs *et al.*, database release). The sequence similarity of ANME-3 16S rRNA gene sequences is high (97-99%). Although the ANME-3 group does not include any cultivated species, it is more closely related to the cultivated genera *Methanosarcina*, *Methanococcoides*, *Methanohalophilus*, *Methanolobus* than the two groups of *Euryarchaeota* so far linked to AOM, ANME-1 and ANME-2. ANME-3 sequences are most similar (93-96%) to *Methanococcoides burtonii* (GenBank acc. no. X65537). ANME-3 sequences were recovered neither from center sediments nor from sediments of the tubeworm site.

Sequences belonging to group ANME-1, which was repeatedly found at other AOM sites [(20, 29, 47, 62-64); T. P. Tourova *et al.*, database release; S. K. Heijs *et al.*, database release] have also been retrieved from HMMV sediments, but only in low numbers (4/44) and from sediments populated with siboglinid tubeworms. So far, no sequences affiliated with ANME-2 were retrieved from HMMV surface sediments.

Crenarchaeota. In oxic sediments from the center all sequences (67/67) belonged to the marine benthic group C (MBGC). This group is often found in marine sediments [(5, 34, 63, 67); Schäfer *et al.*, database release]. Within MBGC HMMV sequences form a separate branch (hereafter "HMMV-Cren") of highly similar sequences often exceeding 99% similarity. The closest relative was a clone sequence derived from a subsurface geothermal water stream (H. Hirayama *et al.*, database release). Most sequences retrieved from the tubeworm site (40/44) were affiliated with the marine benthic group B (MBGB, alternatively designated as DSAG) and marine group I (MGI) (67). The MBGB is generally associated with methane rich surface and subsurface environments (24, 29).

FIGURE 3 Phylogenetic tree showing the affiliations of Haakon Mosby Mud Volcano 16S rDNA clone sequences to selected sequences of the domain *Archaea*. The tree was calculated with nearly full-length sequences by maximum-likelihood analysis in combination with filters, which consider only 50% conserved regions of the 16S rRNA of *Archaea*. Branching orders that were not supported by all calculation methods are shown as multifurcations. Partial sequences were subsequently inserted into the reconstructed consensus tree by parsimony criteria, without allowing changes in the overall tree topology. Clone sequences from HMMV sediments are in boldface type: clones HMMVCen-*, center sediments; clones HMMVBeg-*, *Beggiatoa* site; clone HMMVPog-*, tubeworm site. The bar represents 10% estimated phylogenetic divergence. MBG: marine benthic group; MG: marine group.
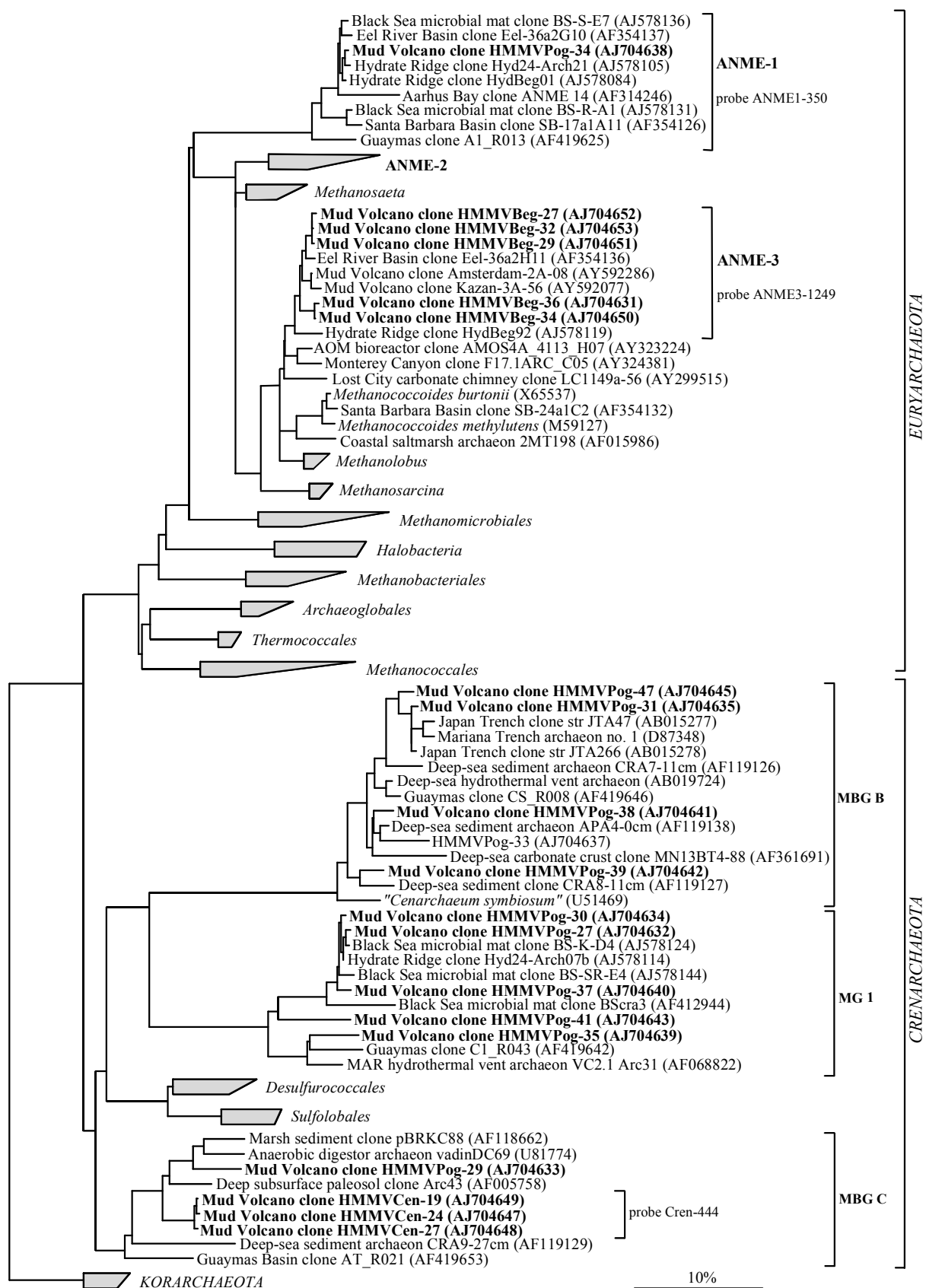
Black Sea microbial mat clone BS-S-E7 (AJ578136)
Eel River Basin clone Eel-36a2G10 (AF354137)
Mud Volcano clone HMMVPog-34 (AJ704638)
Hydrate Ridge clone Hyd24-Arch21 (AJ578105)
Hydrate Ridge clone HydBeg01 (AJ578084)
Aarhus Bay clone ANME 14 (AF314246)
Black Sea microbial mat clone BS-R-A1 (AJ578131)
Santa Barbara Basin clone SB-17a1A11 (AF354126)
Guaymas clone A1_R013 (AF419625)

ANME-1

probe ANME1-350

ANME-2

Methanosaeta

Mud Volcano clone HMMVBeg-27 (AJ704652)
Mud Volcano clone HMMVBeg-32 (AJ704653)
Mud Volcano clone HMMVBeg-29 (AJ704651)
Eel River Basin clone Eel-36a2H11 (AF354136)
Mud Volcano clone Amsterdam-2A-08 (AY592286)
Mud Volcano clone Kazan-3A-56 (AY592077)
Mud Volcano clone HMMVBeg-36 (AJ704631)
Mud Volcano clone HMMVBeg-34 (AJ704650)
Hydrate Ridge clone HydBeg92 (AJ578119)
AOM bioreactor clone AMOS4A_4113_H07 (AY323224)
Monterey Canyon clone F17.1ARC_C05 (AY324381)
Lost City carbonate chimney clone LC1149a-56 (AY299515)
Methanococcoides burtonii (X65537)
Santa Barbara Basin clone SB-24a1C2 (AF354132)
Methanococcoides methylutens (M59127)
Coastal saltmarsh archaeon 2MT198 (AF015986)
Methanolobus

ANME-3

probe ANME3-1249

Methanosarcina

Methanomicrobiales

Halobacteria

Methanobacteriales

Archaeoglobales

Thermococcales

Methanococcales

EURYARCHAEOTA

Mud Volcano clone HMMVPog-47 (AJ704645)
Mud Volcano clone HMMVPog-31 (AJ704635)
Japan Trench clone str JTA47 (AB015277)
Mariana Trench archaeon no. 1 (D87348)
Japan Trench clone str JTA266 (AB015278)
Deep-sea sediment archaeon CRA7-11cm (AF119126)
Deep-sea hydrothermal vent archaeon (AB019724)
Guaymas clone CS_R008 (AF419646)
Mud Volcano clone HMMVPog-38 (AJ704641)
Deep-sea sediment archaeon APA4-0cm (AF119138)
HMMVPog-33 (AJ704637)
Deep-sea carbonate crust clone MN13BT4-88 (AF361691)
Mud Volcano clone HMMVPog-39 (AJ704642)
Deep-sea sediment clone CRA8-11cm (AF119127)
"Cenarchaeum symbiosum" (U51469)

MBG B

Mud Volcano clone HMMVPog-30 (AJ704634)
Mud Volcano clone HMMVPog-27 (AJ704632)
Black Sea microbial mat clone BS-K-D4 (AJ578124)
Hydrate Ridge clone Hyd24-Arch07b (AJ578114)
Black Sea microbial mat clone BS-SR-E4 (AJ578144)
Mud Volcano clone HMMVPog-37 (AJ704640)
Black Sea microbial mat clone BScra3 (AF412944)
Mud Volcano clone HMMVPog-41 (AJ704643)
Mud Volcano clone HMMVPog-35 (AJ704639)
Guaymas clone C1_R043 (AF419642)
MAR hydrothermal vent archaeon VC2.1 Arc31 (AF068822)

MG 1

Desulfurococcales

Sulfolobales

Marsh sediment clone pBRKC88 (AF118662)
Anaerobic digestor archaeon vadinDC69 (U81774)
Mud Volcano clone HMMVPog-29 (AJ704633)
Deep subsurface paleosol clone Arc43 (AF005758)
Mud Volcano clone HMMVCen-19 (AJ704649)
Mud Volcano clone HMMVCen-24 (AJ704647)
Mud Volcano clone HMMVCen-27 (AJ704648)
Deep-sea sediment archaeon CRA9-27cm (AF119129)
Guaymas Basin clone AT_R021 (AF419653)

probe Cren-444

MBG C

CRENARCHAEOTA

10%

KORARCHAEOTA

High *in situ* abundance of free-living methylotrophs in center sediments. Total cell numbers were up to $3.6 \pm 2.1 \times 10^9$ cells cm^{-3} in the uppermost sediment layers and decreased to $1.5 \pm 0.7 \times 10^7$ cells cm^{-3} in 9-10 cm sediment depth (Table 4). FISH detection rates using monolabeled oligonucleotide probes were high with up to 98% of DAPI cell counts. Five 16S rRNA targeted FISH probes have been developed for the clone clusters HMMV-MetI, -MetII, and HMMV-MPH, which are all affiliated with aerobic methylotrophs (Fig. 1). Abundances of target cells were determined in two separate cores retrieved from the HMMV center. Bacteria of cluster HMMV-MetI (probe MetI-444) were most abundant with $48 \pm 2\%$ of total cells and clearly dominated the microbial community in center sediments (Table 3). This percentage corresponds to an absolute number of $1.7 \pm 0.9 \times 10^9$ cells cm^{-3} sediment. HMMV-MetI cells were mainly diplococci of a diameter of 0.7 μm. A second morphotype of MetI-444 was constituted of large cocci of about 2 μm diameter. They occurred in clusters of three or more cells (Fig. 4-1A). The DAPI staining of the clustered cells was irregular, indicating the presence of intracellular membrane systems characteristically for aerobic methanotrophs (19). HMMV-MetI abundance decreased slightly with sediment depth to $26 \pm 11\%$ of total cells in 9-10 cm sediment depth. A second probe (MetI-851) designed for the same cluster confirmed the high abundance of HMMV-MetI at the sediment surface (data not shown). HMMV-MetII (probe MetII-844) could also be detected *in situ*, but in a lower abundance with a maximum of $1.1 \pm 1.3 \times 10^8$ cells cm^{-3} in 0-1 cm sediment depth (Table 3). In general, HMMV-MetII cells occurred as irregular shaped cocci with an average diameter of 1-2 μm (Fig. 4-1B). The identity of HMMV-MetII was confirmed by a second probe (MetII-457) with the same specificity (data not shown). The third abundant clone group in center sediments, HMMV-MPH, which is related to *Methylophaga*, was targeted with probe MPH-732. HMMV-MPH cells accounted for $5 \pm 4\%$ at the sediment surface and abundance decreased with depth. Target cells were morphologically uniform and occurred as small (<1 μm) oval cells (Fig. 4-1C). In addition to aerobic methanotrophs up to 33% of the cells were detected with probe CF319a. Deltaproteobacterial groups (*Desulfosarcina-Desulfococcus* group, *Desulfovibrio*, *Desulforhopalus*, *Desulfobacter*, *Desulfobacula*, *Desulfobulbus*) were detected in low numbers near the detection limit of <0.5%.

Detection rates of *Archaea* ranged from <1% to 17% of total cells, with a maximum in 6-7 cm sediment depth. Members of the crenarchaeotal group HMMV-Cren, which was the only clone group in our archaeal clone library from center sediments, were detected *in situ* but in low abundance (<1%) using probe Cren-444. Target cells were on average 5 μm long, slender rods and occurred as single cells or in chains of up to 10 cells. ANME-1, ANME-2

and ANME-3 archaea could not be detected *in situ* and the major part of *Archaea* at the center site remained unidentified. Most likely, the probe for the crenarchaeal group needs further development and CARD-FISH must be applied to achieve higher detection rates.

High *in situ* abundance of ANME-3 aggregates below *Beggiatoa* mats. Sediments from the *Beggiatoa* area contained a high amount of consortia consisting of archaea and bacteria. Two new probes (ANME3-1249 and ANME3-397) were designed to target specifically ANME-3 sequences (Fig. 3). Both probes identified the coccoid cells in the consortia as ANME-3 cells (0.7 µm diameter). All ANME-3 cells were autofluorescent under UV excitation, indicating the presence of coenzyme F_{420}, which is a characteristic feature of methanogens (66). Hybridization signals of the monolabeled probe ANME3-1249 were dim; therefore we used HRP-labeled probes for CARD-FISH (50), which resulted in much brighter signals. The associated bacteria were identified as rod-shaped SRB (1.1 × 0.5 µm) affiliated with *Desulfobulbus* species (DBB) using the already available probe 660 (10) and a newly designed probe (DBB305). The detected consortia of ANME-3 archaea and SRB of the *Desulfobulbus* branch are in the following referred to as "ANME3/DBB aggregates". The ANME-3/DBB aggregates are mainly built by "shell-type" spheres (29). Mostly several spheres are aligned to an overall cylindrical morphology. Often the DBB layer formed only an incomplete outer shell (Fig. 4-2A/B). Sometimes the acridine orange staining showed the presence of an exopolysaccharide matrix (EPS) enclosing several aggregates. The size spectrum of the diameter of ANME-3/DBB consortia ranged from 2-50 µm with an average diameter of 5 ± 3 µm for spherical aggregates and a diameter of 5 ± 3 and height of 10 ± 5 µm for cylindrical aggregates (several spherical aggregates together). Very few consortia were detected with a yet unidentified bacterial partner. These ANME-3/EUB aggregates were mostly spheres and showed a "mixed-type" morphology, i.e. archaea and bacteria were completely mixed and appeared to grow in direct association (Fig. 4-2D). Almost 25% of HMMV aggregates occurred without any bacterial partners. These monospecific ANME-3 aggregates were more tightly packed, had a spherical morphology and were enclosed by an EPS. High ANME-3/DBB aggregate numbers were restricted to the sediments below the *Beggiatoa* mat (1-3 cm depth) with $1.9 \pm 0.6 \times 10^7$ cm^{-3} sediment (Table 4). Aggregate numbers decreased by two orders of magnitude below 4 cm sediment depth. Calculated cell numbers in the ANME-3 aggregates accounted for 57-95% of total cells (up to 1.5×10^{10} cells cm^{-3}) comprising the major part of the microbial biomass in a 0-5 cm sediment depth interval at the *Beggiatoa* site. In oxic center sediments no ANME-3/DBB aggregates could be detected.

TABLE 3 Quantification of single cells by FISH

Depth [cm]	Bacteria (EUB338 I-III)	Archaea (Arch915)	Deltaproteobacteria				Cytophaga/ Flavobacterium (Cf319a)	HMMV Met I (Met I-444)	HMMV Met II (Met II-844)	HMMV MPH (MPH-732)
			(DSS658)	(DSV698)	(DSR651)	(DSB985)		$\bar{x} \pm SD^a$		
						Center sediment				
0-1	91	<1	0	<0.5	<1	<0.5	23	48 ± 2	3 ± 2	5 ± 4
1-2	97	<1	0	0	0	0	33	44 ± 5	5 ± 0	3 ± 4
2-3	89	6	0	0	<0.5	<0.5	22	43 ± 11	4 ± 2	3 ± 4
3-4	90	9	0	<0.5	0	0	14	43 ± 2	2 ± 1	3 ± 4
4-5	83	8	0	0	<0.5	0	24	33 ± 8	6 ± 4	<1 ± 0
6-7	64	17	ND	ND	ND	ND	22	36 ± 2	1 ± 1	ND
7-8	80	14	0	0	0	0	23	35 ± 13	0 ± 0	<1 ± 0
9-10	61	13	0	<0.5	ND	ND	21	26 ± 11	0 ± 0	ND
						Beggiatoa mat				
0-1	51	<1	4	<0.5	3	<0.5	23	8 ± 1	1 ± 1	<1 ± 0
1-2	40	2	4	<0.5	3	<0.5	16	4 ± 1	1 ± 1	<1 ± 0
2-3	38	2	6	0	<0.5	0	7	4 ± 1	<1 ± 0	ND
3-4	42	4	4	0	0	0	18	1 ± 0	0 ± 0	0 ± 0
4-5	35	4	16	<0.5	0	0	10	<1 ± 0	0 ± 0	ND
6-7	32	6	7	0	ND	ND	ND	ND	ND	0 ± 0
7-8	33	7	12	0	0	0	10	0 ± 0	0 ± 0	ND
8-9	30	22	17	0	ND	ND	10	ND	ND	0 ± 0
9-10	27	25	5	0	0	0	6	0 ± 0	0 ± 0	ND
						Tubeworm field				
0-1	27	<0.5	3	<0.5	<0.5	0	4	0 ± 0	0 ± 0	ND
1-2	22	2	4	<0.5	<0.5	0	10	ND	ND	0 ± 0
2-3	28	3	4	0	<0.5	0	4	0 ± 0	0 ± 0	ND
3-4	18	<0.5	2	<0.5	2	<0.5	<1	ND	ND	0 ± 0
6-7	12	1	6	<0.5	<0.5	<0.5	2	0 ± 0	0 ± 0	ND
7-8	16	<1	5	<1	<0.5	<0.5	2	0 ± 0	0 ± 0	ND
8-9	12	<1	4	1	<0.5	0	<1	ND	ND	0 ± 0
9-10	22	1	7	2	<0.5	0	<0.5	0 ± 0	0 ± 0	ND
12-13	18	1	12	<0.5	<0.5	0	<0.5	ND	ND	0 ± 0
13-14	19	<1	12	<0.5	<1	0	<0.5	0 ± 0	0 ± 0	ND

Numbers are given in percentage of DAPI detected single cells. FISH probe names are in parentheses; for probe specificity confer to Table 1. ND, not determined.
[a] Multiple independent MUC cores were examined for spatial variability: two cores of center sediments, three cores each of sediments covered with *Beggiatoa* mats and sediments from the tubeworm field.

Single cells below *Beggiatoa* mats. FISH detection of single bacterial cells with probe EUB338 I-III was highest near the sediment surface (0-1 cm sediment depth) with 51% of DAPI single cell counts and decreased with depth to a minimum of 27% in 9-10 cm. In contrast, detection rates for single cell archaea increased with sediment depth from 1% at the surface to 25% of single archaeal cells in 9-10 cm (Table 3). Single ANME-3 cells were also observed in *Beggiatoa* sediments, when CARD-FISH was performed. These cells have an oval morphology (Fig. 4-2E) and accounted for 4% of total single cells in 1-2 cm sediment depth. Neither ANME-1 nor ANME-2, which have been found at most other AOM sites, nor the crenarchaeotal group HMMV-Cren, which are the dominant phylotype in center sediments, were detectable at the *Beggiatoa* site.

The CFB cluster dominated the bacterial community beneath the *Beggiatoa* mat, with up to 23% of total single cells in the upper sediment layers. Most targeted cells were short rods, but also slender rods and filaments occurred that could be barely detected by DAPI staining. *Gammaproteobacteria* of the aerobic methanotrophic clusters HMMV-MetI and -MetII were also detected in 0-4 cm sediment depth. HMMV-MetI and -MetII accounted for $9 \pm 2\%$ of total single cells ($3.9 \pm 2.5 \times 10^8$ cells cm^{-3}) in 0-1 cm sediment depth. In deeper sediments layers no hybridized cells were detectable. Members of the *Desulfosarcina/Desulfococcus* branch dominated the SRB community in deeper sediment layers (4-10 cm) with up to 17%. The second dominant SRB population in sediments below *Beggiatoa* mats was related to *Desulforhopalus* species, however, with a much lower relative abundance of only up to 3% in 0-2 cm depth. Single cells of *Desulfobulbus, Desulfovibrio*, *Desulfobacterium* and *Desulfobacula* were below the detection limit of <0.5%.

Bacterial and archaeal abundance in sediments of the tubeworm field. In sediments populated with siboglinid tubeworms, ANME-3/DBB aggregates were detected throughout the sediment core, but with an order of magnitude lower abundance than at the *Beggiatoa* site (max. $6 \pm 5 \times 10^5$ aggregates cm^{-3}, Table 4). FISH detection rates of single cells at the tubeworm site were much lower than at the *Beggiatoa* and center site with a maximum of 32%. In the single cell fraction *Bacteria* dominated and *Archaea* were only found in numbers near the detection limit of <0.5%. Members of the *CFB* cluster were most abundant at this site with up to 10% of total single cells (Table 3). *Gammaproteobacteria* of HMMV specific sequence clusters HMMV-MetI, -MetII and HMMV-MPH were not detectable. The SRB community was dominated *in situ* by complete oxidizers of the *Desulfosarcina-Desulfococcus* branch (12%). Abundance of *Desulforhopalus* species peaked in 3-4 cm sediment depth (2%). *Desulfovibrio* related cells were at the other sampling sites near the detection limit, but one single peak accounting for 2% of total single cells occurred in sediments of the tubeworm site in 9-10 cm sediment depth. Abundance of *Desulfobacterium* and *Desulfobacula* related species was near the detection limit of <0.5%. In contrast to the *Beggiatoa* and center site, ANME-1 archaea were detected (Table 4), but were near the detection limit of <0.5%. ANME-2 cells or members of the HMMV-Cren group were not detected. Unfortunately, we did not sample deeper sediment horizons for FISH counts beneath the roots of the tubeworms, which showed a high AOM activity (46).
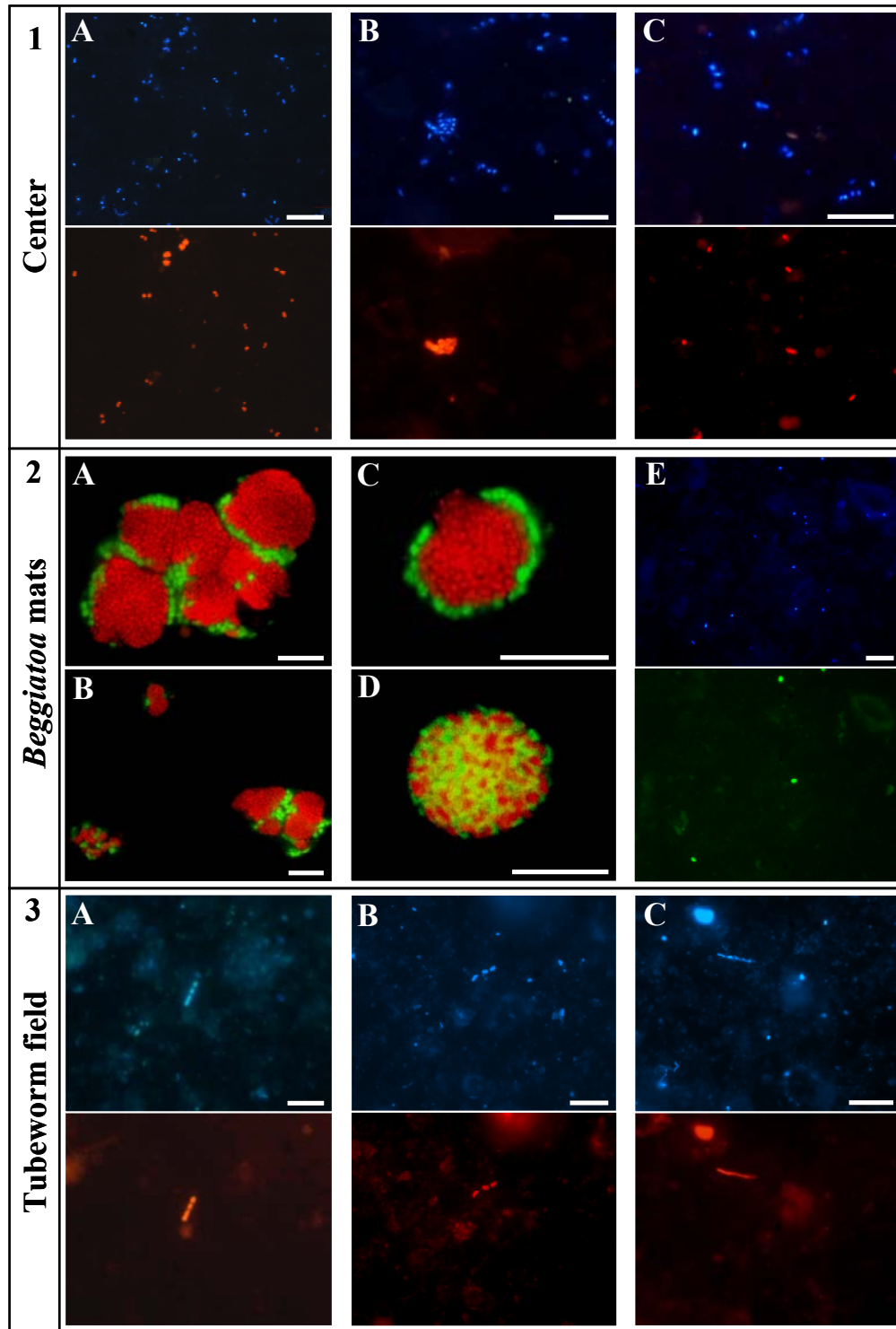
FIGURE 4 Epifluorescence micrographs after *in situ* hybridization with 16S rRNA targeted oligonucleotide probes. Center: DAPI staining and FISH with probes MetI-444 (1A), MetII-844 (1B), MPH-732 (1C) specific for aerobic methanotrophic/methylotrophic bacteria. *Beggiatoa* mat: Color overlays of shell type consortia, probe ANME3-1249 specific for ANME-3 archaea shown in red and probe DBB660 specific for *Desulfobulbus* spp. shown in green (2A-C); color overlay of mixed type consortium, probe ANME3-1249 specific for ANME-3 archaea shown in red and probe EUB338 I-III specific for *Bacteria* shown in green (2D); DAPI staining and CARD-FISH with probe ANME3-1249 showing single ANME-3 cells in green (2E). Tubeworm field: DAPI staining and FISH with probe ANME1-350 specific for ANME-1 archaea (3A), probe DSS658 specific for the *Desulfosarcina/Desulfococcus* branch (3B), and probe Cf319a specific for *Cytophaga/Flavobacterium* (3C). Scale bars, 10 μm.

TABLE 4 Quantification of ANME archaea and total cells

Depth [cm]	Aggregate counts [Aggregates ×10^6/ml] $\bar{x} \pm SD^a$	Total single cell counts [cells ×10^9/ml] $\bar{x} \pm SD^a$	Total cell counts [cells ×10^9/ml] $\bar{x} \pm SD^a$	Aggregated cells Total cells $\bar{x} \pm SD^a$	ANME-1 archaea (ANME1-350)
		Center sediment			
0-1	0.0 ± 0.0	3.6 ± 2.1	3.6 ± 2.1	0.0 ± 0.0	0
1-2	0.0 ± 0.0	1.1 ± 0.1	1.1 ± 0.1	0.0 ± 0.0	ND
2-3	0.0 ± 0.0	0.3 ± 0.3	0.3 ± 0.3	0.0 ± 0.0	0
3-4	0.0 ± 0.0	0.1 ± 0.1	0.1 ± 0.1	0.0 ± 0.0	ND
4-5	0.0 ± 0.0	0.1 ± 0.1	0.1 ± 0.1	0.0 ± 0.0	0
6-7	0.0 ± 0.0	0.1 ± 0.1	0.1 ± 0.1	0.0 ± 0.0	ND
7-8	0.0 ± 0.0	0.1 ± 0.0	0.1 ± 0.0	0.0 ± 0.0	0
9-10	0.0 ± 0.0	0.1 ± 0.0	0.1 ± 0.0	0.0 ± 0.0	0
		***Beggiatoa* mat**			
0-1	8.7 ± 6.3	3.7 ± 1.1	10.2 ± 5.0	0.6 ± 0.2	0
1-2	19.7 ± 0.6	4.8 ± 1.4	19.4 ± 1.6	0.8 ± 0.1	ND
2-3	10.9 ± 2.4	0.5 ± 0.2	8.6 ± 1.9	0.9 ± 0.0	0
3-4	1.0 ± 0.4	0.2 ± 0.1	1.0 ± 0.4	0.8 ± 0.1	ND
4-5	0.8 ± 0.3	0.2 ± 0.2	0.8 ± 0.1	0.7 ± 0.3	0
6-7	0.7 ± 1.1	0.1 ± 0.1	0.6 ± 0.8	0.6 ± 0.5	ND
7-8	0.2 ± 0.3	0.1 ± 0.0	0.2 ± 0.2	0.3 ± 0.5	0
8-9	0.1 ± 0.1	0.1 ± 0.0	0.2 ± 0.1	0.4 ± 0.3	0
9-10	0.3 ± 0.1	0.1 ± 0.0	0.2 ± 0.1	0.5 ± 0.4	0
		Tubeworm field			
0-1	0.1 ± 0.1	0.8 ± 0.6	0.8 ± 0.6	<0.1 ± 0.1	0
1-2	0.1 ± 0.1	0.9 ± 0.3	0.9 ± 0.3	<0.1 ± 0.1	0
2-3	0.3 ± 0.6	1.4 ± 0.5	1.6 ± 0.7	0.1 ± 0.2	0
3-4	0.1 ± 0.1	3.2 ± 3.1	3.3 ± 3.0	<0.1 ± 0.1	0
6-7	0.2 ± 0.2	1.8 ± 1.2	2.0 ± 1.1	0.2 ± 0.2	0
7-8	0.2 ± 0.2	0.7 ± 0.7	0.8 ± 0.8	0.2 ± 0.2	0
8-9	0.4 ± 0.5	0.6 ± 0.6	0.8 ± 0.9	0.1 ± 0.2	0
9-10	0.0 ± 0.0	0.6 ± 0.5	0.6 ± 0.5	0.0 ± 0.0	<0.5
12-13	0.2 ± 0.3	0.6 ± 0.6	0.8 ± 0.5	0.3 ± 0.4	0
13-14	0.6 ± 0.5	0.4 ± 0.6	0.9 ± 0.9	0.4 ± 0.4	0

ANME-1 cells were quantified after hybridization with probe ANME1-350 and numbers are given in percentage of DAPI detected single cells. ND, not determined.
[a] Multiple independent MUC cores were examined for spatial variability: two cores of center sediments, three cores each of sediments covered with *Beggiatoa* mats and sediments from the tubeworm field.

DISCUSSION

Already during the video-guided sampling, but also by *in situ* biogeochemical analyses three clearly distinct habitats - center, *Beggiatoa* mat, tubeworm field - could be distinguished at HMMV (Fig. 5). The biogeochemistry of HMMV is discussed in detail in de Beer *et al.* (2006) (8) and Niemann *et al.* (submitted) (46). Briefly, the center of the HMMV releases high amounts of gaseous and dissolved methane into the water column (56). Here upward subsurface fluid flow is high restricting the diffusion of oxygen in to the seafloor (8). The retrieved push cores showed a high content of gas but had no sulfidic smell. In contrast, samples from the *Beggiatoa* area were highly sulfidic and showed a dark gray color. Here, upward fluid flow rates are still high, restricting sulfate penetration to a few cm (8). Oxygen is

consumed by sulfide-oxidizers within the top few mm. Finally, the tubeworm area is distinctly different from the other sites by relatively lower upward fluid flow and the bioirrigation by the tubeworms, providing oxygen and sulfate as electron acceptors to the microbial communities in the sediments (8). These distinct habitat differences were clearly reflected in the diversity and abundance of microbial populations. Our results show that multiple methanotrophic guilds occupy distinct separate niches at HMMV.
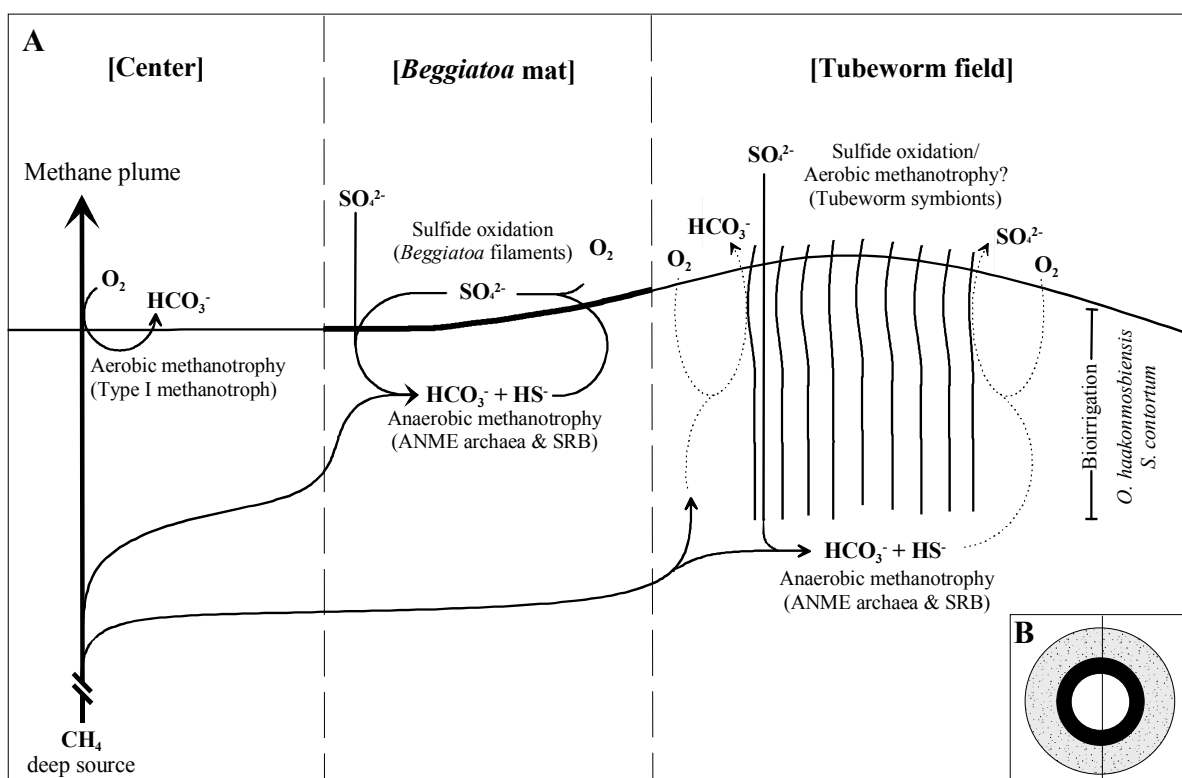
FIGURE 5 Schematic diagram of HMMV. (A) Dominant methane-consuming processes in sediments of the different sampling sites, (B) circular zonation of the mud volcano: the inner circle represents uncovered sediments of the thermal center, the surrounding area is covered with *Beggiatoa* mats, and the rim of the crater is populated by siboglinid tubeworms.

Communities of aerobic methanotrophic bacteria at HMMV. The HMMV is the first cold seep for which high *in situ* abundance of aerobic methanotrophs could be demonstrated. Dense populations of aerobic methanotrophic bacteria were found in freshly expelled surface sediments of the mud volcano center, and to a lesser extent in sediments covered with *Beggiatoa* mats. Both habitats are characterized by high methane concentrations over the entire vertical profile (46) and a limited oxygen penetration depth of a few mm (8).

The specific biogeochemistry of the freshly expelled center sediments promotes the growth of aerobic methanotrophs. The sediments of the volcano center are permanently vented by ascending methane-rich fluids, but also mixed with subsurface sediments during events of

mud eruption. Organic content of the center sediments is very low, and methane is most likely the main carbon source to microbial life. A high upward flow of sulfate-free subsurface fluids limits the penetration of sulfate from the seawater to the uppermost centimeter of the sediment (8) and thereby excludes ANME archaea from these sediments. The sulfide levels at the center were very low (8), confirming that AOM was not a significant process. Analyses of biomarkers and rate measurements of methane oxidation are consistent with 16S rRNA based results of this study. High concentrations of $\delta^{13}C$ depleted (-89‰) bacterial fatty acids (e.g. $C_{16:1\omega8c}$) assigned to *Methylobacter* species were found, whereas archaeal AOM biomarker were below the detection limit (46). Aerobic methane oxidation rates were high [0.9 mol m^{-2} yr^{-1}; (46)], whereas AOM could not be detected. Some aerobic methanotrophs were also found in surface sediments covered with *Beggiatoa* mats. Their distribution is limited by the penetration of oxygen from seawater into the sediments, and the upward diffusion of sulfide into the sediment surface layers.

Communities of anaerobic methane oxidizers at HMMV. The presence of ANME cells was restricted to sediments below *Beggiatoa* mats and sediments populated by siboglinid tubeworms. At the *Beggiatoa* site, high abundance of ANME-3 aggregates was limited to a narrow zone in 1-3 cm sediment depth, due to the limited penetration of sulfate from bottom waters into the sediments (8). AOM rates were high with ca 5 mol m^{-2} yr^{-1} (46). The sediments were covered by vast microbial mats of *Beggiatoa* species. Mats of these giant sulfide-oxidizing bacteria are often found at cold seeps and indicative for high AOM-derived sulfide fluxes from underlying gassy sediments (55, 65).

In deeper sediment layers, ANME aggregates could only be detected at the tubeworm site (throughout the core in low abundance). The site is characterized by the dense colonization of the sediments with tubeworms and most likely a higher input of organic matter (e.g. worm exudates, trapped particles) than at the other sites. Methane and sulfide concentrations in surface sediments were relatively low (8, 46). Sulfate and oxygen penetrated deeper into the sediments [10 cm; (8)] compared to the undisturbed sediments of the *Beggiatoa* site. Sulfide and oxygen profiles overlapped (8) and thereby allow the aerobic sulfide oxidation in the zone, where the tubeworms thrive. The sulfate/methane transition zone is apparently shifted to deeper sediment horizons and growth of AOM aggregates is rather limited in the upper sediment layers. AOM and sulfate reduction rates peaked in deeper sediments [below 60 cm; (46)], indicating the highest activity of anaerobic methane oxidizers in sediment layers which were not investigated in this study.

A new methane-oxidizing consortium of ANME-3/DBB. The sediments below the *Beggiatoa* mats at HMMV are the first habitat known to host a dominant biomass of ANME-3. Sequences of this archaeal clade were previously retrieved from different seep habitats, but were not assigned to a specific AOM consortium. Here we describe the morphology, identity and distribution of a novel consortium of archaea and sulfate-reducing bacteria (SRB) responsible for AOM.

The AOM zone below the *Beggiatoa* mats was restricted to 1-3 cm sediments depth (46). In this zone, ANME-3/DBB aggregates accounted for $95 \pm 2\%$ of total cells. Furthermore, high concentrations of archaeal lipids (dominance of PMI:4 and PMI:5) that were highly depleted in $\delta^{13}C$ (-109‰) were detected in the same layer (45). Biomarker profiles matched perfectly the depth profiles of aggregate counts with highest abundance in 1-2 cm sediment depth. Hence, we conclude that ANME-3 are responsible for AOM at HMMV, and represent a new type of methanotrophic consortium.

In situ analyses showed that ANME-3 occurs in microbial consortia forming a tight physical association with sulfate-reducing bacteria. ANME-1 and ANME-2, which have been proven to oxidize methane anaerobically, occur in similar associations. Whereas ANME-1 and ANME-2 are associated with SRB of the *Desulfosarcina-Desulfococcus* branch, ANME-3 is associated with *Desulfobulbus* species. Of the 132 bacterial clones from the *Beggiatoa* site investigated, none was targeted by probes 660 and DBB305. However, using primer sets specific for *Desulfobulbus* (DBB305/GM4), sequences targeted by probe DBB305 were retrieved from sediments beneath the *Beggiatoa* mat. The *Desulfobulbus* related sequences belong to the recently defined SRB group SEEP-SRB3 which is currently specific to methane rich, anoxic environments (28) and has been discussed to be involved in AOM.

Furthermore, ANME-3 cells occurred without physically associated bacteria or were associated with yet unidentified bacteria forming "mixed-type" aggregates. These observations suggest that a physical association with DBB cells may not be obligatory for ANME-3. However, their sequences have been also detected together with DBB sequences at Eel River basin (47).

Interestingly, we also found a substantial number of single ANME-3 cells below *Beggiatoa* mats at HMMV. FISH-SIMS analysis (48) found that monospecific ANME-2 aggregates and single ANME-1 cells show depletions of ^{13}C in their biomass which are characteristic of methanotrophy. It is not known whether the AOM process requires the physical association between archaea and SRB.

CONCLUSION

At HMMV, we found a relatively high diversity of different aerobic and anaerobic methanotrophs occupying distinct niches defined by the geological and biogeochemical processes (Fig. 5). Three phylotypes of aerobic methanotrophs dominate the highly gassy sediments of the center of the volcano and reach high abundances in a very narrow oxic sediment horizon at the seafloor. Anaerobic archaeal methane oxidizers of a novel consortium type ANME-3/DBB dominate the anaerobic surface sediments limited by sulfate penetration. Microbial diversity increased considerably outside of the zones of highest fluid flow, which was dominated by siboglinid tubeworms. Here, aerobic and anaerobic methane oxidizers were more diverse but less abundant in the top 10 cm of sediment. The presence of the tubeworms likely enhanced availability of other carbon substrates, increasing the diversity of heterotrophic groups of bacteria, but also of crenarchaeal groups.

ACKNOWLEDGEMENTS

REFERENCES

1. **Amann, R. I., L. Krumholz, and D. A. Stahl.** 1990b. Fluorescent-oligonucleotide probing of whole cells for determinative, phylogenetic, and evironmental studies in microbiology. J. Bacteriol. **172:**762-770.
2. **Baer, M., J. Ravel, J. Chun, R. Hill, and H. Williams.** 2000. A proposal for the reclassification of Bdellovibrio stolpii and Bdellovibrio starrii into a new genus, Bacteriovorax gen. nov. as Bacteriovorax stolpii comb. nov. and Bacteriovorax starrii comb. nov., respectively. Int. J. Syst. Evol. Microbiol. **50:**219-224.
3. **Boetius, A., K. Ravenschlag, C. Schubert, D. Rickert, F. Widdel, A. Gieseke, R. Amann, B. B. Jørgensen, U. Witte, and O. Pfannkuche.** 2000. A marine microbial

consortium apparently mediating anaerobic oxidation of methane. Nature **407:**623-626.

4. **Brosius, J., T. Dull, D. D. Sleeter, and H. F. Noller.** 1981. Gene organization and primary structure of a ribosomal RNA operon from *Escherichia coli*. J. Mol. Biol. **148:**107-127.

5. **Chandler, D. P., F. J. Brockman, T. J. Bailey, and J. K. Fredrickson.** 1998. Phylogenetic diversity of archaea and bacteria in a deep subsurface paleosol. Microb. Ecol. **36:**37-50.

6. **Daims, H., A. Brühl, R. Amann, and K. H. Schleifer.** 1999. The domain-specific probe EUB338 is insufficient for the detection of all Bacteria: Development and evaluation of a more comprehensive probe set. Syst. Appl. Microbiol. **22:**434-444.

7. **Damm, E., and G. Budéus.** 2003. Fate of vent-derived methane in seawater above the Haakon Mosby mud volcano (Norwegian Sea). Mar. Chem. **1969:**1-11.

8. **De Beer, D., E. Sauter, H. Niemann, U. Witte, M. Schlüter, and A. Boetius.** 2006. In situ fluxes and zonation of microbial activity in surface sediments of the Haakon Mosby Mud Volcano (in press). Limnol. Oceanogr.

9. **DeLong, E. F.** 1992. Archaea in coastal marine environments. Proc. Natl. Acad. Sci. USA **89:**5685-5689.

10. **Devereux, R., M. D. Kane, J. Winfrey, and D. A. Stahl.** 1992. Genus- and Group-specific hybridization probes for determinative and environmental studies of sulfate-reducing bacteria. System. Appl. Microbiol. **15:**601-609.

11. **Dimitrov, L. I.** 2002. Mud volcanoes - the most important pathway for degassing deeply buried sediments. Earth Sci. Rev. **59:**49-76.

12. **Distel, D. L., and C. M. Cavanaugh.** 1994. Independent phylogenetic origins of methanotrophic and chemoautotrophic bacterial endosymbioses in marine bivalves. J. Bacteriol. **176:**1932-1938.

13. **Distel, D. L., H. K. Lee, and C. M. Cavanaugh.** 1995. Intracellular coexistence of methano- and thioautotrophic bacteria in a hydrothermal vent mussel. Proc. Natl. Acad. Sci. USA **92:**9598-9602.

14. **Dojka, M. A., P. Hugenholtz, S. K. Haack, and N. R. Pace.** 1998. Microbial diversity in a hydrocarbon- and chlorinated-solvent-contaminated aquifer undergoing intrinsic bioremediation. Appl. Environ. Microbiol. **64:**3869-3877.

15. **Eldholm, O., E. Sundvor, P. R. Vogt, B. O. Hjelstuen, K. Crane, A. K. Nilsen, and T. P. Gladczenko.** 1999. SW Barents Sea continental margin heat flow and Haakon Mosby Mud Volcano. Geo-Mar. Lett. **19:**29-37.

16. **Ginsburg, G. D., G. V. Milkov, V. A. Soloviev, A. V. Egorov, G. A. Cherkashev, P. R. Vogt, K. Crane, T. D. Lorenson, and M. D. Khutorskoy.** 1999. Gas hydrate accumulation at the Haakon Mosby Mud Volcano. Geo-Mar. Lett. **19:**57 - 67.

17. **Hallam, S. J., P. R. Girguis, C. M. Preston, P. M. Richardson, and E. F. DeLong.** 2003. Identification of methyl coenzyme M reductase A (mcrA) genes associated with methane-oxidizing archaea. Appl. Environ. Microbiol. **69:**5483-5491.

18. **Hallam, S. J., N. Putnam, C. M. Preston, J. C. Detter, D. Rokhsar, P. M. Richardson, and E. F. DeLong.** 2004. Reverse Methanogenesis: Testing the Hypothesis with Environmental Genomics. Science **305:**1457-1462.

19. **Hanson, R. S., and T. E. Hanson.** 1996. Methanotrophic Bacteria. Microbiol. Rev. **60:**439 - 471.

20. **Hinrichs, K. U., J. M. Hayes, S. P. Sylva, P. G. Brewer, and E. F. DeLong.** 1999. Methane-consuming archaebacteria in marine sediments. Nature **398:**802-805.

21. **Hinrichs, K.-U., L. R. Hmelo, and S. P. Sylva.** 2003. Molecular fossil record of elevated methane levels in late pleistocene coastal waters. Science **299:**1214-1217.

22. **Hjelstuen, B. O., O. Eldholm, J. I. Faleide, and P. R. Vogt.** 1999. Regional setting of Haakon Mosby Mud Volcano, SW Barents Sea margin. Geo-Mar. Lett. **19:**22-28.

23. **Hoehler, T. M., M. J. Alperin, D. B. Albert, and C. S. Martens.** 1994. Field and laboratory studies of methane oxidation in an anoxic marine sediment: Evidence for a methanogen-sulfate reducer consortium. Glob. Biogeochem. Cycles **8:**451-463.

24. **Inagaki, F., T. Nunoura, S. Nakagawa, A. Teske, M. Lever, A. Lauer, M. Suzuki, K. Takai, M. Delwiche, F. S. Colwell, K. H. Nealson, K. Horikoshi, S. D'Hondt, and B. B. Jorgensen.** 2006. Biogeographical distribution and diversity of microbes in methane hydrate-bearing deep marine sediments on the Pacific Ocean Margin. Proc. Natl. Acad. Sci. USA **103:**2815-2820.

25. **Jurkevitch, E.** 2002. The Genus Bdellovibrio. *In* M. Dworkin (ed.), The Prokaryotes (Electronic Version). Springer, New York.

26. **Kane, M. D., L. K. Poulsen, and D. A. Stahl.** 1993. Monitoring the enrichment and isolation of sulfate-reducing bacteria by using oligonucleotide hybridization probes designed from environmentally derived 16S rRNA sequences. Appl. Environ. Microbiol. **59:**682-686.

27. **Klages, M., J. Thiede, and J. P. Foucher (ed.).** 2004. The Expetition ARKTIS XIX/3 of the Research Vessel Polarstern in 2003, vol. 488. Buchhandlung Kamloth, Bremen.

28. **Knittel, K., A. Boetius, A. Lemke, H. Eilers, K. Lochte, O. Pfannkuche, P. Linke, and R. Amann.** 2003. Activity, distribution, and diversity of sulfate reducers and other bacteria in sediments above gas hydrate (Cascadia Margin, Oregon). Geomicrobiol. J. **20:**269-294.

29. **Knittel, K., T. Lösekann, A. Boetius, R. Kort, and R. Amann.** 2005. Diversity and distribution of methanotrophic archaea at cold seeps. Appl. Environ. Microbiol. **71:**467-479.

30. **Kopf, A. J.** 2003. Global methane emission through mud volcanoes and its past and present impact on the Earth´s climate. Int. J. Earth Sci. **92:**806-816.

31. **Krüger, M., A. Meyerdierks, F. O. Glöckner, R. Amann, F. Widdel, M. Kube, R. Reinhardt, J. Kahnt, R. Böcher, R. K. Thauer, and S. Shima.** 2003. A conspicuous nickel protein in microbial mats that oxidize methane anaerobically. Nature **426:**878-881.

32. **Lane, D. J., B. Pace, G. J. Olsen, D. A. Stahl, M. Sogin, and N. R. Pace.** 1985. Rapid determination of 16S ribosomal RNA sequences for phylogenetic analyses. Proc. Natl. Acad. Sci. USA **82:**6955-6959.

33. **Lein, A., P. Vogt, K. Crane, A. Egorov, and M. Ivanov.** 1999. Chemical and isotopic evidence for the nature of the fluid in CH4-containing sediments of the Haakon Mosby Mud Volcano. Geo-Mar. Lett. **19:**76-83.

34. **Li, L., C. Kato, and K. Horikoshi.** 1999. Microbial diversity in sediments collected from the deepest cold-seep area, the Japan trench. Mar. Biotechnol. **1:**391-400.

35. **Ludwig, W., O. Strunk, R. Westram, L. Richter, H. Meier, Yadhukumar, A. Buchner, T. Lai, S. Steppi, G. Jobb, W. Förster, I. Brettske, S. Gerber, A. W. Ginhart, O. Gross, S. Grumann, S. Hermann, R. Jost, A. König, T. Liss, R. Lüßmann, M. May, B. Nonhoff, B. Reichel, R. Strehlow, A. Stamatakis, N. Stuckmann, A. Vilbig, M. Lenke, T. Ludwig, A. Bode, and K. H. Schleifer.** 2004. ARB: a software environment for sequence data. Nucleic Acids Res. **32:**1363-1371.

36. **Manz, W., R. Amann, W. Ludwig, M. Vancanneyt, and K.-H. Schleifer.** 1996. Application of a suite of 16S rRNA-specific oligonucleotide probes designed to investigate bacteria of the phylum cytophaga-flavobacter-bacteroides in the natural environment. Microbiology **142:**1097-1106.

37. **Manz, W., M. Eisenbrecher, T. R. Neu, and U. Szewzyk.** 1998. Abundance and spatial organization of gram negative sulfate-reducing bacteria in activated sludge investigated by in situ probing with specific 16S rRNA targeted oligonucleotides. FEMS Microbiol. Ecol. **25:**43-61.

38. **Massana, R., A. E. Murray, C. M. Preston, and E. F. DeLong.** 1997. Vertical distribution and phylogenetic characterization of marine planktonic Archaea in the Santa Barbara Channel. Appl. Environ. Microbiol. **63:**50-56.

39. **Meyer-Reil, L. A.** 1983. Benthic response to sedimentation events during autumn to spring at a shallow water station in the Western Kiel Bight. Mar. Biol. **77:**247-256.

40. **Michaelis, W., R. Seifert, K. Nauhaus, T. Treude, V. Thiel, M. Blumenberg, K. Knittel, A. Gieseke, K. Peterknecht, T. Pape, A. Boetius, R. Amann, B. B. Jörgensen, F. Widdel, J. Peckmann, N. V. Pimenov, and M. B. Gulin.** 2002. Microbial reefs in the Black Sea fueled by anaerobic oxidation of methane. Science **297:**1013-1015.

41. **Milkov, A., P. Vogt, G. Cherkashev, G. Ginsburg, N. Chernova, and A. Andriashev.** 1999. Sea-floor terrains of Haakon Mosby Mud Volcano as surveyed by deep-tow video and still photography. Geo-Mar. Lett. **19:**38 - 47.

42. **Muyzer, G., A. Teske, C. O. Wirsen, and H. W. Jannasch.** 1995. Phylogenetic relationships of *Thiomicrospira* species and their identification in deep-sea hydrothermal vent samples by denaturing gradient gel electrophoresis of 16S rDNA fragments. Arch. Microbiol. **164:**165-172.

43. **Nauhaus, K., A. Boetius, M. Krüger, and F. Widdel.** 2002. In vitro demonstration of anaerobic oxidation of methane coupled to sulphate reduction in sediment from a marine gas hydrate area. Environ. Microbiol. **4:**296-305.

44. **Nauhaus, K., T. Treude, A. Boetius, and M. Kruger.** 2005. Environmental regulation of the anaerobic oxidation of methane: a comparison of ANME-I and ANME-II communities. Environ. Microbiol. **7:**98-106.

45. **Niemann, H., M. Elvert, T. Lösekann, J. Jakob, T. Nadalig, and A. Boetius.** in prep. Distribution of methanotrophic guilds at Haakon Mosby Mud Volcano, Barents Sea.

46. **Niemann, H., T. Lösekann, D. de Beer, M. Elvert, K. Knittel, R. Amann, E. Sauter, M. Schlüter, M. Klages, J. Foucher, and A. Boetius.** subm. Fluid flow controls distribution of methanotrophic microorganisms at submarine cold seeps. Nature

47. **Orphan, V. J., K.-U. Hinrichs, W. Ussler III, C. K. Paull, L. T. Taylor, S. P. Sylva, J. M. Hayes, and E. F. DeLong.** 2001a. Comparative analysis of methane-oxidizing archaea and sulfate-reducing bacteria in anoxic marine sediments. Appl. Environ. Microbiol. **67:**1922-1934.

48. **Orphan, V. J., C. H. House, K.-U. Hinrichs, K. D. McKeegan, and E. F. DeLong.** 2001b. Methane-consuming archaea revealed by directly coupled isotopic and phylogenetic analysis. Science **293:**484-487.

49. **Orphan, V. J., C. H. House, K.-U. Hinrichs, K. D. McKeegan, and E. F. DeLong.** 2002. Multiple archaeal groups mediate methane oxidation in anoxic cold seep sediments. Proc. Natl. Acad. Sci. USA **99:**7663-7668.

50. **Pernthaler, A., J. Pernthaler, and R. Amann.** 2002. Fluorescence in situ hybridization and catalyzed reporter deposition (CARD) for the identification of marine Bacteria. Appl. Environ. Microbiol. **68:**3094-3101.

51. **Pimenov, N., A. Savvichev, I. Rusanov, A. Lein, A. Egorov, A. Gebruk, L. Moskalev, and P. Vogt.** 1999. Microbial processes of carbon cycle as the base of food chain of Haakon Mosby Mud Volcano. Geo-Mar. Lett. **19:**89 - 96.

52. **Prasolov, E. M., I. V. Tokarev, G. D. Ginsburg, V. A. Soloviev, and G. M. Eltsova.** 1999. Helium and other noble gases in gas-hydrate sediments of the Haakon Mosby Mud Volcano. Geo-Mar. Lett. **19:**84-88.

53. **Ravenschlag, K., K. Sahm, J. Pernthaler, and R. Amann.** 1999. High bacterial diversity in permanently cold marine sediments. Appl. Environ. Microbiol. **65:**3982-3989.

54. **Reeburgh, W. S.** 1996. "Soft spots" in the global methane budget, p. 334–342. *In* M. E. Lidstrom and F. R. Tabita (ed.), Microbial Growth on C1 Compounds. Kluwer Academic Publishers, Dordrecht.

55. **Sahling, H., D. Rickert, R. Lee, P. Linke, and E. Suess.** 2002. Macrofaunal community structure and sulfide flux at gas hydrate deposits from the Cascadia convergent margin, NE Pacific. Mar. Ecol. Prog. Ser. **231:**121 - 138.

56. **Sauter, E. J., S. I. Muyakshin, J. L. Charlou, M. Schlüter, A. Boetius, K. Jerosch, E. Damm, J. P. Foucher, and M. Klages.** in press. Methane discharge from a deep-sea submarine mud volcano into the upper water column by gas hydrate-coated methane bubbles. Earth and Planet. Sci. Lett.

57. **Schmaljohann, R., and H. J. Flügel.** 1987. Methane-oxidizing bacteria in Pogonophora. Sarsia **72:**91-98.

58. **Shilov, V. V., N. I. Druzhinina, L. V. Vasilenko, and V. V. Krupskaya.** 1999. Stratigraphy of sediments from the Haakon Mosby Mud Volcano area. Geo-Mar. Lett. **19:**48-56.

59. **Smirnov, R. V.** 2000. Two new species of Pogonophora from the arctic mud volcano off northwestern Norway. Sarsia **85:**141-150.

60. **Snaidr, J., R. Amann, I. Huber, W. Ludwig, and K. H. Schleifer.** 1997. Phylogenetic analysis and in situ identification of bacteria in activated sludge. Appl. Environ. Microbiol. **63:**2884-2896.

61. **Southward, E. C.** 1982. Bacterial symbionts in Pogonophora. J. Mar. Biol. Ass. U. K. **46:**579-616.

62. **Takai, K., and K. Horikoshi.** 1999. Genetic diversity of archaea in deep-sea hydrothermal vent environments. Genetics **152:**1285-1297.

63. **Teske, A., K.-U. Hinrichs, V. Edgcomb, A. de Vera Gomez, D. Kysela, S. P. Sylva, M. L. Sogin, and H. W. Jannasch.** 2002. Microbial diversity of hydrothermal sediments in the Guaymas Basin: evidence for anaerobic methanotrophic communities. Appl. Environ. Microbiol. **68:**1994-2007.

64. **Thomsen, T. R., K. Finster, and N. B. Ramsing.** 2001. Biogeochemical and molecular signatures of anaerobic methane oxidation in a marine sediment. Appl. Environ. Microbiol. **67:**1646-1656.

65. **Treude, T., A. Boetius, K. Knittel, K. Wallmann, and B. B. Jörgensen.** 2003. Anaerobic oxidation of methane above gas hydrates (Hydrate Ridge, OR). Mar. Ecol. Prog. Ser. **264:**1-14.

66. **Van Bruggen, J. J. A., C. K. Stumm, and G. D. Vogels.** 1983. Symbiosis of methanogenic bacteria and sapropelic protozoa. Arch. Microbiol. **136:**89-95.

67. **Vetriani, C., H. W. Jannasch, B. J. MacGregor, D. A. Stahl, and A. L. Reysenbach.** 1999. Population structure and phylogenetic characterization of marine benthic archaea in deep-sea sediments. Appl. Environ. Microbiol. **65:**4375-4384.

68. **Vogt, P., K. Crane, S. Pfirman, E. Sundvor, N. Cherkis, H. Fleming, C. Nishimura, and A. Shor.** 1991. SeaMARC II sidescan sonar imagery and swath bathymetry in the Nordic Basin. EOS Trans. Am. Geophys. Union **72:**486.

69. **Vogt, P. R., G. Cherkashev, G. Ginsburg, G. I. Ivanov, A. Milkov, K. Crane, A. Lein, E. Sundvor, N. V. Pimenov, and A. Egorov.** 1997. Haakon Mosby Mud

Volcano Provides Unusual Example of Venting. EOS Trans. Am. Geophys. Union Supplement **78 (48):**556-557.

70.   **Vogt, P. R., J. Gardner, and K. Crane.** 1999. The Norwegian-Barents-Svalbard (NBS) continental margin: Introducing a natural laboratory of mass wasting, hydrates, and ascent of sediment, pore water, and methane. Geo-Mar. Lett. **19:**2-21.

71.   **Wallner, G., R. Amann, and W. Beisker.** 1993. Optimizing fluorescent in situ hybridization with rRNA-targeted oligonucleotide probes for flow cytometric identification of microorganism. Cytometry **14:**136-143.

72.   **Zhou, J., M. A. Brunns, and J. M. Tiedje.** 1996. DNA recovery from soils of diverse composition. Appl. Environ. Microbiol. **62:**316-322.

3

Endosymbioses between Bacteria and Deep-Sea Siboglinid Tubeworms from an Arctic Cold Seep (Haakon Mosby Mud Volcano, Barents Sea)

Tina Lösekann, Helge Niemann, Florence Pradillon, Katrin Knittel,

Antje Boetius, and Nicole Dubilier

Preliminary manuscript

Endosymbioses between Bacteria and Deep-Sea Siboglinid Tubeworms from an Arctic Cold Seep (Haakon Mosby Mud Volcano, Barents Sea)

Tina Lösekann[1], Helge Niemann[1,2], Florence Pradillon[1,†], Katrin Knittel[1], Antje Boetius[1,2,3], and Nicole Dubilier[1*]

[1] Max Planck Institute for Marine Microbiology, Celsiusstrasse 1, 28359 Bremen, Germany

[2] Alfred Wegener Institute for Polar and Marine Research, Am Handelshafen 12, 27515 Bremerhaven, Germany

[3] International University Bremen, Research II, Campusring 1, 28759 Bremen, Germany

*Corresponding author. Mailing address: Max Planck Institute for Marine Microbiology, Celsiusstr. 1, D-28359 Bremen, Germany. Phone: 49 (0)4212028932. Fax: 49 (0)4212028580. E-Mail: ndubilie@mpi-bremen.de.

†Present address: Université Pierre et Marie Curie, 7, Quai Saint-Bernard, 75252 Paris Cedex 05, France

Running title: Endosymbioses in deep-sea siboglinid tubeworms

ABSTRACT

Siboglinids, previously referred to as *Pogonophora,* are tube-dwelling worms that live in obligate associations with bacterial endosymbionts. The diversity and phylogeny of symbionts belonging to the vestimentiferan siboglinids has been well described in several species using 16S rDNA based molecular methods (33). In contrast, the symbionts in only two out of 136 frenulate hosts, and no moniliferan species, have been examined to date (27, 37). In this study, the symbionts in *Sclerolinum contortum (Monilifera)* and *Oligobrachia haakonmosbiensis (Frenulata)* were investigated using comparative sequence analysis of 16S rRNA and protein-coding genes, fluorescence *in situ* hybridization, and lipid biomarker analyses. Both host species were found to coexist in the same habitat at a water depth of 1,250 m at an Arctic cold seep (Haakon Mosby Mud Volcano). The symbionts of *S. contortum* and *O. haakonmosbiensis* belong to the *Gammaproteobacteria* based on 16S rRNA gene phylogeny. The *S. contortum* symbiont is closely related to chemoautotrophic sulfur-oxidizing symbionts of vestimentiferan hosts. In *O. haakonmosbiensis*, two very closely related symbionts (97-98% sequence similarity) were found which group with the symbiont of another frenulate siboglinid, *O. mashikoi* from Japan. The symbiont sequences of both *Oligobrachia* species formed a separate clade unaffiliated with known methane- or sulfur-oxidizing bacteria. Fluorescence *in situ* hybridizations with symbiont-specific oligonucleotide probes confirmed that the dominant bacterial phylotypes originated from endosymbionts residing inside the host trophosome. In both host species, genes coding for ribulose-1,5-bisphosphate carboxylase/oxygenase (RubisCO) and adenosine-5'-phosphosulfate reductase (APS) were present, whereas genes diagnostic for methanotrophy, i.e. those coding for the particulate and soluble methane monooxygenase or methanol dehydrogenase were not detected. The molecular data suggest that *S. contortum* harbors chemoautotrophic sulfur-oxidizing symbionts. Average stable carbon isotopic values of bacterial fatty acids and cholesterol of -43‰ were highly negative for a sulfur oxidizer, but may be explained by a ^{13}C-depleted CO_2 source at HMMV. The metabolic mode of the *O. haakonmosbiensis* symbionts remains unclear. The molecular data suggest that *O. haakonmosbiensis* harbors chemoautotrophic sulfur-oxidizing symbionts, but average stable carbon isotope values of bacterial fatty acids and cholesterol of -70‰ appear too negative for chemoautotrophic CO_2 fixation. Such negative values are only known from methane-oxidizing symbionts (18). However, neither genes for methanotrophy nor biomarkers specific for type I and type II methanotrophs were found in *O. haakonmosbiensis*.

119

INTRODUCTION

Symbiotic associations between chemoautotrophic bacteria and marine invertebrates were first discovered about three decades ago during explorations of deep-sea hydrothermal vents (6, 14). It is now known that associations with thiotrophic (sulfur-oxidizing) and methanotrophic (methane-oxidizing) bacteria occur in a wide taxonomic range of invertebrates that live in reducing environments, such as hydrothermal vents, cold seeps, whale and wood falls, and seagrass beds. (7, 15-17). Cold seeps occur worldwide at both passive and active continental margins and support large populations of symbiont-bearing invertebrates, including bivalve clams *(Thyasiridae, Vesicomyidae, Lucinidae)*, bathymodiolid mussels *(Mytilidae)*, and tube-dwelling annelids *(Siboglinidae)* (60).

Within the *Siboglinidae,* four major groups are recognized to date: the *Frenulata* (e.g. *Oligobrachia* spp., *Siboglinum* spp.), the *Monilifera* (only *Sclerolinum* spp.), the *Vestimentifera* (e.g. *Riftia pachyptila, Lamellibrachia* spp., *Escarpia* spp.), and the novel lineage of *Osedax* (21, 52). Siboglinid evolution is likely driven by a trend toward increased habitat specialization (58): frenulates and moniliferans have been mostly reported from low-sulfide sedimentary environments such as continental slopes and deep fjords, whereas vestimentiferans generally inhabit highly sulfidic environments such as hydrothermal vents and cold seeps. *Osedax* species were discovered very recently and live on lipid-rich whale bones (20, 53).

Adult siboglinids lack a digestive system and rely on their endosymbionts for nutrition (14, 64). The morphology of the symbioses is similar in all siboglinids (65): the bacterial symbionts are embedded within host cells (bacteriocytes) in an interior, highly vascularized tissue called the trophosome. Most siboglinid species examined to date harbor sulfur-oxidizing, chemoautotrophic symbionts based on transmission electron microscopy (TEM), stable carbon isotope signatures, and enzyme activity assays (17, 64). Exceptions are the frenulate *Siboglinum poseidoni* from the Skagerrak*,* which contains methanotrophic symbionts (57), and the bone-degrading *Osedax* species, which harbor heterotrophic symbionts (20).

To date, the symbiotic associations of vestimentiferans are well studied with molecular methods and sequences of many host species and their symbionts are published [e.g. (10, 26, 33, 38)]. All vent vestimentiferan symbionts belong to a closely related clade within the *Gammaproteobacteria*. Symbionts of seep vestimentiferans are phylogenetically more diverse and belong to *Alpha-, Beta-, Gamma-* or *Epsilonproteobacteria*. The two described *Osedax* species harbor symbionts that belong to *Oceanospirilliales* (20). Very little is known about

the phylogeny of frenulate hosts and their symbionts, although 136 species of this taxon are known to date (66). Only two species have been studied with molecular methods, *Oligobrachia mashikoi* from muddy shallow sediments off Japan and an undescribed frenulate from the deep Japan Trench (27, 37). Moreover, no molecular data from any moniliferan species and their symbionts are available.

To extend the current knowledge about siboglinid symbioses, we examined the moniliferan and frenulate tubeworms found at an Arctic cold seep, the Haakon Mosby mud volcano (HMMV). The HMMV is a methane-venting cold seep, situated at the Norwegian-Barents-Spitzbergen continental margin (72° 0.25'N, 14° 43.50'E) in a water depth of 1,250 m. Since its discovery in 1990 (72), the HMMV has been intensively studied [reviewed in (34)]. The mud volcano has a circular zonation of three different habitats: 1) in the center, methane-rich muds and fluids are expelled from the deep geosphere to the seafloor, 2) the sediments surrounding the central area are densely covered with bacterial mats of filamentous sulfur-oxidizing bacteria (*Beggiatoa* sp.), and 3) the outer rim is colonized by siboglinid tubeworms (47). During cruises with RV L'Atalante and ROV Victor 6000 in 2001 and with RV Polarstern and ROV Victor 6000 in 2003, the HMMV was revisited to further characterize the distribution and activity of microbial communities and to determine the environmental factors controlling the observed patterns (9, 30, 42-44, 55). One goal was to better understand the nature of the symbioses of the siboglinid tubeworms, which represent the dominant megafauna at HMMV.

We analyzed the phylogenetic placement of *S. contortum* and *O. haakonmosbiensis* within the siboglinid clade based on 18S rRNA gene phylogeny. Comparative analysis of 16S rRNA genes and fluorescence *in situ* hybridizations were used to examine the diversity and phylogeny of the symbionts. In addition, we assessed the metabolic capabilities of the symbionts by examining the following protein-coding genes. All autotrophs that fix CO_2 via the Calvin-Benson-Bassham (CBB) cycle use ribulose-1,5-bisphosphate carboxylase/oxygenase (RubisCO) (69). Two forms of RubisCO have been found in chemoautotrophic symbionts [e.g. (5, 11, 51)]. For the RubisCO form I, the *cbbL* gene is used as a functional marker, whereas the *cbbM* gene is used for Form II. The gene *aprA* codes for the alpha subunit of adenosine-5'-phosphosulfate reductase (APS reductase) (23) and is used to characterize thiotrophic bacteria. The APS reductase catalyzes the oxidation of sulfite and AMP to adenosinephosphosulfate (54) and the *aprA* gene has been found in both free-living and symbiotic sulfur oxidizers (3). To characterize methanotrophic bacteria, the genes encoding the particulate and soluble methane monooxygenase *(pmoA, mmoX)*, and methanol

dehydrogenase *(mxaF)* can be used as functional markers (22). Finally, biomarkers specific to the hosts and symbionts were analyzed and their stable carbon isotopic composition was determined to provide additional information about the nature of the nutritional carbon source.

MATERIAL AND METHODS

Site description and specimen collection. *Sclerolinum contortum* and *Oligobrachia haakonmosbiensis* (61) specimens were collected in 2003 by box coring during cruise ARKXIX-3b with R/V Polarstern in the framework of a German/French collaborative program (28). They were retrieved from position 72° 0.15'N, 14° 44.17'E (box corer 345) of the outer rim of the volcano. On board, specimens were separated from the sediment by washing with filtered seawater, fixed for DNA analyses and FISH, and stored at 4°C until further analyses.

DNA preparation and PCR amplification. Specimens were prepared for DNA extraction by fixation in 70% ethanol. *S. contortum* and *O. haakonmosbiensis* specimens were identified morphologically based on characters described by (61) and selected for construction of clone libraries. Three individuals of each species were prepared individually for DNA extraction. The worms were removed from their tubes by dissection, washed three times in sterile water, and DNA was isolated from the posterior part of the worm (without the opisthosoma). For the protocol applied here, Proteinase K was used for digestion and the reagent GeneReleaser (BioVentures, Murfreesboro, USA) for DNA purification (56).

The 18S rRNA genes of the worms were amplified using 30 PCR cycles with primers specific for the domain *Eukarya,* 1f and 2023r (49). Bacterial 16S rRNA genes were amplified using 20 PCR cycles with primers 8F (36) and 1492R (25) specific for the domain *Bacteria*.

In addition to rRNA genes, genes coding for RubisCO form I *(cbbL)*, RubisCO form II *(cbbM)*, and APS reductase *(aprA)* were amplified using 20 PCR cycles and sequenced. The following primers were used: cbbL-F and cbbL-R for RubisCO form I (12), cbbM-F and cbbM-R for RubisCO form II (12), aps1F and aps4R for APS reductase [designed by Jan Küver, see (4)].

Cloning and sequencing. The 18S rRNA gene of the host was sequenced directly. For PCR products that were cloned (16S rRNA genes, *cbbL, cbbM, aprA*), at least four parallel PCR reactions from each host individual were pooled and purified with the QiaQuick PCR Purification Kit (Qiagen, Hilden, Germany). For cloning, PCR products were ligated in the pCR4 TOPO vector (Invitrogen, Carlsbad, CA) and transformed into *E. coli* TOP10 cells

(Invitrogen, Carlsbad, CA) according to the manufacturer's recommendations. Clones were checked for the correct insert size by PCR with vector primers.

Sequencing was performed by *Taq* cycle sequencing with a model ABI377 sequencer (Applied Biosystems). Sequences were aligned and compared using the BioEdit program (www.mbio.ncsu.edu/BioEdit/bioedit.html). Sequences were grouped in a clone family if they shared more than 99% sequence identity (% identical nucleotides). For each host individual, representative clones from each clone family were chosen for plasmid preparation and fully sequenced in both directions.

Phylogenetic analysis. Sequence comparisons are expressed as sequence identity (% identical nucleotides or amino acids) and were checked against sequences in GenBank using BLAST (1, 70) for similarity searches. Sequence data were analyzed with the ARB software package (31).

Phylogenetic trees of 16S rRNA gene sequences were calculated by parsimony, neighbor-joining, and maximum-likelihood analysis with different sets of filters. For tree calculation, only almost full-length sequences (>1400 bp) were considered. Partial sequences were inserted into the reconstructed tree by parsimony criteria without allowing changes in the overall tree topology.

Phylogenetic trees of the protein-coding genes *cbbL, cbbM,* and *aprA* were generated from deduced amino acid sequences by neighbor-joining and maximum-likelihood analysis with 25% amino acid frequency filters. Sequence positions 102-142 of the *cbbL* gene from *Oligobrachia mashikoi* were excluded from phylogenetic analyses because of poor sequence quality.

Fluorescence *in situ* hybridization (FISH). Specimens were prepared for *in situ* hybridizations by fixation in phosphate-buffered seawater (pH 7.4) with 4% formaldehyde, then dehydrated in an ethanol series, and embedded in low-melting polyester (PE) wax (67). Samples were sectioned serially (6 μm) and mounted on aminosilane-coated slides. PE wax was removed in three rinses in absolute ethanol (5 min each), and sections were rehydrated in an ethanol series. For better penetration of probes, sections were subsequently incubated in Tris-HCl (20 mM, pH 8), Proteinase K (0.05 μg/ml in Tris-EDTA, pH 8, at 37°C), and washed in MilliQ water (5 min each). To prevent mixing or loss of different solutions during hybridization, each section was encircled with a liquid-repellent slide marker pen (Super Pap pen, Kisker Biotechnology, Steinfurt, Germany). For *in situ* hybridizations with mono- or horseradish peroxidase (HRP)-labeled probes (CARD-FISH) and subsequent staining with

4',6'-diamidino-2-phenylindole (DAPI), sections were processed as described previously (45, 62).

Probes and formamide concentrations used are given in Table 1. The specificity of probes developed for this study was determined empirically against reference strains with one or more mismatches. General probes for *Bacteria* and *Gammaproteobacteria* were used as positive controls. Probe NON338 was used as a negative control. All hybridizations were performed using formamide concentrations ensuring high specificity.

Nucleotide sequence accession numbers. The sequences isolated from *S. contortum* and *O. haakonmosbiensis* have the following accession numbers x to x (16S rRNA genes), x and x 18S rRNA genes), x and x *(aprA)*, x to x *(cbbL)*, x to x *(cbbM)*.

Extraction of worm tissue and preparation of derivatives. The extraction procedure and preparation of fatty acid methyl esters (FAMES) was carried out as described (13, 41). Briefly, total lipid extracts (TLE) were obtained from ca. 5 g of worm tissue. Prior to extraction, worm tissue and tube were separated and the tissue washed in artificial seawater to prevent a potential contamination with sedimentary microbes. The TLEs were extracted from whole worms as a separation of host and symbionts was not possible due to the extremely small diameter of the animals. Thus, the TLEs contained host and symbiont lipids. TLE were extracted by ultrasonification using organic solvents of decreasing polarity. Internal standards of known concentration and carbon isotopic compositions were added prior to extraction. Esterified fatty acids (FAs) present in glyco- and phospholipids were cleaved by saponification with methanolic KOH-solution. After extraction of the neutral lipid fraction from this mixture, FAs were methylated for analysis with BF_3 in methanol yielding FAMES.

Neutral lipids were further separated into hydrocarbons, ketones, and alcohols on a SPE silica glass cartridge (0.5 g packing) with solvent mixtures of increasing polarity (41). Alcohols were analyzed as trimethylsilyl (TMS) ethers. Shortly before analysis (<1 wk), aliquots from selected alcohol fractions were methylated with bis(trimethylsilyl)triflouracetamid (41). FAMES and TMS adducts were stored at −20°C until analysis.

Gas chromatography (GC), gas chromatography-mass spectrometry (GC-MS), gas chromatography-isotope ratio mass spectrometry (GC-IRMS). Concentrations, identities, and stable carbon isotope ratios of individual compounds were determined by GC, GC-MS and GC-IRMS analyses, respectively. Instrument specifications and operation modes of the GC, GC-MS and GC-IRMS systems were set according to Elvert and co-workers (13). Concentrations were calculated against internal standards. Identities of acquired mass spectra

were compared to known standards and published data. Stable carbon isotope ratios are given in the δ-notation against Pee Dee Belemnite. δ^{13}C-values of FAs and alcohols were corrected for the introduction of additional carbon atoms during derivatization. Internal standards were used to monitor precision and reproducibility during measurements. Reported δ^{13}C-values have an analytical error of 1-2‰.

Preparation of dimethyl disulphide (DMDS) adducts. Double bond positions of monoenoic FAs were determined by analysis as DMDS adducts as described previously (35, 40). The identities of DMDS adducts was determined by comparing acquired mass spectra to published data (35, 40). Double bond positions of polyunsaturated fatty acids (PUFAs) were not determined. PUFAs of the same carbon chain length and number of double bonds are therefore indicated by roman number suffixes.

TABLE 1 Oligonucleotide probes used in this study

Probe	Specificity	Probe sequence (5′-3′)	FA [%]^a	Label	Reference
NON338	Negative control	ACTCCTACGGGAGGCAGC	10	HRP	(74)
EUB338 I-III	most *Bacteria*	GCTGCCTCCCGTAGGAGT GCAGCCACCCGTAGGTGT GCTGCCACCCGTAGGTGT	55	HRP	(8)
Gam42a	*Gammaproteobacteria*	GCCTTCCCACATCGTTT	55	HRP	(32)
cBet42a	Competitor for probe Gam42a	GCCTTCCCACTTCGTTT	55	None	(32)
Ohaa-130	*O. haakonmosbiensis* symbiont 2	CCCGAACTATTGGGTAGA	35	Cy3	This study
Ohaa-144	*O. haakonmosbiensis* symbionts and rel.	TTTCACCAGGTTGTCCCG	35	Cy3	This study
Ohaa-653	*O. haakonmosbiensis* symbionts and rel.	CTCACCTCTACCAAACTC	55	HRP	This study
Sco-66	*S. contortum* symbiont and rel.	AGCTCTCCTCTGTTACCG	55	HRP	This study
Sco-444	*S. contortum* symbiont	TCCCAAGCCTTTCTTCAC	40	HRP	This study
Sco-467	*S. contortum* symbiont	ACGTCAAGACCCGAGAAT	40	HRP	This study

^{a} Percent (Vol/Vol) formamide (FA) in hybridization buffer for FISH.

RESULTS

Biogeochemical characterization of the siboglinid habitat. About 300-400 m from the geographical centre of the HMMV, the sulfidic zone covered with *Beggiatoa* mats is suddenly replaced by dense tubeworm colonies stretching over an area of about 0.4 km^2 around the HMMV. Two tubeworm species, *Sclerolinum contortum (Monilifera, Siboglinidae)* and *Oligobrachia haakonmosbiensis (Frenulata, Siboglinidae)* (61), coexist at the rim of the HMMV with very high biomasses of 1-2 kg wet weight m^{-2}, as determined by box coring. The posterior parts of their chitin tubes are buried in the reduced sediments (approximately 15 cm and 60 cm depth for *S. contortum* and *O. haakonmosbiensis,* respectively) while the anterior ends extend a few centimeters into the oxygenated water column (-1°C *in situ* temperature).

As measured with *in situ* microsensors, sulfide was depleted to zero at the sediment surface and increased steeply to 0.15 mM at 15 cm bsf. The *in situ* profiles of sulfide and oxygen overlapped in the top centimeters indicating that the tubeworms actively pump seawater into the sulfidic sediments (Fig. 1) (9). Methane concentrations were <0.05 mM down to 50 cm and then increased steeply with depth to 2 mM at 90 cm (43). Just below the base of the *O. haakonmosbiensis* worms and above the first fine layers of gas hydrates, elevated rates of anaerobic methane oxidation were measured (Fig. 1) coinciding with a subsurface peak of microbial aggregates mediating this process (43).
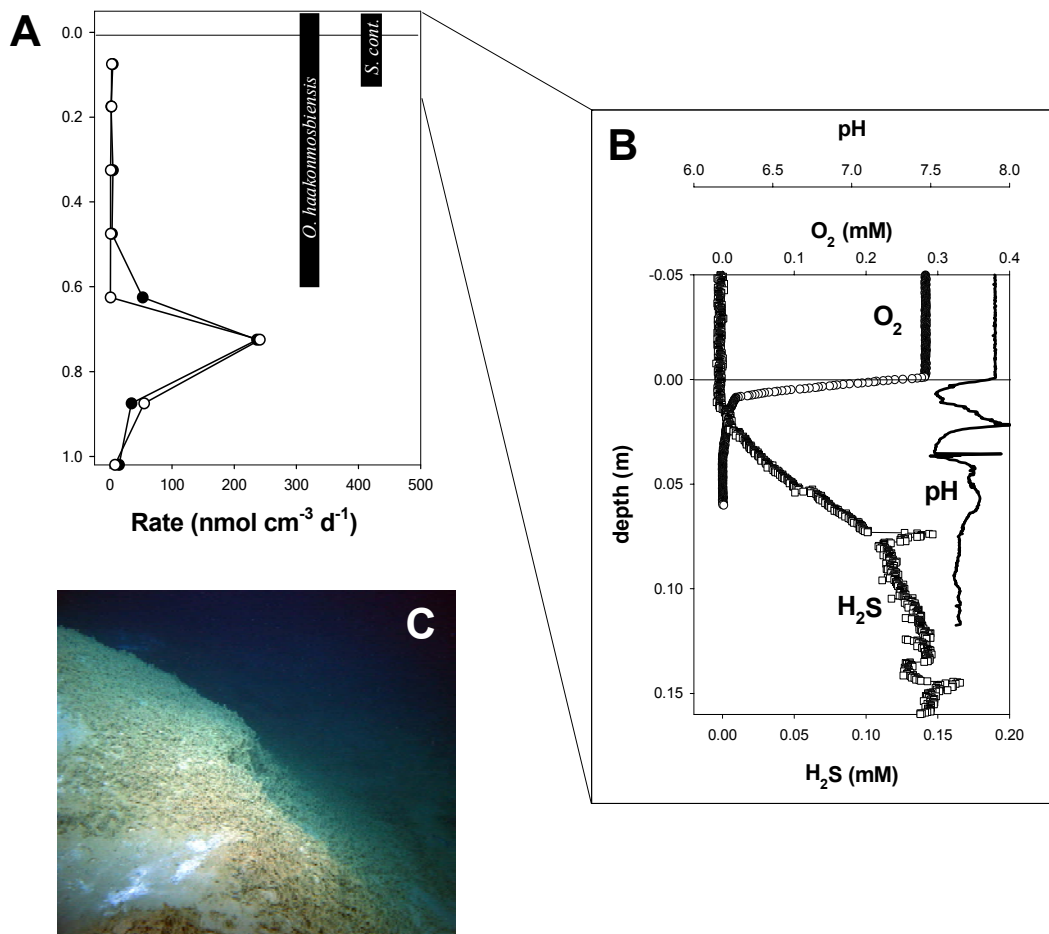
FIGURE 1 The habitat of *S. contortum* and *O. haakonmosbiensis*. (A) *In situ* microsensor measurements of pH (solid line), oxygen (circles) and sulfide (squares). (B) Radiotracer rate measurements of the anaerobic oxidation of methane (filled circles) and sulfate reduction (open circles); bars indicate the maximum tube lengths of *O. haakonmosbiensis* and *S. contortum*. (C) Sediments populated with tubeworms extending into the water column. The tubes are covered with a thin detritus layer. Graphs modified from (8) and (41) with permission.

18S rRNA genes. The morphological identification of worm individuals was confirmed by comparative 18S rRNA gene analysis. The 18S rRNA gene sequences obtained from *S. contortum* and *O. haakonmosbiensis* fell within the siboglinid clade consisting of sequences from other moniliferans, frenulates, and vestimentiferans (Fig. 2). Sequences were identical

between the three individuals from each host species but differed clearly between both species (89%), confirming the morphological identification of the two host species. *O. haakonmosbiensis* grouped with other frenulates, with *Siboglinum fiordicum* from Norwegian fjords as the closest relative (93%) in all three treeing methods. *S. contortum* grouped with *S. brattstromi* from Norwegian fjords (99%) and the sequences fell basal to those of vent and seep vestimentiferans. The *S. contortum* and *S. brattstromi* sequences were almost identical and differed mostly at ambiguous positions. Comparable sequence analysis of genes that are less conserved than 18S rRNA is required to determine whether *S. contortum*
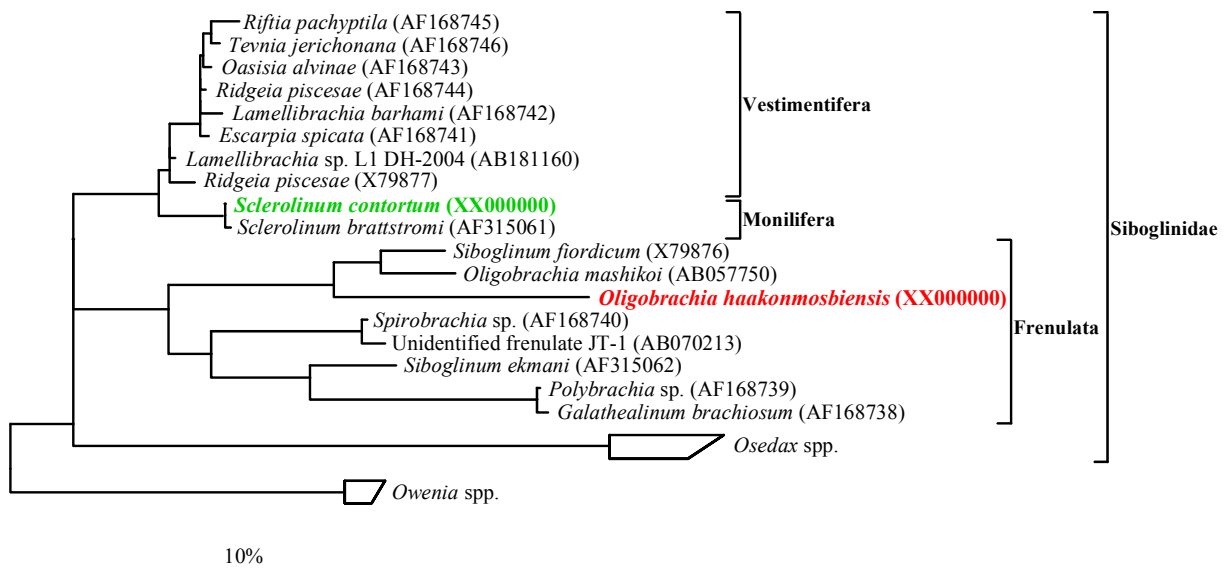
and *S. brattstromi* are indeed two separate species.

FIGURE 2 Phylogenetic placement of *S. contortum* and *O. haakonmosbiensis* based on 18S rRNA gene sequences. Branching orders that were not supported in all three calculation methods are shown as multifurcations. Sequences obtained in this study are enclosed in boxes. The bar represents 10% estimated phylogenetic divergence.

Bacterial 16S rRNA genes. The microbial diversity of clone libraries from *S. contortum* and *O. haakonmosbiensis* specimens was very low (Table 2). The vast majority of bacterial 16S rRNA gene sequences (224 of 226 clones) from *S. contortum* belonged to the *Gammaproteobacteria*. These sequences were nearly identical (99-100%) and grouped within one clone family (ScoSym). Only two out of 226 clones with common marine bacteria of the *Alphaproteobacteria* and the *Bacteroidetes*. Parsimony, distance, and maximum-likelihood analyses revealed that the gammaproteobacterial 16S rRNA gene sequence from *S. contortum* belongs to a clade of sulfide-oxidizing symbionts (Fig. 3). This clade contains symbionts of several host taxa belonging to the *Vestimentifera, Lucinacea,* and *Solemyidae* and is hereafter referred to as the '*Riftia*-lucinid' clade. The relationship between the *S. contortum* symbiont

127

and symbionts of various vestimentiferans was very close. The closest relative was the sulfide-oxidizing symbiont of the vestimentiferan *Escarpia spicata* from a hydrothermal vent in the Guaymas Basin (99%).

Almost all bacterial 16S rRNA gene sequences (220 of 223 clones) from *O. haakonmosbiensis* were also affiliated with the *Gammaproteobacteria* (Table 2). Two clone families (OhaaSym1 and OhaaSym2) sharing 97-98% sequence similarity to each other were found. Sequences were highly similar (>99%) within each clone family. Group OhaaSym1 sequences were found in individuals #1 and #2, while group OhaaSym2 sequences only occurred in individual #3. Only three out of 223 clones did not belong to the OhaaSym1 or 2 clone family and fell instead within the *Deltaproteobacteria* and CFB. The gammaproteobacterial sequences from *O. haakonmosbiensis* belong to a clade that includes environmental sequences from gas hydrate bearing lake sediments (96-97%), hydrothermal sediments (95-96%), shellfish-aquaculture sediments (92-93%), and the symbiont of another frenulate, *O. mashikoi* from muddy shallow sediments off Japan (92-93%). The closest cultivated relative was the heterotrophic sulfide-oxidizer *Leucothrix mucor* (89-90%). The phylogenetic placement of these sequences to each other was stable in all three treeing methods, but the relationship of this clade to other methane-oxidizing and sulfide-oxidizing symbionts was inconsistent (multifurcations shown in Fig. 3).

TABLE 2 Gene libraries from *S. contortum* and *O. haakonmosbiensis* individuals

Specimen	Number of clones								
	16S rRNA Genes						Protein-coding Genes		
	Gamma			Alpha	Delta	*Bacteroidetes*	RubisCO		APS
	ScoSym	OhaaSym1	OhaaSym2				*cbbL*	*cbbM*	*aprA*
S. contortum 1	113	0	0	1	0	0	-	16	30
S. contortum 2	58	0	0	0	0	1	-	10	ND
S. contortum 3	53	0	0	0	0	0	-	1	ND
O. haakonmosbiensis 1	0	55	0	0	0	0	6	5	12
O. haakonmosbiensis 2	0	113	0	0	2	0	25	23	25
O. haakonmosbiensis 3	0	0	52	0	0	1	2	2	ND

16S rRNA gene clones: Gamma *(Gammaproteobacteria)*, Alpha *(Alphaproteobacteria)*, Delta *(Deltaproteobacteria)*, ScoSym and OhaaSym (symbiont groups defined in this study). -, no PCR product; ND, not determined.

FIGURE 3 Phylogenetic placement of bacterial symbionts from *S. contortum* and *O. haakonmosbiensis* based on 16S rRNA gene sequences. Branching orders that were not supported in all three calculation methods are shown as multifurcations. Clone sequences from symbionts are in boldface type. Symbiont sequences obtained in this study are enclosed in boxes, sulfur-oxidizing bacteria (SOx), methane-oxidizing bacteria (MOx). The bar represents 10% estimated phylogenetic divergence.

Bathymodiolus puteoserpentis symbiont (U29164)
Bathymodiolus japonicus symbiont (AB036711)
Bathymodiolus sp. symbiont, Louisiana Slope mussel species Ia (U05595)
Methylomicrobium agile (X72767)
Methylomonas rubra (AF304194)
Methylobacter marinus (AF304197)
Frenulate *Oligobrachia haakonmosbiensis* symbiont 1 (XX000000)
Frenulate *Oligobrachia haakonmosbiensis* symbiont 2 (XX000000)
Sea of Okhotsk clone OHKB4.35 (AB094842)
Rainbow hydrothermal vent clone pIR3BC07 (AY354137)
Frenulate *Oligobrachia mashikoi* symbiont (AB057751)
Shellfish-aquaculture sediment clone Y94 (AB116468)
Hydrate Ridge surface sediment clone Hyd89-87 (AJ535246)
Marine sediment clone s11 (AY171372)
Cold-seep sediment clone CS043 (AY279067)
Leucothrix mucor (X87277)
Lucina pectinata symbiont (X84980)
Thyasira flexuosa symbiont (L01575)
Moniliferan *Sclerolinum contortum* symbiont (XX000000)
Vestimentiferan *Escarpia spicata* symbiont 'Alvin #2837' (AF165909)
Vestimentiferan *Riftia pachyptila* symbiont (U77478)
Vestimentiferan *Ridgeia piscesae* symbiont (U77480)
Vestimentiferan *Lamellibrachia columna* symbiont (U77481)
Inanidrilus leukodermatus Gamma 1 symbiont (AJ890100)
Olavius ilvae Gamma 1 symbiont (XX000000)
Allochromatium vinosum (M26629)
Thiorhodovibrio winogradskyi (AB016986)
Thiobacillus prosperus (AY034139)
Unidentified frenulate JT-1 symbiont (AB070215)
Olavius crassitunicatus Gamma 2 symbiont (AJ620508)
Beggiatoa alba (AF110274)
Thioploca ingrica (L40998)
Ectenagena extenta symbiont (AF035725)
Vesicomya gigas symbiont (AF035726)
Calyptogena elongata symbiont (AF035719)
Bathymodiolus septemdierum symbiont (AB178222)
Desulfosarcina variabilis (M34407)

MOx

SOx

10%

Protein-coding genes. In both host species, the presence of the following genes diagnostic for certain metabolic pathways were examined. Markers for methanotrophy *(pmoA, mmoX, mxaF)* could not be amplified despite many PCR attempts using different conditions, while RubisCO genes *(cbbL, cbbM)* and APS reductase genes *(aprA)* were successfully amplified (Table 2).

Fragments of *aprA* genes encoding the alpha-subunit of APS reductase were amplified from both *S. contortum* and *O. haakonmosbiensis*. Deduced amino acid sequences (152 amino acids) were identical between the individuals of each host species. The sequences from *S. contortum* and *O. haakonmosbiensis* were closely related to each other (92% sequence identity, Fig. 4) and to sequences from thiotrophic symbionts of gutless oligochaete worms (*S. contortum* 90-93%, *O. haakonmosbiensis* 85-87% sequence identity, respectively). The closest cultivated relatives were sulfur oxidizers such as *Thiobacillus denitrificans* (*Betaproteobacteria,* 88-92% sequence identity) and *Chlorobium chlorochromatii* (green sulfur bacteria, 67-70% sequence identity).
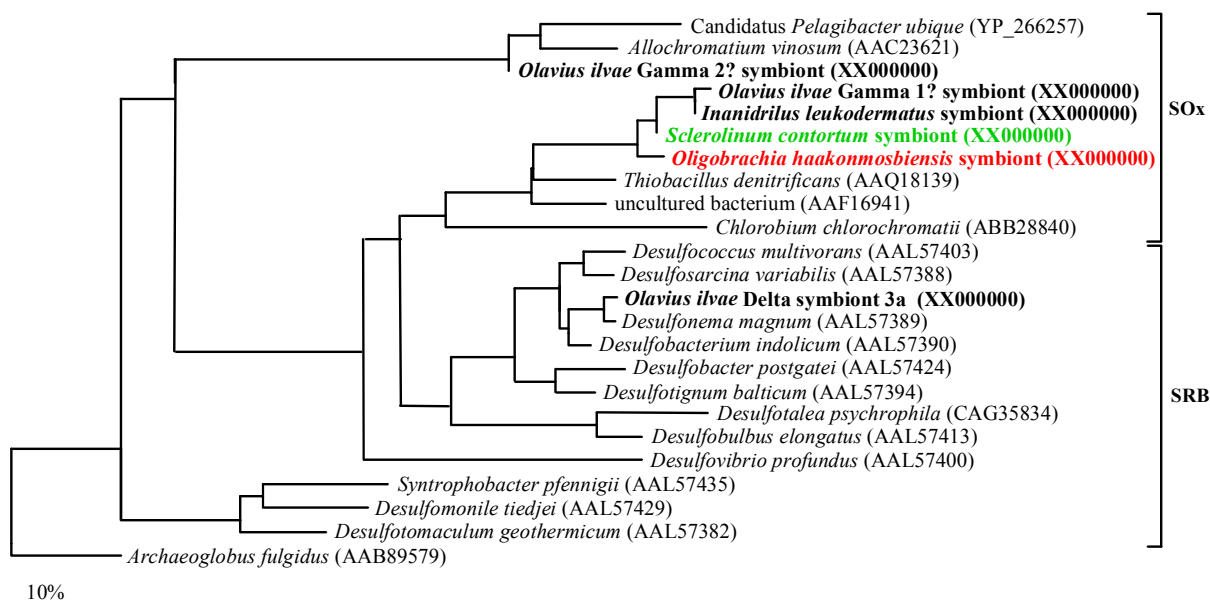
FIGURE 4 Phylogenetic placement of APS genes *(aprA)* from *S. contortum* and *O. haakonmosbiensis* symbionts based on deduced amino acid sequences. Clone sequences from symbionts are in boldface type. Symbiont sequences obtained in this study are enclosed in boxes, sulfate-reducing bacteria (SRB), sulfur-oxidizing bacteria (SOx). The bar represents 10% estimated phylogenetic divergence.

The *cbbM* gene of RubisCO form II was amplified from all *S. contortum* specimens, whereas the *cbbL* gene of RubisCO form I was not detectable despite multiple PCR attempts with different primer sets. Deduced amino acid sequences of the *cbbM* gene were identical in all 3 individuals (134 amino acids). Comparative sequence analysis (Fig. 5) showed that the *cbbM* sequence from *S. contortum* was closely related to a sequence from the seep vestimentiferan *Lamellibrachia* sp. symbiont-1 (Sagami Trough at 1,200 m water depth) and sequences isolated from hydrothermal vent bacteria (87-88% sequence identity). These sequences formed a distinct clade that also included the sulfide-oxidizer *Thiomicrospira crunogena*.

Both RubisCO form I and form II genes were found in *O. haakonmosbiensis* with two closely related sequences present for each RubisCO form (Fig. 5). Deduced amino acid sequences of the two *O. haakonmosbiensis cbbM* genes were highly similar to each other (133 amino acids, 97% sequence identity) and most closely related to environmental sequences from a hydrothermal vent (94% sequence identity) and Monterey Bay bacterioplankton (91-93% sequence identity). Deduced amino acid sequences of the two *cbbL* genes from *O. haakonmosbiensis* were almost identical (99% amino acid identity). The closest relatives were sequences from hydrothermal vent bacteria and symbionts from the frenulate *O. mashikoi* (91%), the vent mussel *Bathymodiolus azoricus cbbL*-1 and -2 (93%), the clam *Solemya velum* (91%), and a Suiyo seamount vent mussel (90%).
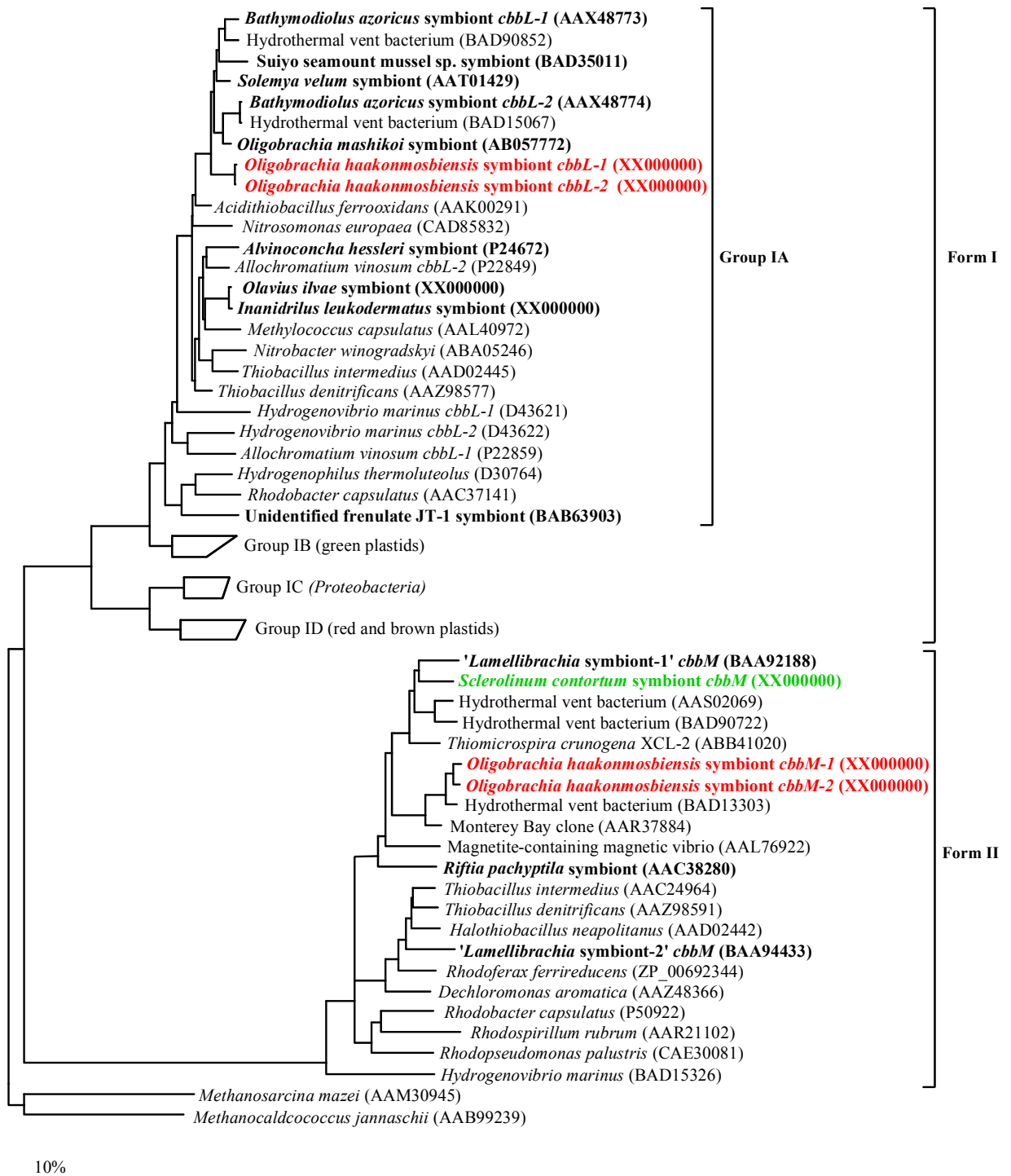
FIGURE 5 Phylogenetic placement of RubisCO form I and form II genes *(cbbL, cbbM)* from *S. contortum* and *O. haakonmosbiensis* symbionts based on deduced amino acid sequences. Branching orders that were not supported by the two calculation methods are shown as multifurcations. Clone sequences from symbionts are in boldface type. Symbiont sequences obtained in this study are enclosed in boxes. The bar represents 10% estimated phylogenetic divergence.

***In situ* identification.** Fluorescence *in situ* hybridization (FISH) with 16S rRNA targeted oligonucleotide probes specific to the dominant 16S rRNA phylotypes isolated from *S. contortum* and *O. haakonmosbiensis* (Table 2), confirmed that these originated from endosymbionts and not from bacteria on the worm surfaces or contaminants (Fig. 6). In both host species, coccoid-shaped bacteria (0.5-1.0 μm in diameter) were observed only in the symbiont-containing trophosome, while no bacteria were detected in other tissues or the space between the worm and its tube. The hybridization patterns of the symbiont-specific probes were similar to those of the general probes for all *Bacteria* and *Gammaproteobacteria*. The trophosome was only sparsely filled with endosymbiotic cells and their distribution was patchy with cells occurring mainly in clumps.

In situ hybridizations with general probes for the *Alphaproteobacteria*, *Deltaproteobacteria*, and *Bacteroidetes* gave no signals indicating that the 16S rRNA phylotypes found in low frequency in the clone libraries did not originate from endosymbionts. This conclusion was supported by double hybridizations with general probes for the domain *Bacteria* and for *Gammaproteobacteria* showing that cells other than *Gammaproteobacteria* were not present or extremely rare.
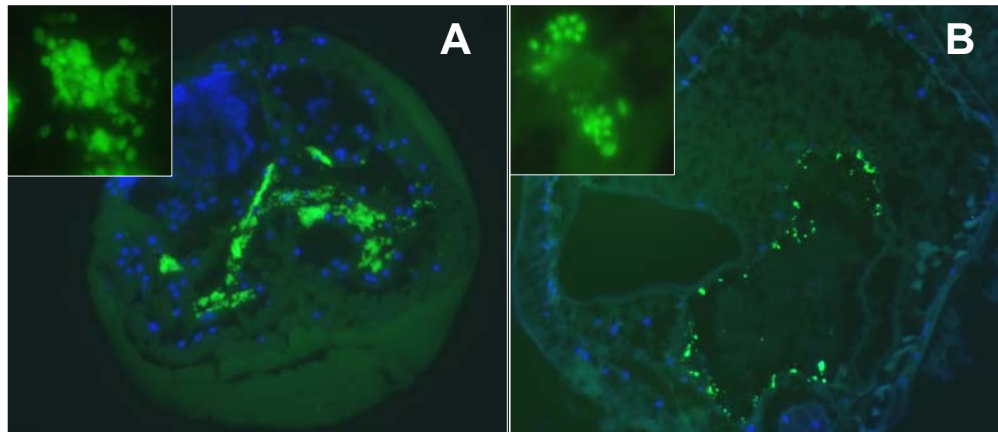
FIGURE 6 *In situ* identification of bacterial symbionts: epifluorescence micrographs of cross-sections through the entire worm and the symbiont-containing trophosome (inserts). (A) Endosymbionts of *S. contortum* stained by probe Sco-444 (green). (B) Endosymbionts of *O. haakonmosbiensis* stained by probe Ohaa-653 (green). Host nuclei and sperm of *S. contortum* are stained with DAPI (blue). Scale bars, 50 μm and 5 μm, respectively.

Biomarker analyses. The total lipid extracts (TLE) of both worm species were dominated by fatty acids (FA) and cholesterol (Table 3). Bacteria-specific steroids such as diplopterol, as well as hopanes were not present in the alcohol and hydrocarbon fraction, respectively (Table 3). The FA fingerprint showed considerable differences in both host species (Fig. 7). *S. contortum* was dominated by the FAs $C_{18:1\omega7}$ followed by $C_{16:1\omega7}$, $C_{16:0}$, $C_{20:4}$, $C_{22:2}$, and

$C_{18:1\omega9}$. Minor amounts of monoenoic C_{19} and C_{20} as well as polyunsaturated C_{20} and C_{22} FAs were also present. δ^{13}C-values ranged from -36‰ ($C_{18:1\omega9}$) to -53.5‰ ($C_{20:1\omega7}$) with a median of -43‰. In comparison to the FAs, cholesterol had a slighter higher δ^{13}C-value of -38.5‰. *O. haakonmosbiensis* was dominated by

the FAs $C_{18:1\omega7}$ followed by $C_{16:0}$, $C_{20:2}$, $C_{16:1\omega7}$, $C_{20:1\omega7}$, and $C_{20:4}$. FAs specific to type I and II methanotrophs such as $C_{16:1\omega8c}$ and $C_{18:1\omega8c}$ were not detected. Similar to *S. contortum,* minor amounts of monoenoic C_{18} - C_{20} as well as poly-unsaturated C_{18}, C_{20} and C_{22} FAs were also present. δ^{13}C-values of FAs ranged from -46‰ ($C_{14:0}$) to -81.5‰ ($C_{14:1\omega7}$) with a median of -70‰. As in *S. contortum*, cholesterol had a slightly higher δ^{13}C-value than the median of the FAs, but reached -65.5‰ in *O. haakonmosbiensis*. Bulk δ^{13}C measurements confirmed the average values measured for the host biomarkers with a δ^{13}C-value of -47.9‰ in *S. contortum* and -66.7‰ in *O. haakonmosbiensis*.

TABLE 3 Lipid biomarker concentrations extracted from *S. contortum* and *O. haakonmosbiensis*

	S. contortum	*O. haakonmosbiensis*
	concentration [µg g^{-1} dw]	concentration [µg g^{-1} dw]
Fatty Acids		
C14:1ω7	10	34
C14:0	8	28
C15:0	8	11
C16:1ω7	773	349
C16:0	376	525
C17:1ω7	3	17
C17:0	42	19
C18:3	8	120
C18:2-I	-	89
C18:2-II	-	38
C18:2-III	8	42
C18:1ω9	129	200
C18:1ω7	852	1485
C18:0	77	123
C19:1ω7	32	84
C20:5	60	80
C20:4	367	251
C20:3	7	118
C20:2	16	401
C20:1ω8	81	79
C20:1ω7	51	343
C22:4	44	103
C22:2	158	145
Steroids		
Cholesterol	544	2622

-, not detected.
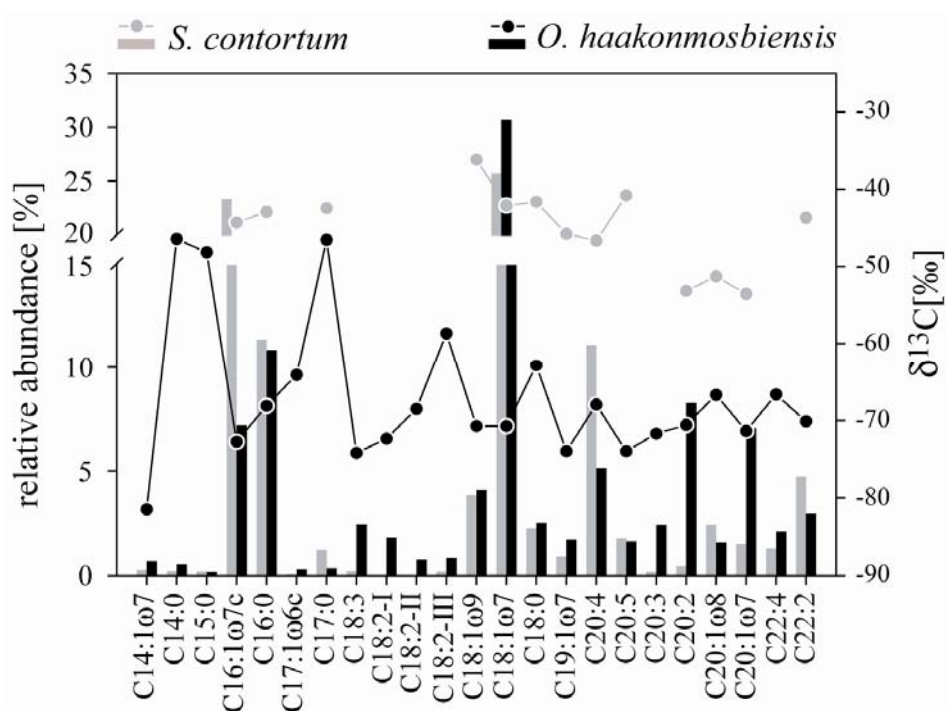
FIGURE 7 Abundance (bars) and stable carbon isotope composition (circles, triangles) of fatty acids extracted from *S. contortum* and *O. haakonmosbiensis* tissues.

DISCUSSION

Phylogeny of hosts and symbionts. Comparative 16S rRNA gene analysis confirmed that the siboglinids studied here live in symbiosis with *Gammaproteobacteria*. The *S. contortum* symbiont is the first one described for moniliferan siboglinids and falls into the monophyletic *Riftia*-lucinid clade. The *Riftia*-lucinid clade comprises most symbiont sequences of vestimentiferans known to date [(33), but also see (26, 38)]. Previous studies have shown that the phylogeny of vestimentiferan hosts is not congruent with the phylogeny of their symbionts (33). Symbionts are acquired from the locally available population of free-living bacteria (environmental transmission) and in seep vestimentiferans water depth appears to be the main selective factor for the symbiont phylotype in a given habitat (33). Both *S. contortum* (this study) and its closest relative *S. brattstromi*, (21), are related to the vestimentiferans, not to the frenulate species. Hence, it is intriguing that also the *S. contortum* symbiont is most closely related to vestimentiferan symbionts. Clearly, further studies on additional moniliferan species and their symbionts are needed to resolve the evolutionary relationships in these symbioses.

Comparative 18S rRNA phylogeny placed *O. haakonmosbiensis* in the siboglinid clade with other frenulates as its closest relatives. Two closely related symbiont sequences (97-98% sequence identity) were obtained from the different individuals of *O. haakonmosbiensis*. One

phylotype was found in two individuals investigated, while the other phylotye was only retrieved from the third individual investigated. Both phylotypes could be present in each individual as analytical constrains such as selective amplification during PCR cannot be ruled out. However, the co-occurrence of both phylotypes in the same individual is unlikely as PCR bias was minimized by a low number of PCR cycles. Moreover, the screening of 50-100 clones of each host individual should be sufficient to detect both phylotypes if they were present. This indicates microheterogeneity of symbionts which is probably due to the uptake of closely related symbiont species from the environment. Dual hybridization with probes specific for each phylotype could be used to prove this assumption. For symbionts of bathymodiolid mussels, it has been shown that microheterogeneity occurs on the level of ITS sequences (75). Moreover in gutless oligochaetes, closely related symbionts (≥92% sequence identity) may co-occur in the same host individual (4). Microheterogeneity of symbiotic 16S rRNA gene sequences has not been reported from chemosynthetic symbioses before but might be widespread in symbioses with environmentally transmitted symbionts. For most host species, only one to three individuals have been examined and this number might be too low to unveil the symbiont microheterogeneity within a given host population. The *O. haakonmosbiensis* symbionts grouped with environmental sequences from sediments and the symbiont of the frenulate *O. mashikoi* from muddy shallow sediments off Japan (25 m depth). This clade is only distantly related to the siboglinid symbionts of the *Riftia*-lucinid clade. The only other described frenulate symbiont from the unidentified seep species JT-1 from the Japan Trench (7,300 m depth) falls in a separate clade with the Gamma 2 symbiont of the gutless oligochaete *Olavius crassitunicatus* (3). However, there is no *in situ* evidence for the JT-1 sequence to confirm that it originated from endosymbionts. The three frenulate symbionts examined to date are not closely related to the major clades of methanotrophic and chemoautotrophic symbionts from other host species including those from vestimentiferans and the moniliferan species described in this study.

***In situ* identification and distribution of the symbionts.** Like all other siboglinids examined to date, *S. contortum* and *O. haakonmosbiensis* harbor endosymbiotic bacteria in their trophosomes as confirmed by FISH. In *O. haakonmosbiensis*, the symbiotic cells make up only a very small proportion of the trophosomal tissue. This observation is consistent with previous reports based on TEM analyses which show that the volume occupied by the symbionts of the closely related frenulate *S. fiordicum* is less than 1% of the whole animal (65). The low number of symbiotic cells may be attributed to the life style of these animals which are slow-growing organisms with a presumably low energy demand. Furthermore, the

posterior parts of frenulate tubes are permeable for dissolved organic matter and the worms may absorb these organic compounds through their epidermis, enabling them to supplement the nutritional input provided by the endosymbionts (63).

Metabolic capabilities of the symbionts. In addition to our molecular data, we analyzed biomarkers such as long chain polyunsaturated fatty acids (PUFAs) and their stable carbon isotope composition to gain further insights into the nutritional modes of the symbioses investigated here. PUFAs are essential membrane compounds of higher eukaryotes (73), but most animals lack the ability to synthesize them *de novo* [(48) and references therein]. Marine animals therefore rely on a dietary input of long chain PUFAs and to a limited extent on the uptake of shorter precursor C_{18} PUFAs, which are converted to C_{20} and C_{22} PUFAs by the animals. For *S. contortum* and *O. haakonmosbiensis,* a dietary input can be excluded, because the adult worms lack a digestive system (66). Moreover, the PUFAs detected in *S. contortum* and *O. haakonmosbiensis* were not present in lipid extracts from the sediments inhabited by the worms. Hence, symbiotic bacteria are the most likely source for the PUFAs.

Our molecular analyses clearly suggest that *S. contortum* harbors chemoautotrophic sulfur-oxidizing symbionts. This conclusion is supported by comparative 16S rRNA gene analyses showing that the symbiont falls into the *Riftia*-lucinid clade, which is assumed to consist of only chemoautotrophic sulfur-oxidizing symbionts (17). Moreover, chemoautotrophy was confirmed by the presence of a RubisCO form II gene *(cbbM)*, which indicates CO_2 fixation via the CBB cycle (69). RubisCO form II has also been found in the symbionts of the vestimentiferans *R. pachyptila* (51) and *Lamellibrachia* sp. (11). The presence of an *aprA* gene that groups with *aprA* sequences from symbiotic and free-living sulfur oxidizers provides further evidence for the thiotrophic nature of the *S. contortum* symbiont. These results correspond well with enzyme assays demonstrating APS and RubisCO activity in tissues of the closely related *S. brattstromi* (64) and indicate that both *Sclerolinum* hosts are associated with chemoautotrophic sulfur-oxidizing symbionts.

The δ^{13}C-values of *S. contortum* bulk tissue (-47.9‰) and biomarkers (Fig. 7) are highly negative for sulfur oxidizers that possess RubisCO form II, but in the range of reported for cold seep vestimentiferan tubeworms that harbor chemoautotrophic sulfur oxidizers (-18.6‰ to -51.3‰) (39). A likely explanation for the pronounced ^{13}C depletion of *S. contortum* tissue would be an isotopically light CO_2 pool. Lein *et al.* (29) found highly varying δ^{13}C-values for bicarbonate in sediments of the HMMV ranging from -32‰ to +2‰. CO_2 is fractionated upon autotrophic fixation via the CBB cycle. The isotopic fractionation factor of the RubisCO form II gene from the *R. pachyptila* symbiont (which is closely related to the *S. contortum*

RubisCO form II gene) is -19.5‰ (50). Thus, chemoautotrophic fixation of light ambient CO_2 coupled to the high isotopic fractionation of RubisCO form II may account for the observed stable carbon isotope composition of *S. contortum* (Fig. 8).
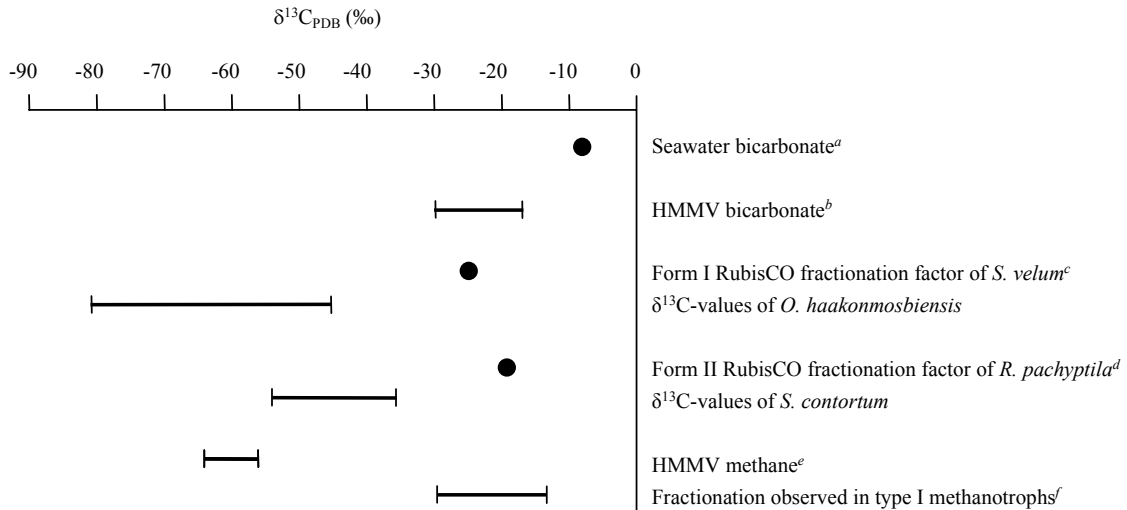
FIGURE 8 Stable carbon isotope signatures and ^{13}C fractionation. Sources: a (18), b+e (28), c (57), d (48), f (66).

Our results are in contrast to previous studies of *S. contortum* specimens, which were also sampled at HMMV. Stacked membrane structures typical for type I methanotrophs were visualized by TEM inside the symbiotic cells and methane oxidation was measured in homogenized tissues (46, 47). These observations suggest a methanotrophic symbiosis in *S. contortum* and for which we did not find any indications in this study.

The metabolic mode of the *O. haakonmosbiensis* symbionts could not be unambiguously determined based on 16S rRNA gene phylogeny. The 16S rRNA gene sequences of the symbionts are too distantly related to cultivated bacteria to infer the symbionts metabolism. Moreover, the phylogenetic position of the sequences could not be clearly resolved as they fall between clades of known thiotrophic and methanotrophic symbionts. However, the additional molecular data presented in this study argues for a thiotrophic nature of the *O. haakonmosbiensis* symbionts. We did not detect *pmoA* genes indicative of methanotrophy. However, *aprA* genes were present in the trophosome related to those from chemoautotrophic, sulfur-oxidizing symbionts of gutless oligochaetes. Moreover, APS activity based on enzyme assays has been reported previously in another frenulate, *Oligobrachia gracilis* (64). The presence of genes encoding RubisCO *(cbbL, cbbM)* confirms the metabolic potential for autotrophic CO_2 fixation, but RubisCO form I have been reported from both thiotrophs and

type X methanotrophs (2). The occurrence of both RubisCO forms has not been described for any symbiont previously, but is known from free-living bacteria such as *Allochromatium vinosum* (71). Furthermore, TEM analysis of *O. haakonmosbiensis* from HMMV showed that the symbiont ultrastructure was similar to thiotrophic symbionts reported from other chemoautotrophic symbioses and membrane stacks typical of methanotrophic bacteria were not detected (47).

The stable carbon isotope composition of *O. haakonmosbiensis* was even more negative than that of *S. contortum* with values never measured before in a chemoautotrophic symbiosis (18). The bulk δ^{13}C-value of -66.7‰ was 69-35‰ lighter than the ambient bicarbonate (Fig. 8) (29). The *O. haakonmosbiensis* symbionts possess genes for both RubisCO form I and form II, but known isotopic fractionation factors for these genes are not large enough to explain such highly negative tissue values. The RubisCO form I genes from *O. haakonmosbiensis* are related to RubisCO form I of *S. velum*, which shows a fractionation effect of 24.4‰ (59). Thus, the lightest δ^{13}C-value observed in *O. haakonmosbiensis* biomarkers (-81.5‰, compound C14:1ω7) cannot be explained by chemoautotrophic CO_2 fixation alone and strongly indicates an incorporation of methane derived carbon (Fig. 8).

A dual symbiosis in *O. haakonmosbiensis* may be an explanation for the highly negative stable carbon isotopic composition. Type I methanotrophs fractionate methane-derived carbon upon oxidation by up to -35‰ (24, 68). The ambient methane has a δ^{13}C-value of -60‰ (29). Hence, methane oxidation by methanotrophic symbionts possibly accounts for the highly negative biomarker signatures (Fig. 8). Moreover, *O. haakonmosbiensis* extends with its root into the methane rich zone of the sediments and putative methanotrophic symbionts could exploit the ambient methane, but could also profit from the sulfide provided by the anaerobic oxidation of methane (Fig. 1). In contrast, our biogeochemical data indicate that methane would not be available for symbionts of *S. contortum*, because it is already depleted before it reaches the surface sediments that are inhabited by *S. contortum*. Here, sulfide concentrations reach up to 0.15 mM, which may be enough to fuel a thiotrophic life style.

The hypothesis of a dual symbiosis in *O. haakonmosbiensis* implies that we were not able to detect the methanotrophic symbiont despite the analysis of a large number of 16S rRNA sequences and three genes involved in methanotrophy, as well as FISH data indicating that no further symbionts are present, at least in significant amounts, in these worms. Moreover, biomarkers that are characteristic for type I and type II methanotrophs such as $C_{16:1\omega8}$ and $C_{18:1\omega8}$ fatty acids (22) were not found in *O. haakonmosbiensis*. Instead, substantial amounts

of PUFAs were detected, which have not been found in known lineages of methanotrophic bacteria. In conclusion, the molecular data indicates that *O. haakonmosbiensis* harbors a chemoautotrophic, sulfur-oxidizing symbiont while the highly negative δ^{13}C values suggest that these worms harbor an additional symbiont belonging to a novel lineage of methanotrophs. Clearly, further molecular studies as well as stable carbon isotope analyses of inorganic carbon sources at HMMV are necessary to resolve if additional symbionts beyond the ones described in this study also occur in *O. haakonmosbiensis* worms.

REFERENCES

1. **Altschul, S. F., T. L. Madden, A. A. Schäffer, J. Zhang, Z. Zhang, W. Miller, and D. J. Lipman.** 1997. Gapped BLAST and PSI-BLAST: a new generation of protein database search programs. Nucleic Acids Res. **29:**2994-3005.
2. **Baxter, N., R. Hirt, L. Bodrossy, K. Kovacs, M. Embley, J. Prosser, and C. Murrell.** 2002. The ribulose-1,5-bisphosphate carboxylase/oxygenase gene cluster of Methylococcus capsulatus (Bath). Arch. Microbiol. **177:**279-289.
3. **Blazejak, A., C. Erseus, R. Amann, and N. Dubilier.** 2005. Coexistence of Bacterial Sulfide Oxidizers, Sulfate Reducers, and Spirochetes in a Gutless Worm (Oligochaeta) from the Peru Margin. Appl. Environ. Microbiol. **71:**1553-1561.
4. **Blazejak, A., J. Kuever, C. Erséus, R. Amann, and N. Dubilier.** in press. Phylogeny of 16S rRNA, RubisCO, and APS reductase genes from gamma- and alphaproteobacterial symbionts in gutless marine worms (Oligochaeta) from Bermuda and Bahamas. Appl. Environ. Microbiol.
5. **Cavanaugh, C. M., M. S. Abbott, and M. Veenhuis.** 1988. Immunochemical Localization of Ribulose-1,5-bisphosphate Carboxylase in the Symbiont-Containing Gills of Solemya velum (Bivalvia: Mollusca) Proc. Natl. Acad. Sci. **85:**7786-7789.

6.   **Cavanaugh, C. M., S. L. Gardiner, M. L. Jones, H. W. Jannasch, and J. B. Waterbury.** 1981. Prokaryotic cells in the hydrothermal vent tube worm Riftia pachyptila Jones: possible chemoautotrophic symbionts. Science **213:**340-342.

7.   **Childress, J. J., C. R. Fisher, J. M. Brooks, M. C. Kennicutt II, R. Bidigare, and A. E. Anderson.** 1986. A methanotrophic marine molluscan (Bivalvia, Mytilidae) symbiosis: mussels fueled by methane. Science **233:**1306-1308.

8.   **Daims, H., A. Brühl, R. Amann, and K. H. Schleifer.** 1999. The domain-specific probe EUB338 is insufficient for the detection of all Bacteria: Development and evaluation of a more comprehensive probe set. Syst. Appl. Microbiol. **22:**434-444.

9.   **De Beer, D., E. Sauter, H. Niemann, U. Witte, M. Schlüter, and A. Boetius.** 2006. In situ fluxes and zonation of microbial activity in surface sediments of the Haakon Mosby Mud Volcano (in press). Limnol. Oceanogr.

10.   **Di Meo, C. A., A. E. Wilbur, W. E. Holben, R. A. Feldman, R. C. Vrijenhoek, and S. C. Cary.** 2000. Genetic Variation among Endosymbionts of Widely Distributed Vestimentiferan Tubeworms. Appl. Environ. Microbiol. **66:**651-658.

11.   **Elsaied, H., H. Kimura, and T. Naganuma.** 2002. Molecular characterization and endosymbiotic localization of the gene encoding D-ribulose 1,5-bisphosphate carboxylase-oxygenase (RuBisCO) form II in the deep-sea vestimentiferan trophosome. Microbiology **148:**1947-1957.

12.   **Elsaied, H., and T. Naganuma.** 2001. Phylogenetic Diversity of Ribulose-1,5-Bisphosphate Carboxylase/Oxygenase Large-Subunit Genes from Deep-Sea Microorganisms. Appl. Environ. Microbiol. **67:**1751-1765.

13.   **Elvert, M., A. Boetius, K. Knittel, and B. B. Jörgensen.** 2003. Characterization of specific membrane fatty acids as chemotaxonomic markers for sulfate-reducing bacteria involved in anaerobic oxidation of methane. Geomicrobiol. J. **20:**403-419.

14.   **Felbeck, H.** 1981. Chemoautotrophic potential of the hydrothermal vent tube worm, Riftia pachyptila Jones (Vestimentifera). Science **213:**336-338.

15.   **Felbeck, H., J. J. Childress, and G. N. Somero.** 1981. Calvin-Benson cycle and sulfide oxidation enzymes in animals from sulfide-rich habitats. Nature **293:**291.

16.   **Feldman, R. A., T. M. Shank, M. B. Black, A. R. Baco, C. R. Smith, and R. C. Vrijenhoek.** 1998. Vestimentiferan on a whale fall. Biol Bull **194:**116-119.

17.   **Fisher, C. R.** 1990. Chemoautotrophic and methanotrophic symbioses in marine invertebrates. Rev. Aquat. Sci. **2:**399-436.

18.   **Fisher, C. R.** 1995. Toward an appreciation of hydrothermal vent animals: their environment, physiological ecology, and tissue stable isotope values, p. 297-316. *In* S. E. Humphris, R. A. Zierenberg, L. S. Mullineaux, and R. E. Thomson (ed.), Seafloor hydrothermal systems: Physical, Chemical, Biological, and Geological Interactions, vol. Geophysical Monograph 91. American Geophysical Union, Washington D.C.

19.   **Goericke, R., J. P. Montoya, and B. Fry.** 1994. Physiology of isotopic fractionation in algae and cyanobacteria. *In* K. Lajtha and R. H. Michener (ed.), Stable isotopes in ecology and environmental science. Blackwell Scientific Publications, Oxford.

20.   **Goffredi, S. K., V. J. Orphan, G. W. Rouse, L. Jahnke, T. Embaye, K. Turk, R. Lee, and R. C. Vrijenhoek.** 2005. Evolutionary innovation: a bone-eating marine symbiosis. Environ. Microbiol. **7:**1369-1378.

21.   **Halanych, K. M., R. A. Feldman, and R. C. Vrijenhoek.** 2001. Molecular Evidence that Sclerolinum brattstromi Is Closely Related to Vestimentiferans, not to Frenulate Pogonophorans (Siboglinidae, Annelida) Biol. Bull. **201:**65-75.

22.   **Hanson, R. S., and T. E. Hanson.** 1996. Methanotrophic Bacteria. Microbiol. Rev. **60:**439 - 471.

23. **Hipp, W., A. Pott, N. Thum-Schmitz, I. Faath, C. Dahl, and H. Truper.** 1997. Towards the phylogeny of APS reductases and sirohaem sulfite reductases in sulfate-reducing and sulfur-oxidizing prokaryotes. Microbiology **143:**2891-2902.

24. **Jahnke, L. L., R. E. Summons, J. M. Hope, and D. J. Des Marais.** 1999. Carbon isotopic fractionation in lipids from methanotrophic bacteria II: the effects of physiology and environmental parameters on the biosynthesis and isotopic signatures of biomarkers. Geochim. Cosmochim. Acta **63:**79-93.

25. **Kane, M. D., L. K. Poulsen, and D. A. Stahl.** 1993. Monitoring the enrichment and isolation of sulfate-reducing bacteria by using oligonucleotide hybridization probes designed from environmentally derived 16S rRNA sequences. Appl. Environ. Microbiol. **59:**682-686.

26. **Kimura, H., Y. Higashide, and T. Naganuma.** 2003. Endosymbiotic Microflora of the Vestimentiferan Tubeworm (Lamellibrachia sp.) from a Bathyal Cold Seep. Mar. Biotechnol. **5:**593-603.

27. **Kimura, H., M. Sato, Y. Sasayama, and T. Naganuma.** 2003. Molecular characterization and in situ localization of endosymbiotic 16S ribosomal RNA and RuBisCO genes in the pogonophoran tissue. Mar. Biotechnol. **5:**261-269.

28. **Klages, M., J. Thiede, and J. P. Foucher (ed.).** 2004. The Expetition ARKTIS XIX/3 of the Research Vessel Polarstern in 2003, vol. 488. Buchhandlung Kamloth, Bremen.

29. **Lein, A., P. Vogt, K. Crane, A. Egorov, and M. Ivanov.** 1999. Chemical and isotopic evidence for the nature of the fluid in CH4-containing sediments of the Haakon Mosby Mud Volcano. Geo-Mar. Lett. **19:**76-83.

30. **Lösekann, T., T. Nadalig, H. Niemann, K. Knittel, A. Boetius, and R. Amann.** in prep. Novel clusters of aerobic and anaerobic methane oxidizers at an Arctic cold seep (Haakon Mosby Mud Volcano, Barents Sea).

31. **Ludwig, W., O. Strunk, R. Westram, L. Richter, H. Meier, Yadhukumar, A. Buchner, T. Lai, S. Steppi, G. Jobb, W. Förster, I. Brettske, S. Gerber, A. W. Ginhart, O. Gross, S. Grumann, S. Hermann, R. Jost, A. König, T. Liss, R. Lüßmann, M. May, B. Nonhoff, B. Reichel, R. Strehlow, A. Stamatakis, N. Stuckmann, A. Vilbig, M. Lenke, T. Ludwig, A. Bode, and K. H. Schleifer.** 2004. ARB: a software environment for sequence data. Nucleic Acids Res. **32:**1363-1371.

32. **Manz, W., R. Amann, W. Ludwig, M. Wagner, and K.-H. Schleifer.** 1992. Phylogenetic oligodeoxynucleotide probes for the major subclasses of proteobacteria: problems and solutions. Syst. Appl. Microbiol. **15:**593-600.

33. **McMullin, E. R., S. Hourdez, S. Schaeffer, and C. Fisher.** 2003. Phylogeny and Biogeography of Deep Sea Vestimentiferan Tubeworms and Their Bacterial Symbionts. Symbiosis **34:**1-40.

34. **Milkov, A. V., P. R. Vogt, K. Crane, A. Y. Lein, R. Sassen, and G. A. Cherkashev.** 2004. Geological, geochemical, and microbial processes at the hydrate-bearing Haakon Mosby mud volcano: a review. Chem. Geol. **205:**347-366.

35. **Moss, C. W., and M. A. Lambert-Fair.** 1989. Location of Double Bonds in Monounsaturated Fatty Acids of Campylobacter cryaerophila with Dimethyl Disulfide Derivatives and Combined Gas Chromatography-Mass Spectrometry. J. Clin. Microbiol. **27:**1467-1470.

36. **Muyzer, G., A. Teske, C. O. Wirsen, and H. W. Jannasch.** 1995. Phylogenetic relationships of *Thiomicrospira* species and their identification in deep-sea hydrothermal vent samples by denaturing gradien gel electrophoresis of 16S rDNA fragments. Arch. Microbiol. **164:**165-172.

37. **Naganuma, T., H. Elsaied, D. Hoshii, and H. Kimura.** 2005. Bacterial Endosymbioses of Gutless Tube-Dwelling Worms in Nonhydrothermal Vent Habitats. Mar. Biotechnol. **7:**416-428.

38. **Naganuma, T., C. Kato, H. Hirayama, N. Moriyama, J. Hashimoto, and K. Horikoshi.** 1997. Intracellular occurrence of epsilon-proteobacterial 16S rDNA sequences in the vestimentiferan trophosome. J. Oceanogr. **53:**193-197.

39. **Nelson, D. C., and C. R. Fisher.** 1995. Chemoautotrophic and methanotrophic endosymbiotic bacteria at deep-sea vents and seeps, p. 125-167. *In* D. M. Karl (ed.), Deep-sea hydrothermal vents. CRC Press, Boca Raton.

40. **Nichols, P. D., J. B. Guckert, and D. C. White.** 1986. Determination of monounsaturated fatty acid double-bond position and geometry for microbial monocultures and complex consortia by capillary GC-MS of their dimethyl disulphide adducts. J. Microbiol. Methods **5:**49-55.

41. **Niemann, H., M. Elvert, M. Hovland, B. Orcutt, A. G. Judd, I. Suck, J. Gutt, S. B. Joye, E. Damm, K. Finster, and A. Boetius.** 2005. Methane emission and consumption at a North Sea gas seep (Tommeliten area). Biogeosciences **2:**335-351.

42. **Niemann, H., M. Elvert, T. Lösekann, J. Jakob, T. Nadalig, and A. Boetius.** in prep. Distribution of methanotrophic guilds at Haakon Mosby Mud Volcano, Barents Sea.

43. **Niemann, H., T. Lösekann, D. de Beer, M. Elvert, K. Knittel, R. Amann, E. Sauter, M. Schlüter, M. Klages, J. Foucher, and A. Boetius.** subm. Fluid flow controls distribution of methanotrophic microorganisms at submarine cold seeps. Nature.

44. **Niemann, H., E. Sauter, M. Krüger, F. Heinrich, T. Lösekann, M. Elvert, and A. Boetius.** in prep. Aerobic and anaerobic methane oxidation in sediments of Haakon Mosby Mud Volcano, Barents Sea.

45. **Pernthaler, A., J. Pernthaler, and R. Amann.** 2002. Fluorescence in situ hybridization and catalyzed reporter deposition (CARD) for the identification of marine Bacteria. Appl. Environ. Microbiol. **68:**3094-3101.

46. **Pimenov, N., A. Savvichev, I. Rusanov, A. Lein, A. Egorov, A. Gebruk, L. Moskalev, and P. Vogt.** 1999. Microbial processes of carbon cycle as the base of food chain of Haakon Mosby Mud Volcano. Geo-Mar. Lett. **19:**89 - 96.

47. **Pimenov, N. V., A. S. Savvichev, I. I. Rusanov, A. Y. Lein, and M. V. Ivanov.** 2000. Microbiological processes of the carbon and sulfur cycles at cold methane seeps of the North Atlantic. Microbiology **69:**709-720.

48. **Pond, D. W., C. E. Allen, M. V. Bell, C. L. Van Dover, A. E. Fallick, D. R. Dixon, and J. R. Sargent.** 2002. Origins of long-chain polyunsaturated fatty acids in the hydrothermal vent worms Ridgea piscesae and Protis hydrothermica. Mar. Ecol. Prog. Ser. **225:**219-226.

49. **Pradillon, F., A. Schmidt, J. Peplies, and N. Dubilier.** subm. Identification of early life history stages of marine invertebrate species with whole-larvae in situ hybridisation. Mar. Ecol. Prog. Ser.

50. **Robinson, J. J., K. M. Scott, S. T. Swanson, M. H. O'Leary, K. Horken, F. R. Tabita, and C. M. Cavanaugh.** 2003. Kinetic istotope effect and characterization of form II RuBisCO from the chemoautotrophic endosymbionts of the hydrothermal vent tubeworm Riftia pachyptila. Limnol. Oceanogr. **48:**48-54.

51. **Robinson, J. J., J. L. Stein, and C. M. Cavanaugh.** 1998. Cloning and Sequencing of a Form II Ribulose-1,5-Bisphosphate Carboxylase/Oxygenase from the Bacterial Symbiont of the Hydrothermal Vent Tubeworm Riftia pachyptila. J. Bacteriol. **180:**1596-1599.

52.   **Rouse, G. W.** 2001. A cladistic analysis of Siboglinidae Caullery, 1914 (Polychaeta, Annelida): formerly the phyla Pognophora and Vestimentifera. Zoo. J. Linn. Soc. **132:**55-80.

53.   **Rouse, G. W., S. K. Goffredi, and R. C. Vrijenhoek.** 2004. Osedax: Bone-Eating Marine Worms with Dwarf Males. Science **305:**668-671.

54.   **Sanchez, O., I. Ferrera, C. Dahl, and J. Mas.** 2001. In vivo role of adenosine-5'-phosphosulfate reductase in the purple sulfur bacterium Allochromatium vinosum. Arch. Microbiol. **176:**301-305.

55.   **Sauter, E. J., S. I. Muyakshin, J. L. Charlou, M. Schlüter, A. Boetius, K. Jerosch, E. Damm, J. P. Foucher, and M. Klages.** in press. Methane discharge from a deep-sea submarine mud volcano into the upper water column by gas hydrate-coated methane bubbles. Earth Planet. Sci. Lett.

56.   **Schizas, N. V., G. T. Street, B. C. Coull, G. T. Chandler, and J. M. Quattro.** 1997. An efficient DNA extraction method for small metazoans. Mol. Mar. Biol. Biotech. **6:**381-383.

57.   **Schmaljohann, R., and H. J. Flügel.** 1987. Methane-oxidizing bacteria in Pogonophora. Sarsia **72:**91-98.

58.   **Schulze, A., and K. M. Halanych.** 2003. Siboglinid evolution shaped by habitat preference and sulfide tolerance. Hydrobiologia **496:**199-205.

59.   **Scott, K. M., J. Schwedock, D. P. Schrag, and C. M. Cavanaugh.** 2004. Influence of form IA RubisCO and environmental dissolved inorganic carbon on the delta 13C of the clam-chemoautotroph symbiosis Solemya velum. Environ. Microbiol. **6:**1210-1219.

60.   **Sibuet, M., and K. Olu.** 1998. Biogeography, biodiversity and fluid dependence of deep-sea cold-seep communities at active and passive margins. Deep-Sea Res. II **45:**517 - 567.

61.   **Smirnov, R. V.** 2000. Two new species of Pogonophora from the arctic mud volcano off northwestern Norway. Sarsia **85:**141-150.

62.   **Snaidr, J., R. Amann, I. Huber, W. Ludwig, and K. H. Schleifer.** 1997. Phylogenetic analysis and in situ identification of bacteria in activated sludge. Appl. Environ. Microbiol. **63:**2884-2896.

63.   **Southward, A. J., and E. C. Southward.** 1981. Dissolved organic matter and the nutrition of the Pogonophora: a reassessment based on recent studies of their morphology and biology. Kieler Meeresforsch. **5:**445-453.

64.   **Southward, A. J., E. C. Southward, P. R. Dando, R. L. Barrett, and R. Ling.** 1986. Chemoautotrophic Function of Bacterial Symbionts in Small Pogonophora. Journal of the Marine Biological Association of the United Kingdom **66:**415-437.

65.   **Southward, E. C.** 1982. Bacterial symbionts in Pogonophora. J. Mar. Biol. Ass. U. K. **46:**579-616.

66.   **Southward, E. C., A. Schulze, and S. L. Gardiner.** 2005. Pogonophora (Annelida): form and function. Hydrobiologia **535-536:**227-251.

67.   **Steedman, H. F.** 1957. Polyester wax: A new ribboning embedding medium for histology. Nature **457:**1345.

68.   **Summons, R. E., L. L. Jahnke, and Z. Roksandic.** 1994. Carbon isotopic fractionation in lipids from methanotrophic bacteria: Relevance for interpretion of the geochemical record of biomarkers. Geochim. Cosmochim. Acta **58:**2853-2863.

69.   **Tabita, F. R.** 1988. Molecular and cellular regulation of autotrophic carbon dioxide fixation in microorganisms. Microbiol. Rev. **52:**155-189.

70.   **Tatusova, T. A., and T. L. Madden.** 1999. Blast 2 sequences - a new tool for comparing protein and nucleotide sequences. FEMS Microbiol. Letters **174**.

71. **Viale, A. M., H. Kobayashi, and T. Akazawa.** 1989. Expressed genes for plant-type ribulose 1,5-bisphosphate carboxylase/oxygenase in the photosynthetic bacterium Chromatium vinosum, which possesses two complete sets of the genes. J. Bacteriol. **171:**2391-2400.

72. **Vogt, P., K. Crane, S. Pfirman, E. Sundvor, N. Cherkis, H. Fleming, C. Nishimura, and A. Shor.** 1991. SeaMARC II sidescan sonar imagery and swath bathymetry in the Nordic Basin. EOS Trans. Am. Geophys. Union **72:**486.

73. **Wallis, J. G., J. L. Watts, and J. Browse.** 2002. Polyunsaturated fatty acid synthesis: what will they think of next? Trends in Biochemical Sciences **27:**467-473.

74. **Wallner, G., R. Amann, and W. Beisker.** 1993. Optimizing fluorescent in situ hybridization with rRNA-targeted oligonucleotide probes for flow cytometric identification of microorganism. Cytometry **14:**136-143.

75. **Won, Y.-J., S. J. Hallam, G. D. O'Mullan, I. L. Pan, K. R. Buck, and R. C. Vrijenhoek.** 2003. Environmental Acquisition of Thiotrophic Endosymbionts by Deep-Sea Mussels of the Genus Bathymodiolus. Appl. Environ. Microbiol. **69:**6785-6792.

4

Microbial Diversity and Community Composition
Gas Hydrates and Hydrate-Bearing Sediments
of the Cascadia Margin (Hydrate Ridge)

Tina Lösekann, Katrin Knittel, Tina Treude, Katja Nauhaus, Klaus Wallmann,

Antje Boetius, and Rudolf Amann

Preliminary manuscript

Microbial Diversity and Community Composition in Gas Hydrates and Hydrate-

Bearing Sediments of the Cascadia Margin (Hydrate Ridge)

Tina Lösekann[1], Katrin Knittel[1]*, Tina Treude[1]†, Katja Nauhaus[1]‡, Klaus Wallmann[2],

Antje Boetius[1,3,4], and Rudolf Amann[1]

[1] Max Planck Institute for Marine Microbiology, Bremen, Germany

[2] Leibniz Institute for Marine Sciences – IFM-GEOMAR, Kiel, Germany

[3] International University Bremen, Bremen, Germany

[4] Alfred Wegener Institute for Polar and Marine Research, Bremerhaven, Germany

*Corresponding author. Mailing address: Max Planck Institute for Marine Microbiology,
Celsiusstr. 1, D-28359 Bremen, Germany. Phone: +49 (0)4212028936. Fax: 49
(0)4212028580. E-Mail: kknittel@mpi-bremen.de.

†Present address: University of Southern California, Department of Marine Environmental
Biology, Los Angeles, USA
‡Present address: Ludwig-Maximilians-Universität, Department Biology I, Munich, Germany

Preliminary manuscript version, intended as an article in Geobiology

Running title: Microorganisms in gas hydrates and hydrate-bearing sediments

146

ABSTRACT

The cold seep ecosystem Hydrate Ridge (Cascadia margin) is characterized by high and variable rates of fluid and gas venting, surface and subsurface gas hydrate deposits, abundant carbonate precipitates and a rich microbial and faunal community. High numbers of microbial consortia consisting of methanotrophic archaea (ANME) and sulfate-reducing bacteria are present in the surface sediments mediating the anaerobic oxidation of methane (AOM). In this study, we describe the microbial diversity, community composition, and methanotrophic activity in subsurface gas hydrates and hydrate-bearing sediments from a 1.5 m gravity core collected at Hydrate Ridge. Comparative sequence analysis of 16S rRNA genes indicated the dominance of microbial lineages involved in AOM. Microbial diversity at 1 m sediment depth above a gas hydrate layer was as high as in surface sediments, whereas diversity was very low in pure gas hydrates. Fluorescence *in situ* hybridizations confirmed the presence of ANME throughout the 1.5 m sediment core. Subsurface abundance of ANME was highest (10^9 cells cm^{-3}) in 23 and 73 cm depth in sediments directly above two gas hydrate layers. When integrated over depth, cells of ANME-1 dominated the archaeal community. Cells collected from solid gas hydrates had very low rRNA contents, indicating that they may have been inactive for extended periods. In contrast, ANME cells in the vicinity of gas hydrates had high rRNA contents even at 1 m depth below the seafloor indicating that sulfate and methane are available for the microbial community in distinct subsurface horizons. Interestingly, various types of consortia morphologies were found: ANME-1 and sulfate-reducing *Desulfosarcina/Desulfococcus* (DSS), occurred as shell-type ANME-1/DSS aggregates in relatively high abundance. ANME-3, previously reported to be associated with *Desulfobulbus* species, formed shell-type consortia with DSS showing that these archaea can interact with different groups of sulfate-reducing bacteria.

INTRODUCTION

Gas hydrates are crystalline deposits composed of highly compressed gas (predominantly methane) encaged in water crystals. They are formed at low temperatures and high hydrostatic pressures when gas is present in excess of solubility (Bohrmann et al. 1998). Marine gas hydrates occur at active and passive continental margins (Kvenvolden 1988) and are estimated to represent the largest reservoir of reduced carbon on earth (Kvenvolden 1995, Collett & Kuuskraa 1998).

Cold seeps are hot spot ecosystems characterized by high fluxes of methane released from subsurface gas reservoirs. When methane ascends to the sulfate penetrated anoxic zone of the sediments, most of it is microbially converted to CO_2 with sulfate as the electron acceptor before it reaches the seafloor (Treude et al. 2003, Joye et al. 2004). This microbial process, the anaerobic oxidation of methane (AOM), is an effective biological barrier to methane in marine sediments, and controls oceanic emissions of the aggressive greenhouse to the atmosphere [(Hinrichs & Boetius 2002) and references therein]. AOM is coupled to sulfate reduction (SR), presumably through the syntrophic interaction between methanotrophic archaea (ANME) and sulfate-reducing bacteria (SRB) [(Valentine & Reeburgh 2000 and references therein]. ANME and SRB oxidize methane with sulfate yielding equimolar amounts of sulfide and bicarbonate (Nauhaus et al. 2002). Three AOM mediating archaeal clades (ANME-1, ANME-2, ANME-3) have been identified with culture-independent methods: ANME-1 archaea are distantly related to *Methanosarcinales* and *Methanomicrobiales* and occur in sediments as single cells (Orphan et al. 2001b, Knittel et al. 2005, Orcutt et al. 2005, Lösekann et al. in prep), aggregated cells (Orphan et al. 2002, Orcutt et al. 2005) or in microbial mats associated with SRB of the *Desulfosarcina-Desulfococcus* branch (DSS) (Michaelis et al. 2002, Knittel et al. 2005). ANME-2 archaea are more closely related to *Methanosarcinales*, whereas ANME-3 archaea are related to *Methanococcoides*. Both lineages were found to form shell-type or mixed consortia with DSS and *Desulfobulbus* species (DBB), respectively (Boetius et al. 2000, Lösekann et al. in prep, Niemann et al. subm). A recent study of the microbial diversity in the deep subsurface of Hydrate Ridge did not detect the presence of ANME 16S rRNA genes in cores from depths of 2-60 m below seafloor (Inagaki et al. 2006), suggesting that they may be restricted by energy constraints to the more active upper surface. All attempts to isolate microorganisms capable of AOM failed so far. Insights into genomes of ANME and their physiology have been provided recently by metagenomic libraries (Hallam et al. 2003, Krüger et al. 2003, Hallam et al. 2004, Meyerdierks et al. 2005) and studies of enrichment cultures (Nauhaus et al. 2002, Girguis et al. 2003, Girguis et al. 2005, Nauhaus et al. 2005).

In this study, we investigated the microbial diversity, community structure, and methanotrophic activity in subsurface sediments (down to 1.5 m below seafloor) and gas hydrates at Hydrate Ridge (Cascadia convergent margin off Oregon, USA). Hydrate Ridge is an accretionary structure formed as the result of the subduction of the Juan de Fuca plate underneath the North American plate (Suess et al. 1999). Fluids rich in methane rise from deep sediments and form massive gas hydrates (methane vol% >95, Suess et al. 1999) in the

overlying sediments at about 60 m below seafloor and above, some of which outcrop at the seafloor. *In situ* methane concentrations reach up to 70 mM (Torres et al. 2002), which is the equilibrium solubility at *in situ* conditions (600-800 m water depth, 4-6°C). AOM rates reported for surface sediments of Hydrate Ridge were extremely high (several μmol cm^{-3} d^{-1}) and correlated with the presence of high amounts of ANME-2/DSS aggregates (>10^{10} cells/ml sediment) (Boetius et al. 2000, Knittel et al. 2003, Treude et al. 2003, Boetius & Suess 2004, Knittel et al. 2005).

The microbial diversity in Cascadia margin sediments, especially of Hydrate Ridge, has been intensively studied including surface, subsurface and gas hydrate samples (Bidle et al. 1999, Boetius & Suess 2004, Cragg et al. 1996, Inagaki et al. 2006, Lanoil et al. 2005, Marchesi et al. 2001), but an analysis of the shallow subsurface (>20 cm to a few meters below seafloor) and pure gas hydrates has been lacking. Understanding the diversity and activity of anaerobic methanotrophs in hydrate-bearing sediments is highly interesting, because they may affect methane concentrations and hence processes of decomposition and formation of hydrates.

Here, we report the analysis of sediment samples from a 1.5 m long gravity core bearing two distinct gas hydrate layers. Additionally, we examined massive gas hydrates and sediments directly attached to the outside of gas hydrates. To assess the microbial diversity and community structure, 16S rRNA gene analyses and fluorescence *in situ* hybridizations were conducted. Microbial methane oxidation was determined by *ex situ* and *in vitro* rate measurements.

MATERIAL AND METHODS

Site description and sample collection. Sediment samples and gas hydrates were collected during R/V 'Sonne' cruise SO-165/2 (OTEGA-I) in August 2002 at the southern summit of Hydrate Ridge at the Cascadia convergent margin coast off Oregon, USA (Table 1). Gas hydrate bearing subsurface sediments were recovered with a gravity corer (station 176-3: 44°34.204'N, 125°08.807'W). Gas hydrate layers were observed in two depths of the core (35-50 cm and 110-140 cm, respectively). This layering was confirmed by *ex situ* temperature anomalies (Fig. 1).

Pure gas hydrates were retrieved with a piston corer (station 167-2: 44°34.209'N, 125°08.812'W). Pieces of massive hydrates were obtained devoid of any sediment particles and melted to a clear solution. The *in situ* depth of these gas hydrates is unknown, since sediments were washed out the core liner during recovery. Total length of the piston corer

149

was 5 m. Additional gas hydrate samples with very few sediment inclusions (station 162-1: 44°34.171'N, 125°08.791'W; and station 169: 44°34.207'N, 125°08.090'W) and sediments directly attached to gas hydrates (station 154-1: 44°34.211'N, 125°08.803'W; and station 162-1: 44°34.171'N, 125°08.791'W) were obtained with TV-operated grabs. A detailed description of Hydrate Ridge and research that has been conducted at this site is given by Boetius & Suess (2004).

Pore water analyses. Pore waters were separated from the sediment matrix by squeezing in a cold room at 4°C temperature and 2-4 bar using a polypropylene apparatus pressurized with argon and equipped with 0.45 μm cellulose acetate membrane filters. All vials used for pore water storage were previously washed with acid and Milli-Q water to prevent sample contamination.

Sulfide samples were conserved with zinc acetate gelatine solution (23.8 mM in Zn acetate) adding 4 ml solution to 1 ml pore water. The Zn-bearing solution was added to fix sulfide as colloidal zinc sulfide whereas the gelatine was used to inhibit ZnS precipitation. The resulting ZnS colloidal solution was mixed with 40 μl phenylen-diamine and 40 μl $FeCl_3*6H_2O$ and the absorbance was measured after 10 min to 1 hour at 670 nm using a Hitachi UV/VIS Spectrometer. A linear calibration curve was obtained in the concentration range of 0-57 μM ΣH_2S. The sulfide standard solution was titrated with sodium thiosulfate to determine the true concentration of the standard. Samples were diluted to the calibration range before reagent addition.

Dissolved sulfate was determined using ion-chromatography. A Methrom ion-chromatograph equipped with a conventional anion-exchange column was used with carbonate-bicarbonate solution as solvent. A conductivity sensor was applied for the measurement of sulfate anions.

Total carbon was determined by combustion of squeezed sediment samples and gas-chromatographic detection of CO_2 produced in the combustion process using a Carlo-Erba element analyzer (NA 1500). Additional samples were repeatedly acidified with HCl and desiccated till complete dryness to release CO_2 from carbonate minerals. The residues were analyzed for the contents of particulate organic carbon. The carbonate content was determined from the difference between total and particulate organic carbon. Sediment and soil standards with certified concentrations of carbon were analyzed during each run (marine sediment MAG-1, United States geological Survey; soil standard 1, HEKAtech

GmbH). The recovered values were always within the certified range. Replicate measurements of sediment samples (n = 5) revealed a relative standard deviation of 1%.

Methane concentration. On board, 2 cm^3 sediment was taken from the bisected gravity core at 15 cm depth intervals with cut-off syringes immediately after recovery and transferred into 10 ml glass vials filled with 5 ml sodium hydroxide (2.5 % w/w). The vials were closed quickly with butyl rubber stoppers, sealed with aluminum crimps, and shaken thoroughly to equilibrate the pore water methane into the headspace. In the laboratory, the methane concentrations were determined by injection of 200 μl headspace into a gas chromatograph (5890A, Hewlett Packard) equipped with a packed stainless steel Porapak-Q column (183 m, 0.32 cm, 80/100 mesh, Agilent Technologies) and a flame ionization detector. The carrier gas was helium at a flow rate of 30 ml min^{-1}. The column temperature was 40°C.

DNA extraction. The gravity core of station 176-3 was sampled in 5-10 cm intervals and sediments were frozen at -20°C for DNA extraction. Total community DNA was extracted directly from 5 g wet sediments (sediments of the gravity corer: 95 cm and 110 cm, respectively) using the method of Zhou *et al.* (Zhou et al. 1996). Crude DNA was purified with the Wizard DNA Clean-Up Kit (Promega, Madison, WI).

PCR amplification and clone library construction. Domain-specific primers were used to amplify almost full-length 16S rRNA genes from the environmental DNA: for *Bacteria* the primer set 8F (Muyzer et al. 1995) and 1492R (Kane et al. 1993), and for *Archaea* the primer set 20F (Massana et al. 1997) and Uni1392R (Lane et al. 1985) was used. Templates for amplification were either DNA extracted directly from the sediments (sediments of the gravity core) or pure melted gas hydrate from which cells have been concentrated by centrifugation (station 167-2). PCRs were performed and purified as described previously (Ravenschlag et al. 1999). The annealing temperatures for amplification of archaeal 16S rRNA genes were 58°C, and for bacterial genes 42°C. DNA was ligated in the pCR4 TOPO vector (Invitrogen, Carlsbad, CA) and transformed into *E. coli* TOP10 cells (Invitrogen, Carlsbad, CA) according to the manufacturer's recommendations. Clones were checked for the correct insert size by PCR with vector primers.

Sequencing and phylogenetic analysis. Sequencing was performed by *Taq* cycle sequencing with a model ABI377 sequencer (Applied Biosystems) using vector primers and universal 16S rRNA gene specific primers. Sequences were grouped in phylotypes (>97% sequence similarity) and representatives of most phylotypes were chosen for plasmid preparation and full length sequencing. The presence of chimeric sequences was determined with programs Bellerophon (http://foo.maths.uq.edu.au/~huber/bellerophon.pl) and CHIMERA_CHECK

(Ribosomal Database Project II, http://rdp.cme.msu.edu/html/analyses.html). Potential chimeras were eliminated before phylogenetic trees were constructed. Sequence data were analyzed with the ARB software package (Ludwig et al. 2004). Phylogenetic trees were calculated by parsimony, neighbor-joining, and maximum-likelihood analysis with different sets of filters. For tree calculation, only almost full-length sequences (>1315 bp) were considered. Partial sequences were inserted into the reconstructed tree by parsimony criteria without allowing changes in the overall tree topology.

Fluorescence *in situ* hybridization (FISH). Samples were obtained from 19 depths (3, 13, 23, 33, 43, 53, 63, 73, 75, 80, 85, 90, 95, 108, 118, 128, 138, 148 and 155 cm sediment depth) of the gravity core (station 176-3) and from several gas hydrate samples (Table 1). Preparation of samples for FISH analysis, hybridization with monolabeled probes and microscopy counting of hybridized and 4',6'-diamidino-2-phenylindole (DAPI)-stained cells was performed as described previously (Snaidr et al. 1997, Ravenschlag et al. 2000). For each filter section, 700 to 1,000 DAPI-stained cells were counted or at least 50 randomly chosen microscopic fields were examined and means were calculated. The average standard deviation for single cell counts was relatively high with 42% of the mean of the counted microscopic fields. This is probably due to low cell numbers and the presence of microbial aggregates, which were counted separately. For *in situ* hybridizations with horseradish peroxidase (HRP)-conjugated probes followed by tyramide signal amplification (CARD-FISH), samples were processed as described previously by Pernthaler *et al.* (Pernthaler et al. 2002) with the following specifications: For bacterial cell wall permeabilization, filters were treated with lysozyme (10 mg/ml of lysozyme in 50 mM EDTA and 0.1 M Tris-HCl, pH 8.0), and incubated in a humid chamber at 37°C for 1 h. For archaeal cell wall permeabilization, filters were incubated in 1% Triton X-100 or Proteinase K (10 µg/ml in 50 mM EDTA and 0.1 M Tris-HCl, pH 8.0) for 15 min at room temperature. After permeabilization, filters were washed in MilliQ water, dehydrated in absolute ethanol, and stored at 20°C until further processing. For inactivation of endogenous peroxidases, filters were covered with 0.01 M HCl for 10 min at room temperature and washed in MilliQ water. Filters were hybridized on microscopic slides in a humid chamber over night at 46°C with probes purchased from Biomers (Ulm, Germany) and washed in prewarmed washing buffer at 48°C for 10 min. CARD was performed at 46°C for 10 min with tyramide concentrations adjusted for each probe. After hybridization and CARD procedure, cells were counterstained with DAPI (1 µg/ml in MilliQ).

Probes and formamide concentrations used in this study are given in Table 2. Hybridized samples were examined with an Axioskop II epifluorescence microscope (Carl Zeiss, Jena, Germany). Micrographs were taken with an Axiocam MRm camera (Carl Zeiss, Jena, Germany).

Background signal of samples observed with the nonsense probe NON338 was negligible (<0.1%). Other probes specific for SEEP-SRB2 and aerobic methanotrophs, respectively, did not result in any hybridization signals [SEEP-SRB2-204, (unpublished); MetI-444 and MetII-844, (Niemann et al. subm); Mγ84, Mγ705, (Eller et al. 2000); MTMC-701, (Boetius et al. 2000)].

Nucleotide sequence accession numbers. The sequence data reported here will appear in the EMBL, GenBank, and DDBJ nucleotide sequence databases under the accession numbers AM229185 to AM229261.

Radiotracer rate measurements. AOM and sulfate reduction was measured in gas-hydrate melts. Gas hydrates were collected with a TV-guided grab and with a piston corer, respectively (Tab. 1). Pieces of pure hydrate were transferred into a nitrogen pre-flushed glass bottle (1,000 ml). The gas bottle was closed with a rubber stopper and a screw cap. Methane gas released during gas-hydrate dissociation escaped from the bottle via a small tube opening. After complete dissociation of the gas hydrates, the remaining fluid was filled anoxically into three to five replicate Hungate tubes (5 ml) for AOM and sulfate reduction measurements, respectively. The fluid of sediment-rich gas hydrates was homogenously mixed before transfer. Purified radioactive methane ($^{14}CH_4$ dissolved in water, injection volume 30 μl, activity 1 kBq, specific activity 2.28 GBq mmol^{-1}) and carrier-free radioactive sulfate ($^{35}SO_4^{2-}$ dissolved in water, injection volume 12 μl, activity 200 kBq, specific activity 37 TBq mmol^{-1}) were injected into AOM and sulfate-reduction samples, respectively, and the tubes were incubated for 2 days at 4ºC in the dark. After incubation, AOM samples were transferred into 50 ml glass vials filled with 25 ml sodium hydroxide (2.5% w/w) and closed quickly with rubber stoppers. The glass vials were shaken thoroughly to equilibrate the pore water methane between the aqueous and gaseous phase. One control sample (5 ml anoxic gas-hydrate fluid) was first transferred into glasses with sodium hydroxide before addition of tracer. AOM was analyzed and calculated according to (Treude et al. 2003). Sulfate-reduction samples were transferred into 50 ml plastic centrifuge vials filled with 20 ml zinc acetate (20% w/w). One control sample (5 ml anoxic gas-hydrate fluid) was first transferred into plastic tubes with zinc acetate before addition of tracer. Sulfate reduction rates were determined using the single step acid Cr-II method according to (Fossing & Jørgensen 1989).

Anoxic incubations. Melted gas hydrate from station 167-2 and 154-1 was incubated in glass tubes (20 ml) with butyl-rubber stoppers and screw caps. The final volume of 8 ml consisted of 2 ml (station 154-1) or 1.5 ml (station 167-2) melted hydrate and artificial seawater medium for sulfate reducing bacteria (Widdel & Bak 2002). The headspace of the three parallels each contained methane, one control contained N_2/CO_2 (90/10 v/v). One set of samples (3+1 control) for each station was incubated under elevated methane partial pressure as described in Nauhaus *et al.* (2002) (Nauhaus et al. 2002), the other set at atmospheric pressure. Incubation temperature was 12°C.

Sediment from the gravity core (station 176-3) was split into 19 depths (3, 13, 23, 33, 43, 53, 63, 73, 75, 80, 85, 90, 95, 108, 118, 128, 138, 148 and 155 cm sediment depth). Sample manipulation and incubations were performed as described in Nauhaus *et al.* (2002). Each tube contained 0.5 g of sediment and 12 ml of artificial seawater medium. The headspace was filled with methane for three parallels for each depth and one control with N_2/CO_2 (90/10 v/v). The samples were incubated at atmospheric pressure at 12°C.

For both experiments the development of sulfide was determined as a measure of methane dependent sulfate reduction by the formation of colloidal copper sulfide (Cord-Ruwisch 1985).

FIGURE 1 Lithostratigraphic description of gas hydrate bearing sediments of the gravity core (station 176-3, modified from Pfannkuche et al. 2002).

TABLE 1 Samples used for this study (expedition SO-165/2)

Sample	Description	Station	Date [d.m.y]	Position	Depth [m]	Device	Types of analysis
Sediments	'Gravity core': recovery of 178 cm sediment, two gas hydrate layers (Fig. 1)	176-3	09.08.02	44° 34.204'N, 125° 08.807'W	776	Gravity corer	16S: 95 cm, 110 cm; FISH: 0-148 cm in 5-10 cm intervals; TCC; agg. no.; Rates: *in vitro*
Gas hydrates	'Pure gas hydrates': devoid of any sediment particles	167-2	08.08.02	44° 34.2090'N, 125° 08.8120'W	775	Piston corer	16S; FISH; TCC; agg. no.; Rates: *in vitro, ex situ*
Gas hydrates	Gas hydrates cleaned manually, very few sediment inclusions	162-1	07.08.02	44° 34.1710'N, 125° 08.7910'W	775	TV grab	FISH; TCC; agg. no.
Gas hydrates	Gas hydrates cleaned manually, very few sediment inclusions	169	09.08.02	44° 34.1713'N, 125° 08.7685'W	776	TV grab	FISH; TCC; agg. no.
Interface sediments	Sediments scraped off from massive gas hydrates	169	09.08.02	44° 34.1713'N, 125° 08.7685'W	776	TV grab	FISH; TCC; agg. no.
Interface sediments	Sediments scraped off from massive gas hydrates	154-1	07.08.02	44° 34.2114'N, 125° 08.8031'W	776	TV grab	FISH; TCC; agg. no.

Types of analysis: 16S rDNA cloning (16S), fluorescence *in situ* hybridization (FISH), total cell counts (TCC), aggregate numbers (agg. no.), *in vitro/ex situ* incubations for activity measurements (rates).

TABLE 2 Oligonucleotide probes used in this study

Probe	Specificity	Probe sequence (5´-3´)	FA [%][a]	Label	Reference
NON338	Negative control	ACTCCTACGGGAGGCAGC	10	HRP	(Wallner et al. 1993)
EUB338 I-III	most *Bacteria*	GCTGCCTCCCGTAGGAGT GCAGCCACCCGTAGGTGT GCTGCCACCCGTAGGTGT	35	HRP	(Daims et al. 1999)
Arch915	most *Archaea*	GTGCTCCCCGCCAATTCCT	35	HRP	(Amann et al. 1990b)
DSS658	*Desulfosarcina* spp., *Desulfofaba* spp., *Desulfococcus* spp., *Desulfofrigus* spp.	TCCACTTCCCTCTCCCAT	40	HRP	(Manz et al. 1998)
DSV698	*Desulfovibrio* spp.	GTTCCTCCAGATATCTACGG	35	HRP	(Manz et al. 1998)
cDSV698	Competitor for probe DSV698	GTTCCTCCAGATATCTACGC	35	None	(Mussmann et al. 2005)
DSB985	*Desulfobacter* spp., *Desulfobacula* spp.	CACAGGATGTCAAACCCAG	20	HRP	(Manz et al. 1998)
660	*Desulfobulbus* spp.	GAATTCCACTTTCCCCTCTG	60	HRP	(Devereux et al. 1992)
Gam42a	*Gammaproteobacteria*	GCCTTCCCACATCGTTT	35	HRP	(Manz et al. 1992)
cBet42a	Competitor for probe Gam42a	GCCTTCCCACTTCGTTT	35	None	(Manz et al. 1992)
Cf319a	*Cytophaga/Flavobacterium*	TGGTCCGTGTCTCAGTAC	35	HRP	(Manz et al. 1996)
ANME1-350	ANME-1 archaea	AGTTTTCGCGCCTGATGC	40	HRP	(Boetius et al. 2000)
EelMS-932	ANME-2 archaea	AGCTCCACCCGTTGTAGT	65	Cy3	(Boetius et al. 2000)
ANME2-712	ANME-2 archaea	TTCGCCACAGATGGTCCC	40	Cy3	This study
ANME2a-647	Subgroup a of ANME-2 archaea	TCTTCCGGTCCCAAGCCT	50	Cy3	(Knittel et al. 2005)
ANME2c-622	Subgroup c of ANME-2 archaea	CCCTTGGCAGTCTGATTG	50	Cy3	(Knittel et al. 2005)
ANME3-1249	ANME-3 archaea	TCGGAGTAGGGACCCATT	20	Cy3	(Niemann et al. subm)
h1-ANME3-1249	Helper for probe ANME3-1249	GTCCCAATCATTGTAGCCCGC	20	None	This study
h2-ANME3-1249	Helper for probe ANME3-1249	TTATGAGATTACCATCTCCTT	20	None	This study

[a] Percent (Vol/Vol) formamide (FA) in hybridization buffer for FISH.
DSS were only hybridized by CARD-FISH at FA concentrations lower than those for FISH with a monolabeled probe (positive control: DSS associated with AOM aggregates in sediments of the gravity core). To ensure that *Gammaproteobacteria* were not targeted unspecifically, CARD-FISH double hybridizations with probes Gam42a and DSS658 were carried out but no false positives were detected.

RESULTS

Pore water chemistry of the gravity core. Methane concentrations measured *ex situ* were very low at the surface (0.07 mM) of the gravity core and increased with sediment depth (up to 3.6 mM in 120 cm). Sulfate concentrations showed a sharp decrease with depth, indicating consumption by AOM, but remained relatively constant (1-3 mM) below 27 cm sediment depth (uncorrected depth) (Fig. 2A).

Calcium carbonate precipitates due to localized increases in alkalinity caused by AOM activity and the availability of cations from the overlying seawater (Bohrmann et al. 1998). Carbonates can therefore be considered as secondary indicators for recent or former AOM activity. Extensive deposits were observed in two depth intervals (15 cm and 80-90 cm, Fig. 2B) above sediment layers with abundant gas hydrates (35-50 cm and 110-140 cm depth, Fig. 1).

Elevated sulfide concentrations (4 mM and 6-8 mM, Fig. 2C) coincided with high carbonate concentrations. Highest sulfide concentrations (11 mM) were found deeper in the sediment at >130 cm depth.
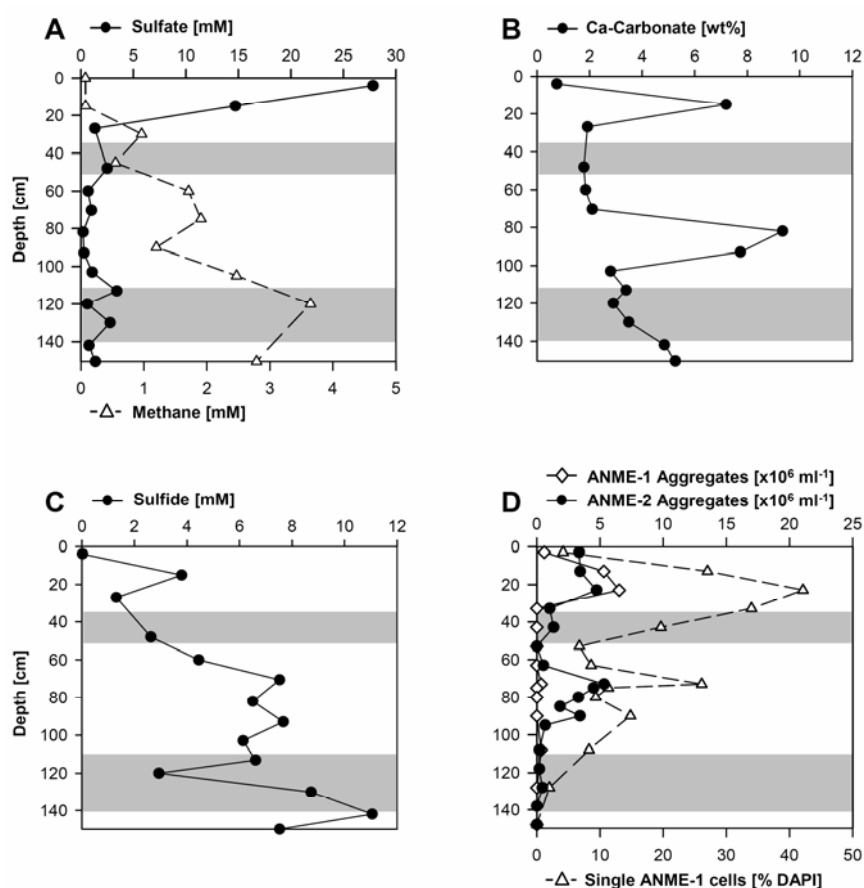
FIGURE 2 Depth profiles of sediments of the gravity core. (A) Sulfate and methane concentrations. (B) Calcium carbonate mineral concentration. (C) Sulfide concentration. (D) *In situ* abundance of AOM mediating microorganisms as quantified by *in situ* hybridization. Shaded areas indicate the occurrence of gas hydrates.

Microbial methane turnover in hydrates and hydrate-bearing sediments. AOM and SR activity was below detection limit in sediments of the gravity core and the hydrate melts. The AOM enrichments were incubated for nine months and did not result in significant sulfide productions. The radiotracer experiments were only incubated for four days, which was probably too short given the relatively low biomass of AOM consortia. However, we cannot exclude other sources of error, such as a toxic effect on the ANME cells by exposure to oxygen during subsampling.

TABLE 3 Phylogenetic affiliations and frequencies of 16S rRNA gene sequences obtained in this study

Phylogenetic affiliation	Next cultivated relative	*Station 176-3* **Gravity core** No. of clones	*Station 167-2* **Pure gas hydrates** No. of clones
Gammaproteobacteria	*Lysobacter brunescens* (AB161360)	1	0
Deltaproteobacteria			
SEEP-SRB1	*Desulfosarcina variabilis* (M26632)	77	46
	Desulfosarcina variabilis (M26632)	1	0
SEEP-SRB2	*Desulfobulbus propionicus* (M34410)	5	2
Desulfobacterales	*Desulfobacterium anillini* (AJ237601)	3	0
Syntrophobacterales	*Syntrophus gentianae* (X85132)	1	0
Desulfovibrionales	*Desulfonatronum lacustre* (AF418171)	2	0
Spirochaetes	*Spirochaeta thermophila* (X62809)	2	0
	Leptospira parva (Z21636)	3	0
Bacteroidetes	*Flexibacter canadensis* (AB078046)	1	2
Planctomycetes	*Pirellula marina* (X62912)	4	0
Chlamydiae/Verrucomicrobia	*Victivallis vadensis* (AY049713)	1	1
OP9	No close cultivated relative	20	0
Nitrospirae	*Nitrospira marina* (X82559)	6	1
OP8	No close cultivated relative	4	0
Actinobacteria	*Rubrobacter xylanophilus* (AJ243871)	1	0
Thermomicrobia	*Sphaerobacter thermophilus* (X53210)	2	0
OD1 (OP11 derived)	No close cultivated relative	3	1
OP5 Relatives	No close cultivated relative	1	0
Unaffiliated bacteria		6	0
Subtotal *Bacteria*		**144**	**53**
Methanosarcinales			
ANME-3	*Methanococcoides methylutens* (M59127)	40	0
ANME-2a		22	0
ANME-2c		77	34
ANME-1a		3	2
ANME-1b		9	14
	Methanosaeta concilii (X16932)	1	0
Marine benthic group D	No close cultivated relative	47	0
Guaymas Euryarchaeota Group	No close cultivated relative	1	0
Miscellaneous Euryarchaeota Group	No close cultivated relative	6	0
Subtotal *Archaea*		**206**	**50**

Microbial diversity in sediments of the gravity core and pure gas hydrates. To study the microbial diversity, 16S rRNA gene libraries for *Bacteria* and *Archaea* were constructed using sediments of the gravity core (station 176-3, clones "HydGC", ca. 1 m below seafloor) and melted pure gas hydrates (station 167-2, clones "HydGH"), respectively. A total of 197 bacterial 16S rRNA gene sequences and 256 archaeal 16S rRNA gene sequences were analyzed. The vast majority of 16S rRNA gene sequences were affiliated with AOM specific taxa (Table 3). Lineages unique to gas hydrates were not detected in the 16S rRNA gene libraries. The closest relatives to our sequences were mainly sequences retrieved from other methane rich sites, e.g. Hydrate Ridge surface sediments (Knittel et al. 2003), an ODP borehole and surface sediments at the Cascadia margin (Lanoil et al. 2005), Gulf of Mexico gas hydrates (Mills et al. 2005), Eel River Basin sediments (Orphan et al. 2001a), Eastern Mediterranean Mud Volcanoes (Heijs et al. 2005), or an AOM bioreactor (Girguis et al. 2003).

Bacterial diversity in pure gas hydrates was reduced compared to sediments of the gravity core: Bacterial lineages present in both samples include the *Deltaproteobacteria*, *Bacteroidetes*, *Chlamydiae/Verrucomicrobia*, *Nitrospirae*, and the OP11 derived candidate division OD1. Members of *Gammaproteobacteria*, *Spirochaetes*, *Actinobacteria*, *Thermomicrobia*, and the yet uncultivated clades OP5, OP8 and OP9 were only found in sediments of the gravity core but were not present in pure gas hydrate (Table 3).

Sequences within *Deltaproteobacteria* were diverse and several orders were represented (Fig. 3). The majority of sequences (HydGC: 77 of 144 clones, HydGH: 45 of 53 clones) was affiliated with the recently defined sulfate-reducing group SEEP-SRB1 of DSS (Knittel et al. 2003). Hydrate Ridge sequences within SEEP-SRB1 showed a maximum similarity (95%) to *Desulfosarcina variabilis*. Sequences of the second seep-specific sulfate-reducing clade, SEEP-SRB2 (Knittel et al. 2003), were also found in our clone libraries but only in lower numbers (HydGC: 5 of 144 clones, HydGH: 2 of 53 clones). The closest cultured relative *Desulfobulbus propionicus* is distantly related (86-90%) to SEEP-SRB2.

In addition to *Deltaproteobacteria*, many sequences from sediments of the gravity core (HydGC: 19 of 144 clones) grouped in OP9, a candidate division that was first discovered in a Yellowstone hot spring environment (Hugenholtz et al. 1998) but none of pure gas hydrate sequences. No member of this group is cultivated yet and the physiology of this group remains unknown. However, it is emerging from recent studies that members of OP9 are present in many methane rich habitats (e.g. Bowman et al. 2000, Dhillon et al. 2003, Knittel et al. 2003, Kormas et al. 2003, Mills et al. 2003, Mills et al. 2005).
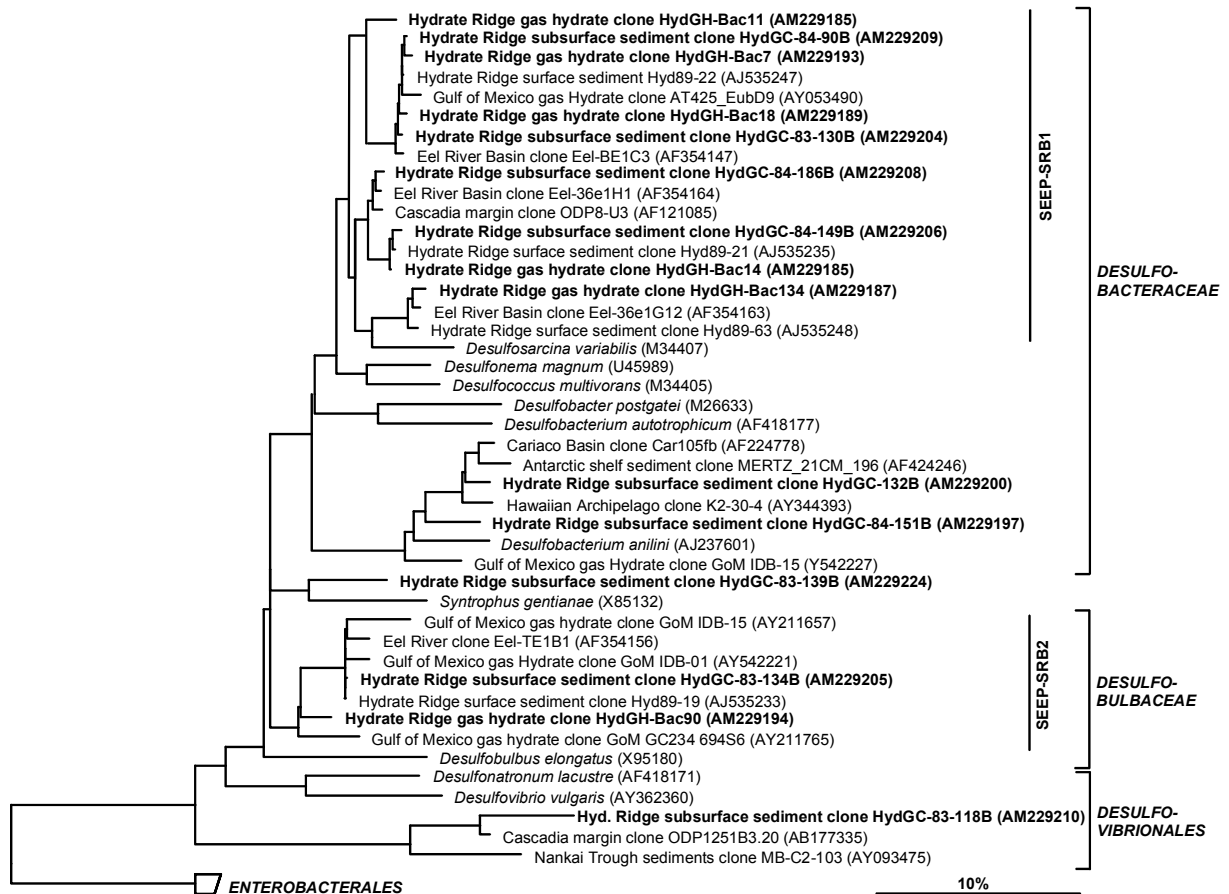
FIGURE 3 Phylogenetic tree showing the affiliations of Hydrate Ridge16S rRNA gene sequences to selected reference sequences of the *Deltaproteobacteria*. The tree was calculated with nearly full-length sequences by maximum-likelihood analysis in combination with filters, which consider only 50% conserved regions of the 16S rRNA of *Deltaproteobacteria* to exclude the influence of highly variable positions. Branching orders that were not supported by all calculation methods are shown as multifurcations. Partial sequences were subsequently inserted into the reconstructed consensus tree by parsimony criteria, without allowing changes in the overall tree topology. Sequences from Hydrate Ridge are in boldface type: clones HydGC-* are from sediments of the gravity core (station 176-3); clones HydGH-* from pure gas hydrates (station 167-2). The bar represents 10% estimated phylogenetic divergence.

Archaeal diversity was lower and only six major lineages became evident in sediments of the gravity core (Table 3). Sequences from pure gas hydrates were phylogenetically even less diverse and included only two major archaeal lineages (Table 3). The vast majority of archaeal 16S rRNA gene sequences grouped in clades of anaerobic methanotrophs (Fig. 4). In both clone libraries most clones were affiliated with group ANME-2c (HydGC: 77 of 206 clones, HydGH: 34 of 50 clones) and were highly similar (98-100%). Members of ANME-1a (HydGC: 3 of 206 clones, HydGH: 2 of clones 50) and ANME-1b (HydGC: 9 of 206 clones, HydGH: 14 of 50 clones) were also obtained from both samples. Sequence similarities of our clones within ANME-1a were 96-99% and ANME-1b 94-100%. 16S rRNA gene sequences affiliated with the other known groups of anaerobic methanotrophs,

ANME-2a (HydGC: 22 of 206 clones, HydGH: 0 of 50 clones) and ANME-3 (HydGC: 40 of 206 clones, HydGH: 0 of 50 clones), were only found in clone libraries constructed from sediments of the gravity core.

Members of the marine benthic group D (MGBD) were second most abundant in the archaeal library from GC sediments (HydGC: 47 of 206 clones), but absent in pure gas hydrates. This group is distantly related to *Thermoplasmales* (Fig. 4) and comprised of yet uncultivated species. Two distinct clusters became evident and sequence similarity of our clones within MBGD ranged from only 80 up to 99%. MBGD affiliated 16S rRNA gene sequences are highly diverse, not seep specific and have been recovered from a variety of limnic and marine habitats (e.g. Munson et al. 1997, Dojka et al. 1998, Hinrichs et al. 1999, Takai & Horikoshi 1999, Vetriani et al. 1999, Reysenbach et al. 2000, Takai et al. 2001, Galand et al. 2003, Mills et al. 2003, Coolen et al. 2004).

Crenarchaeotal sequences were absent in the 16S rRNA gene libraries of this study.

Microbial community structure in sediments of the gravity core and pure gas hydrates. FISH analysis was performed to gain insights into microbial community structures and interspecies associations. Total single cell numbers in sediments of the gravity core were highest in 13 cm and 75 cm sediment depth (5.3×10^9 cells cm^{-3} and 1.3×10^9 cells cm^{-3}, respectively) but more than one order of magnitude lower in depths of 43-63 cm and below 80 cm ($\leq 1 \times 10^8$ cells cm^{-3}, Table 4). CARD-FISH detection rates were very high in most sediment layers (mean 67% of total cells). Single bacterial cells were dominant over the whole depth of the core (up to 66% of total cells). Single archaeal cells were rare, and only frequently detected at 23 cm sediment depth (44% of total cells).

The sediments of the gravity core contained a high amount of microbial aggregates (Table 4) as quantified with the general archaeal probe Arch915. Aggregate counts were highest in 23-24 cm and 73-74 cm sediment depth with 10.1×10^6 aggregates cm^{-3} and 5.7×10^6 aggregates cm^{-3}, respectively. In all other sediment layers investigated, aggregate abundance was low ($< 10^5$) or aggregates were not detectable at all.

FIGURE 4 Phylogenetic tree showing the affiliations of Hydrate Ridge 16S rRNA gene sequences to selected reference sequences of the domain *Archaea*. The tree was calculated with nearly full-length sequences by maximum-likelihood analysis in combination with filters, which consider only 50% conserved regions of the 16S rRNA of *Archaea* to exclude the influence of highly variable positions. Branching orders that were not supported by all calculation methods are shown as multifurcations. Partial sequences were subsequently inserted into the reconstructed consensus tree by parsimony criteria, without allowing changes in the overall tree topology. Sequences from Hydrate Ridge are in boldface type: clones HydGC-* are from sediments of the gravity core (station 176-3); clones HydGH-* from pure gas hydrates (station 167-2). The bar represents 10% estimated phylogenetic divergence.

Methanosarcina
Methanococcoides burtonii (X65537)
Hydrate Ridge subsurface sediment clone HydGC-83-600A (AM229241)
Arctic mud volcano clone HMMVBeg-32 (AJ704653)
Hydrate Ridge subsurface sediment clone HydGC-84-548A (AM229234)
Arctic mud volcano clone HMMVBeg-36 (AJ704631)
Hydrate Ridge subsurface sediment clone HydGC-84-212A (AM229243)
Eel River Basin clone Eel-36a2H11 (AF354136)
Eastern Mediterranean mud volcano clone Kazan-3A-16/BC19-3A-16 (AY592040)
Hydrate Ridge surface sediment clone HydBeg92 (AJ578119)

ANME-3

Hydrate Ridge surface sediment clone HydBeg134 (AJ578116)
Black Sea microbial mat clone BS-K-H6, LOGA 0114 (AJ578128)
Santa Barbara Basin clone SB-24a1F10 (AF354134)
Hydrate Ridge subsurface sediment clone HydGC-84-213A (AM229254)
Hydrate Ridge subsurface sediment clone HydGC-83-548A (AM229240)
Eastern Mediterranean mud volcano clone Kazan-3A-23/BC19-3A-23 (AY592047)
Blake Ridge clone BR34ARC_C05 (AY324379)
Gulf of Mexico gas hydrate clone GoM GC185 517R (AY211687)

a

Hydrate Ridge gas hydrate clone HydGH40-Arch247 (AM229226)
Hydrate Ridge subsurface sediment clone HydGC-84-86A (AM229244)
Hydrate Ridge surface sediment clone HydBeg05 (AJ578098)
Guaymas Basin clone C1_R004 (AF419635)
Hydrate Ridge gas hydrate clone HydGH40-Arch271 (AM229227)
AOM bioreactor clone AMOS4A_4113_B05 (AY323218)
Gulf of Mexico gas hydrate clone GoM GC234 019R (AY211694)
Hydrate Ridge subsurface sediment clone HydGC-83-640A (AM229250)
Hydrate Ridge surface sediment clone HydBeg125 (AJ578115)
Eel River Basin clone Eel-36a2A1 (AF354129)
Hydrate Ridge subsurface sediment clone HydGC-84-251A (AM229242)
Hydrate Ridge gas hydrate clone HydGH40-Arch201 (AM229230)

ANME-2

c

Methanosaeta thermoacetophila (M59141)
Hydrate Ridge subsurface sediment clone HydGC-83-654A (AM229252)
Guaymas Basin clone 7F07 (AY835417)
Hydrate Ridge gas hydrate clone HydGH40-Arch207 (AM229231)
Hydrate Ridge subsurface sediment clone HydGC-84-267A (AM229258)
Eel River Basin clone Eel-36a2G10 (AF354137)
Eel River Basin fosmid GZfosARC_25D1 (AY324375)
Hydrate Ridge surface sediment clone HydCal61 (AJ578089)
Black Sea microbial mat clone BS-S-E1, LOGA 0155-4 (AJ578135)
Hydrate Ridge surface sediment clone HydBeg01 (AJ578084)
Hydrate Ridge subsurface sediment clone HydGC-83-532A (AM229246)
Black Sea microbial mat clone BS-M-A7, LOGA 0155-4 (AJ578129)
Hydrate Ridge gas hydrate clone HydGH40-Arch254 (AM229232)
Gulf of Mexico gas hydrate clone GoM GC234 616R (AY211707)
Hydrate Ridge gas hydrate clone HydGH40-Arch264 (AM229228)
Mud volcano carbonate crust clone Napoli-MN16BT2-131 (AY593330)

ANME-1

Methanomicrobium

Halobacteriales

Eastern Mediterranean mud volcano clone Napoli-2A-14 16S (AY592479)
Gulf of Mexico gas hydrate clone GoM GC234 011A (AY211722)
Hydrate Ridge subsurface sediment clone HydGC-83-611A (AM229248)
AOM bioreactor clone AMOS1B_4113_A05 (AY323217)
Hydrate Ridge subsurface sediment clone HydGC-83-644A (AM229251)
Ace Lake clone DGGE gel bands 3 and 12 (AY291551)
Hydrate Ridge surface sediment clone HydCal69 (AJ578091)
Gulf of Mexico clone GoM HDA-13 (AY542186)
Black Sea microbial mat clone BS-S-316, LOGA 0121-1 (AJ578149)
Hydrate Ridge subsurface sediment clone HydGC-83-542A (AM229233)
Hydrate Ridge subsurface sediment clone HydGC-84-66A (AM229260)
Eel River Basin clone TA1c9 (AF134388)
Hydrate Ridge subsurface sediment clone HydGC-84-48A (AM229259)
Eastern Mediterranean mud volcano clone Napoli-3A-07 (AY592518)
Hydrate Ridge subsurface sediment clone HydGC-83-585A (AM229247)
Hydrothermal vent clone pMC2A33 (AB019738)
Hydrate Ridge subsurface sediment clone HydGC-84-240A (AM229257)
Peru margin subseafloor sediment clone (AB177119)
NW Atlantic Ocean Continental Rise clone CRA12-27cm (AF119123)
MAR hydrothermal vent clone VC2.1 Arc6 (AF068817)
Hydrate Ridge subsurface sediment clone HydGC-83-658A (AM229253)
Kuroshima Knoll clone KAMR-7.23 (AB178093)
Contaminated aquifer clone WCHD3-16 (AF050618)
Hydrate Ridge subsurface sediment clone HydGC-83-656A (AM229237)
Hydrate Ridge subsurface sediment clone HydGC-84-92A (AM229261)
Eastern Mediterranean mud volcano clone Napoli-1A-07 (AY592440)
Hydrate Ridge subsurface sediment clone HydGC-83-623A (AM229235)
Aegean Sea sediments clone 19b-30 (AJ294863)

Marine Benthic Group D (MBGD)

Thermoplasmales

Black smoker chimney clone FZ1aA153 (AY165971)
Hydrate Ridge subsurface sediment clone HydGC-84-221A (AM229255)
Cold seep clone FE2MidArch10 (AY769051)
Hydrate Ridge subsurface sediment clone HydGC-84-22A (AM229256)
Eastern Mediterranean mud volcano clone Kazan-3A-27/BC19-3A-27 (AY592049)

Miscellaneous Euryarchaeotic Group (MEG)

Methanobacterium

Methanococcales

EURYARCHAEOTA

CRENARCHAEOTA

KORARCHAEOTA

10%

161

In order to identify the AOM mediating populations in 23 cm and 73 cm sediments, probes specific for ANME archaea were applied. The single archaeal cells at 23 cm sediment depth were ANME-1 archaea accounting for 42% of total single cells (1×10^9 cells cm^{-3}). In addition, high numbers of ANME-1 aggregates were detected (5.4×10^6 aggregates cm^{-3}), which have not been found in Hydrate Ridge sediments before (Knittel et al. 2003, Knittel et al. 2005). Most ANME-1 aggregates consisted of tightly associated ANME-1 archaea and sulfate-reducing DSS (ANME-1/DSS) forming shell type consortia (Fig. 5A-C). Furthermore, we observed not only ANME-1 cells surrounded by DSS but also vice versa (Fig. 5B). ANME-1/DSS aggregates were relatively large and ranged from 5-30 μm in diameter with small aggregates being more frequently observed. A minor percentage of aggregates were monospecifically composed of ANME-1 cells. ANME-2/DSS aggregates were also detected in high numbers (4.7×10^6 aggregates cm^{-3}). However, aggregated and single ANME-1 archaea clearly dominated the 23 cm sediment layer. In deeper sediments at 73 cm depth, abundance of ANME-1 aggregates was one order of magnitude lower (4×10^5 aggregates-cm^{-3}). Here, most microbial aggregates consisted of ANME-2 archaea (5.3×10^6 aggregates cm^{-3}). However, calculated cell numbers for ANME-2 cells living in aggregates [5.3×10^8 cells cm^{-3}; 100 cells on average per aggregate; (Boetius et al. 2000)] were only twice as high than the number of ANME-1 single cells (2.6×10^8 cells cm^{-3}). Comparing the identity of ANME-2 subgroups showed that ANME-2c aggregates were predominant in both sediment layers (70-80% of ANME-2 aggregates, Fig. 5D), whereas ANME-2a aggregates were only found in low numbers (Fig. 5E).

Since ANME-3 sequences were found in our 16S rRNA gene libraries, a probe specific for this novel type of AOM consortium (Lösekann et al. in prep, Niemann et al. subm) was applied to obtain quantitative *in situ* data. ANME-3 single cells could be detected in 73 cm sediment depth at very low abundance. To check whether ANME-3 cells are more abundant close to the surface, we reinvestigated sediment samples from a previous study (Knittel et al. 2003). Indeed, presence of ANME-3 could be confirmed and aggregates were detected more frequently (estimated 1×10^4 aggregates cm^{-3}) in 3-4 cm sediment depth of Hydrate Ridge sediments covered with *Beggiatoa* mats (station 19-2). Here, ANME-3 formed spherical or irregular shaped consortia that were partially surrounded by DSS cells (Fig. 5F).

TABLE 4 Quantification of single cells and AOM aggregates

Station No.	Depth [cm]	Total single cell counts[a] [cells x 10^9/ml]	AOM Aggregate counts[b] [Aggregates x 10^6/ml]	Bacteria (EUB338 I-III)	Archaea (Arch915)	Deltaproteobacteria (DSS658)	(DSV698)	(DSB985)	Gammaproteobacteria (Gam42a)	Cytophaga/Flavobacterium (Cf319a)	ANME-1 (ANME1-350)
					Gravity core						
176-3	3	2.5	3.9	66	6	7	4	<1	17	8	4
	13	5.3	6.6	55	33	6	<1	1	1	4	27
	23	2.5	10.1	35	44	13	<1	<1	<1	<1	42
	33	1.3	1.0	62	37	1	0	0	0	<1	34
	43	0.9	1.3	52	21	3	<1	0	3	<1	20
	53	0.2	0.0	13	8	0	0	0	0	0	7
	63	0.6	0.5	34	15	14	0	0	4	<1	9
	73	1.0	5.7	44	30	15	<1	<1	0	0	26
	75	1.3	4.5	28	12	3	<1	0	<1	<1	11
	80	1.0	3.3	40	29	3	0	0	0	0	9
	85	0.2	1.8	ND	ND	ND	ND	ND	ND	ND	ND
	90	0.3	3.4	63	32	12	0	0	0	0	15
	95	0.1	0.7	ND	ND	ND	ND	ND	ND	ND	ND
	108	0.1	0.6	48	25	4	0	0	0	0	8
	118	<0.1	0.2	ND	ND	ND	ND	ND	ND	ND	ND
	128	0.1	0.4	45	20	<1	0	0	0	0	2
	138	0.1	0.0	ND	ND	ND	ND	ND	ND	ND	ND
	148	0.1	0.0	44	3	<1	0	0	0	0	0
					Gas hydrates						
162-1		0.03	0.003	7	84	4	0	<1	0	<1	57[c]
167-2		0.002	0.04	46	33	11	0	0	<1	<1	1[c]
169		0.0006	0.003	58	32	17	0	4	<1	1	16[c]
					Interface sediments						
154-1		0.0006	0.2	56	19	18	<1	2	1	<1	10
162-1		0.004	0.02	74	15	25	0	<1	<1	<1	8

FISH counts of single cells are given in percentage of DAPI detected single cells. FISH probe names are in parentheses; for probe specificity confer to Table 2. ND, not determined.

[a] Total single cells were quantified by DAPI staining of unhybridized samples.

[b] AOM aggregates were quantified after hybridization with the general archaeal probe Arch915. Numbers given represent the sum of ANME-1, ANME-2, and ANME-3 aggregates.

[c] Abundance of ANME-1 is likely underestimated, because not all morphologically distinguishable ANME-1 cells were stained after hybridization.

Abundant groups that are not directly linked to AOM were single deltaproteobacterial SRB, *Gammaproteobacteria*, and members of the *Cytophaga/Flavobacterium* group (Table 4). Cells of *Gammaproteobacteria* and *Cytophaga/Flavobacterium* were most abundant in the uppermost sediment layers (17% and 8% of total cells, respectively) as previously described for coastal sediments (Llobet-Brossa et al. 1998, Ravenschlag et al. 2001). In order to characterize the gammaproteobacterial population in more detail, several probes specific for aerobic methane oxidizers were applied (see methods). However, aerobic methane oxidizers were not detectable using these probes. Within the *Deltaproteobacteria*, DSS were most abundant. Abundance of single DSS peaked in 23 cm, 73 cm, and 90 cm sediment depth, i.e. in sediment layers of highest ANME aggregate abundance. Members of the SEEP-SRB2 group of *Deltaproteobacteria*, and *Desulfobulbus* species were not detected. *Desulfovibrio* spp., *Desulfobacter* spp., and *Desulfobacula* spp. were rarely detected throughout the sediment core.

The gas hydrate samples (stations 162-1, 167-2, 169) were characterized by relatively low and highly variable total cell numbers that differed by three orders of magnitude (10^5-10^7 cells cm^{-3}). FISH with monolabeled probes resulted in weak hybridization signals suggesting a low rRNA content of target cells. To improve signal intensities, CARD-FISH was performed for further analysis. Using CARD-FISH, detection rates of single *Bacteria* and *Archaea* were high in all gas hydrates ranging from 79%-91% of total cells. The microbial communities were dominated by single *Archaea* (46-84% of total cells), whereas single *Bacteria* were less abundant (7-33% of total cells). Relative abundance of AOM mediating archaea was high in all samples and either ANME-1 or ANME-2 archaea dominated the methanotrophic community (Table 4). Although CARD-FISH was performed, ANME-1 hybridization signals often only filled partially the target cells (Fig. 5H, e.g. arrowhead). Additionally, many cells showed the characteristic rectangular ANME-1 morphology, but were not stained with the ANME-1 probe (Fig. 5H, e.g. arrows). In pure gas hydrates (station 167-2), ANME-2 aggregates were abundant (4×10^4 aggregates cm^{-3}, Fig. 5G). Detection of single ANME-1 cells was near the detection limit (>1% of total cells). In gas hydrates with few sediment inclusions (stations 162-1, 169), abundance of ANME-2 aggregates was approximately one order of magnitude lower (3×10^3 aggregates cm^{-3}). Here, a large fraction of the microbial community could be assigned to ANME-1 (16-57% of total cells). The major fraction of the bacterial community could be assigned to sulfate-reducing DSS (4-17% of total cells). Total cell numbers in 'interface sediments' (stations 154-1 and 162-1) physically attached to the outside of massive gas hydrates were low (6×10^5 cells cm^{-3} and

4×10^6 cells cm^{-3}, respectively), but detection rates were high (Table 4). In contrast to the gas hydrate samples, the microbial community of these sediments were dominated by single *Bacteria* (59-74% of total cells), whereas single *Archaea* comprised only a minor fraction (15-19% total cells). Abundance of microbial aggregates varied and ranged from 0.2-2 $\times 10^6$ aggregates cm^{-3}. In both samples single DSS (18-25% of total cells) and ANME-1 cells (8-10% total cells) were highly abundant. Furthermore, the hybridization signals of ANME-1 cells were bright and filled the whole cell.
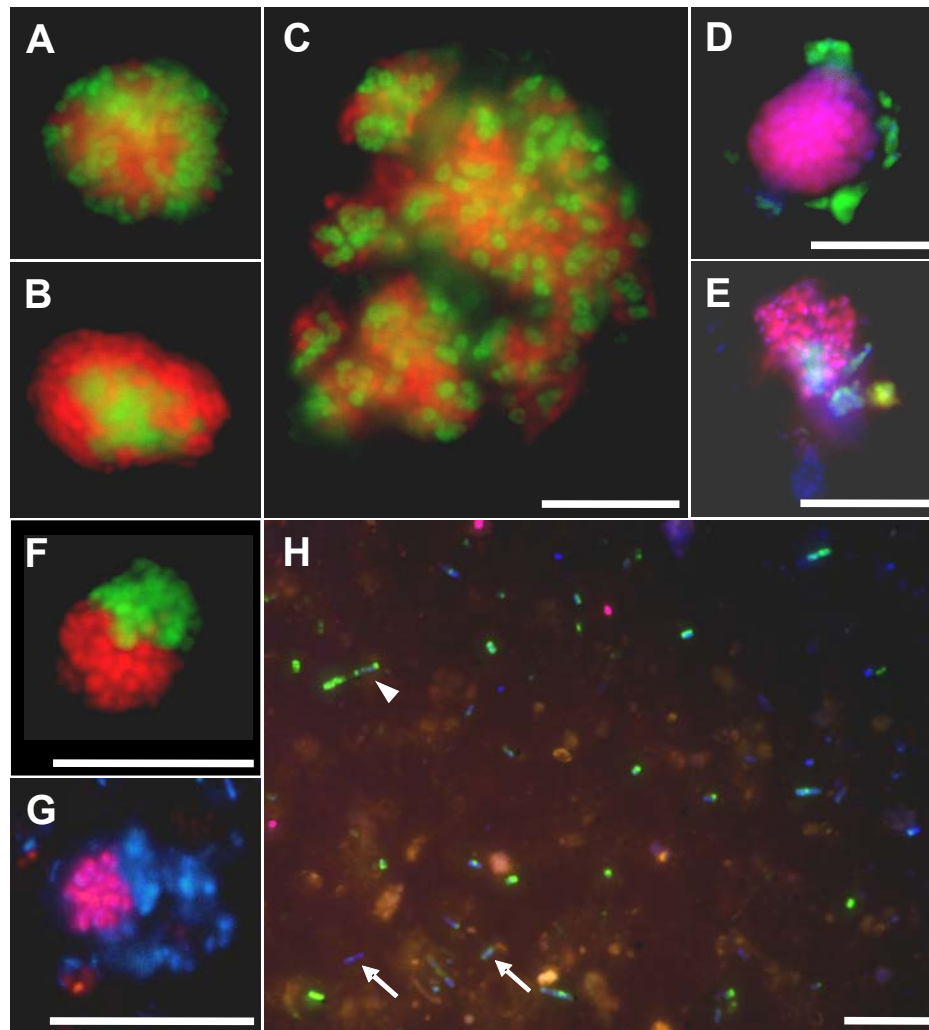
FIGURE 5 Epifluorescence micrographs of AOM mediating microorganisms in (A-E) sediments of the gravity core at 73 cm sediment depth, (F) surface sediments covered with *Beggiatoa* mats of 3-4 cm sediment depth, and (G, H) pure gas hydrates as identified by *in situ* hybridization. (A-C) ANME-1/DSS aggregates stained by probe ANME1-350 specific for ANME-1 archaea (red) and probe DSS658 for SRB of the *Desulfosarcina/Desulfococcus* branch (green), the scale bar is valid for all three pictures. (B) ANME-2c/DSS aggregate stained with DAPI and by probe ANME2c-622 for ANME-2c archaea (magenta) and probe DSS658 (cyan). (C) ANME-2a/DSS aggregate stained with DAPI and by probe ANME2a-647 (magenta) and probe DSS658 (cyan). (D) ANME-3/DSS aggregates detected by probe ANME3-1249 for ANME-3 archaea (red) and probe DSS658 (green). (E) ANME-2 aggregate stained with DAPI and by probe EelMS-932 (magenta). (F) Single ANME-1 cells stained with DAPI and by probe ANME1-350 (green-cyan) and single DSS stained with DAPI and by probe DSS658 (magenta). Many cells showed the characteristic rectangular ANME-1 morphology, but were not stained with probe ANME1-350 (e.g. arrows) or stained only partially (e.g. arrowhead). Scale bars, 10 μm.

<div align="center">DISCUSSION</div>

Microbial diversity in sediments of the gravity core. Bacterial diversity in gas hydrate bearing subsurface sediments (ca. 1 m below seafloor) was comparable to that of surface sediments of Hydrate Ridge (Knittel et al. 2003, Knittel et al. 2005). This was unexpected given the reduced microbial biomass and energy availability in deep sediment layers. All other published studies of methane rich subsurface sediments (1-300 m depth, (Marchesi et al. 2001, Kormas et al. 2003, Reed et al. 2002, Inagaki et al. 2006) investigated mainly much deeper sediments with even lower energy availability and revealed a lower bacterial diversity.

Archaeal diversity was low in sediments of the gravity core and most 16S rRNA gene sequences grouped within clades of anaerobic methane oxidizers. Again, the detected diversity was similar to the diversity in surface sediments (Knittel et al. 2005). This is in good agreement with previous studies, reporting low archaeal diversity and occurrence of ANME groups in methane rich, anoxic sediments (e.g. Lanoil et al. 2001, Madrid et al. 2001, Orphan et al. 2001a, Mills et al. 2003, Knittel et al. 2005).

Presence of two zones with enhanced ANME biomass at different depths. Generally, the cell counts in the hydrate-bearing subsurface sediments were relatively high compared to other deep water ecosystems at similar water and sediment depths (Parkes et al. 1994). FISH surveys on the gravity core revealed two distinct zones (23 and 73 cm depth) with relatively high abundant ANME populations in sediments above gas hydrate bearing layers. Indirect evidence for accumulations of AOM mediating microorganisms in deeper sediments of Hydrate Ridge in association with hydrate zones has been provided previously by biomarker analyses (Elvert et al. 2005). In a gravity core similar to the one examined in this study, concentrations of strongly 13-C depleted specific biomarkers increased just above gas hydrate layers. Biomarker concentrations were only one third of those found in the surface sediments, which is consistent with our finding of reduced total ANME cell counts in the subsurface compared to the surface.

Previous biogeochemical studies of Hydrate Ridge sediments illustrated that AOM and SR rates are highest in the uppermost sediment layers and drop dramatically with depth (Treude et al. 2003). The near-surface peak of ANME abundance detected in this study was expected and is located at a sediment depth where environmental parameters favour AOM as indicated by pore water profiles of sulfate and methane (SMT zone, Fig. 2A). Elevated concentrations of sulfide and carbonate are indicative for AOM activity and were found in both sediment layers. The near-surface ANME population likely performs AOM, whereas it is unclear

166

whether the deeper subsurface ANME population was still active at the time of sampling. In the following, we discuss two hypotheses:

AOM communities are active throughout the gravity corer sediments: An indication for an active ANME population in the subsurface are bright FISH signals with monolabeled probes. Pure culture studies demonstrated that the fluorescence intensity of a hybridization signal correlates well with the ribosome content of the target cell (Oda et al. 2000). A high rRNA content is often indicative for metabolically active cells and has been proved to be a proxy for specific growth rates under steady state conditions (Binder & Liu 1998, Kerkhof & Kemp 1999). ANME cells are slow-growing (Girguis et al. 2005; K. Nauhaus, unpublished data) and have to face unfavorable conditions in dynamic cold seeps. Although there are other studies reporting the storage of ribosomes during prolonged starvation (Eilers et al. 2000, Flardh et al. 1992, Morgenroth et al. 2000), it seems reasonable that inactive ANME cells rather reduce their cellular machinery in order to survive starvation periods and dispersal.

Sulfate (1-3 mM, Fig. 2A) is low in the subsurface sediments of the gravity core and sulfide accumulates. Cells in the sediments need to tolerate high levels of sulfide and be able to utilize low sulfate concentrations. Half-saturation constants (K_m) for SR in marine systems [70-200 µM, (Ingvorsen & Jørgensen 1984a, Ingvorsen et al. 1984b)] show that SR is kinetically feasible for microbial ecotypes adapted to low sulfate concentrations. However, preliminary experiments with sediments from Hydrate Ridge have shown that the K_m for AOM may be between 2-5 mM. Additional sulfate supporting the microbial community may originate from hydrate formation processes: during hydrate crystallization, pore water ions are excluded from the gas hydrate lattice and may be concentrated in the surrounding sediments. Over a short period, sulfate concentrations near gas hydrates may be locally enhanced and promote microbial AOM activity.

Subsurface AOM mediating community is inactive; signatures found mark a former AOM zone: The ANME subsurface zone might be caused by a recent shift of the former deep AOM zone to the sediment surface due to an increased methane flux from below. This scenario would explain the two distinct carbonate layers observed in sediments of the gravity core (Fig. 2B). The formation of carbonate crusts is a common feature of high fluid flow in cold seep systems. Luff and co-workers developed a model for changes in carbonate and aragonite concentration at Hydrate Ridge over time (Luff et al. 2005). Their calculations showed that the carbonate profile observed in the sediments of the gravity core might represent an intermediate state of carbonate crust formation. The model predicts a time scale of 3,000 years to generate a carbonate profile as observed in the sediments of the gravity core.

The calculations are based on the assumption that the pressure gradient is stable over time and methane is transported only dissolved in pore water fluids. When rapid alterations in fluid flow are considered, the observed profiles could be generated within months. This interpretation implies a -at this time- inactive microbial community in subsurface sediments with the deep carbonate peak representing former, ancient AOM activity. The scattered, relaxing sulfide profile observed in 13-60 cm sediment depth supports this hypothesis. The upper smaller sulfide peak may indicate the formation of a new growing AOM community, which started to be active not long ago.

Microbial life in gas hydrates. In Hydrate Ridge pure gas hydrates only a subset of microbial lineages present in the surrounding sediment were found and most of them belonged to groups involved in AOM (ANME-1, -2, DSS). The reduced microbial diversity might be caused by the dilution of sedimentary microorganisms during the process of gas hydrate formation. Since the microbial community in the sediments is strongly dominated by anaerobic methanotrophs, these microorganisms are likely among those that are trapped within the gas hydrate lattice. A contamination with sediments attached to the outside of the gas hydrates can be excluded, because the gas hydrates used for clone library construction melted to a clear solution without sediment pellet formation. Our results are in contrast to studies on gas hydrates of the Gulf of Mexico (GoM), where a high microbial diversity was detected (Lanoil et al. 2001, Mills et al. 2005). The higher diversity at the GoM may be due to the presence of non-methane hydrocarbons, which can be oxidized by microorganisms other than ANMEs. Furthermore, the gas hydrates analyzed in the GoM were of different physical and chemical structure (structure II hydrates). Our *in situ* analyses of gas hydrate melts and attached sediments showed the presence of microbial cells. Sulfate dependent AOM has been demonstrated for GoM gas hydrates and it has been proposed that pores and channels within the gas hydrate lattice could serve as ecological niches for metabolically active microorganisms (Orcutt et al. 2004). However, total cell numbers were low compared to surrounding sediments in Hydrate Ridge and GoM gas hydrates (Lanoil et al. 2001) suggesting that the highly crystallized gas hydrate structure is not as favorable for microbial life as the sediments.

For the first time, the microbial community structure in gas hydrates was characterized by FISH. Abundance of ANME-1 cells was high as identified by their conspicuous morphology, i.e. characteristic rectangular shape. However, many cells had very low ribosome content and showed no hybridization signals with ANME-1 probes but only a fuzzy DAPI signal. AOM activity could not be measured in melted pure gas hydrates (station 176-2) with *ex situ* and *in*

vitro rate measurements, although samples were taken as fast as possible after gas hydrate recovery and stored under anoxic conditions immediately. These findings suggest that ANME cells frozen in gas hydrates are inactive or even dead and decaying.

The interface sediments, which were physically attached to gas hydrates, showed high accumulations of ANME-1 cells. In contrast to cells entrapped in gas hydrates, they had bright hybridization signals suggesting high/recent metabolic activity. The close vicinity to gas hydrates might be a favorable niche for AOM mediating microorganisms due to locally elevated methane concentrations. Sedimentary ANME cells may even induce gas hydrate decomposition by lowering the methane partial pressure.

Novel types of ANME aggregates. The major fraction of ANME aggregates in surface sediments of the gravity core was identified as shell-type ANME-1 aggregates associated with sulfate-reducing DSS. This novel type of structured AOM consortium (ANME-1/DSS) has not been detected in Hydrate Ridge surface sediments (Knittel et al. 2003) nor described for any other seep system. ANME-1 cells have been repeatedly described as single cells or chains of 4 cells (Orphan et al. 2002, Blumenberg et al. 2005, Eller et al. 2005, Knittel et al. 2005, Orcutt et al. 2005). ANME-1 aggregations have only been described for Eel River Basin sediments (Orphan et al. 2002) and GoM cold seeps (Orcutt et al. 2005), but without any known sulfate-reducing partner. In thick microbial mats from the Black Sea ANME-1 cells accounted for more than 40% of the total biomass, with DSS cells distributed irregularly as single cells or colonies throughout the mat [mat type consortia, (Michaelis et al. 2002)].

In addition, novel types of ANME-3 aggregates have been detected in Hydrate Ridge surface sediments. ANME-3 has recently been described to live in a consortium with sulfate reducers of the genus *Desulfobulbus* (DBB) and mediate AOM at an Arctic mud volcano (Lösekann et al. in prep, Niemann et al. subm). Numerous ANME-3 16S rRNA gene sequences have been found in Hydrate Ridge surface sediments and other methane rich habitats (Orphan et al. 2001a, Knittel et al. 2005, Meyerdierks et al. 2005; Heijs, S.K., Aloisi, G., Boulobassi, I., Pancost, R.D., Pierre, C., Sinninghe Damste, J.S., Gottschall, J.C. and Forney, L.J., database release]. Interestingly, ANME-3 aggregates described in this study were associated with sulfate-reducing DSS but not with DBB. Thus, ANME-3 cells seem not to depend on a specific sulfate-reducing partner but can be associated with at least a second type of syntrophic SRB. In contrast, in all habitats investigated ANME-1 and ANME-2 have yet been found always in consortia with DSS (Boetius et al. 2000, Orphan et al. 2001a, Knittel et al. 2005). Abundance of ANME-3 consortia was low compared with the cell numbers of ANME-1 and ANME-2. The low *in situ* abundance of this group is supported by sequence

information derived from metagenomic libraries. Meyerdierks and colleagues (Meyerdierks et al. 2005) constructed large-insert libraries from Hydrate Ridge surface sediments and identified four fosmids carrying ANME-2 16S rRNA genes but only one fosmid carrying the ANME-3 16S rRNA gene. Both studies indicate that ANME-3 seems to play a minor role in the ANME-1/-2 dominated cold seep of Hydrate Ridge.

REFERENCES

Amann RI, Krumholz L, Stahl DA (1990b) Fluorescent-oligonucleotide probing of whole cells for determinative, phylogenetic, and environmental studies in microbiology. Journal of Bacteriology 172:762-770

Bidle KA, Kastner M, Bartlett DH (1999) A phylogenetic analysis of microbial communities associated with methane hydrate containing marine fluids and sediments in the Cascadia margin (ODP8 site 892B). FEMS Microbiology Letters 177:101-108

Binder BJ, Liu YC (1998) Growth-rate regulation of ribosomal-rna content of a marine *Synechococcus* (cyanobacterium) strain. Applied and Environmental Microbiology 64:3346-3351

Blumenberg M, Seifert R, Nauhaus K, Pape T, Michaelis W (2005) In Vitro Study of Lipid Biosynthesis in an Anaerobically Methane-Oxidizing Microbial Mat. Applied and Environmental Microbiology 71:4345-4351

Boetius A, Ravenschlag K, Schubert C, Rickert D, Widdel F, Gieseke A, Amann R, Jørgensen BB, Witte U, Pfannkuche O (2000) A marine microbial consortium apparently mediating anaerobic oxidation of methane. Nature 407:623-626

Boetius A, Suess E (2004) Hydrate Ridge: a natural laboratory for the study of microbial life fueled by methane from near-surface gas hydrates. Chemical Geology 205:291-310

Bohrmann G, Greinert J, Suess E, Torres M (1998) Authigenic carbonates from the Cascadia subduction zone and their relation to gas hydrate stability. Geology 26:647-650

Bowman JP, Rea SM, McCammon SA, McMeekin TA (2000) Diversity and community structure within anoxic sediment from marine salinity meromictic lakes and a coastal meromictic marine basin, Vestfold Hills, eastern Antarctica. Environmental Microbiology 2:227-237

Collett TS, Kuuskraa VA (1998) Hydrates contain vast store of world gas resources. Oil Gas Journal 96:90-95

Coolen MJL, Hopmans EC, Rijpstra WIC, Muyzer G, Schouten S, Volkman JK, Sinninghe Damsté JS (2004) Evolution of the methane cycle in Ace Lake (Antarctica) during the Holocene: response of methanogens and methanotrophs to environmental change. Organic Geochemistry 35:1151-1167

Cord-Ruwisch R (1985) A quick method for the determination of dissolved and precipitated sulfides in cultures of sulfate-reducing bacteria. Journal of Microbiological Methods 4:33-36

Cragg BA, Parkes RJ, Fry JC, Weightman AJ, Rochelle PA, Maxwell JR (1996) Bacterial populations in sediments containing gas hydrates (ODP Leg 146: Cascadia Margin). Earth and Planetary Science Letters 139:497-507

Daims H, Brühl A, Amann R, Schleifer KH (1999) The domain-specific probe EUB338 is insufficient for the detection of all Bacteria: Development and evaluation of a more comprehensive probe set. Systematic and Applied Microbiology 22:434-444

Devereux R, Kane MD, Winfrey J, Stahl DA (1992) Genus- and Group-specific hybridization probes for determinative and environmental studies of sulfate-reducing bacteria. Systematic and Applied Microbiology 15:601-609

Dhillon A, Teske A, Dillon J, Stahl DA, Sogin ML (2003) Molecular characterization of sulfate-reducing bacteria in the Guaymas Basin. Applied and Environmental Microbiology 69:2765-2772

Dojka MA, Hugenholtz P, Haack SK, Pace NR (1998) Microbial diversity in a hydrocarbon- and chlorinated-solvent-contaminated aquifer undergoing intrinsic bioremediation. Applied and Environmental Microbiology 64:3869-3877

Eilers H, Pernthaler J, Amann R (2000b) Succession of Pelagic Marine Bacteria during Enrichment. Applied and Environmental Microbiology 66:4634 - 4640

Eller G, Kanel L, Kruger M (2005) Cooccurrence of Aerobic and Anaerobic Methane Oxidation in the Water Column of Lake Plußsee. Applied and Environmental Microbiology 71:8925-8928

Eller G, Stubner S, Frenzel P (2000) Group-specific 16S rRNA targeted probes for the detection of type I and type II methanotrophs by fluorescence in situ hybridisation. FEMS Microbiology Letters 198:91-97

Elvert M, Hopmans EC, Treude T, Boetius A, Suess E (2005) Spatial variations of methanotrophic consortia at cold methane seeps: implications from a high-resolution molecular and isotopic approach. Geobiology 3:195-209

Flardh K, Cohen P, Kjelleberg S (1992) Ribosomes exist in large excess over the apparent demand for protein synthesis during carbon starvation in marine *Vibrio* sp. strain CCUG 15956. Journal of Bacteriology 174:6780-6788

Fossing H, Jørgensen BB (1989) Measurement of bacterial sulfate reduction in sediments: Evaluation of a single-step chromium reduction method. Biogeochemistry 8:205-222

Galand PE, Fritze H, Yrjala K (2003) Microsite-dependent changes in methanogenic populations in a boreal oligotrophic fen. Environmental Microbiology 5:1133-1143

Girguis PR, Cozen AE, DeLong EF (2005) Growth and Population Dynamics of Anaerobic Methane-Oxidizing Archaea and Sulfate-Reducing Bacteria in a Continuous-Flow Bioreactor. Applied and Environmental Microbiology 71:3725-3733

Girguis PR, Orphan VJ, Hallam SJ, DeLong EF (2003) Growth and methane oxidation rates of anaerobic methanotrophic archaea in a continuous-flow bioreactor. Applied and Environmental Microbiology 69:5472-5482

Hallam SJ, Girguis PR, Preston CM, Richardson PM, DeLong EF (2003) Identification of methyl coenzyme M reductase A (*mcrA*) genes associated with methane-oxidizing archaea. Applied and Environmental Microbiology 69:5483-5491

Hallam SJ, Putnam N, Preston CM, Detter JC, Rokhsar D, Richardson PM, DeLong EF (2004) Reverse Methanogenesis: Testing the Hypothesis with Environmental Genomics. Science 305:1457-1462

Heijs SK, Sinninghe Damste JS, Forney LJ (2005) Characterization of a deep-sea microbial mat from an active cold seep at the Milano mud volcano in the Eastern Mediterranean Sea. FEMS Microbiology Ecology 54:47-56

Hinrichs K-U, Boetius A (2002) The anaerobic oxidation of methane: New insights in microbial ecology and biogeochemistry. In: Wefer G, Billett D, Hebbeln D, Jørgensen BB, Schlüter M, Van Weering TC (eds) Ocean Margin Systems. Springer, Berlin

Hinrichs KU, Hayes JM, Sylva SP, Brewer PG, DeLong EF (1999) Methane-consuming archaebacteria in marine sediments. Nature 398:802-805

Hugenholtz P, Pitulle C, Hershberger KL, Pace NR (1998) Novel division level bacterial diversity in a Yellowstone hot spring. Journal of Bacteriology 180:366-376

Inagaki F, Nunoura T, Nakagawa S, Teske A, Lever M, Lauer A, Suzuki M, Takai K, Delwiche M, Colwell FS, Nealson KH, Horikoshi K, D'Hondt S, Jørgensen BB (2006) Biogeographical distribution and diversity of microbes in methane hydrate-bearing deep marine sediments on the Pacific Ocean Margin. Proceedings of the National Academy of Sciences USA 103:2815-2820

Ingvorsen K, Jørgensen BB (1984a) Kinetics of sulfate uptake by freshwater and marine species of Desulfovibrio. Archives of Microbiology 139:61

Ingvorsen K, Zehnder AJB, Jørgensen BB (1984b) Kinetics of sulfate and acetate uptake by Desulfobacter postgatei. Applied and Environmental Microbiology 47:403-407

Joye SB, Boetius A, Orcutt BN, Montoya JP, Schulz HN, Erickson MJ, Lugo SK (2004) The anaerobic oxidation of methane and sulfate reduction in sediments from Gulf of Mexico cold seeps. Chemical Geology 205:219-238

Kane MD, Poulsen LK, Stahl DA (1993) Monitoring the enrichment and isolation of sulfate-reducing bacteria by using oligonucleotide hybridization probes designed from environmentally derived 16S rRNA sequences. Applied and Environmental Microbiology 59:682-686

Kerkhof L, Kemp P (1999) Small ribosomal RNA content in marine Proteobacteria during non-steady growth. FEMS Microbiology Ecology 30:253-260

Knittel K, Boetius A, Lemke A, Eilers H, Lochte K, Pfannkuche O, Linke P, Amann R (2003) Activity, distribution, and diversity of sulfate reducers and other bacteria in sediments above gas hydrate (Cascadia Margin, Oregon). Geomicrobiology Journal 20:269-294

Knittel K, Lösekann T, Boetius A, Kort R, Amann R (2005) Diversity and distribution of methanotrophic archaea at cold seeps. Applied and Environmental Microbiology 71:467-479

Kormas KA, Smith DC, Edgcomb V, Teske A (2003) Molecular analysis of deep subsurface microbial communities in Nankai Trough sediments (ODP leg 190, site 1176). FEMS Microbiology Ecology 45:115-125

Krüger M, Meyerdierks A, Glöckner FO, Amann R, Widdel F, Kube M, Reinhardt R, Kahnt J, Böcher R, Thauer RK, Shima S (2003) A conspicuous nickel protein in microbial mats that oxidize methane anaerobically. Nature 426:878-881

Kvenvolden K (1988) Methane hydrate - a major reservoir of carbon in the shallow geosphere? Chemical Geology 71:41 - 51

Kvenvolden K (1995) A review of the geochemistry of methane in natural gas hydrate. Organic Geochemistry 23:997 - 1008

Lane DJ, Pace B, Olsen GJ, Stahl DA, Sogin M, Pace NR (1985) Rapid determination of 16S ribosomal RNA sequences for phylogenetic analyses. Proceedings of the National Academy of Sciences USA 82:6955-6959

Lanoil BD, Duc MTL, Wright M, Kastner M, Nealson KH, Bartlett D (2005) Archaeal diversity in ODP legacy borehole 892b and associated seawater and sediments of the Cascadia Margin. FEMS Microbiology Ecology 54:167-177

Lanoil BD, Sassen R, La Duc MT, Sweet ST, Nealson KH (2001) *Bacteria* and *Archaea* physically associated with Gulf of Mexico Gas Hydrates. Applied and Environmental Microbiology 67:5143-5153

Llobet-Brossa E, Rossello-Mora R, Amann R (1998) Microbial community composition of wadden sea sediments as revealed by fluorescence in situ hybridization. Applied and Environmental Microbiology 64:2691-2696

Lösekann T, Nadalig T, Niemann H, Knittel K, Boetius A, Amann R (in prep) Novel clusters of aerobic and anaerobic methane oxidizers at an Arctic cold seep (Haakon Mosby Mud Volcano, Barents Sea).

Ludwig W, Strunk O, Westram R, Richter L, Meier H, Yadhukumar, Buchner A, Lai T, Steppi S, Jobb G, Förster W, Brettske I, Gerber S, Ginhart AW, Gross O, Grumann S, Hermann S, Jost R, König A, Liss T, Lüßmann R, May M, Nonhoff B, Reichel B, Strehlow R, Stamatakis A, Stuckmann N, Vilbig A, Lenke M, Ludwig T, Bode A, Schleifer KH (2004) ARB: a software environment for sequence data. Nucleic Acids Research 32:1363-1371

Luff R, Greinert J, Wallmann K, Klaucke I, Suess E (2005) Simulation of long-term feedbacks from authigenic carbonate crust formation at cold vent sites. Chemical Geology 216:157-174

Madrid V, Taylor G, Scranton M, Christoserdov A (2001) Phylogenetic Diversity of Bacterial and Archaeal Communities in the Anoxic Zone of the Cariaco Basin. Applied and Environmental Microbiology 67:1663 - 1674

Manz W, Amann R, Ludwig W, Vancanneyt M, Schleifer K-H (1996) Application of a suite of 16S rRNA-specific oligonucleotide probes designed to investigate bacteria of the phylum cytophaga-flavobacter-bacteroides in the natural environment. Microbiology 142:1097-1106

Manz W, Amann R, Ludwig W, Wagner M, Schleifer K-H (1992) Phylogenetic oligodeoxynucleotide probes for the major subclasses of proteobacteria: problems and solutions. Systematic and Applied Microbiology 15:593-600

Manz W, Eisenbrecher M, Neu TR, Szewzyk U (1998) Abundance and spatial organization of gram negative sulfate-reducing bacteria in activated sludge investigated by in situ probing with specific 16S rRNA targeted oligonucleotides. FEMS Microbiology Ecology 25:43-61

Marchesi JR, Weightman AJ, Cragg BA, Parkes RJ, Fry JC (2001) Methanogen and bacterial diversity and distribution in deep gas hydrate sediments from the Cascadia Margin as revealed by 16S rRNA molecular analysis. FEMS Microbiology Ecology 34:221-228

Massana R, Murray AE, Preston CM, DeLong EF (1997) Vertical distribution and phylogenetic characterization of marine planktonic Archaea in the Santa Barbara Channel. Applied and Environmental Microbiology 63:50-56

Meyerdierks A, Kube M, Lombardot T, Knittel K, Bauer M, Glockner FO, Reinhardt R, Amann R (2005) Insights into the genomes of archaea mediating the anaerobic oxidation of methane. Environmental Microbiology 7:1937-1951

Michaelis W, Seifert R, Nauhaus K, Treude T, Thiel V, Blumenberg M, Knittel K, Gieseke A, Peterknecht K, Pape T, Boetius A, Amann R, Jørgensen BB, Widdel F, Peckmann J, Pimenov NV, Gulin MB (2002) Microbial reefs in the Black Sea fueled by anaerobic oxidation of methane. Science 297:1013-1015

Mills HJ, Hodges C, Wilson K, MacDonald IR, Sobecky PA (2003) Microbial diversity in sediments associated with surface-breaching gas hydrate mounds in the Gulf of Mexico. FEMS Microbiology Ecology 46:39-52

Mills HJ, Martinez RJ, Story S, Sobecky PA (2005) Characterization of Microbial Community Structure in Gulf of Mexico Gas Hydrates: Comparative Analysis of DNA- and RNA-Derived Clone Libraries. Applied and Environmental Microbiology 71:3235-3247

Morgenroth E, Obermayer A, Arnold E, Brühl A, Wagner M, Wilderer PA (2000) Effect of long-term idle periods on the performance of sequencing batch reactors. Water Science and Technology 41:105-113

Munson MA, Nedwell DB, Embley TM (1997) Phylogenetic diversity of Archaea in sediment samples from a coastal salt marsh. Applied and Environmental Microbiology 63:4729-4733

Mussmann M, Ishii K, Rabus R, Amann R (2005) Diversity and vertical distribution of cultured and uncultured *Deltaproteobacteria* in an intertidal mud flat of the Wadden Sea. Environmental Microbiology 7:405-418

Muyzer G, Teske A, Wirsen CO, Jannasch HW (1995) Phylogenetic relationships of *Thiomicrospira* species and their identification in deep-sea hydrothermal vent samples by denaturing gradient gel electrophoresis of 16S rDNA fragments. Archives of Microbiology 164:165-172

Nauhaus K, Boetius A, Krüger M, Widdel F (2002) In vitro demonstration of anaerobic oxidation of methane coupled to sulfate reduction in sediment from a marine gas hydrate area. Environmental Microbiology 4:296-305

Nauhaus K, Treude T, Boetius A, Kruger M (2005) Environmental regulation of the anaerobic oxidation of methane: a comparison of ANME-I and ANME-II communities. Environmental Microbiology 7:98-106

Niemann H, Lösekann T, de Beer D, Elvert M, Knittel K, Amann R, Sauter E, Schlüter M, Klages M, Foucher J, Boetius A (subm) Fluid flow controls distribution of methanotrophic microorganisms at submarine cold seeps.

Oda Y, Slagman S-J, Meijer WG, Forney LJ, Gottschal JC (2000) Influence of growth rate and starvation on fluorescent in situ hybridization of *Rhodopseudomonas palustris*. FEMS Microbiology Ecology 32:205-213

Orcutt B, Boetius A, Elvert M, Samarkin V, Joye SB (2005) Molecular biogeochemistry of sulfate reduction, methanogenesis and the anaerobic oxidation of methane at Gulf of Mexico cold seeps. Geochimica et Cosmochimica Acta 69:4267-4281

Orcutt BN, Boetius A, Lugo SK, MacDonald IR, Samarkin VA, Joye SB (2004) Life at the edge of methane ice: microbial cycling of carbon and sulfur in Gulf of Mexico gas hydrates. Chemical Geology 205:239-251

Orphan VJ, Hinrichs K-U, Ussler III W, Paull CK, Taylor LT, Sylva SP, Hayes JM, DeLong EF (2001a) Comparative analysis of methane-oxidizing archaea and sulfate-reducing bacteria in anoxic marine sediments. Applied and Environmental Microbiology 67:1922-1934

Orphan VJ, House CH, Hinrichs K-U, McKeegan KD, DeLong EF (2001b) Methane-consuming archaea revealed by directly coupled isotopic and phylogenetic analysis. Science 293:484-487

Orphan VJ, House CH, Hinrichs K-U, McKeegan KD, DeLong EF (2002) Multiple archaeal groups mediate methane oxidation in anoxic cold seep sediments. Proceedings of the National Academy of Sciences USA 99:7663-7668

Parkes RJ, Cragg BA, Bale SJ, Getliff JM, Goodman K, Rochelle PA, Fry JC, Weightman AJ, Harvey SM (1994) Deep bacterial biosphere in Pacific Ocean sediments. Nature 371:410-413

Pernthaler A, Pernthaler J, Amann R (2002) Fluorescence in situ hybridization and catalyzed reporter deposition (CARD) for the identification of marine Bacteria. Applied and Environmental Microbiology 68:3094-3101

Pfannkuche O, Eisenhauer A, Linke P, Utecht C (2002) RV SONNE Cruise Report SO165: OTEGA I. GEOMAR reports

Ravenschlag K, Sahm K, Amann R (2001) Quantitative molecular analysis of the microbial community in marine Arctic sediments (Svalbard). Applied and Environmental Microbiology 67:387-395

Ravenschlag K, Sahm K, Knoblauch C, Jørgensen BB, Amann R (2000) Community structure, cellular rRNA content and activity of sulfate-reducing bacteria in marine Arctic sediments. Applied and Environmental Microbiology 66:3592-3602

Ravenschlag K, Sahm K, Pernthaler J, Amann R (1999) High bacterial diversity in permanently cold marine sediments. Applied and Environmental Microbiology 65:3982-3989

Reed DW, Fujita Y, Delwiche ME, Blackwelder DB, Sheridan PP, Uchida T, Colwell FS (2002) Microbial communities from methane-bearing deep marine sediments in a forearc basin. Appl. Environm. Microbiol. 68:3759-3770

Reysenbach A-L, Longnecker K, Kirshtein J (2000) Novel bacterial and archaeal lineages from an in situ growth chamber deployed at a Mid-Atlantic Ridge hydrothermal vent. Applied and Environmental Microbiology 66:3798-3806

Snaidr J, Amann R, Huber I, Ludwig W, Schleifer KH (1997) Phylogenetic analysis and in situ identification of bacteria in activated sludge. Applied and Environmental Microbiology 63:2884-2896

Suess E, Torres ME, Bohrmann G, Collier RW, Greinert J, Linke P, Rehder g, Trehu A, Wallmann K, Winckler G, Zuleger E (1999) Gas hydrate destabilization: enhanced dewatering, benthic material turnover and large methane plumes at the Cascadia convergent margin. Earth and Planetary Sciences Letters 170:1-5

Takai K, Horikoshi K (1999) Genetic diversity of archaea in deep-sea hydrothermal vent environments. Genetics 152:1285-1297

Takai K, Moser DP, DeFlaun M, Onstott TC, Fredrickson JK (2001) Archaeal Diversity in Waters from Deep South African Gold Mines. Applied and Environmental Microbiology 67:5750-5760

Torres ME, McManus J, Hammond DE, De Angelis MA, Heeschen KU, Colbert SL, Tryon MD, Brown KM, Suess E (2002) Fluid and chemical fluxes in and out of sediments hosting methane hydrate deposits in Hydrate Ridge, OR, I: Hydrological provinces. Earth and Planetary Sciences Letters 201:525-540

Treude T, Boetius A, Knittel K, Wallmann K, Jørgensen BB (2003) Anaerobic oxidation of methane above gas hydrates (Hydrate Ridge, OR). Marine Ecology Progress Series 264:1-14

Valentine DL, Reeburgh WS (2000) New perspectives on anaerobic methane oxidation. Environmental Microbiology 2:477-484

Vetriani C, Jannasch HW, MacGregor BJ, Stahl DA, Reysenbach AL (1999) Population structure and phylogenetic characterization of marine benthic archaea in deep-sea sediments. Applied and Environmental Microbiology 65:4375-4384

Wallner G, Amann R, Beisker W (1993) Optimizing fluorescent in situ hybridization with rRNA-targeted oligonucleotide probes for flow cytometric identification of microorganism. Cytometry 14:136-143

Widdel F, Bak F (2002) Gram-negative mesophilic sulfate-reducing bacteria. In: Dworkin M (ed) The Prokaryotes (Electronic Version). Springer Verlag, New York, p 3352-3378

Zhou J, Brunns MA, Tiedje JM (1996) DNA recovery from soils of diverse composition. Applied and Environmental Microbiology 62:316-322

5

Diversity and Distribution of
Methanotrophic Archaea at Cold Seeps

Katrin Knittel, Tina Lösekann, Antje Boetius, Renate Kort,

and Rudolf Amann

Diversity and Distribution of Methanotrophic Archaea at Cold Seeps†

Katrin Knittel,[1]* Tina Lösekann,[1] Antje Boetius,[1,2] Renate Kort,[3] and Rudolf Amann[1]

Max Planck Institute for Marine Microbiology[1] and International University of Bremen,[2] Bremen, and ICBM-Geomicrobiology Group, University of Oldenburg, Oldenburg,[3] Germany

In this study we investigated by using 16S rRNA-based methods the distribution and biomass of archaea in samples from (i) sediments above outcropping methane hydrate at Hydrate Ridge (Cascadia margin off Oregon) and (ii) massive microbial mats enclosing carbonate reefs (Crimea area, Black Sea). The archaeal diversity was low in both locations; there were only four (Hydrate Ridge) and five (Black Sea) different phylogenetic clusters of sequences, most of which belonged to the methanotrophic archaea (ANME). ANME group 2 (ANME-2) sequences were the most abundant and diverse sequences at Hydrate Ridge, whereas ANME-1 sequences dominated the Black Sea mats. Other seep-specific sequences belonged to the newly defined group ANME-3 (related to *Methanococcoides* spp.) and to the *Crenarchaeota* of marine benthic group B. Quantitative analysis of the samples by fluorescence in situ hybridization (FISH) showed that ANME-1 and ANME-2 co-occurred at the cold seep sites investigated. At Hydrate Ridge the surface sediments were dominated by aggregates consisting of ANME-2 and members of the *Desulfosarcina-Desulfococcus* branch (DSS) (ANME-2/DSS aggregates), which accounted for >90% of the total cell biomass. The numbers of ANME-1 cells increased strongly with depth; these cells accounted 1% of all single cells at the surface and more than 30% of all single cells (5% of the total cells) in 7- to 10-cm sediment horizons that were directly above layers of gas hydrate. In the Black Sea microbial mats ANME-1 accounted for about 50% of all cells. ANME-2/DSS aggregates occurred in microenvironments within the mat but accounted for only 1% of the total cells. FISH probes for the ANME-2a and ANME-2c subclusters were designed based on a comparative 16S rRNA analysis. In Hydrate Ridge sediments ANME-2a/DSS and ANME-2c/DSS aggregates differed significantly in morphology and abundance. The relative abundance values for these subgroups were remarkably different at *Beggiatoa* sites (80% ANME-2a, 20% ANME-2c) and *Calyptogena* sites (20% ANME-2a, 80% ANME-2c), indicating that there was preferential selection of the groups in the two habitats. These variations in the distribution, diversity, and morphology of methanotrophic consortia are discussed with respect to the presence of microbial ecotypes, niche formation, and biogeography.

The microbially mediated anaerobic oxidation of methane (AOM) is the major biological sink of the greenhouse gas methane in marine sediments (49) and serves as an important control for emission of methane into the hydrosphere. The AOM metabolic process is assumed to be a reversal of methanogenesis coupled to the reduction of sulfate to sulfide involving methanotrophic archaea (ANME) and sulfate-reducing bacteria (SRB) as syntrophic partners (7, 20, 21, 23, 69). Neither the ANME groups nor their sulfate-reducing partners have been isolated yet, and the enzymes and biochemical pathways involved in AOM remain unknown (18, 19). Very recently, however, Krüger et al. described a candidate enzyme (Ni-protein I) that may catalyze methane activation in a reverse terminal methyl-coenzyme M reductase reaction (27), supporting the hypothesis that reverse methanogenesis occurs in the ANME groups. Field and laboratory studies have provided ample evidence that AOM can be mediated by structured consortia consisting of archaea (ANME group 2 [ANME-2]) belonging to the order *Methanosarcinales* and SRB

belonging to the *Desulfosarcina-Desulfococcus* branch (DSS) of the *Deltaproteobacteria* (7, 40); below these consortia are referred to as ANME-2/DSS aggregates. These consortia oxidize methane with sulfate, yielding equimolar amounts of carbonate and sulfide (37). A second archaeal group (ANME-1), which is distantly related to the *Methanosarcinales* and *Methanomicrobiales*, has also been shown to mediate AOM (34, 41). Using fluorescence in situ hybridization (FISH) combined with secondary ion mass spectrometry, Orphan and coworkers were able to measure carbon isotopic signatures of single aggregates of ANME-1 and ANME-2 cells (40, 41). Their $\delta^{13}C$ values were extremely low and thus provided direct evidence for methanotrophy in both phylogenetic clusters. At hot spot sites of AOM in different marine environments phylogenetic analyses based on 16S rRNA gene sequencing of microbial communities showed that there was relatively low diversity of archaea compared to the bacterial diversity in these habitats (21, 26, 28, 39, 58) (GenBank accession numbers AY593257 to AY593349 and AF357889 to AF361694 [http://www.ncbi.nlm.nih.gov]) and indicated the co-occurrence of several ANME-1 and ANME-2 populations. However, such studies so far have not provided quantification of the biomasses of the different groups and their distribution in the environment.

The presence of several microbial populations with essentially the same function in a given environment is still a major puzzle in our concept of biodiversity and microbial ecology. In this study we dealt with methanotrophic archaea, which are

---

* Corresponding author. Mailing address: Max Planck Institute for Marine Microbiology, Department of Molecular Ecology, Celsiusstrasse 1, 28359 Bremen, Germany. Phone: 49-421-2028936. Fax: 49-421-2028580. E-mail: kknittel@mpi-bremen.de.

TABLE 1. Geochemical characterization of Hydrate Ridge and Black Sea stations and abundance of ANME-2a/DSS and ANME-2c/DSS aggregates[a]

Parameter	Hydrate Ridge						Black Sea mats
	Beggiatoa mat		Calyptogena field		Acharax field		
	105-1	19-2	185	38-1	139	51-1	55-4
Station	105-1	19-2	185	38-1	139	51-1	55-4
Depth (m)	780	777	785	787	830	775	230
In situ pressure (10^5 Pa)	80 (38)		80 (38)		80 (38)		23 (38)
Position	44°34.140'N, 125°08.810'W	44°34.104'N, 125°08.807'W	44°34.190'N, 125°08.830'W	44°34.186'N, 125°08.847'W	44°34.100'N, 125°08.380'W	44°34.198'N, 125°08.858'W	31°59.530'N, 44°46.479'E
Temp (°C)	2–4[b]		2–4[b]		2–4[b]		8[b]
Ex situ CH_4 concn (mM)	50 (63)		1 to 10 (63)		<1		ND[c]
Theoretical methane concn at saturation (mM)	138 (38)		138 (38)		ND		40 (38)
CH_4 flux (mmol m^{-2} day^{-1})	30 to 90 (63)		<1 – (63)		0		ND
Fluid flux (cm yr^{-1})	10 to 250 (63, 67)		2 to –10 (63, 67)		0		ND
Oxygen penetration	ca. 1 mm		ca. 10 mm		Several centimeters		Anoxic
Hydrogen sulfide concn (mM)	10 to 26 (50)		0 to 10 (50)		<0.1 (0–15 cm); 0.1–0.3 mM (15–25 cm) (50)		ca 1
Sulfate concn (mM)	<18 (0–10 cm) (8)		18 to 28 (0–10 cm) (8)		28 (8)		17 (38)
AOM rate (µmol cm^{-3} day^{-1})	ND	Up to 0.24 (other mats up to 3) (65)	ND	Up to 2.7 (65)	ND	Up to 0.065 (65)	18 (34)[d]
SRR (µmol cm^{-3} day^{-1})[e]	ND	Up to 2.1 (65)	ND	Up to 3.6 (65)	ND	Up to 0.0016 (65)	19 (34)[d]
Mixed type ANME-2a/DSS consortia (%)	45 (this study)	80 (this study)	20 (this study)	20 (this study)	ND	ND	0 (this study)
Shell type ANME-2c/DSS consortia (%)	25 (this study)	16 (this study)	80 (this study)	75 (this study)	ND	ND	90–100 (this study)

[a] The diagram of the chemosynthetic communities at Hydrate Ridge is from reference 65. The numbers in parentheses are references.
[b] Shipboard measurement.
[c] ND, not determined.
[d] The units are micromoles per gram (dry weight) per day.
[e] SRR, sulfate reduction rate.

179

limited to extreme environments with anoxic, methane-rich, and sulfate-containing sediments. Hence, the rest of the ocean represents a barrier to the dispersal of these organisms, making them an interesting case study for the central question of microbial biogeography, which is "Is everything everywhere?" (3, 5, 15, 71). To find clues to potential niche occupation by the different ANME groups, we investigated the phylogenetic diversity, distribution, and abundance of the methanotrophs at selected seep sites with high rates of AOM (34, 65), including sediments from three different types of chemosynthetic communities (*Beggiatoa* mats, *Calyptogena* fields, and *Acharax* fields) above outcropping methane hydrate at Hydrate Ridge (Cascadia margin off Oregon) and massive methanotrophic microbial mats at Black Sea methane seeps.

MATERIALS AND METHODS

Study sites, sampling, and geochemical description. Sediment samples from Hydrate Ridge were obtained during R/V *SONNE* cruises SO143-2 in August 1999 (9) and SO148-1 in August 2000 (30) at the crest of southern Hydrate Ridge at the Cascadia convergent margin off the coast of Oregon. At Hydrate Ridge, discrete methane hydrate layers occur on the seafloor at a water depth of 600 to 800 m, which corresponds to the hydrate stability limit (50, 57). The hydrates are located a few centimeters beneath the sediment surface and form mounds that are several meters in diameter (56). The mounds are covered by sediment and are populated by sulfide-oxidizing communities, which benefit from large quantities of hydrogen sulfide generated as a by-product of AOM (4, 37, 50, 67). The sediments above the hydrates were covered by mats of giant filamentous sulfur-oxidizing bacteria belonging to the genus *Beggiatoa* extending several millimeters into the overlying bottom water (stations 105–1 and 19–2; referred to as *Beggiatoa* mats below) or by clam fields consisting of *Calyptogena* spp. (stations 185-1 and 38-1; referred to as *Calyptogena* fields below). Layers of gas hydrate were found in cores with *Beggiatoa* mats at sediment depths of >13 cm and in cores with *Calyptogena* fields at sediment depths of >16 cm. Strong degassing from decomposing hydrates was observed. Sediments not covered by either community often contained subsurface-dwelling chemosynthetic *Acharax* bivalves. The concentrations of methane and sulfide were low in the upper 15 cm in these *Acharax* fields. Sediment cores that were 20 to 40 cm long were obtained by using a video-guided multiple corer from gas hydrate-bearing sediments and from *Acharax* fields not enriched in methane in the surface sediments. Geochemical parameters are described in detail in Table 1. Upon recovery all sediment cores were immediately transferred to a cold room (4°C). Samples were processed within 4 h after sampling by using the methods described below.

The second study area is located in the Black Sea and represents a field in which there is active seepage of free gas on the slope of the northwestern Crimea area. Here, a field of conspicuous microbial reefs forming chimney-like structures was discovered at a water depth of 230 m in anoxic waters (29, 34, 46). The reef structure consists of porous carbonate structures covered by microbial mats that are up to 10 cm thick. The chimneys are up to 4 m high and 1 m wide. They are composed mainly of magnesium calcite and aragonite with δ¹³C values of ca. −30‰, indicating that the carbonate is predominantly derived from AOM (59). Gas seeping from the seafloor at the Ukrainian shelf edge contains 95 to 99% methane and minor amounts of N₂, CO₂, and H₂. In cross sections of the mat, the outside is dark gray to black. The interior part of the mat is pink to brownish (34). Major portions of the mat (ca. 30%; Knittel et al., unpublished data) consist of irregularly distributed cavities and channels containing seawater and gases. Nodules had the same morphology but contained less carbonate. The microbial mats were sampled by using the manned submersible *JAGO* during the R/V *Prof. LOGACHEV* cruise in July 2001 (Table 1, station 55-4). Furthermore, material from a nodule (station 14; 31°58.877′N, 44°46.616′E; depth, 182 m) and material

from a gel within the mat cavities and channels (station 10; 31°59.559′N, 44°46.515′E; depth, 235 m) were used in this study.

DNA extraction, PCR amplification, and clone library construction. Sediment cores from Hydrate Ridge were sectioned into 1-cm layers and deep frozen (−20°C) for DNA extraction at the home laboratory. Total community DNA was directly extracted from 2 g of sediment from station 19–2 (depths, 2 to 4 and 6 to 7 cm) and station 38 (depth, 2 to 6 cm) as described by Zhou et al. (72). The following two primer sets were used for PCR amplification of 16S rRNA genes from extracted chromosomal DNA: (i) primers ARCH20F (33) and Uni1392 (42), which resulted in an almost 1,400-bp product; and (ii) primers ARCH20F and ARCH958R (10), which resulted in a ca. 950-bp product. Both primer sets were used with an annealing temperature of 58°C. PCR products were purified with a QiaQuick PCR purification kit (QIAGEN, Hilden, Germany). Clone libraries in pGEM-T-Easy (Promega, Madison, Wis.) or the TOPO pCR4 vector (Invitrogen, Karlsruhe, Germany) were constructed as described previously (48).

For construction of Black Sea clone libraries, a fresh mat (station 55–4) was cut into the following sections: (i) surface biomass, which was dark gray to black (thickness, ca. 1 to 2 mm; clones having designations beginning with BS-S); (ii) material from the black-to-pink transition zone (ca. 2 to 4 mm below the mat surface; clones having designations beginning with BS-M); and (iii) the interior portion of the mat, which was pink (ca. 4 to 8 mm below the mat surface; clones having designations beginning with BS-R). DNA was extracted with a FASTDNA spin kit for soil (Bio 101 Inc., Carlsbad, Calif.). In addition, two clone libraries were constructed from formaldehyde-fixed samples from station 14 (clones having designations beginning with BS-K) and station 55–4 (clones having designations beginning with BS-SR). Aliquots (1 μl) of fixed cells were directly used for PCR and cloning as described above.

Amplified rRNA gene restriction analysis. Clones known to contain the inserts that were the correct size (ca. 1.4 or 0.95 kb) were screened by amplified rRNA gene restriction analysis in order to identify clones with different inserts. Two restriction enzymes (HaeIII and RsaI) were used for screening as described previously (48).

Sequencing and phylogenetic analysis. *Taq* cycle sequencing of plasmid DNAs from selected clones with vector primers and universal rRNA gene-specific primers was performed by GATC Biotech (Konstanz, Germany) and AGOWA (Berlin, Germany). Sequence data were analyzed with the ARB software package (31). Phylogenetic trees were calculated with sequences from Hydrate Ridge sediments and Black Sea microbial mats together with sequences which are available in the EMBL, GenBank, and DDJB databases by performing parsimony, neighbor-joining, and maximum-likelihood analyses with a subset of 200 nearly full-length sequences (>1,300 bp). Filters which excluded highly variable positions were used. In all cases, general tree topology and clusters were stable (a maximum-likelihood tree is shown in Fig. 1). Partial sequences (<1,300 bp) were inserted into the reconstructed tree by parsimony criteria with global-local optimization with no changes in the overall tree topology.

Quantification and measurement of ANME-2/DSS aggregates. 4′,6′-Diamidino-2-phenylindole staining (DAPI) was used to measure sizes of ANME-2a/ DSS and ANME-2c/DSS aggregates by epifluorescence microscopy of FISH-treated samples (Hydrate Ridge stations 19–2 and 38 [depth, 1 to 2 cm] and Black Sea mats from station 55–4). The numbers of cells in the aggregates were calculated based on the assumptions that the aggregates were completely surrounded by SRB and that both the aggregates and the cells within the aggregates were spheres.

FISH. Subsamples of Hydrate Ridge sediment cores were sliced into 1-cm sections, fixed for 2 to 3 h in 3% formaldehyde, washed twice with 1× phosphate-buffered saline (130 mM NaCl, 10 mM sodium phosphate; pH 7.2), and finally stored in 1× phosphate-buffered saline–ethanol (1:1) at −20°C. A Black Sea microbial mat was fixed with paraformaldehyde, embedded in Tissue Tek OCT compound (Ted Pella Inc., Redding, Calif.), and sectioned with a cryostat (HM505 E; Microm, Walldorf, Germany) as previously described (52). Hybridization and microscopic counting of hybridized and DAPI-stained cells were performed as described previously (55). Means were calculated by using 10 to 40 randomly chosen fields for each filter section, which corresponded to 800 to 1,000

FIG. 1. Phylogenetic tree showing the affiliations of 16S rRNA gene sequences retrieved from Hydrate Ridge sediments and Black Sea microbial mats (boldface type) with selected reference sequences of the domain *Archaea*. Besides cultivated organisms all previously published clone sequences from methane-rich sites are included as references (at least one representative per phylogenetic group). The tree was constructed by using maximum-likelihood analysis in combination with filters excluding highly variable positions in a subset of 200 nearly full-length sequences (>1,300 bp). Partial sequences were inserted into the reconstructed tree by using parsimony criteria with global-local optimization, without allowing changes in the overall tree topology. Probe specificity is indicated by brackets. Bar = 10% estimated sequence divergence.
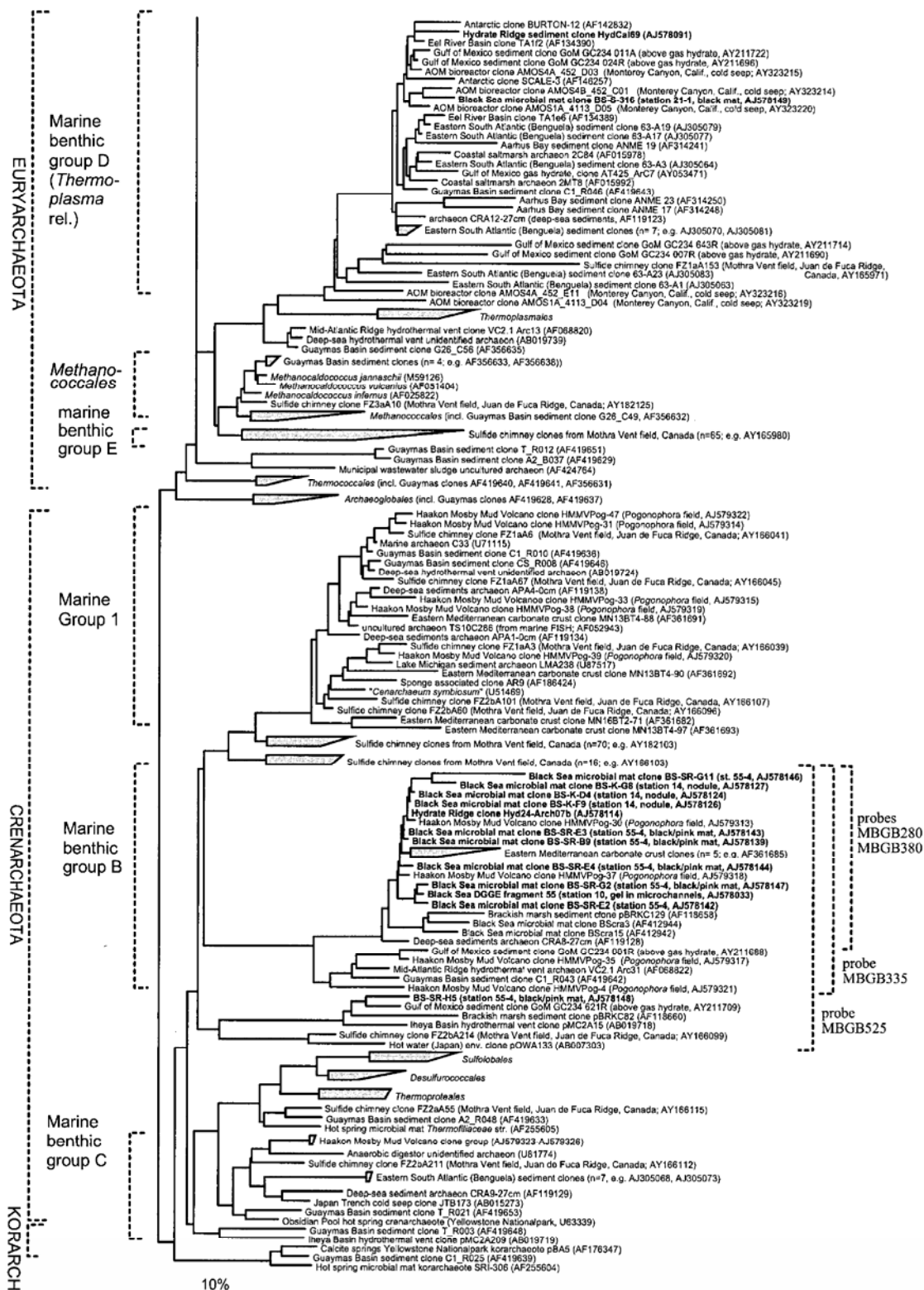
FIG. 1—*Continued*.

471
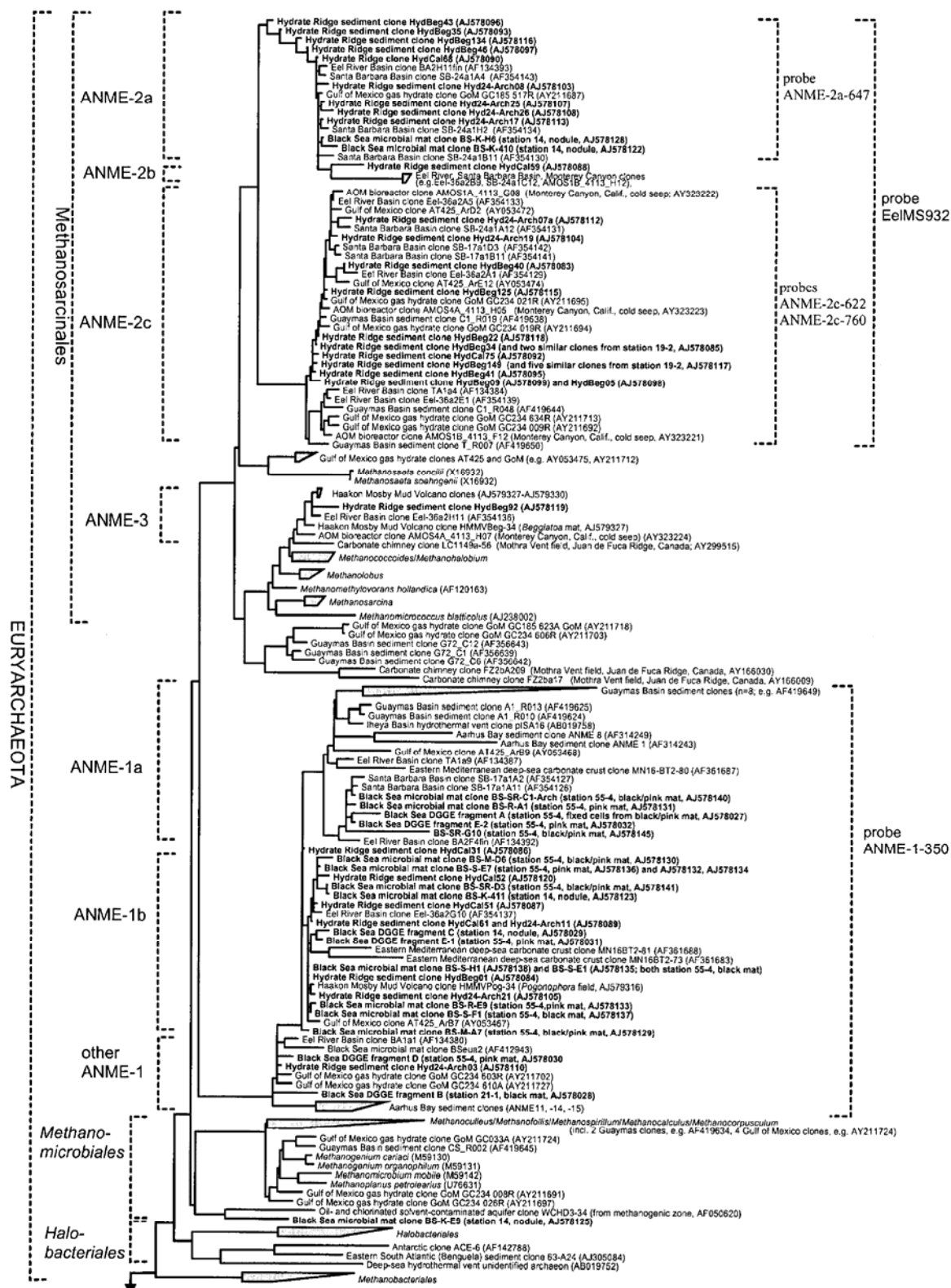
TABLE 2. Oligonucleotide probes used in this study

Probe	Specificity		Sequence (5' to 3')	Position[a]	Formamide concn (%, vol/vol)[b]	Reference
	Group	Taxon				
DSS658	*Desulfosarcina-Desulfococcus*	SRB of *Delta-proteobacteria*	TCC ACT TCC CTC TCC CAT	658–685	60	32
ARCH915	Most archaea	*Archaea*	GTG CTC CCC CGC CAA TTC CT	915–934	35	2
ANME-1-350	ANME-1	*Euryarchaeota*	AGT TTT CGC GCC TGA TGC	350–367	40	7
EeIMS932	ANME-2	*Euryarchaeota*	AGC TCC ACC CGT TGT AGT	932–949	65	7
ANME-2a-647	ANME-2a	*Euryarchaeota*	TCT TCC GGT CCC AAG CCT	647–664	50	This study
ANME-2c-622	ANME-2c	*Euryarchaeota*	CCC TTG GCA GTC TGA TTG	622–639	50	This study
ANME-2c-760	ANME-2c	*Euryarchaeota*	CGC CCC CAG CTT TCG TCC	760–777	60	This study
MBGB-280	Marine benthic group B	*Crenarchaeota*	TCA CGG CCC CTA TCG ATT	280–297	50	This study
MBGB-335	Marine benthic group B	*Crenarchaeota*	TGC GCC TCG TAA GGC CTG	335–352	50–60	This study
MBGB-380	Marine benthic group B	*Crenarchaeota*	GTA ACC CCG TCA CAC TTT	380–397	50	This study
MBGB-525[c]	Marine benthic group B	*Crenarchaeota*	AGA GCT GGT TTT ACC GCG	525–542	40–50	This study

[a] Position in the 16S rRNA of *Escherichia coli*.
[b] Formamide concentration in the hybridization buffer.
[c] Probe MBGB-525 also targets several sequences from korarchaeota and other archaea due to a single terminal mismatch.

DAPI-stained cells. Cy3-, Cy5-, and fluorescein-monolabeled oligonucleotides were purchased from ThermoHybaid (Ulm, Germany). Probes and formamide concentrations used in this study are listed in Table 2. The background signals of samples, observed with the nonsense probe NON338, were negligible (<0.1%).

Scanning electron microscopy (SEM). Black Sea microbial mat sections (treated as described above for FISH) were directly placed on aluminum specimen mounts. The OCT compound was washed out with sterile water three times for 3 to 5 min each time, and mat sections were dehydrated by covering the samples with 50, 80, and 96% ethanol for 3 min each. Air-dried samples were gold sputtered with a BAL-TEC SCD005 sputter coater for 100 s at 30 mA and were viewed with a Hitachi S-3200N scanning electron microscope operating at 20 kV.

Nucleotide sequence accession numbers. The nucleotide sequence data reported in this paper have been deposited in the EMBL, GenBank, and DDBJ nucleotide sequence database under accession numbers AJ578027 to AJ578033 and AJ578083 to AJ578150.

RESULTS

Archaeal diversity in Hydrate Ridge sediments and Black Sea microbial mats. Compared to the previously discovered high bacterial diversity at methane seeps (6, 26, 28, 39, 58), the archaeal diversity was relatively low in the Hydrate Ridge sediments and Black Sea microbial mats. Seven different phylogenetic groups were detected; five of these groups belong to the *Euryarchaeota*, and two belong to the *Crenarchaeota* (Table 3 and Fig. 1). Archaea belonging to ANME-2 dominated the libraries from Hydrate Ridge sediments and accounted for 76% (*n* = 82) of all archaeal clones. These archaea could be assigned to subgroups ANME-2a (13%) and ANME-2c (62%). In contrast, only low numbers of ANME-2 representatives were retrieved from Black Sea microbial mats (station 14; *n* = 2). Both ANME-2 sequences belonged to ANME-2a. The levels of sequence similarity to cultivated species were in all cases less than 91%. However, the levels of similarity to sequences from uncultivated organisms were high and often exceeded 99%. Together with environmental sequences from the Eel River and the Santa Barbara Basin (21, 39), from Monterey Canyon (18), from the Guaymas Basin (58), and from the Gulf

TABLE 3. Phylogenetic affiliations of 16S rRNA gene clones retrieved from Hydrate Ridge sediments and Black Sea microbial mats

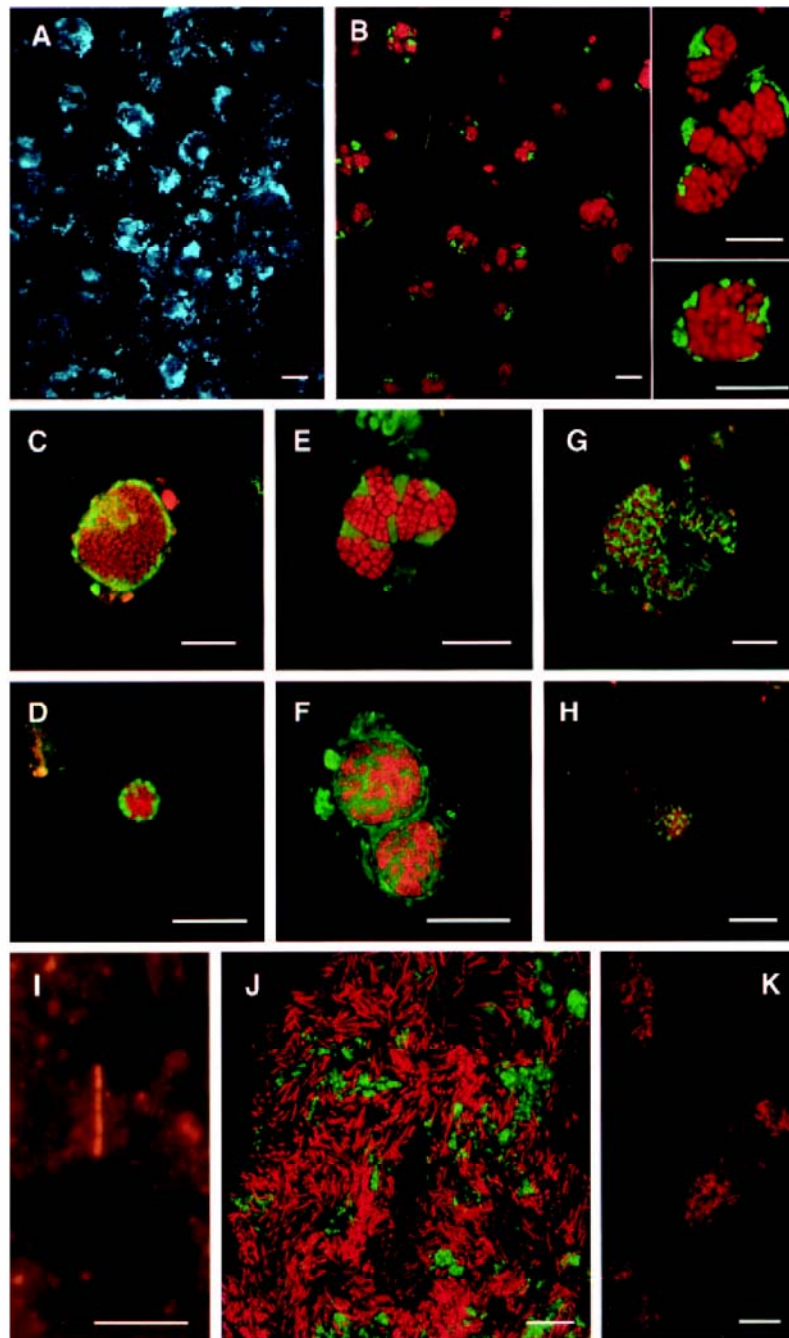| Phylogenetic group	No. of clones							
	Hydrate Ridge			Black Sea microbial mat				
	Beggiatoa mat (station 19-2)	*Beggiatoa* mat (station 19-2)	*Calyptogena* field (station 38-1)	PCR from extracted DNA			PCR from fixed cells	
				Station 55-4			Station 55-4 (black/pink)	Station 14 (nodule)
	2–4 cm	6–7 cm	2–6 cm	Black	Black/pink	Pink		
Euryarchaeota								
ANME-1a							13	1
ANME-1b	4	3	14	29	25	32	8	2
ANME-1 unaffiliated			1					
ANME-2a	7	5	2					2
ANME-2c	20	46	1					
ANME-2 unaffiliated			1					
ANME-3		3						
Methanomicrobiales								1
Marine benthic group D			1					
Crenarchaeota								
Marine benthic group B							30	9
Unaffiliated							3	
Total no. of clones per library	31	57	20	29	25	33	21	6

FIG. 2. Single cells and cell aggregates of ANME-1 and ANME-2 archaea in sediments from Hydrate Ridge sediments and thin sections of Black Sea microbial mats, visualized by FISH. Scale bars = 10 μm. Panels A to H, J, and K are confocal laser scanning micrographs. Panel I is a regular epifluorescence micrograph. (A) DAPI staining showing the embedded aggregates in the bulk biomass in Black Sea microbial mats. (B) Corresponding FISH image of ANME-2/DSS aggregates (probe ANME-2c-760 labeled with Cy5 [red] and probe DSS658 labeled with Cy3 [green]). DSS cells surrounded the archaea partially or completely. In many aggregates the ANME cells had only a few or no DSS partners. (C to F) Different types of ANME-2c/DSS aggregates (probe ANME-2c-622 labeled with Cy3 [red] and probe DSS658 labeled with Cy5 [green]), including aggregates with an inner core of archaea surrounded by a shell of SRB (shell type). (G and H) ANME-2a/DSS aggregates (probe ANME-2a-647 labeled with Cy3 [red] and probe DSS658 labeled with Cy5) from *Beggiatoa* site station 38 (depth, 1 to 2 cm), showing cell-to-cell association of the partners (mixed type). (I) ANME-1 cells stained with Cy3-labeled probe ANME-1-350 in Hydrate Ridge sediments (*Beggiatoa* site station 19–2 [depth, 5 to 6 cm]) (J) Color overlay of ANME-1 cells targeted with probe ANME-1-350 labeled with Cy3 (red) and SRB of the *Desulfosarcina-Desulfococcus* branch labeled with fluorescein (probe DSS658; green) in a Black Sea mat section. (K) Marine benthic group B *Crenarchaeota* targeted with probe MBGB-380 labeled with Cy3 in a Black Sea mat section.

473

184
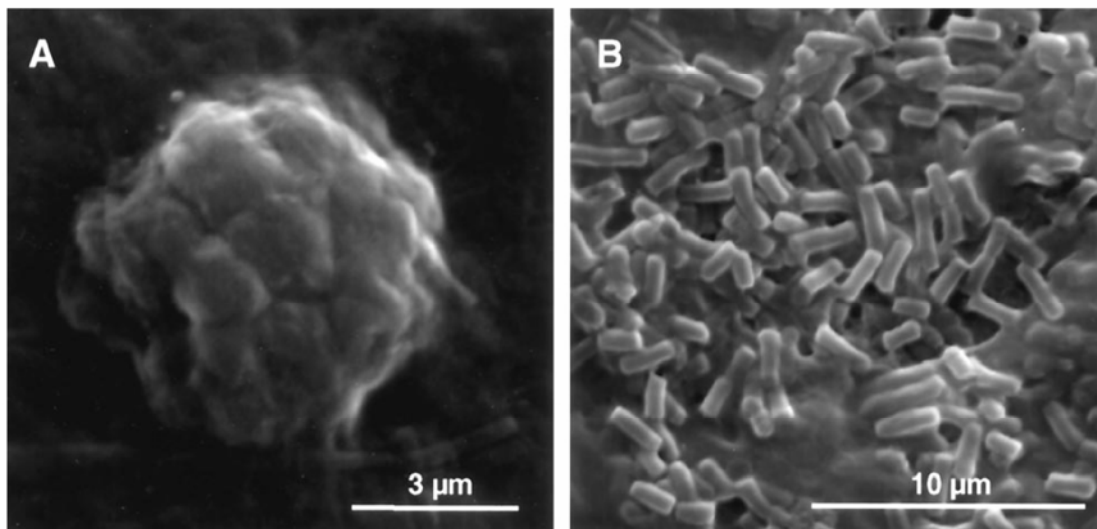
FIG. 3. ANME-1 archaea and ANME-2/DSS aggregates in the Black Sea microbial mat: SEM images of a gold-sputtered formaldehyde-fixed mat section. (A) ANME-2/DSS aggregate, showing the typical spherical structure. (B) Cylindrical ANME-1 cells.

of Mexico (28, 35), ANME-2c and ANME-2a form a clade specific for AOM sites. Today, ANME-2b consists only of sequences from Eel River and Santa Barbara Basin sediment (39), as well as Monterey Canyon (18).

The second archaeal group mediating AOM is ANME-1 (34, 41), which is distantly related to the *Methanosarcinales* and *Methanomicrobiales*. ANME-1 can be divided into two subgroups, ANME-1a and ANME-1b, and other sequences which cannot be affiliated with these subgroups (Fig. 1). Like the subgroups of ANME-2, both of the ANME-1 subgroups do not contain any cultivated species but comprise only uncultivated species from methane seeps with levels of similarity up to 99% (21, 28, 39, 58, 62) (GenBank accession numbers AY593257 to AY593349, AF357889 to AF361694, AJ704631 to AJ704652, and AJ579313 to AJ579330 [http://www.ncbi.nlm.nih.gov]). Sequences belonging to ANME-1 were most abundant in Black Sea clone libraries (71% of all archaeal clones; $n = 111$) (Fig. 1 and Table 3). The major portion was affiliated with ANME-1b (61%), and only a minor fraction (10%) belonged to ANME-1a. At Hydrate Ridge ANME-1 sequences were the second most abundant phylotype recovered; they accounted for 20% of the sequences, all of which were affiliated with ANME-1b.

Few sequences from Hydrate Ridge ($n = 3$) could be affiliated with a third seep-specific clade, ANME-3. This group is phylogenetically closely related to methanogenic bacteria belonging to the *Methanococcoides* (94 to 96%). Besides Hydrate Ridge sequences this group comprises mainly sequences from Haakon Mosby Mud Volcano (GenBank accession numbers AJ704631 to AJ704652 and AJ579313 to AJ579330 [http://www.ncbi.nlm.nih.gov]) and some sequences from the Eel River Basin (39), from Monterey Canyon (18), and from a sulfide chimney from the Mothra Vent Field in Canada (53). A single sequence from the Black Sea was related to the *Methanomicrobiales*, and another sequence from Hydrate Ridge was af-

filiated with the *Euryarchaeota* of marine benthic group D (70), which is related to the order *Thermoplasmales*.

Marine benthic group B (MBGB) belonging to the *Crenarchaeota* was abundant in the clone libraries constructed by using fixed cells from Black Sea mat stations 55–4 (56%; $n = 30$) and 14 (60%; $n = 9$). None of the members of this group have been cultivated yet. The diversity within the group is high; the levels of sequence similarity are between 82 and 99%.

ANME-2 abundance. Hydrate Ridge sediments were dominated by high numbers of ANME-2/DSS aggregates, which accounted for more than 90% of the total cells (i.e., aggregated cells plus single archaea and bacteria [7, 65]). Single ANME-2 cells accounted for only around 1% of the total cells, and this value did not vary significantly with depth (data not shown). We rarely detected aggregated ANME-2 cell clusters without any bacterial partner. These aggregates were smaller than average aggregates (7) and consisted of 4 to 36 cells. At the *Acharax* stations no single ANME-2 cells and only a few aggregated ANME-2 cells were found.

ANME-2 cells were also detected in Black Sea microbial mats (Fig. 2A and B); however, they were limited to microenvironments in regions that were 3 to 6 mm below the mat surface. Like the cells at Hydrate Ridge, the ANME-2 cells formed spherical aggregates associated with SRB belonging to the *Desulfococcus-Desulfosarcina* branch (Fig. 3B). SEM analysis showed high levels of these aggregates (Fig. 3A) restricted to specific areas of the mat section. In these areas almost no cylindrical ANME-1 cells were detected. An average ANME-2/DSS aggregate in the Black Sea mat consisted of an inner core of about 100 coccoid archaeal cells, similar to the Hydrate Ridge consortia (7). However, the archaeal cells were each 1.2 to 1.4 μm in diameter and thus substantially larger than those at Hydrate Ridge. The Black Sea aggregates were only partially surrounded by *Desulfosarcina-Desulfococcus* cells (diameter, 1 μm). The diameters of 60 ANME-2/DSS aggregates from the
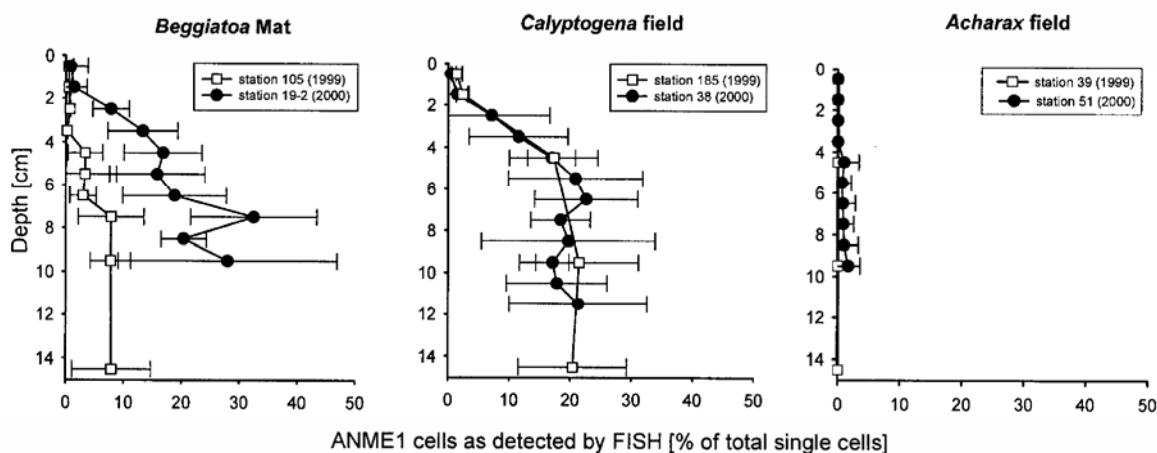
FIG. 4. Detection and quantification of ANME-1 cells in Hydrate Ridge sediments by FISH.

Black Sea ranged from 4 to 20 µm, and the average was 8.3 ± 4.0 µm; hence, these aggregates were significantly larger than the average consortium at Hydrate Ridge (diameter, ca. 3 µm [7, 26]). We also detected a few aggregates which seemed to have a bacterial partner other than DSS. A minimum of three ANME-2 cells together were observed, and a relatively large percentage of the ANME-2 aggregates did not have any tightly associated partner (ca. 10%). In total, we estimated that ANME-2 cells accounted for 5% of the total cells in the 3- to 6-mm subsurface mat horizons in which they were detected (ca. 1×10^{10} cells cm of mat^{-3}). For the total mat they were insignificant in terms of biomass (<1%).

ANME-2 subgroup detection. The ANME-2 cluster can be divided into three subgroups, ANME-2a, ANME-2b, and ANME-2c (39). To study the distribution and abundance of these subgroups, we developed several new oligonucleotide probes, one probe specific for ANME-2a (ANME-2a-647) and two probes specific for ANME-2c (ANME-2c-622 and ANME-2c-760). No probe was developed for ANME-2b since we did not obtain ANME-2b sequences from our samples. Sequences belonging to ANME-2c had at least four mismatches with the probe specific for ANME-2a; sequences belonging to ANME-2a had at least five mismatches with probe ANME-2c-622 and two mismatches with probe ANME-2c-760 (one central mismatch and one terminal mismatch). In sections from Black Sea microbial mats (station 55–4) only cells belonging to ANME-2c could be detected. ANME-2a cells were not detected in the sections; however, due to the great complexity of the mat they may have occurred in other regions.

In Hydrate Ridge sediments two different types of ANME-2/DSS aggregates were detected. At the *Beggiatoa* sites ANME-2a/DSS aggregates were the most abundant aggregates, and they accounted for ca. 80% of all aggregates at station 19–2 (depth, 1 to 2 cm) and 45% of all aggregates at station 105 (depth, 1 to 2 cm). At both *Calyptogena* sites (stations 38 and 185) ANME-2a/DSS aggregates accounted for only ca. 20% of all aggregates (depth, 1 to 2 cm). At these sites, ANME-2c/DSS aggregates were the most abundant aggre-

gates, and they accounted for 75% of the aggregates at station 38 and 80% of the aggregates at station 185. At the *Beggiatoa* sites only 16% (station 19–2) and 25% (station 105–1) of the total ANME-2/DSS aggregates belonged to ANME-2c. In addition to the difference in phylogenetic origin, the two populations could be distinguished from each other by the morphology of the aggregates which they formed. The ANME-2c/DSS aggregates represented the common spherical type with an inner archaeal core which was partially or fully surrounded by an outer shelf of SRB (Fig. 2C and F) (referred to as the shell type below). In the shell type, sometimes the SRB cells grew into the inner ANME-2c core colony, but in general they were not completely mixed with the archaeal cells. In contrast, in the ANME-2a/DSS aggregates the SRB and archaea were completely mixed, and the resulting aggregates were not always spherical (Fig. 2G and H); below we refer to these consortia as the mixed type. Only a very few ANME-2a/DSS aggregates which were the shell type were detected.

ANME-1 abundance. The ANME-1 cells were cylindrical and were, like ANME-2 cells, autofluorescent under UV light, a feature typical of methanogenic archaea containing coenzyme F_{420}. The length varied between 1.5 and 3 µm, and the diameter was about 0.6 µm. At Hydrate Ridge these cells mostly occurred as single cells without any directly associated bacterial or archaeal partner. However, they often formed long chains of 2 to 10 cells (Fig. 2I). We rarely detected spherically aggregated ANME-1 cells. At the *Beggiatoa* and *Calyptogena* sites at Hydrate Ridge the FISH detection rates for ANME-1 cells were comparable and increased strongly with depth (Fig. 4). In the surface layers (depth, 0 to 2 cm) the ANME-1 cells accounted for between 1 and 2% of the total single cells (≪1% of the total cells). At the *Beggiatoa* sites the percentage of ANME-1 cells strongly increased to 8% of the total DAPI-detected single cells at a depth of 7 to 15 cm at station 105 and to 20 to 33% of the total DAPI-detected single cells at a depth of 7 to 10 cm at station 19–2. These percentages correspond to absolute ANME-1 cell numbers of 1×10^8 and 5×10^8 cells cm of sediment^{-3}, respectively. In samples from *Calyptogena* sites

(stations 185 and 38) the ANME-1 abundance was comparable; the highest percentages were 21 to 23% at a depth of 6 to 12 cm (up to 1.0×10^9 cells cm^{-3}). The ANME-1 abundance at the *Acharax* sites ranged between 0 and 2% of the single cells in the upper 15 cm of the sediment. On the basis of the total cell numbers, including the cells in the aggregates (7, 65), ANME-1 comprised up to 5% of all archaea throughout the sediment column.

In contrast to the Hydrate Ridge sediments, the Black Sea microbial mats (stations 14 and 55–4) were clearly dominated by ANME-1 cells (34). These cells were highly active, as indicated by a bright FISH signal, and had the same morphology as the cells at Hydrate Ridge (Fig. 2J). SEM analysis of mat sections revealed very abundant cylindrical microorganisms embedded in a thick extracellular polysaccharide matrix (Fig. 3B). On average, throughout the mat ANME-1 cells accounted for 20% of the total cells (ca. 4×10^{10} cells cm of mat^{-3}); the maximum was ca. 50% (ca. 9×10^{10} cells cm of mat^{-3}) in the samples analyzed here. Values up to 70% were reported for similar samples analyzed in a previous study (34).

Detection of MBGB. Many clone sequences retrieved from the Black Sea microbial mats and other methane seeps were affiliated with *Crenarchaeota* belonging to MBGB (Fig. 1). To quantify the in situ abundance of these clones, we designed four FISH probes specific for the Black Sea sequences and several other sequences in this cluster. With these probes very small cocci (diameter, 0.2 to 0.4 μm) could be detected in the Black Sea mats (Fig. 2K). To our knowledge, this is the first in situ visualization of this group. The organisms occurred mostly in large clusters and were abundant in regions with lower cell densities (e.g., the channels through the mats). Clear signals were available but did not allow quantification because of the very small size of the cells. DAPI signals were also hardly detectable. However, dual hybridization of mat sections with the MBGB-specific probes in combination with the general archaeal probe ARCH915 showed a clear overlay of the two signals. In Hydrate Ridge sediments at *Calyptogena* site 38 (depths, 1 to 2 and 7 to 8 cm) very few cocci (<1%) showed weak signals with the new Cy3-monolabeled MBGB probes. Tourova et al. proposed that these organisms might be a new form of sulfate reducers (64). The metabolism of most *Crenarchaeota* other than the cultivated thermophilic extremophiles is not known yet (11, 25, 51). Their high abundance and association with seeps might indicate that the MBGB are also involved in AOM or may use specific carbon intermediates generated from AOM. However, so far, based on isotopic signatures of biomarker lipids there is no clear evidence for involvement of *Crenarchaeota* in AOM (51).

DISCUSSION

Diversity of methanotrophic guilds at cold seeps. The overall archaeal diversity in the Black Sea and Hydrate Ridge clone libraries was low; these libraries contained only five and four phylogenetic groups, respectively. Similar low diversities (only two to five major groups) have been reported for all but one of the methane seeps investigated so far (1, 6, 21, 28, 35, 39, 62) (GenBank accession numbers AY593257 to AY593349 and AF357889 to AF361694 [http://www.ncbi.nlm.nih.gov]). The archaeal community of hydrothermally active sediments of

Guaymas Basin (58) consists of 13 phylogenetic lineages. At this site, a variety of methanogens and other thermophilic archaea not related to ANME groups have been isolated. However, AOM appeared not be the dominant carbon cycling process in the Guaymas sediments (24), in contrast to the other methane seeps.

Compared to the overall low archaeal diversity at cold seeps, the 16S rRNA diversity within and between the individual ANME groups appears to be relatively high. ANME-1 and ANME-2 show <85% similarity to each other and hence are two different lineages. The phylogenetic distance is so large that members of ANME-1 and ANME-2 certainly belong to different orders or families, which, however, have apparently similar physiological properties. Based on 16S rRNA gene similarity values of <96%, ANME-1a and ANME-1b contain different species or even genera. The same applies to the ANME-2 subgroups ANME-2a and ANME-2c.

Co-occurrence of methanotrophic groups. ANME-1 and ANME-2 co-occur in Hydrate Ridge sediments and in Black Sea microbial mats, as well as in many other methane-rich habitats. In situ quantification of these groups, however, showed that they were present at very different levels, indicating that there were different mechanisms of selection of the different groups by the habitat. ANME-1 dominated the Black Sea microbial mats (40 to 50% of the total cells), and ANME-2/DSS aggregates were restricted to small microenvironments and accounted for only 1% of the total cells. In contrast, ANME-2/DSS aggregates dominated the Hydrate Ridge sediments (>90% of the total cells), and ANME-1 cells were detected only in deeper sediment layers and the number of cells was at least 1 order of magnitude less. The environmental conditions at the Hydrate Ridge and Black Sea habitats were compared (Table 1) to identify possible factors that determined niches for ANME-1 and ANME-2. At both sites excess methane was available as the main carbon and energy source (the in situ concentrations were 10 to 60 and 20 mM). Sulfate at concentrations of >2 mM was found to be the only known electron acceptor in the horizons with abundant ANME biomass. Hence, the availability of an electron donor and an electron acceptor obviously did not directly exert selective pressure. The parameter that differed the most between the two locations is oxygen. The Black Sea microbial mats thrive in a permanently anoxic habitat because oxygen is depleted in the subsurface waters beneath a depth of ca. 120 m. In contrast, the bottom waters at Hydrate Ridge are oxic, and the surface sediments are sporadically flushed with oxygen by bottom water currents, bioturbation, and gas ebullition (67). Thus, ANME-1 may be more sensitive to oxygen than ANME-2. This hypothesis is supported by the very low ANME-1 abundance (≪1% of the total cells) in the surface sediments at Hydrate Ridge and the increase in the abundance with depth to 5% of the total cells despite the concurrent decrease in sulfate availability and the increase in sulfide concentrations. Furthermore, ANME-1 was completely absent in the oxygenated surface sediments at the *Acharax* site, although ANME-2/DSS aggregates were present in these layers (26).

Environmental niches of the ANME-2a/DSS and ANME-2c/DSS aggregates. ANME-2a and ANME-2c co-occur in Hydrate Ridge sediments; however, the abundance varies greatly on a meter to decimeter scale according to the type of chemo-

synthetic community (the sulfide-oxidizing bacterium *Beggiatoa* or the symbiotic clam *Calyptogena*) populating the surface sediments. Both sites have steep gradients of pore water sulfate (7, 12), high hydrogen sulfide concentrations (50), and high rates of AOM and sulfate reduction (7, 65) (Table 1). However, the fluid flow and methane fluxes from the seafloor are substantially greater but also more variable at *Beggiatoa* sites than at *Calyptogena* sites (50, 63, 68). At *Beggiatoa* sites oxygen had a maximum penetration of a few millimeters. In contrast, at *Calyptogena* sites oxygen penetrated deeper into the sediments due to the bioturbating activity of the clams, which live with their feet in the sulfide-rich zones of the sediment. The dominance of ANME-2a/DSS and ANME-2c/DSS aggregates is clearly linked with a specific type of chemosynthetic communities populating the surface sediment for reasons that are not known yet.

Biogeography of the anaerobic methanotrophs (ANME). Methanotrophic archaea were first detected in sediments of cold seeps of the northeast Pacific continental margin, such as the sediments from Eel River (21, 39, 41) and Hydrate Ridge (7). The data for lipid biomarker and DNA signatures indicate the global presence of these archaea in anoxic methane-rich sediments. So far, ANME signatures have been detected at all methane seeps investigated, including seeps in the north Pacific Ocean, north and south Atlantic Ocean, Mediterranean Sea, Black Sea, and North Sea (1, 7, 13, 14, 18, 21, 22, 26, 28, 34, 35, 40, 41, 43, 44, 53, 58, 60–62). Furthermore, ANME groups have also been found in the methane-sulfate transition zones of different coastal environments (23a, 66). An analysis of the current data set for the 16S rRNA genes of the ANME groups indicates that their occurrence is limited to the upper few meters of subsurface sediments, as no genes have been retrieved from any deep biosphere core yet. Since so far the presence of ANME-1, ANME-1, and ANME-3 is restricted to anoxic, methane-rich, and sulfate-containing sediments and the oxic bottom waters of the ocean present a barrier to their distribution, these groups are an interesting case for the study of microbial biogeography, as are all extremophiles. The occurrence of biogeographical trends in the distribution of microorganisms is debated (16, 17, 45, 71) because such trends contradict a basic paradigm of microbial ecology, that everything is everywhere—the environment selects (3, 5). Based on 16S rRNA genes as the evolutionary marker, the present data do not indicate the biogeography of ANME-1, ANME-1, and ANME-3 or subclusters of these groups, in contrast to various thermophilic microorganisms (45, 71). Other globally abundant groups of microbes, such as *Alphaproteobacteria* belonging to the SAR11 clade (36, 47) or the *Roseobacter* clade-affiliated cluster (54), do not have a biogeography based on oceanic regions or latitudes. Instead, as observed in this study, clusters appear to be formed by subgroups, which are specifically adapted to certain niches (e.g., water depth, light availability, and temperature). However, these results may be related to insufficient phylogenetic resolution of 16S rRNA sequences. Recently, Whitaker et al. (71) and Papke et al. (45) used high-resolution multilocus sequence analysis to show that the genetic distances between thermophilic prokaryotes having almost identical 16S rRNAs increased proportionally with geographic distance. These findings revealed that populations are isolated from one another by geographic barriers and have

diverged over the course of their recent evolutionary history. Besides multilocus sequence analysis, other markers, such as functional genes specific for methanotrophs, or simply a clear increase in the size of the ANME 16S rRNA data set to several thousand sequences could be used to address the biogeography of ANME.

Conclusions. A comparison of 16S rRNA gene sequences showed the ubiquitous presence of methanotrophic archaea in almost all environments investigated so far independent of the in situ temperature, depth, pressure, and methane and sulfate concentrations. ANME-1 and ANME-2, as well as their phylogenetic subgroups, co-occur at all seep sites that have been investigated quantitatively; however, microscopic analysis of the distribution of the subgroups has revealed the dominance of certain types within microniches in the environments. To single out the factors responsible for the selection of certain ecotypes of methanotrophs, environmental conditions and geochemical gradients need to be analyzed in situ with a high resolution relevant to the scale of the microenvironments detected in this study. This would require parallel investigations with microsensors in the field or experimental studies in flowthrough microcosms.

REFERENCES

1. **Aloisi, G., I. Bouloubassi, S. K. Heijs, R. D. Pancost, C. Pierre, J. S. S. Damsté, J. C. Gottschal, L. J. Forney, and J.-M. Rouchy.** 2002. CH₄-consuming microorganisms and the formation of carbonate crusts at cold seeps. Earth Planet. Sci. Lett. **203:**195–203.
2. **Amann, R. I., B. J. Binder, R. J. Olson, S. W. Chisholm, R. Devereux, and D. A. Stahl.** 1990. Combination of 16S rRNA-targeted oligonucleotide probes with flow cytometry for analyzing mixed microbial populations. Appl. Environ. Microbiol. **56:**1919–1925.
3. **Baas-Becking, L. G. M.** 1934. Geobiologie of Inleiding Tot de Milieukunde. In W. P. van Stockum and N. V. Zoon (ed.), Diligentia Wetensch. serie 18/19. van Stockum's Gravenhange, The Hague, The Netherlands.
4. **Barry, J. P., R. E. Kochevar, and C. H. Baxter.** 1997. The influence of pore-water chemistry and physiology in the distribution of vesicomyid clam at cold seeps in Monterey Bay: implications for patterns of chemosynthetic community organization. Limnol. Oceanogr. **42:**318–328.
5. **Beijerinck, M. W.** 1913. De infusies en de ontdekking der backteriën. In Jaarboek van de Koninklijke Akademie v. Wetenschappen. Müller, Amsterdam, The Netherlands.
6. **Bidle, K. A., M. Kastner, and D. H. Bartlett.** 1999. A phylogenetic analysis of microbial communities associated with methane hydrate containing marine fluids and sediments in the Cascadia margin (ODP8 site 892B). FEMS Microbiol. Lett. **177:**101–108.
7. **Boetius, A., K. Ravenschlag, C. Schubert, D. Rickert, F. Widdel, A. Gieseke, R. Amann, B. B. Jørgensen, U. Witte, and O. Pfannkuche.** 2000. A marine microbial consortium apparently mediating anaerobic oxidation of methane. Nature **407:**623–626.
8. **Boetius, A., and E. Suess.** 2004. Hydrate Ridge: a natural laboratory for the

study of microbial life fueled by methane from near-surface gas hydrates. Chem. Geol. **205**:291–310.

9. **Bohrmann, G., P. Linke, P. Suess, and O. Pfannkuche.** 2000. R.V. SONNE cruise report SO143: TECFLUX-I (June 29-September 6, 1999; Honolulu-Astoria-San Diego). GEOMAR Rep. **93**:217.

10. **DeLong, E. F.** 1992. Archaea in coastal marine environments. Proc. Natl. Acad. Sci. USA **89**:5685–5689.

11. **DeLong, E. F.** 1998. Everything in moderation: Archaea as 'non-extremo-philes.' Curr. Opin. Genet. Dev. **8**:649–654.

12. **Elvert, M., J. Greinert, E. Suess, and M. J. Whiticar.** 2001. Carbon isotopes of biomarkers derived from methane-oxidizing microbes at Hydrate Ridge, Cascadia convergent margin, p. 115–129. *In* C. K. Paull and W. P. Dillon (ed.), Natural gas hydrates: occurrence, distribution, and dynamics, vol. 124. American Geophysical Union, Washington, D.C.

13. **Elvert, M., E. Suess, J. Greinert, and M. J. Whiticar.** 2000. Archaea mediating anaerobic methane oxidation in deep-sea sediments at cold seeps of the eastern Aleutian subduction zone. Org. Geochem. **31**:1175–1187.

14. **Elvert, M., E. Suess, and M. J. Whiticar.** 1999. Anaerobic methane oxidation associated with marine gas hydrates: superlight C-isotopes from saturated and unsaturated C^{20} and C_{25} irregular isoprenoids. Naturwissenschaften **86**:295–300.

15. **Fenchel, T.** 2003. Biogeography for bacteria. Science **301**:925–926.

16. **Fenchel, T.** 2002. Microbial behavior in a heterogeneous world. Science **296**:1068–1071.

17. **Finlay, B. J.** 2002. Global dispersal of free-living microbial eukaryote species. Science **296**:1061–1063.

18. **Girguis, P. R., V. J. Orphan, S. J. Hallam, and E. F. DeLong.** 2003. Growth and methane oxidation rates of anaerobic methanotrophic archaea in a continuous-flow bioreactor. Appl. Environ. Microbiol. **69**:5472–5482.

19. **Hallam, S. J., P. R. Girguis, C. M. Preston, P. M. Richardson, and E. F. DeLong.** 2003. Identification of methyl coenzyme M reductase A (*mcrA*) genes associated with methane-oxidizing archaea. Appl. Environ. Microbiol. **69**:5483–5491.

20. **Hansen, L. B., K. Finster, H. Fossing, and N. Iversen.** 1998. Anaerobic methane oxidation in sulfate depleted sediments: effects of sulfate and molybdate additions. Aquat. Microb. Ecol. **14**:195–204.

21. **Hinrichs, K. U., J. M. Hayes, S. P. Sylva, P. G. Brewer, and E. F. DeLong.** 1999. Methane-consuming archaebacteria in marine sediments. Nature **398**:802–805.

22. **Hinrichs, K.-U., and A. Boetius.** 2002. The anaerobic oxidation of methane: new insights in microbial ecology and biogeochemistry, p. 457–477. *In* G. Wefer, D. Billett, D. Hebbeln, B. B. Jørgensen, M. Schlüter, and T. Van Weering (ed.), Ocean margin systems. Springer-Verlag, Berlin, Germany.

23. **Hoehler, T. M., M. J. Alperin, D. B. Albert, and C. S. Martens.** 1994. Field and laboratory studies of methane oxidation in an anoxic marine sediment: evidence for a methanogen-sulfate reducer consortium. Glob. Biogeochem. Cycles **8**:451–463.

23a.**Ishii, K., M. Mußmann, B. J. MacGregor, and R. Amann.** 2004. An improved fluorescence in situ hybridization protocol for the identification of bacteria and archaea in marine sediments. FEMS Microbiol. Ecol. **50**:203–212.

24. **Kallmeyer, J., and A. Boetius.** 2004. Effects of temperature and pressure on sulfate reduction and anaerobic oxidation of methane in hydrothermal sediments of Guaymas Basin. Appl. Environ. Microbiol. **70**:1231–1233.

25. **Karner, M. B., E. F. DeLong, and D. M. Karl.** 2001. Archaeal dominance in the mesopelagic zone of the Pacific Ocean. Nature **409**:507–510.

26. **Knittel, K., A. Boetius, A. Lemke, H. Eilers, K. Lochte, O. Pfannkuche, P. Linke, and R. Amann.** 2003. Activity, distribution, and diversity of sulfate reducers and other bacteria in sediments above gas hydrate (Cascadia Margin, OR). Geomicrobiol. J. **20**:269–294.

27. **Krüger, M., A. Meyerdierks, F. O. Glöckner, R. Amann, F. Widdel, M. Kube, R. Reinhardt, J. Kahnt, R. Böcher, R. K. Thauer, and S. Shima.** 2003. A conspicuous nickel protein in microbial mats that oxidize methane anaerobically. Nature **426**:878–881.

28. **Lanoil, B. D., R. Sassen, M. T. La Duc, S. T. Sweet, and K. H. Nealson.** 2001. *Bacteria* and *Archaea* physically associated with Gulf of Mexico gas hydrates. Appl. Environ. Microbiol. **67**:5143–5153.

29. **Lein, A. Y., M. V. Ivanov, N. V. Pimenov, and M. B. Gulin.** 2002. Geochemical peculiarities of the carbonate constructions formed during microbial oxidation of methane under anaerobic conditions. Mikrobiologiya **71**:78–90. (In Russian.)

30. **Linke, P., and E. Suess.** 2001. R.V. SONNE cruise report SO148 TEC-FLUX-II-2000 (Victoria-Victoria; July 20-August 12, 2000). GEOMAR Rep. **98**:122.

31. **Ludwig, W., O. Strunk, R. Westram, L. Richter, H. Meier, Yadhukumar, A. Buchner, T. Lai, S. Steppi, G. Jobb, W. Förster, I. Brettske, S. Gerber, A. W. Ginhart, O. Gross, S. Grumann, S. Hermann, R. Jost, A. König, T. Liss, R. Lüßmann, M. May, B. Nonhoff, B. Reichel, R. Strehlow, A. Stamatakis, N. Stuckmann, A. Vilbig, M. Lenke, T. Ludwig, A. Bode, and K.-H. Schleifer.** 2004. ARB: a software environment for sequence data. Nucleic Acids Res. **32**:1363–1371.

32. **Manz, W., M. Eisenbrecher, T. R. Neu, and U. Szewzyk.** 1998. Abundance and spatial organization of gram negative sulfate-reducing bacteria in acti-

vated sludge investigated by in situ probing with specific 16S rRNA targeted oligonucleotides. FEMS Microbiol. Ecol. **25**:43–61.

33. **Massana, R., A. E. Murray, C. M. Preston, and E. F. DeLong.** 1997. Vertical distribution and phylogenetic characterization of marine planktonic archaea in the Santa Barbara Channel. Appl. Environ. Microbiol. **63**:50–56.

34. **Michaelis, W., R. Seifert, K. Nauhaus, T. Treude, V. Thiel, M. Blumenberg, K. Knittel, A. Gieseke, K. Peterknecht, T. Pape, A. Boetius, R. Amann, B. B. Jørgensen, F. Widdel, J. Peckmann, N. V. Pimenov, and M. B. Gulin.** 2002. Microbial reefs in the Black Sea fueled by anaerobic oxidation of methane. Science **297**:1013–1015.

35. **Mills, H. J., C. Hodges, K. Wilson, I. R. MacDonald, and P. A. Sobecky.** 2003. Microbial diversity in sediments associated with surface-breaching gas hydrate mounds in the Gulf of Mexico. FEMS Microbiol. Ecol. **46**:39–52.

36. **Morris, R. M., M. S. Rappé, S. A. Connon, K. L. Vergin, W. A. Siebold, C. A. Carlson, and S. J. Giovannoni.** 2002. SAR11 clade dominates ocean surface bacterioplankton communities. Nature **420**:806–810.

37. **Nauhaus, K., A. Boetius, M. Krüger, and F. Widdel.** 2002. In vitro demonstration of anaerobic oxidation of methane coupled to sulphate reduction in sediment from a marine gas hydrate area. Environ. Microbiol. **4**:296–305.

38. **Nauhaus, K., T. Treude, A. Boetius, and M. Krüger.** 11 November 2004. Environmental regulation of the anaerobic oxidation of methane: a comparison of ANME-I- and ANME-II-communities. Environ. Microbiol. 10.1111/j.1462-2920.2004.00669.x.

39. **Orphan, V. J., K.-U. Hinrichs, W. Ussler III, C. K. Paull, L. T. Taylor, S. P. Sylva, J. M. Hayes, and E. F. DeLong.** 2001. Comparative analysis of methane-oxidizing archaea and sulfate-reducing bacteria in anoxic marine sediments. Appl. Environ. Microbiol. **67**:1922–1934.

40. **Orphan, V. J., C. H. House, K.-U. Hinrichs, K. D. McKeegan, and E. F. DeLong.** 2001. Methane-consuming archaea revealed by directly coupled isotopic and phylogenetic analysis. Science **293**:484–487.

41. **Orphan, V. J., C. H. House, K.-U. Hinrichs, K. D. McKeegan, and E. F. DeLong.** 2002. Multiple archaeal groups mediate methane oxidation in anoxic cold seep sediments. Proc. Natl. Acad. Sci. USA **99**:7663–7668.

42. **Pace, N. R.** 1996. New perspective on the natural microbial world: molecular microbial ecology. ASM News **62**:463–470.

43. **Pancost, R. D., E. C. Hopmans, and J. S. S. Damsté.** 2001. Archaeal lipids in Mediterranean cold seeps: molecular proxies for anaerobic oxidation. Geochim. Cosmochim. Acta **65**:1611–1627.

44. **Pancost, R. D., S. J. Sinninghe Damsté, S. de Lint, M. J. E. C. van der Maarel, J. C. Gottschal, and T. M. S. S. Party.** 2000. Biomarker evidence for widespread anaerobic methane oxidation in Mediterranean sediments by a consortium of methanogenic archaea and bacteria. Appl. Environ. Microbiol. **66**:1126–1132.

45. **Papke, R. T., N. B. Ramsing, M. M. Bateson, and D. M. Ward.** 2003. Geographical isolation in hot spring cyanobacteria. Environ. Microbiol. **5**:650–659.

46. **Pimenov, N. V., I. I. Rusanov, M. N. Poglazova, L. L. Mityushina, D. Y. Sorokin, V. N. Khmelenina, and Y. A. Trotsenko.** 1997. Bacterial mats on coral-like structures at methane seeps in the Black Sea. Mikrobiologiya **66**:354–360. (In Russian.)

47. **Rappe, M. S., S. A. Connon, K. L. Vergin, and S. J. Giovannoni.** 2002. Cultivation of the ubiquitous SAR11 marine bacterioplankton clade. Nature **418**:630–633.

48. **Ravenschlag, K., K. Sahm, J. Pernthaler, and R. Amann.** 1999. High bacterial diversity in permanently cold marine sediments. Appl. Environ. Microbiol. **65**:3982–3989.

49. **Reeburgh, W. S.** 1996. "Soft spots" in the global methane budget, p. 334–342. *In* M. E. Lidstrom and F. R. Tabita (ed.), Microbial growth on C_1 compounds. Kluwer Academic Publishers, Dordrecht, The Netherlands.

50. **Sahling, H., D. Rickert, R. W. Lee, P. Linke, and E. Suess.** 2002. Macrofaunal community structure and sulfide flux at gas hydrate deposits from the Cascadia convergent margin, NE Pacific. Mar. Ecol. Prog. Ser. **231**:121–138.

51. **Schouten, S., E. C. Hopmans, E. Schefuss, and J. S. S. Damsté.** 2002. Distributional variations in marine crenarchaeotal membrane lipids: a new tool for reconstructing ancient sea water temperatures. Earth Planet. Sci. Lett. **204**:265–274.

52. **Schramm, A., L. H. Larsen, N. P. Revsbech, N. B. Ramsing, R. Amann, and K.-H. Schleifer.** 1996. Structure and function of a nitrifying biofilm as determined by in situ hybridization and the use of microelectrodes. Appl. Environ. Microbiol. **62**:4641–4647.

53. **Schrenk, M. O., D. S. Kelley, J. R. Delaney, and J. A. Baross.** 2003. Incidence and diversity of microorganisms within the walls of an active deep-sea sulfide chimney. Appl. Environ. Microbiol. **69**:3580–3592.

54. **Selje, N., M. Simon, and T. Brinkhoff.** 2004. A newly discovered *Roseobacter* cluster in temperate and polar oceans. Nature **427**:445–448.

55. **Snaidr, J., R. Amann, I. Huber, W. Ludwig, and K. H. Schleifer.** 1997. Phylogenetic analysis and in situ identification of bacteria in activated sludge. Appl. Environ. Microbiol. **63**:2884–2896.

56. **Suess, E., G. Bohrmann, D. Rickert, W. Kuhs, M. E. Torres, A. Trehu, and P. Linke.** 2002. Properties and fabric of near-surface hydrates at Hydrate Ridge, Cascadia Margin, p. 740–744. *In* Proceedings of the Fourth International Conference on Gas Hydrates, Yokohama, Japan.

57. **Suess, E., M. E. Torres, G. Bohrmann, R. W. Collier, J. Greinert, P. Linke, G. Rehder, A. Trehu, K. Wallmann, G. Winckler, and E. Zuleger.** 1999. Gas hydrate destabilization: enhanced dewatering, benthic material turnover and large methane plumes at the Cascadia convergent margin. Earth Planet. Sci. Lett. **170:**1–15.

58. **Teske, A., K.-U. Hinrichs, V. Edgcomb, A. de Vera Gomez, D. Kysela, S. P. Sylva, M. L. Sogin, and H. W. Jannasch.** 2002. Microbial diversity of hydrothermal sediments in the Guaymas Basin: evidence for anaerobic methanotrophic communities. Appl. Environ. Microbiol. **68:**1994–2007.

59. **Thiel, V., M. Blumenberg, T. Pape, R. Seifert, and W. Michaelis.** 2003. Unexpected occurrence of hopanoids at gas seeps in the Black Sea. Org. Geochem. **34:**81–87.

60. **Thiel, V., J. Peckmann, H. H. Richnow, U. Luth, J. Reitner, and W. Michaelis.** 2001. Molecular signals for anaerobic methane oxidation in Black Sea seep carbonates and a microbial mat. Mar. Chem. **73:**97–112.

61. **Thiel, V., J. Peckmann, R. Seifert, P. Wehrung, J. Reitner, and W. Michaelis.** 1999. Highly isotopically depleted isoprenoids: molecular markers for ancient methane venting. Geochim. Cosmochim. Acta **63:**3959–3966.

62. **Thomsen, T. R., K. Finster, and N. B. Ramsing.** 2001. Biogeochemical and molecular signatures of anaerobic methane oxidation in a marine sediment. Appl. Environ. Microbiol. **67:**1646–1656.

63. **Torres, M. E., J. McManus, D. Hammond, M. A. de Angelis, K. Heeschen, S. Colbert, M. D. Tryon, K. M. Brown, and E. Suess.** 2002. Fluid and chemical fluxes in and out of sediments hosting methane hydrate deposits on Hydrate Ridge, OR. I. Hydrological provinces. Earth Planet. Sci. Lett. **201:**525–540.

64. **Tourova, T. P., T. V. Kolganova, B. B. Kuznetsov, and N. V. Pimenov.** 2002. Phylogenetic diversity of the archaeal component in microbial mats on coral-like structures associated with methane seeps in the Black Sea. Mikrobiologiya **71:**230–236. (In Russian.)

65. **Treude, T., A. Boetius, K. Knittel, K. Wallmann, and B. B. Jørgensen.** 2003. Anaerobic oxidation of methane above gas hydrates at Hydrate Ridge, NE Pacific Ocean. Mar. Ecol. Prog. Ser. **264:**1–14.

66. **Treude, T., M. Krüger, A. Boetius, and B. B. Jørgensen.** Unpublished data.

67. **Tryon, M. D., K. M. Brown, and M. E. Torres.** 2002. Fluid and chemical fluxes in and out of sediments hosting methane hydrate deposits on Hydrate Ridge, OR. II. Hydrological processes. Earth Planet. Sci. Lett. **201:**541–557.

68. **Tryon, M. D., K. M. Brown, M. E. Torres, A. M. Tréhu, J. McManus, and R. W. Collier.** 1999. Measurements of transience and downward fluid flow near episodic methane gas vents, Hydrate Ridge, Cascadia. Geology **27:**1075–1078.

69. **Valentine, D. L., and W. S. Reeburgh.** 2000. New perspectives on anaerobic methane oxidation. Environ. Microbiol. **2:**477–484.

70. **Vetriani, C., H. W. Jannasch, B. J. MacGregor, D. A. Stahl, and A. L. Reysenbach.** 1999. Population structure and phylogenetic characterization of marine benthic archaea in deep-sea sediments. Appl. Environ. Microbiol. **65:**4375–4384.

71. **Whitaker, R. J., D. W. Grogan, and J. W. Taylor.** 2003. Geographic barriers isolate endemic populations of hyperthermophilic archaea. Science **301:**976–978.

72. **Zhou, J., M. A. Brunns, and J. M. Tiedje.** 1996. DNA recovery from soils of diverse composition. Appl. Environ. Microbiol. **62:**316–322.

Part III

Appendix

List of clones that are not presented in a manuscript

Archaeal 16S rRNA Gene Sequences

Phylogenetic affiliation	Next cultivated relative	HMMV Surface Sediment	HMMV Deep Sediment		
		Grey Mat	Center	Beg	Worm
EURYARCHAEOTA					
Methanosarcinales					
	Methanosarcina semesiae		1		
	Methanosaeta concilii			2	1
ANME-3	*Methanococcoides methylutens*	30			
ANME-2a	-	8			26
ANME-2c	-	87			9
Methanomicrobiales					
	Methanofollis aquaemaris		50		
	Methanoplanus limicola	1			
Marine benthic group D	-	2			
Miscellaneous Euryarchaeota Group	-	10			
Unaffiliated euryarcheaeota	-			1	
CRENARCHAEOTA					
Marine benthic group C	-		67	56	69
SUBTOTAL		**138**	**118**	**59**	**105**

Bacterial 16S rRNA Gene Sequences

Phylogenetic affiliation	Next cultivated relative	HMMV Bacterial Mats		HMMV Surface Sediment		HMMV Deep Sediment		
		Grey Mat	White Mat	Grey Mat	Beg-DBB*	Center	Beg	Worm
Alphaproteobacteria								
Sphingomonadales	*Sphingomonas yanoikuyae*					1		
Betaproteobacteria								
Herbaspirillum et rel	*Ultramicrobacterium* str. D-7					3		
Burkholderiales	*Aquabacterium citratiphilum*						1	
Gammaproteobacteria								
Alteromonadales	*Endobugula glebosa*			1				
Xanthomonadales	*Hydrocarbophaga effusa*		1					
HMMV-MPH	*Methylophaga sulfidovorans*	2						
HMMV-MetI	*Methylobacter marinus*	14		1		2	1	
HMMV-MetII	*Methylobacter marinus*	6		1	1	1		
Thiotrichales	*Leucothrix mucor*	8				1		
Unaffiliated	-		1					
Epsilonproteobacteria								
Campylobacterales	Distantly related to *Arcobacter* spp.	31		5	2			
Deltaproteobacteria								
Desulfobacteraceae	*Desulfosarcina variabilis*		4	1		1		
SEEP-SRB1	*Desulfosarcina* spp.		17	22				17
	Desulfobacterium anillini		6					
	Desulfobacterium catecholicum		1					
	Desulfobacula phenolica				8			2
SEEP-SRB2	-			2		1		
Desulfobulbaceae	*Desulfobulbus propionicus*		4		1	1		
SEEP-SRB3	*Desulfobulbus* spp.		1				10	
	Desulforhopalus singaporensis	1						
	Desulforhopalus vacuolatus				6			
SEEP-SRB4	*Desulforhopalus* spp.	6	1	1	54	2		1

Bacterial 16S rRNA Gene Sequences cont.

Phylogenetic affiliation	Next cultivated relative	HMMV Bacterial Mats		HMMV Surface Sediment		HMMV Deep Sediment		
		Grey Mat	White Mat	Grey Mat	Beg-DBB*	Center	Beg	Worm
Deltaproteobacteria								
Syntrophobacterales	*Desulfacinum infernum*	1				1		1
	Syntrophus gentianae							
Desulfonatronumaceae	*Desulfonatronum lacustre*					6		6
Desulfuromonadaceae	*Desulfuromonas palmitatis*				1			
Polyangiaceae	*Polyangium vitellinum*			1				
Bdellovibrionaceae	*Bdellovibrio bacteriovorus*					1		
Unaffiliated	-		2					
Fusobacteria								
	Propionigenium maris		2					
Bacteroidetes	*Flexibacter canadensis*	84		1	10	3	1	
	Flexibacter tractuosus	1						
	Flexibacter aggregans	3		1				
	Chryseobacterium spp.					5		
	Fibrobacter succinogenes		1					
	Sphingobacterium comitans		1	1	1	2		
Unaffiliated	-	1	8		7			5
Chlorobi	*Fibrobacter succinogenes*		1					
Unaffiliated	-		4	1	10	3	1	
Planctomycetes	*Pirellula marina*		5			1		4
	Candidatus Scalindua		1					
Unaffiliated	-		21	2				1
Verrucomicrobia	*Candidatus Xiphinematobacter*	2			1			
	Victivallis vadensis		1	1				
Unaffiliated	-							
WS3	-		8					

Bacterial 16S rRNA Gene Sequences cont.

Phylogenetic affiliation	Next cultivated relative	HMMV Bacterial Mats		HMMV Surface Sediment		HMMV Deep Sediment		
		Grey Mat	White Mat	Grey Mat	Beg-DBB*	Center	Beg	Worm
OP9	-		1			14	2	10
Gemmatimonadales	Unaffiliated, -		1					
Acidobacteria	Unaffiliated, -		1					1
Nitrospira	Unaffiliated, -					1		
OP8	-		3			7	34	3
TM6	-		3					
Nitrospina	*Nitrospira marina*		2					
Firmicutes	*Bacillus jeotgali*					1		
	Fusibacter paucivorans	1	1	3				
	Desulfotomaculum et rel.					3		
	Syntrophomonas erecta					2		
Actinobacteria	Unaffiliated, -		1			3		1
Thermomicrobia	Unaffiliated, -		16			5		4
OP11	-		4					1
WS6	-		2					
OD1	-		3	3	1			1
WS1	-							1
OP5	-		2					
Unaffiliated bacteria	-		2					
SUBTOTAL		**159**	**133**	**48**	**102**	**71**	**50**	**59**

Clone library	Sample used for clone library construction				Primer set	Clone names in ARB
	Cruise	Core location	Sample	Depth		
HMMV Bacterial Mats						
Grey mat	ARKXIX	N72° 0.17', E14 43.55'	144	0-1 cm	GM3 + GM4 *(Bacteria)*	HMMV-SOG*
White mat	ARKXIX	N72° 0.30', E14° 43.40'	113	0-0.5 cm	GM3 + GM4 *(Bacteria)*	HMMV-SOW*
HMMV Surface sediment						
Grey mat	ARKXIX	N72° 0.30', E14° 43.40'	81 + 82	0-2 cm	GM3 + GM4 *(Bacteria)*	HMMV-GM02*
					Arch20f + Uni1392R *(Archaea)*	HMMV-GM02*
Grey mat	ARKXIX	N72° 0.30', E14° 43.40'	83	2-3 cm	GM3 + GM4 *(Bacteria)*	HMMV-GM83*
					Arch20f + Uni1392R *(Archaea)*	HMMV-GM83*
Grey mat	ARKXIX	N72° 0.30', E14° 43.40'	83 + 84	2-4 cm	GM3 + GM4 *(Bacteria)*	HMMV-GM24*
					Arch20f + Uni1392R *(Archaea)*	HMMV-GM24*
Beg-DBB (White mat)	ATL	N72° 0.26', E14° 43.00'	27	1-2 cm	DBB305F + GM4 *(D'bulbus* spp.)	HMMVBeg-DBB*
HMMV Subsurface						
Center	ARKXIX	N72° 0.26', E14° 43.59'	151	465 cm	GM3 + GM4 *(Bacteria)*	HMMVCen-DS*
					Arch20f + Uni1392R *(Archaea)*	HMMVCen-DS*
Beg (White mat)	ARKXIX	N72° 0.20', E14° 43.88'	145	458 cm	GM3 + GM4 *(Bacteria)*	HMMVBeg-DS*
					Arch20f + Uni1392R *(Archaea)*	HMMVBeg-DS*
Worm (Tubeworm field)	ARKXIX	N72° 0.02', E14° 43.57'	63	410 cm	GM3 + GM4 *(Bacteria)*	HMMVPog-DS*
					Arch20f + Uni1392R *(Archaea)*	HMMVPog-DS*

Acknowledgement